Proceedings of the 2nd International Workshop on Groundwater Risk Assessment at Contaminated Sites (GRACOS) and Integrated Soil and Water Protection (SOWA)

Held in Tübingen, Germany, from 20 to 21 March 2003.

Edited by

DIETRICH HALM and PETER GRATHWOHL
Center for Applied Geoscience, Chair of Applied Geology, Eberhard Karls University of Tübingen,
Sigwartstraße 10, 72076 Tübingen, Germany

This workshop was organised by:

EBERHARD KARLS
UNIVERSITÄT
TÜBINGEN

Eberhard-Karls-University of Tübingen
Center for Applied Geoscience

ATTEMPTO SERVICE GMBH
RESEARCH • CONFERENCES • INNOVATION

Attempto Service GmbH
Tübingen Germany

GRACOS

Soil and Water
Integrated
SO
WA
Protection

GRACOS, SOWA: EU projects funded under Framework 5

Herausgeber:	Institut und Museum für Geologie und Paläontologie der Universität Tübingen Sigwartstraße 10, D-72076 Tübingen
Schriftleitung der Reihe C:	Lehrstuhl für Angewandte Geologie Prof. Dr. Peter Grathwohl & Prof. Dr. Georg Teutsch
Redaktion:	Dipl.-Geol. Björn Sack-Kühner

ISSN 0935-4948

Foreword

Welcome to the 2nd International Workshop on Groundwater Risk Assessment at Contaminated Sites and Integrated Soil and Water Protection in Tübingen.

One year ago, the 1st International Workshop on Groundwater Risk Assessment at Contaminated Sites mainly addressed methodologies for groundwater risk assesment such as leaching tests, in situ measurement of volatile organic compounds, and the development of low cost concepts and procedures.

The background given for the 2nd International Workshop on Groundwater Risk Assessment at Contaminated Sites and Integrated Soil and Water Protection is:

- contaminated sites (1st day)
- large-scale diffuse pollution of soils from disposal of non-regulated waste on land, agricultural activities, atmospheric deposition of pollutants, etc. (2nd day)

A major risk at most contaminated sites is that of groundwater pollution by organic and inorganic compounds. Since complete restoration of all these contaminated sites is economically and often technically not feasible, advanced procedures and guidelines of groundwater risk assessment are needed as innovative tool for the ranking of sites, decision making on further use, and remediation standards. The first part of the workshop focuses on the discussion of these new, innovative procedures for groundwater risk assessment at contaminated sites.

Diffuse pollution can affect large bodies of water where restoration is hardly reversible within reasonable periods of time. The second part of the workshop focuses thus on the protection of soil as the most active resource in the hydro- and biosphere and as the essential environmental compartment for food production and finally human health. Soil has to be recognised as key zone between the land surface and groundwater.

Participants from regulatory agencies (EPAs), consulting companies and academia will attend the workshop and therefore an unique forum for knowledge transfer between involved scientists, enterprises, authorities and the public is provided. We hope that the participants will benefit from the workshop and the inspiring ambience of Tübingen.

Tübingen, March 2003

Dietrich Halm, Peter Grathwohl

Acknowledgements

The workshop organisers are grateful to all who assisted in preparing this conference. They especially would like to thank the members of the Scientific Committee and the four invited Key Note Speakers who brought new and specific input to the workshop.

Scientific Committee:

Erwin Appel	University of Tübingen, D
Damiá Barcelò	IIQAB-CSIC Barcelona, E
Alberto Bonilla	LABEIN, E
Vasilis Burganos	Foundation for Research and Technology, GR
Mette Christophersen	Technical University of Denmark, DK
Rob Comans	Netherlands Energy Research Foundation, NL
Kim Dahlstrøm	Danish EPA, DK
Iñaki Gorostiza	GAIKER, E
Peter Grathwohl	University of Tübingen, D
Rolf Hahn	State EPA Baden-Württemberg, D
Dietrich Halm	University of Tübingen, D
Patrick Höhener	Federal Technical Institute of Lausanne, CH
Michel Jauzein	University Henri Poincaré Nancy 1, F
Kevin Jones	Lancaster University, UK
Peter Kjeldsen	Technical University of Denmark, DK
Knud Erik Klint	Geological Survey of Denmark and Greenland, DK
Tadeusz Magiera	Polish Academy of Sciences, PL
Rainer Schulin	Swiss Federal Institute of Technology Zurich, CH
Hans van der Sloot	Netherlands Energy Research Foundation, NL
Zygmunt Strzyszcz	Polish Academy of Sciences, PL
Kai Uwe Totsche	Technical University of Munich, D
Christos Tsakiroglou	Foundation for Research and Technology, GR
Tomas Vogel	Czech Technical University of Prague, CZ
Wolfgang Walther	Technical University of Dresden, D
Christoph Wenger	BUWAL, CH
Sjoerd van der Zee	Wageningen University, NL
Urs Ziegler	BUWAL, CH

Key Note Speakers:

Damià Barceló, Department of Environmental Chemistry, IIQAB-CSIC, Barcelona (E)
Peter Kjeldsen, Environment and Resources, Danish Technical University, Lyngby (DK)
Hans A. van der Sloot, ECN - Netherlands Energy Research Foundation ECN (NL)
Christos Tsakiroglou, Foundation for Research and Technology – Hellas (GR)

The editors wish to acknowledge the conference authors for their patience and cooperation during the editing process.

Table of Contents

page

LECTURES

GROUNDWATER RISK ASSESSMENT AT CONTAMINATED SITES (GRACOS)

KEY NOTE: Impact of inorganic contaminants from contaminated sites using an integrated approach assisted by a database/expert system

H.A.van der Sloot, P. Seignette, R.N.J. Comans, A. van Zomeren, J.J.Dijkstra, H. Meeussen.

ECN, Petten, The Netherlands.

Abstract: An important aspect of evaluating contaminated sites is to what extent they pose a risk of contaminant release to soil and groundwater in the short and the long term. Clearly, the common evaluation of soil contamination based on total composition does not assess the long-term risk properly. Recently, more sophisticated test methods have been or are standardised at European (CEN/TC292/WG6) and at international level (ISO/TC 190/SC7/WG6). A single step extraction test can not provide the relevant information needed either, as an understanding of the chemistry and controlling factors are needed to properly assess the potential for release. In addition, such understanding can provide insight in possible mitigating measures. Apart from the leaching behaviour of the material other aspects, such as hydrology and external influencing factors need to be taken into account to allow predictions on long-term behaviour. By setting up a database/expert system a comparison between materials from the GRACOS project and materials already studied before (Harmonisation project) can be made, thus gaining from existing knowledge and behaviour for the case at hand. The database contains results of pH-static experiments, column leaching tests, CEN tests, availability tests and diffusion tests on soil, contaminated soil, sediment, sewage sludge, compost and other related materials. This makes the database/expert system a unique tool to study correlation between parameters, comparison of different soil types, biodegradation aspects for organic rich materials and the comparison of data from laboratory leaching, lysimeter scale studies and field measurements. This information can be used to derive a time-variable source term for contaminated sites to be used as input to subsoil and groundwater impact studies.

Modelling chemical speciation

Saturation indices of potentially concentration controlling precipitates in landfilled materials proves to be very useful information (Van der Sloot et al., 2002 (Sardinia abstract). These saturation indices can be calculated with geochemical models such as PHREEQC (Parkhurst and Appelo, 1999), ECOSAT (Keizer and Van Riemsdijk, 1998) or the modelling environment ORCHESTRA (Meeussen et al., ES&Taccepted for publication). The recent recognition of the concentration enhancing effect of DOC with respect to heavy metals, makes it desirable that these calculations include adsorption of metals by DOC, for example by using the NICA-Donnan approach (Kinniburgh, 1999, Milne, 2000). However, this type of geochemical modelling, especially when applied to many different leachates/materials with different properties, is time-consuming and requires specialists skills. The development of a database/expert system, in which landfill leachate data is grouped in a systematic way, opens the possibility of a instantaneously coupled geochemical model, saving time and effort. For example, saturation indices can be calculated relatively simple using measured concentrations in the leachate (e.g., pH, redox potential, macro-elements, heavy metals, DOC) and an extensive, up-to-date and consistent thermodynamic database. Such a 'coupled' approach requires some adaptation of the geochemical software used for this purpose, and the possibility to read the appropriate data from the leaching/expert system database. Currently, tests of database-coupled PHREEQC and ORCHESTRA versions are ongoing and very promising. The program is made to communicate with the database/expert system to obtain the necessary input data, and a large thermodynamic database for the calculations of

speciation and mineral saturation indices (over 600 species and 450 minerals). Results of the modelling are readily spreadsheet- importable and can be interpreted more efficiently.

Potential for comparison of data from laboratory, from lysimeter studies and from field measurements

Results from laboratory tests on individual soil, treated soil and soil related materials can be compared to the leachate quality of a contaminated site and hence will help to improve management decisions site restoration.

DOC mobilization aspects

Because the database consists of a very large dataset it is possible to compare the behaviour of contaminants in soil and soil like materials with different organic matter contents. The data range from different types of soil and sediments (of marine and fresh water origin) at different contamination levels, a predominantly inorganic waste landfill taking soil cleanup residues (Van der Sloot et al., 2001) to sewage sludge and compost. The comparison has shown that organic matter rich materials in different stages of degradation exhibit different levels of DOC leaching and hence comparable differences are observed in heavy metal leaching (Cu, Cd, Zn, Fe). The DOC level is also important for release of organic micro-contaminants. In the latter case, the nature of the DOC must be further characterised as particularly high molecular weight DOC is of importance for the generally poorly water-soluble substances.

References

Keizer, MG, Van Riemsdijk WH, ECOSAT: Equilibrium Calculation Of Speciation And Transport, user manual, version 4, subdepartment of soil science and plant nutrition, Wageningen University and Research Centre, Wageningen, 1998.

Kinniburgh DG, van Riemsdijk WH, Koopal LK, Borkovec M, Benedetti MF, Avena MF. Ion bining to natural organic matter: competition, heterogeneity, stoichiometry and thermodynamic consistency, Colloids and Surfaces A: Physicochemical and Engineering Aspects 151 (1999) 147-166.

Milne CJ. Measurement and modelling of ion binding by humic substances. Ph. D. Thesis, University of Reading, Reading, 2000.

Parkhurst DL, Appelo CAJ. User's guide to PHREEQC (version 2)- a computer program for speciation, batch-reaction, one-dimensional transport, and inverse geochemical calculations. Water Resour. Inv. Report 99-4259, Denver CO: U.S. Geol. Surv., 1999.

Meeussen JCL., ORCHESTRA. Accepted for publication

Modelling processes controlling metal leaching from contaminated and remediated soils

Rob N.J. Comans[1], Joris J. Dijkstra[1] & Hans Meeussen[1]

Energy research Centre of the Netherlands (ECN), P.O. Box 1, 1755 ZG Petten, The Netherlands, tel. (+31) 224 564218, fax (+31) 224 568163, E-mail: comans@ecn.nl

Abstract: A combination of analytical measurements and geochemical modelling was used to identify the adsorption/desorption and aqueous complexation processes that control the leaching of metals from sets of contaminated and remediated soils. The results have provided important insights in the speciation of the environmentally relevant available metal fraction in the soils before and after remediation. The effect of soil remediation on metal leachability was not generally found to be favourable. Along with the removal of the metals, remediation techniques also tend to remove a substantial fraction of the sorption sites, while the available metal concentrations often remain relatively unaffected and do sometimes even increase, e.g. after thermal treatment. It is demonstrated that the effect of soil remediation on metal leachability needs to be evaluated with great care.

1. Introduction

The effect of soil remediation is often evaluated on the basis of the reduction of total contaminant concentration, rather than the mobile (leachable) fraction, which is the relevant property for risk-assessment purposes. It is only the leachable fraction that can be mobilised and taken up by soil biota, and soil remediation technologies should, therefore, be evaluated on their ability to reduce the leachable contaminant fractions. In this study, the processes controlling metal leaching from contaminated and remediated soils have been investigated in support of the development of a risk-assessment strategy for the reuse of remediated soils (Comans et al., 2003). A combination of analytical measurements and geochemical modelling was used to identify the adsorption/desorption and aqueous complexation processes that control the leaching of metals from sets of contaminated and remediated samples from a number of different soils and remediation techniques.

2. Materials and methods

Soil samples were leached in a pH-stat system to obtain geochemical fingerprints of the leaching processes over a wide pH range (pH = 2-10). Leachates were analysed for major elements, dissolved total inorganic (TIC) and organic (DOC) carbon and the metals Cd, Cu, Pb, and Zn. Amorphous iron (hydr)oxides and natural organic material were considered to constitute the major binding sites in these soils. Selective extractions were used to quantify their amounts: the ascorbic acid method according to Kostka & Luther (1994) was used for amorphous iron (hydr)oxides and a 0.1 M NaOH extraction (liquid/solid ratio of 10 L/kg) for natural organic (humic) material. Geochemical speciation modelling, including the diffuse double layer surface complexation model for hydrous ferric oxide (Dzombak & Morel, 1990) and the non-ideal competitive adsorption (NICA) model for natural organic material (Kinniburgh et al., 1996), was used to calculate metal partitioning between the leachate and sorption sites in the soil matrix. The “available” metal fraction in the soils was estimated on the basis of the amount leached at both pH = 2 and pH = 4. Further binding parameters for hydrous ferric oxide and natural organic material were used as recommended by Dzombak &

Morel (1990) and Kinniburgh et al. (1996), respectively. The geochemical speciation code ECOSAT (Keizer & van Riemsdijk, 1994) was used for the geochemical modelling.

3. Results and discussion

Figure 1 shows an example of cadmium leaching as a function of pH from two soils, before and after remediation. The leaching of cadmium is well-predicted on the basis of adsorption to natural organic matter (humic acid) and amorphous iron (hydr)oxides. Model calculations show that Cd in these soils is predominantly (>98%) bound to organic matter.

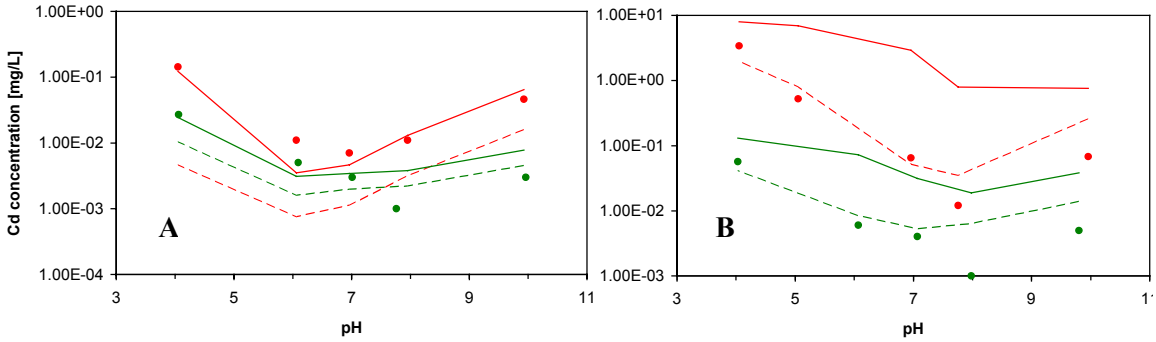

Figure 1. Example of cadmium leaching from two sets of contaminated (red symbols and lines) and remediated soils (green symbols and lines). Solid and broken lines represent model predictions based on "available" metal fractions estimated by leaching at pH = 2 and pH = 4, respectively. Soil A (Huizen Roden) was contaminated by electroplating industry and remediated by flotation; Soil B (Sparrenlaan Veenendaal) was contaminated by textile painting industry and remediated by chemical extraction.

An interesting feature illustrated in Figure 1 is the fact that in some soils the best match between modelling predictions and measurements of metal leaching is obtained using estimates of the availability of metals on the basis of their leachability at pH = 4, while in others on the basis of their leachability at pH = 2. Obviously, inaccuracies in quantifying the sorption capacity of the soils in terms of organic matter and hydrous ferric oxide may also contribute to the observed differences.

The model was also used to calculate speciation diagrams for the distribution of metals in the soils before and after remediation, as function of leachate pH (Figures 2 and 3). These diagrams give an indication of how the remediation process has affected the metal speciation in the soil and of the resulting leachability. Some generally observed features indicated by the geochemical modelling are that the available metal fractions are predominantly bound to particulate organic matter in the soil matrix and to dissolved organic carbon (DOC) in the leachate. Only at pH 4 and lower, the free metal ion, and to a lesser extent inorganically complexed metal, become important.

Figure 2 shows an example of a positive effect of remediation on cadmium leachability for a soil contaminated by electroplating industry and remediated by flotation. Both the total availability and leaching of Cd as a function of pH are reduced by a factor of approx. 5-10. Figure 3 gives an example of an adverse effect of remediation on Cd leachability, for a former gasworks soil remediated by thermal treatment. Both the total availability and leaching of Cd as a function of pH are increased by a factor of 2-5. The latter effect is caused by the thermal degradation of the organic binding sites in the soil. Cadmium in the soil after remediation is bound almost only to the remaining iron (hydr)oxides.

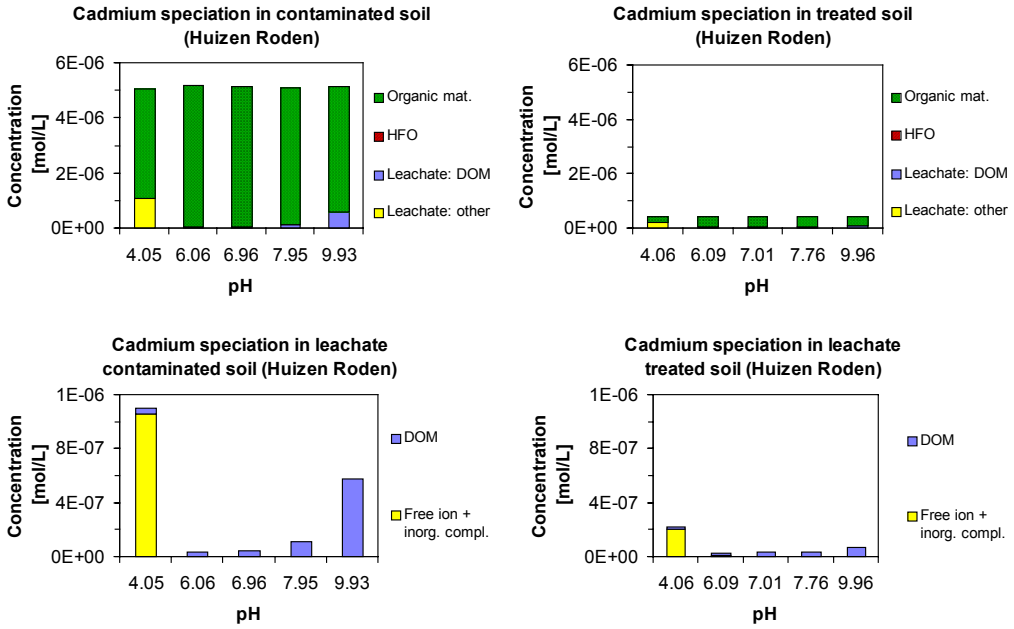

Figure 2. Speciation of cadmium as a function of leachate pH in Huizen Roden soil before (left) and after (right) remediation. The soil was contaminated by electroplating industry and remediated by flotation. The diagrams at the top indicate how the total available fraction of cadmium in the soil is distributed among particulate organic matter and hydrous ferric oxide (HFO) in the soil matrix, DOC- (dissolved organic carbon) bound Cd and free ionic + inorganically complexed Cd in the soil leachate. The bottom diagrams focus on the latter two fractions in the leachate.

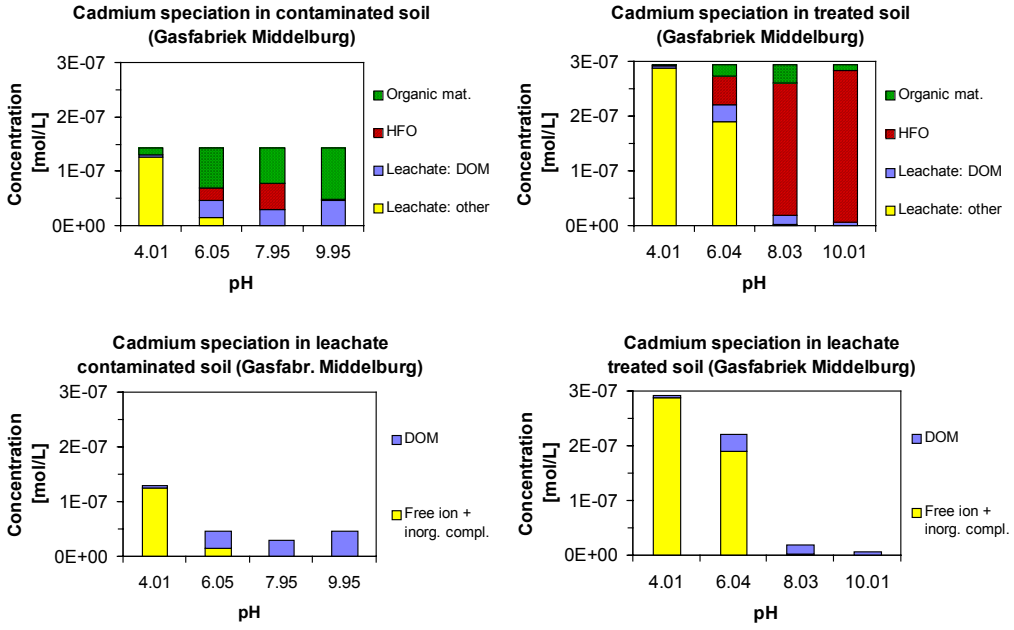

Figure 3. Speciation of cadmium as a function of leachate pH in Gasfabriek Middelburg soil before (left) and after (right) remediation. The soil was contaminated by a former gasworks plant and remediated by thermal treatment. The diagrams at the top indicate how the total available fraction of cadmium in the soil is distributed among particulate organic matter and hydrous ferric oxide (HFO) in the soil matrix, DOC- (dissolved organic carbon) bound Cd

and free ionic + inorganically complexed Cd in the soil leachate. The bottom diagrams focus on the latter two fractions in the leachate.

It is noteworthy that the soil pH after thermal treatment increased to a value of 10-11 and resulted in lower metal leaching compared to the soil before remediation at its near-neutral native pH. However, as Figure 3 indicates, this apparent positive effect will be lost after natural carbonation/pH-restoration of the remediated soil.

4. Conclusions

The results of this study have provided valuable insights in the speciation of the environmentally relevant available metal fraction in contaminated soils before and after remediation. pH-static leaching experiments and geochemical modelling have particularly demonstrated the importance of organic matter in controlling metal leaching from the soils. The results have shown that the effect of soil remediation on metal leachability is not necessarily favourable and that observed effects have to be evaluated with great care. Along with the removal of the metals, remediation techniques also tend to remove a substantial fraction of the sorption sites, *in casu* amorphous iron (hydr)oxides and organic material. The available metal concentrations often remain relatively unaffected by the investigated remediation techniques and do sometimes even increase, e.g. after thermal treatment.

References

Comans, R.N.J., Dijkstra, J.J. & Meeussen, J.C.L. (2003) *Manuscript in preparation.*

Dzombak, D.A. & F.M.M. Morel (1990) Surface complexation modeling. Hydrous ferric oxide. John Wiley & Sons, New York, 393 p.

Keizer, M.G. & van Riemsdijk, W.H. (1994) ECOSAT: A computer program for the calculation of speciation and transport in soil-water systems. Department of Soil Science and Plant Nutrition, Wageningen Agricultural University.

Kinniburgh, D.G., Milne, C.J., Benedetti, M.F., Pinheiro, J.P., Filius, J., Koopal, L.K. & van Riemsdijk, W.H. (1996) Metal ion binding by humic acid: application of the NICA-Donnan Model. *Environ. Sci. Technol.* **30,** 1687-1698.

Kostka, J.E. & Luther, G.W. (1994) Partitioning and speciation of solid phase iron in salt marsh sediments. *Geochim. Cosmochim. Acta* **58,** 1701-1710.

Leaching of PAHs from soil, sediment and waste materials in relation to dissolved organic matter characteristics

Gerlinde D. Roskam and Rob N.J. Comans,

Energy research Centre of the Netherlands (ECN)
Postbus 1, 1755 ZG Petten,
Tel +31-224 568309; Fax +31-224 568488; g.roskam@ecn.nl

Abstract: Batch pH-static leaching experiments were performed with a number of soil, sediment and waste materials to investigate the effect of pH on the character of DOC in the leachates and its role in facilitating the leaching of PAHs. In order to investigate the relationship between DOC and PAHs more directly, PAHs were analysed in NaOH-extracts of the samples before and after flocculation of DOC. Analysis of these extracts by High Performance Size Exclusion Chromatography (HPSEC) shows that especially the larger DOC molecules are responsible for the leaching of the least soluble PAHs. The smaller and more soluble PAHs are less influenced by the amount and character of DOC. Radiotracer experiments with ^{14}C-labelled PAHs confirm the preferential association with the higher-molecular humic acid fraction.

1. Introduction

The significance of the association with DOC on the fate of organic contaminants depends on properties such as the character, concentration, and mobility of the DOC, the characteristics of the contaminant, and the nature of the interaction (Kan and Tomson, 1990). Generally mentioned characteristics of DOC that affect the binding of PAHs are aromaticity, elemental composition, and molecular weight. For example, a correlation has been found between molecular weight and the number of aromatic domains; i.e. larger molecules are more aromatic (Chin *et al.*, 1997). This indicates that the larger molecules tend to cause a stronger interaction (Luthy *et al.*, 1997). However, their relatively low concentration in solution at low and neutral pH might limit their influence on the solubility enhancement. Therefore, due to its effect on the DOC concentration, pH should also be taken into account when evaluating the aqueous mobility of hydrophobic organic contaminants.

The objective of our research was to investigate the DOC enhanced leaching of PAHs and the influence of the characteristics of DOC on this process. Solutions with different DOC concentrations and characteristics were obtained by leaching three different samples at different pH-values. In order to investigate the relationship between DOC and PAHs more directly, PAHs were analysed in NaOH-extracts of the three samples before and after flocculation of DOC. In addition, DOC containing solutions spiked with ^{14}C-labeled PAHs were fractionated by HPSEC (high performance size exclusion chromatography) followed by radio-analysis of the DOC size fractions.

2. Materials and Methods

Materials: Three materials contaminated with PAHs have been used for this study, a PAH-contaminated soil from a former gasworks site and two waste materials: tar-containing asphalt granulate and the mechanically-biologically separated organic-rich fraction of municipal solid waste (referred to as OF-MSW). These three samples are believed to cover a wide spectrum of soil/waste materials with high PAH content and low (asphalt-granulate), intermediate

(gasworks soil) and high (OF-MSW) DOC concentrations in the leachates. Moreover, the properties of DOC in the three materials are likely to be different from one another. Therefore, this selection of samples is believed to facilitate a wide validity of observed leaching processes.

Batch pH-static leaching: Suspensions (liquid/solid ratio of 10 L/kg) of the three samples mentioned above were automatically adjusted to 6 different pH-values. After 48 hours reaction time, the leachates were obtained by centrifugation and analysed for DOC and PAHs (after extraction with dichloromethane). In addition, the size distribution of DOC was analysed by High Performance Size Exclusion Chromatography (HPSEC).

DOC-flocculation: Flocculation of DOC was based on a complexation/flocculation method developed by Laor and Rebhun (1997), with some modifications. The large amounts of aluminiumsulphate that were required to flocculate the high concentrations of DOC in the leachates were added as solid salt rather than as a concentrated solution. Moreover, the pH of the solution was not set to pH 6 in advance, because the addition of $Al_2(SO_4)_3$ already decreased the pH sufficiently. In order to determine the effect of pH reduction, one batch of each sample was adjusted to pH 6 without addition of $Al_2(SO_4)_3$. In addition, one batch was adjusted to pH 1, a procedure that is frequently used to precipitate humic acids (Stevenson, 1994).

Modelling of the experiments: Burkhard (2000) has recently reviewed DOC partition coefficients for nonionic organic contaminants, and found the following relationship between naturally occurring DOC and individual PAHs:

$$\log K_{DOC} = 1.18\ (\pm 0.13) \cdot \log K_{OW} - 1.56\ (\pm 0.72) \qquad \text{(eq. 1)}$$

based on 33 data points resulting in a correlation coefficient of 0.76.

Based on the above K_{DOC} values for individual PAHs and the leachate sample with the lowest pH-value, which is usually the sample with the lowest amount of DOC, we have estimated the amount of freely dissolved PAHs. It is assumed that the concentration of freely dissolved PAHs is independent of pH and constant throughout the pH-static experiments.

3. Results and Discussion

The results of the pH-static experiment shown in Figure 1 are consistent with the general behaviour of natural organic matter: the DOC concentrations increase towards higher pH values and HPSEC reveals that especially the larger molecules are more abundant (Figure 1, on the right). The DOC fraction that elutes first is humic acid size/type DOC; fulvic acids elute from this column after about 10 minutes (van Zomeren and Comans, 2003).

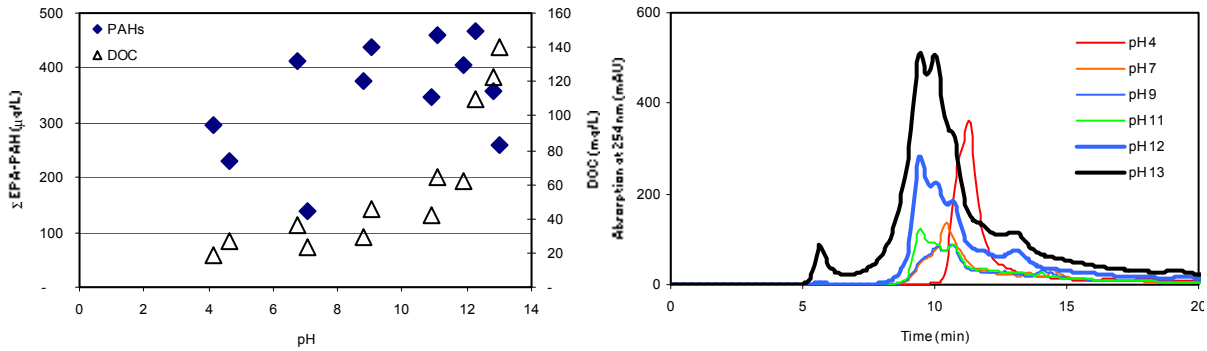

Figure 1 - Leaching of Σ EPA-PAHs and DOC from a gasworks soil as function of pH (left) and the influence of the leachate pH on the size distribution of DOC (right)

However, unlike preliminary experiments, the PAH concentrations do not increase likewise. According to the literature K_{DOC} values, one would expect a minor effect on the solubility of the smaller PAHs and an increase by a factor 5 for the largest PAHs over this range of DOC concentrations. When the data are separated into different PAH size fractions (results are not shown), only the 3-ring PAHs can be predicted reasonably well by the calculations using literature K_{DOC} values (eq. 1).

A factor that might bias the results is the ionic strength, as the aqueous solubility of PAHs is reduced by the presence of salts (Schwarzenbach, 1993). The ionic strength can be as high as 1 M for the pH 13 leachates. A non-automated pH-static experiment at a constant ionic strength for all pH values (I = 0.1 M or 1 M) does indeed show a difference in leaching of especially the 2- and 3-ring PAHs between the different ionic strength conditions, but a parallel increase with DOC towards high pH is still absent (results not shown).

Another potential cause for the apparent inconsistency of our results could be related to changes in the conformation of DOC. If a change in conformation towards higher pH-values (or ionic strength) would make DOC less prone to binding PAHs, due to increased charging and hydrophilic properties, the increase in the DOC concentration is counteracted by a reduced affinity (i.e. lower K_{DOC} values). This factor is currently being investigated.

By fractionating DOC by HPSEC, the binding of PAHs to specific size fractions of DOC can be measured. We have spiked DOC solutions with either ^{14}C-radiolabeled pyrene or benzo(*a*)pyrene and have thus been able to measure the amount of PAH in each DOC fraction. The HPSEC chromatogram shows a strong increase of the PAH signal in the humic acid like DOC fraction (Figure 2).

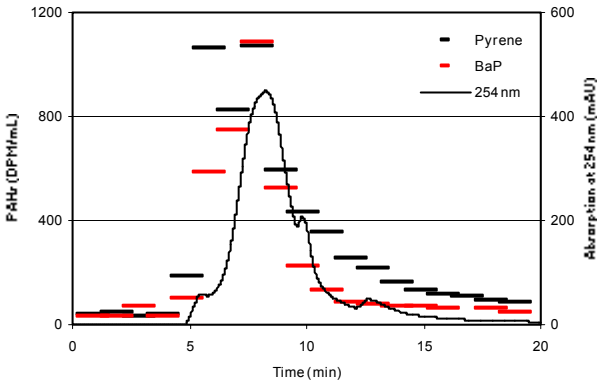

Figure 2 – Distribution of ^{14}C-labeled pyrene and benzo(a)pyrene over different DOC size fractions

Furthermore, flocculation experiments show a strong relationship between the leaching of DOC and PAHs. Addition of 1 g $Al_2(SO_4)_3$ per litre to 1 M NaOH extracts of the three samples reduced the DOC concentration to 53%, 51%, and 78% for asphalt granulate, gasworks soil and OF-MSW, respectively, whereas the PAH concentrations declined to 55%, 20%, and 9%. Figure 3 (left) clearly shows that in particular the concentrations of the least soluble PAHs decrease upon flocculation.

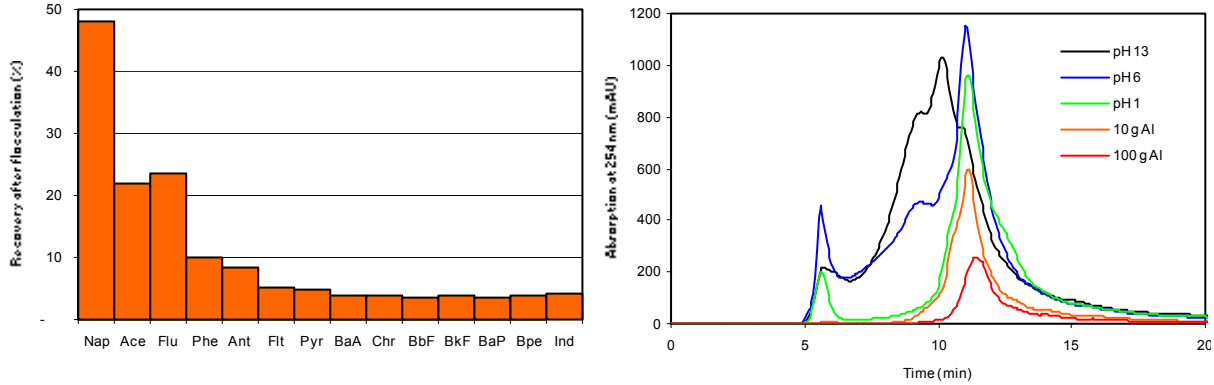

Figure 3 - The effect of flocculation of DOC from OF-MSW extract (by addition of 1 g/L $Al_2(SO_4)_3$) on individual PAHs (left), and the influence of flocculation on the size distribution of DOC (right)

Increasing the addition to 100 g $Al_2(SO_4)_3$ per litre for OF-MSW reduced the DOC concentration to 48% and the PAH concentration to 6% of the concentrations in the original leachate. Those results make clear that the fraction of DOC that is easily flocculated is most relevant for the solubility enhancement of PAHs. Analysis of the samples with HPSEC shows that mainly the higher-molecular DOC is removed by flocculation (Figure 3, on the right). The strong decrease in the PAH concentrations upon flocculation reconfirms the suggestion that this DOC fraction is mainly responsible for the solubility enhancement of PAHs.

4. Conclusions

There are various reports in the literature on natural (soil/sediment) organic matter that have shown that particularly the larger and relatively apolar DOC molecules strongly bind hydrophobic organic contaminants (Chin *et al.*, 1997; Luthy *et al.*, 1997). In this paper results are presented that confirm the relationship between the size-distribution of DOC and the extent of PAH leaching from contaminated soil/waste materials. Up till now, we have not been able to establish the same relationship in pH-static experiments, but several factors that might bias our results are under investigation. Our results are, to the best of our knowledge, among the first to show similar effects of DOC on PAHs in waste material leachates. It appears that the relevant DOC fraction in waste material leachates has very similar properties to that in natural systems.

References

Burkhard, L.P., *Environ. Sci. Technol.*, 2000, **34**, 4663.
Chin, Y.-P., Aiken, G.R. and Danielsen, K.M., *Environ. Sci. Technol.*, 1997, **31**, 1630.
Kan, A.T. and Tomson, M.B., *Environ. Tox. Chem.*, 1990, **9**, 253.
Laor, Y. and Rebhun, M., *Environ. Sci. Technol.*, 1997, **31**, 3558.

Luthy, R.G. *et al.*, *Environ. Sci. Technol.*, 1997, **31,** 3341.
Schwarzenbach, R.P., Gschwend, P.M. and Imboden, D.M., 'Environmental Organic Chemistry', John Wiley & Sons, New York, 1993.
van Zomeren, A. and Comans, R.N.J., 2003, submitted

PAHs leaching test for solidified waste

Rainer Henzler, Peter Grathwohl

University Tübingen, Center for Applied Geoscience, Sigwartstr. 10, 72072 Tübingen, Tel. +49-7071/2977452, Fax: +49-7071/295727, E-Mail: rainer.henzler@uni-tuebingen.de

Abstract: The treatment of waste materials to allow recycling or safe disposal is a rapidly expanding businesss, but also subject to increasing public awareness of enviromental issues and tightening of the regularise governing in many countries. One of the most widely used treatment for wastes is stabilisation /solidification using a cement matrix to obtain a monolithic residue. The most common test procedure to assess the risks of contaminant release into water (seepage, surface and groundwater) is the so-called „tank leaching test" or „diffusion test" (NEN 7345, Mulder et al 2001, Hohberg et al 2000), in which a solidified specimen is leached with water during different periods of time. The tests are usually done at room temperatures between 20 °C and 25 °C. However, the temperature under natural conditions are lower resulting in lower contaminant release rates. (subsurface temperature: 5 °C - 10 °C). If the thermodynamics of the contaminant release, especially the activation energy of desorption and diffusion, is known, it is possible to estimate the contaminant release for lower temperatures, e.g. down to groundwater temperatures. In addition the test can be accelerated if performed at high temperatures.

Theoretical backround

During relatively short time ranges and at an adequately high water / solid ratio the release of contaminants from a monolithic specimen is limited by diffusion in the matrix. The flux decrease over time (Fig. 1) and can be calculated with Equation 1 (Grathwohl 1998):

$$F = \frac{A}{V} M_0 \sqrt{\frac{D_a}{t\ \pi}} \qquad [1]$$

F, A/V, M_0, t and D_a denote the flux [µg kg^{-1} d^{-1}], the surface / volume ratio of the specimen [cm^{-1}], the initial contaminant content in the sample [µg kg^{-1}], the leaching time [d] and the apparent diffusion coefficient [cm^2 d^{-1}], respectively.

F decreases proportional $\sqrt{/t}$, i.e. very rapidly initially (Fig.1). After the specimen is leached under nonequilibrium conditions over a relative long time period, the flux change during a relatively small time interval is only minimal (Fig. 1) and "quasi" steady state condition can be assumed. In such a time interval the influence of elevated temperatures on contaminant release can be investigated.

The flux F is proportional to the apparent diffusion coefficient D_a under quasi steady state conditions. With increased temperatures D_a and thus F from the specimen increase because of two reasons: 1) sorption decreases and 2) diffusion gets faster. The temperature dependence of F can be described with an Arrhenius equation.

$$-E_a = \frac{}{\Delta\left(\frac{1}{R\,T}\right)} \qquad [2]$$

E_a, R and T are the activation energy [kJ mol^{-1}], the gas constant [kJ mol^{-1} K^{-1}] and the temperature [K], respectively.
Plotting ln F versus 1 / (T R) gives in ideale cases a linear relationship and the slope from the regression line corresponds to the activation energy E_a.

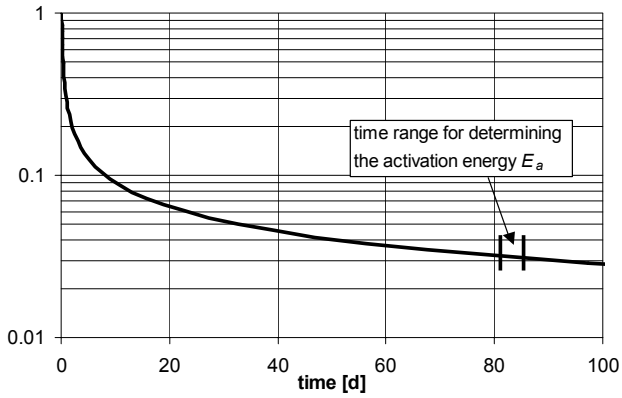

Figure 1: After leaching 82 days the flux F is quasi constant for a short time interval, which allows to investigate the temperature influence on contaminant release under quasi steady state condition.

Material and Methods

The sieve fraction 0.1 mm – 2 mm of a contaminated soil sample (reference material from the Bundesanstalt für Materialkunde und – prüfung) was chosen. The equilibrium concentration of the sum 16 EPA-PAHs in an aqueous leachate (dynamic column test) was 1700 µg l^{-1}. The total loading on the solid material amounts to 50 mg kg^{-1}.

A Recyclingbinder from Heidelberger Zement (Germany) was used as hydraulic setting cement. It contains 6 % organic carbon and thus it has a high sorption capacity for PAHs. The total amount of the sum 16 EPA-PAHs in the cement was 0.7 mg kg^{-1}.

The mixture chosen for the solidified specimen consisted of 70 % contaminated material and 30 % cement. 20 % water by weight was added to the mixture. After mixing, the sample was filled in to zylindric glass vials with a radius of 1.6 cm and a height of 9 cm. After 3 days of drying the glass was broken and the cement body was allowed to air-dry for another 30 days.

The specimen was saturated with water under low pressure in an exciccator and then stored in a glass bottle filled with 0.5 l Millipore water at 20 °C. In the first 10 days the water was exchanged every day and after 10 days every third day to determine the time dependent PAH flux. The experimental setup is shown in Fig. 2.

After 82 days at 20 °C, the cement body was leached at 6 different temperatures for one day each to determine the temperature dependency of the flux (Fig 1). The temperatures were 4 °C, 20 °C, 39 °C, 49 °C, 70 °C and 88 °C. The same experimental setup as for the 20 °C leaching test was used (Fig. 2) while the bottle was kept in a water bath.

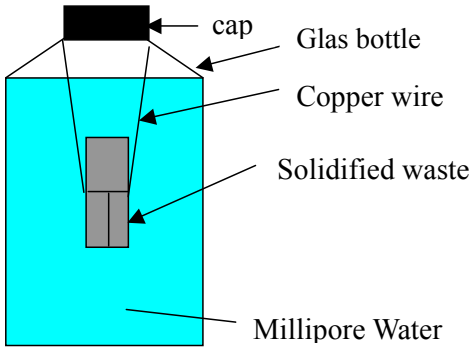

Figure 2: Experimental scheme for the tank leaching test. The water in the bottle was exchanged after certain time intervals.

Results

The contaminant fluxes from the zylindric specimen decreased proportional to the square root of time for all investigated PAHs as expected for a transient diffusion process. In a double-logarithmic scale plot the slope of the fluxes over time are consequently close to – 0.5 (Fig.3).

Fig. 3 shows results at 20 °C for the sum 15 EPA-PAHs (sum 16 EPA-PAHs without Naphthalene) and for some specific PAHs.

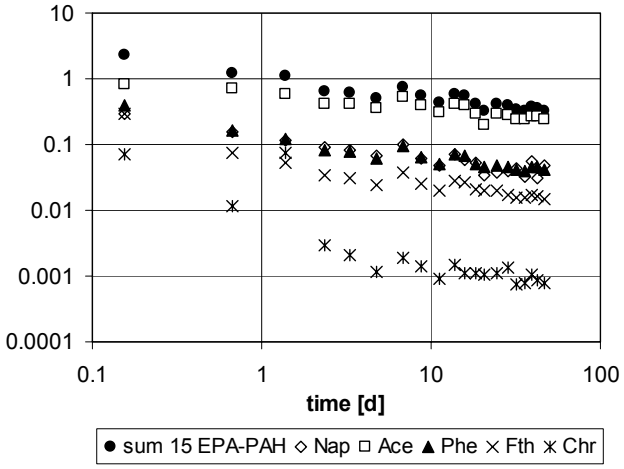

Figure 3: PAH fluxes over time at 20 °C for Naphtalene (Nap) Acenaphtylene (Ace), Phenanthrene (Phe), Fluoranthene (Fth), Chyrsene (Chr) and the sum 16 EPA-PAHs without Naphtalene (sum 15 EPA-PAH).

Fig. 4 compares model [eq. 1] and measurement for Phenanthrene using the apparent diffusion coefficient D_a as fitting parameter.

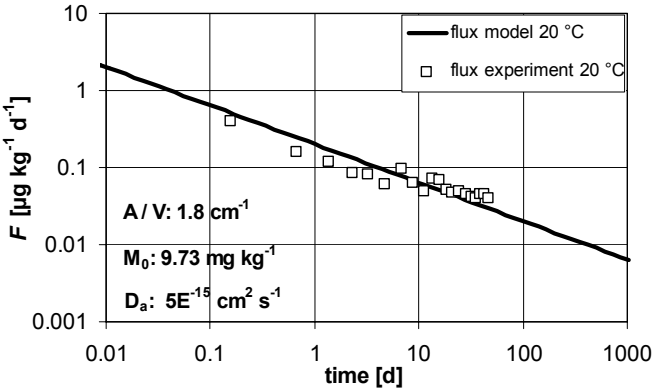

Figure 4: Measured and modelled Phenanthrene flux over time at 20 °C in double logarithmic scale.

After the tank leaching test at 20 °C, the specimen was leached at 6 different temperatures to determine the activation energy E_a [eq. 2]. Fig. 5 shows the results and the Arrhenius equation for Phenanthrene.

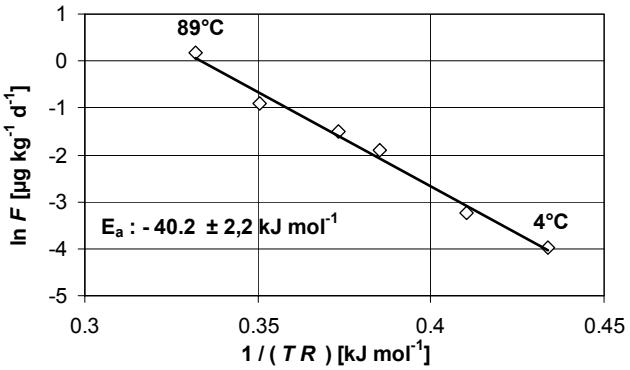

Figure 5: Arrhenius plot to determine the activation energy E_a. The slope of the regression line corresponds to E_a.

Fig. 6 shows the release rates of Phenanthrene versus time calculated with equation 1 at three different temperatures based on D_a determined at 20 °C.

The modelled data show, that Phenanthrene fluxes determined at room temperatures 20 °C should be corrected by a factor of 0.75 (E_a = 40 kJ mol^{-1}), if they are used for 10 °C field conditions. If the field temperature is 5 °C, a correction factor of 0.65 is needed. If the experiment is done at 30 °C or 50 °C, then the fluxes of Phenanthrene would increase by a factor of 1.30 and 2.1, respectively.

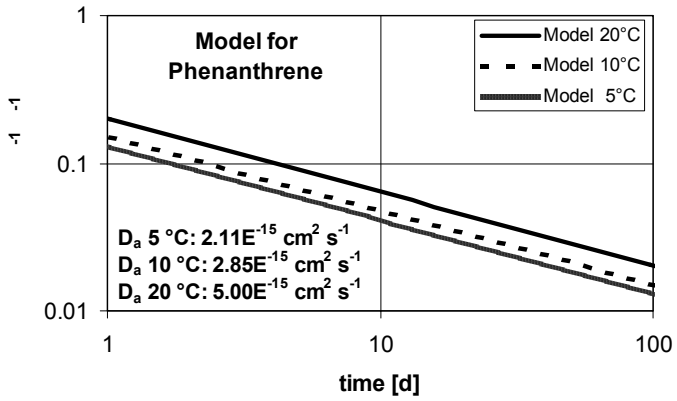

Figure 6: Flux versus time calculated with equation 1 at three different temperatures based on D_a determined at 20 °C.

References

Grathwohl, P. (1998): Diffusion in Natural Porous Media: Contaminant Transport, Sorption/Desorption and Dissolution Kinetics.- Kluwer Academic Publishers, Boston, 224p.

Hohberg, I., de Groot, G.J., van der Veeen, A., Wassing, W. (2000): Development of a leaching protocol for concrete.- Waste Management 20, p. 177-184.

NEN7345 (1995): Leaching Characteristics of soil and stony building and waste materials-Leaching tests-Determination of the leaching of inorganic components from building and monolithic waste materials with the didffusion test.-NNI, Delft, The Netherlands.

Mulder, E., Brouwer, J.P., Blaakmeer.J., Frenay.J.W. (2001): Immobilisation of PAH in waste materials.- Waste Management 21, p. 247-253.

A multicriteria approach for environmental impact assessment of contaminated materials

E. Cagigal[1], A. Bonilla[1], A. Urzelai[1], A. Díaz[2], I. Gorostiza[2]

[1]LABEIN, Cuesta de Olabeaga, 16, 48013 Bilbao, SPAIN
Phone: +34 94 4892400, Fax: +34 94 4892460, E-mail: ecagigal@labein.es
[2]GAIKER, Parque Tecnológico de Zamudio. Edf. 202, 48170 Zamudio, SPAIN

Abstract: This project aims to develop a method for the environmental assessment of contaminated materials. The core of the study is based on the ecotoxicological characterisation of the mobile/bioavailable fraction of the materials. In order to achieve this objective several assays were carried out divided into mobility/bioavailability tests and toxicitiy tests on mobile fractions. Mobility procedures involved batch leaching tests, column tests and sequential extraction tests. Microtox™ tests were employed for the measurement of the toxicological response of the extracted fractions. Toxicity tests on solid phase (Microtox SP and worms) were also carried out in order to assess correlation between both toxicity responses. This combination of leaching/toxicity tests provides a fast/low cost procedure for the ecotoxicological characterisation and the study of potential hazards associated to contaminated materials. In addition, an ecological risk assessment of the contaminated materials was carried out comparing chemical results with bibliographical toxicity data. According to obtained information, a stepwise methodology for the environmental risk assessment of contaminated materials was proposed. This protocol could be a very useful tool for the evaluation of potential risks for the ecosystems due to the presence of contaminated materials.

1. Introduction

Chemical characterisation of leachates and speciation tests could be not enough for the prediction of potential hazards or ecological effects of contaminated materials, since sinergic effects of contaminants and influence of non-analysed pollutants are not considered. Bioassays provide direct evidence of ecological effects associated with soil and groundwater pollution, complementing conventional chemical analysis. Current study aims to assess the environmental/ecological risks associated to contaminated soil, sediments or wastes. This assessment takes in consideration the analysis of leachate toxicity using bioassays. Conventional biological tests are based on the exposition of organisms to the pollutants and contaminated media of interest. These tests are performed in solid phase being expensive, and space and time consuming. This new approach considers the use of bioassays traditionally applied in water monitoring or leachate ecotoxicity assessment. These methods are cheaper and have a quick response. This approach requires the development of extraction procedures to be used together with bioassays to determine the hazards due to soluble molecules, less soluble, soil bound molecules, etc. The combined application of extraction-leaching tests/bioassays/physico-chemical analysis on samples will provide us a wide and complete information about the presence, behaviour and toxicity of pollutants in the tested materials.

Final objective of the project is the development of a procedure to be used as a tool for the assessment of environmental impact of contaminated materials. On the framework of the project two mobility/bioavailability tests for both inorganic and organic compounds, and an ecotoxicological assay of the mobile/bioavailable fractions have been applied. Toxicity tests on solid phase were also carried out in order to assess the representativeness of the leaching protocols as a method to reproduce bioavailability of contaminants.

2. Methods and Materials

Contaminated materials

Materials used for the experiences were selected from different contaminated sites. Samples (sediments, soils and wastes) were from different sources and with different features.

Table 1. Description of contaminated materials

Sample	Type of material	Description of material
M-1	Sediment	Dredged sediment from disposal of river freshwater in an industrial area
M-2	Sediment	Dredged sediment (harbour sludge), salty-brackish water
M-3	Sediment	Dredged sediment (harbour sludge), salty-brackish water
M-4	Sediment	Dredged sediment from river freshwater
M-5	Waste	Bottom ashes
M-6	Waste	Tar-road containing asphalt granulate
M-7	Waste	Sifter-sand
M-8	Soil	Coal

Due to the origin of most of the materials, large contents of heavy metals were expected, hence As, Cd, Cr, Cu, Hg, Ni, Pb, and Zn were analysed. Since it was not so clear the composition of organic compounds in the materials, a screening procedure was carried out on solid phase in order to determine main organic contaminants.

Experimental work for the assessment of the mobility/bioavailability/toxicity of these materials involved: 1) batch leaching tests, 2) sequential extraction tests, 3) column leaching tests, and 4) toxicity tests.

Batch leaching tests

Batch leaching tests are based on a continuous contact between sample material and leaching agent (distilled water), according to EN-12457-1. The material (4 mm) was leached employing distilled water with a liquid/solid ratio of 2 L/Kg. Using an end-over-end tumbler (15 r.pm.) samples with leaching agent were shaken during 48 hours. After this period pH measurements of the solution were carried out and extracted solutions were separated using centrifugation and vacuum filtration. Chemical analysis were performed in these extraction solutions in order to determine the concentration of heavy metals (As, Hg, Zn, Cu, Cd, Pb, Ni, Cr).

Mobilisation of heavy metals is strongly influenced by pH and organic matter conditions. As these two parameters are key factors to understand heavy metals mobility, additional leaching studies were carried out based on the batch leaching tests described above. Eight extractions were performed at different values of pH (ranging 2 to 12), using HCl and NaOH as extractants. Batch leaching tests were also performed varying the organic matter content by means of additions of humic acid at different concentrations, with constant pH at 12.

Sequential extraction tests

Sequential extraction procedure was based on the BCR scheme for soils and sediments. This method includes three extraction stages corresponding to different fractions of metals in soils/sediments. Extractant solutions were: 1) acetic acid 0.11 $mol \cdot l^{-1}$, 2) hydroxylamine

hydrochloride 0.1 mol·l^{-1} pH 2, and 3) hydrogen peroxide 30% pH 2 and ammonium acetate 1 mol·l^{-1} pH 2.

Column leaching tests

Experimental setup tries to simulate real leaching process pumping water through a glass column filled with sample material. This procedure is based on DIN V 19736 standard for the derivation of concentrations of organic pollutants. The water was pumped upwards into the column at a rate of 0.8 mL/min using a peristaltic pump. Chemical analysis were performed in the extraction solutions in order to determine the concentration of organic pollutants (PCB, PAH, mineral oil).

Toxicity tests

Toxicity tests were carried out on the leachates from batch and column tests. The aim of these tests was the assessment of potential toxicity to the groundwater due to contaminants mobilisation. Toxicity measurement on leachates was carried out using Microtox™ equipment. This method is based on the exposition of a luminiscent organism (*Vibrio fischeri*) to the contaminated leachates. The luminiscence reduction is in direct relation with the organism lethality. Toxicity tests performed directly on solid phase were Solid Phase Microtox Test (*Vibrio fischeri*) and Earthworms toxicity test (*Eisenia foetida*).

3. Results

Solid phase characterisation

Chemical characterisation of the materials was performed, analysing heavy metals (As, Cd, Cr, Cu, Hg, Ni, Pb, and Zn), mineral oil, PCB and PAH. High contents of heavy metals were detected in most of the contaminated materials, especially for M-3 and M-5. Main organic contaminant was PAH, while mineral oil was only significant in samples M-6, M-7, and M-8. Therefore, subsequent analyses were focused on heavy metals and PAH.

Mobility/Bioavailability

Mobilisation of inorganic contaminants was studied by means of batch leaching tests. Heavy metals and pH were measured in the extracts. Among studied metals, mobilisation rates of Cd and Zn were the highest. On the contrary, no fractions of Pb and Hg were detected and it is supposed to be associated to low mobility fractions.

Concerning the metal mobilisation in function of pH of extractant agent, two samples (M-3 and M-5) were selected for these tests at different value of pH. There is a clear dependence of heavy metals mobilisation rates on this parameter for both materials, as it can be seen in Figure 1. Metal release is maximum at acid pH, it reaches a minimum around pH 7, and then increases moderately with alkaline pH. However, it does not seem to be a clear relation between heavy metals mobilisation and organic matter content in the studied range of humic acid addition.

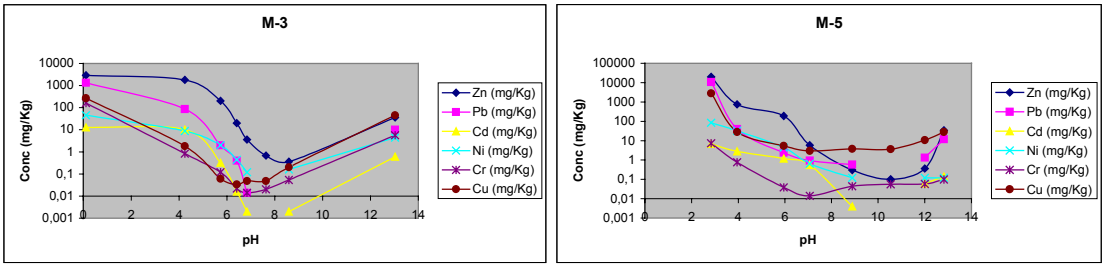

Figure 1. Heavy metals mobilisation rates depending on pH for samples M-3 and M-5.

Organic compounds leaching behaviour was studied using column tests and they were determined in the eluates from the column. Organic compounds mobility resulted very low and only mineral oil and PAH concentrations were significant in samples M-6 and M-7

Sequential extraction tests

Different distributions of chemical fractions were found in the sequential extraction tests depending on the metal mobility. In general, the distribution of heavy metals in the different fractions indicates that Hg and Pb are associated to low mobility fractions (residual fraction), while Cd and Zn are the most mobile metals. These results have a good concordance with results from batch extraction tests.

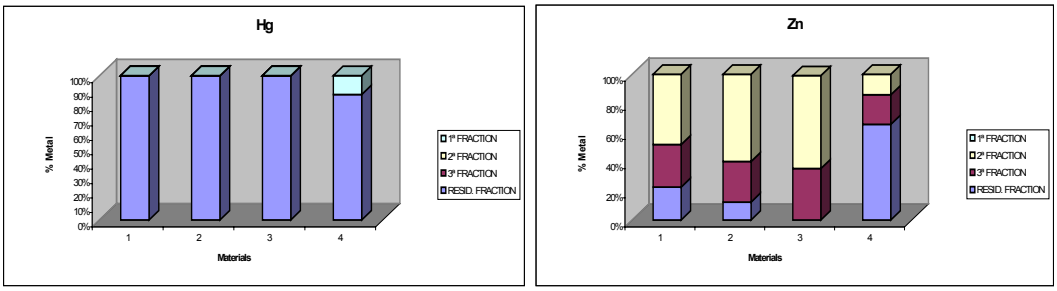

Figure 2. Percentage distribution of heavy metals (Hg and Zn) in samples M-1, M-2, M-3 and M-4.

Toxicity tests

Toxicity assessment of ecological impact of the studied materials was carried out by means of the methods described above. Leachates from batch leaching tests and column tests were assayed. Table 2 includes toxicological results of the contaminated materials.

Table 2. Toxicity tests results of the contaminated materials.

Sample	Microtox Solid Phase (EC50, mg/l)	Worms (EC50, %)	Batch leaching tests (EC50, mg/l)	Column tests (EC50, mg/l)
M-1	---	25.8	No effect	No effect
M-2	No effect	No effect	No effect	No effect
M-3	1070	No effect	31500	No effect
M-4	2234	No effect	No effect	No effect
M-5	1589	42.3	No effect	98120
M-6	252700	---	367900	No effect
M-7	3898	No effect	No effect	No effect
M-8	No effect	No effect	No effect	No effect

Toxicity response of mobile/bioavailable fraction correlates with tests on solid phase in samples M-3, M-5, and M-6. No toxicological effect was detected in the other cases.

In the studies of metal mobilisation vs pH a good correlation between toxicity and heavy metals content was obtained in the batch tests. Toxicity of solutions increases in those cases where the pH causes a higher release of metals. Same conclusion was obtained from the study of the influence of organic matter in the available fraction: Toxicity response correlates with heavy metals content of leachates.

Ecotoxicological assessment based on chemical data (solid phase and mobile fractions)

This assessment procedure was applied to the four sediments involved in the project, which implies the study of an estuarine environment for three of them (samples M-1, M-2 and M-3) and a freshwater environment for sample M-4. These case studies must be considered only as examples to show this procedure, since a more complex sampling design would be required for a detailed environmental impact assessment. The assessment procedure considers the analysis of relevance of pollutants concentrations determined in the fractions obtained in the previous tests and assays, comparing them with bibliographical toxicological data.

Two approaches were considered in the study: 1) Effects of pollutants on organisms associated to the sediment (NOAA reference values), and 2) Effects of contaminants on the aquatic media (EQG reference values and PAF calculation). Results from these evaluations are compiled on Table 3.

Table 3. Results of the ecotoxicological assessment.

	Samples	Benthic communities (ER-L, ER-M)*	Aquatic communities (%PAF)**
Estuarine environment	M-1, M-2, M-3	Hg, Zn > ER-L As, Cd, Cr, Cu, Ni, Pb > ER-M	Zn 40%, Ni 23%, Cr 18%
Freshwater environment	M-4	Cu, Hg, Ni > ER-L	Ni 37%, Zn 28%, Cd 12%

* >ER-L: Potential risk for the ecosystem, >ER-M: Real risk for the ecosystem.

** PAF: Potentially Affected Fraction of species of the ecosystem.

4. Conclusion

As it has been described, the development of combined toxicity/mobility methods is a very useful tool for the ecological risks assessment of groundwaters. In order to achieve this objective a procedure for the environmental impact assessment has been applied based on ecotoxicological characterisation of the mobile/bioavailable fraction in contaminated sites. This methodology can be structured as follows.

This easy stepwise protocol allows evaluating ecological impact of a contaminated material considering different approaches. The procedure aims to combine all the information obtained from toxicity tests and chemical analyses. For each scenario several risk assessment steps of increasing complexity can be considered. As much complex is the assessment step higher is the cost and the time consuming. The significance of their results can also vary a lot. From this point of view groundwater environmental impact assessment involves several levels or steps that include procedures of increasing cost and difficulty.

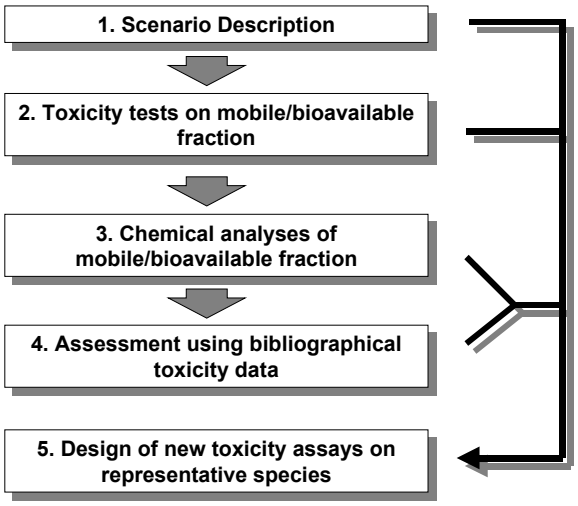

Firstly, a good description of the contaminated site is required. The description must include points such as type and features of contaminants, hydrogeological, geological and other aspects related to mobilisation pathways, potential receptors of contaminants (human beings, aquatic ecosystem -freshwater/marine environments-, terrestrial ecosystems), etc. Mobility and toxicity tests described above are included in a second phase of the methodology. This experimental work provides data for the evaluation of the potential risk associated to a contaminated material. Finally, the last step of the ecological risk assessment involves the analysis of significance of pollutants concentrations determined in the fractions obtained in the previous tests and assays.

As additional stage of the presented methodology, toxicity assays (bioassays) on representative species of the scenario could be developed. Obtained information from previous steps can be useful for the planning of more valuable bioassays (selection of sensible species, for instance). These assays are usually expensive and space and time consuming but offers a very accurate information about the effects on specific organisms and they would be very useful in detailed environmental risk assessment of the contaminated scenario.

Importance of parameter uncertainty for groundwater risk assessment – a case study

Heinke Stöfen, Wilfried Schneider

Corresponding author: Heinke Stöfen, Technical University of Hamburg-Harburg, Department of Water Management and Water Supply, Schwarzenbergstr. 95, 21073 Hamburg, phone: +49 40 42878-3177, fax: +49 40 42878-2999, E-Mail: stoefen@tuhh.de

Abstract: According to the German ordinance to protect the soil (BBodSchV 1999) transport models can be used to predict the maximum concentration that will reach the point of compliance. The calculated maximum concentration at the point of compliance is compared to the limiting value to determine if the site endangers the groundwater. In early stages of site evaluation literature values have to be used for the transport and reaction parameters of the contaminants. Especially sorption and biodegradation parameters from the literature differ by orders of magnitude. In this case study we will show that using the minimum or maximum values to estimate a worst respectively best case does not lead to results which allows one to decide whether the site is a threat to the groundwater or not. The resulting maximum concentration at the point of compliance is far below or far above the limiting value, in the case of maximum respectively minimum values. Uncertainty analysis is a possible technique to assess this dilemma. If the parameter uncertainty is considered and a Monte Carlo simulation is performed the risk evaluation becomes more reliable. The case study is another example which shows that uncertainty analysis should become a standard procedure for decision-making in the context of groundwater risk assessment.

1. Introduction

Following the federal soil protection ordinance (BBodSchV 1999) sites suspected to endanger the groundwater must be evaluated. Limiting concentrations have been defined at a point of compliance, which is located at the transition between the unsaturated and the saturated zone. Transport models can be used to calculate the concentrations of contaminants at the point of compliance. In early stages of site evaluation input parameters for the transport models have to be estimated from literature data. Because of the uncertainty inherent in subsurface transport prediction, an integral part of predictive modeling should be uncertainty analysis (James and Oldenburg 1997). Using a case study we show the importance of considering parameter uncertainty for groundwater risk assessment.

2. Basics of Uncertainty Analysis

One approach to uncertainty analysis is the Monte Carlo method. The Monte Carlo analysis is especially appropriate for input variables which are affected by large uncertainties and where a nonlinear relationship between input and output variables exits. The Monte Carlo analysis is based on performing multiple model evaluations with randomly selected model input and then using the results to determine the uncertainty in model predictions. The procedure consists of four steps: (1) select a range and a probability distribution function (pdf) for each input variable and impose a correlation among the variables, if present, (2) generate multiple sample sets from the pdf's specified before, (3) evaluate the model for each sample set, (4) use the resulting output values as the basis for uncertainty analysis. A histogram of the output variables is the outcome. From this the mean, the variance, and different percentiles of the output variables can be estimated (Tarantola et al. 2002).

To generate the sample sets different sampling techniques can be used, e.g. random or Latin hyper-cube sampling. Desirable features of Latin hyper-cube sampling include unbiased estimates for means and distribution functions and dense stratification across the range of each sampled variable. For a description of the Latin hyper-cube sampling, refer to McKay et al. (1979). In particular, uncertainty analysis results, obtained with Latin hyper-cube sampling, have been observed to be quite robust even when a relatively small number of sample sets are used (Helton and Davis 2000). Therefore, this method is used here to produce the sample sets. For this first approach the input variables are assumed to be uncorrelated.

3. Case study

A hypothetical contaminated site is used for this case study. The contamination consists of polychlorinated hydrocarbons. The most critical contaminant is 1,2-dichloroethane with a concentration of 1 mg/L determined in a leaching test. The limiting value according to the German ordinance to protect the soil (10 µg/L) is exceeded by a factor of 100. A 10 m thick unsaturated zone at the site consisting of sand is assumed. It should therefore be evaluated if biodegradation and volatilization can reduce the concentration to observe the limiting value. To determine whether the contamination threatens the groundwater the transport code HYDRUS 1D (Simunek et al. 1998) in conjunction with the sampling tool SimLab 1.1 (SimLab 2000) is applied.

3.1 Uncertainty in Input Parameters

To conduct an uncertainty analysis the range and the pdf of input parameters have to be selected. Some parameters are assumed to be measured and are therefore relatively certain.. The diffusivity in air is estimated with the equation of Fuller et al. (1966) for 10°C, the diffusivity in water is taken from the literature (Montgomery 1996, Wiedemeier et al. 1999). The values of the relatively certain parameters are shown in Table 1. For these parameters uncertainty exists due to heterogeneity but since this uncertainty is small compared to the uncertainty in not measured data it is neglected.

Table 1 – Relatively certain parameters

Parameter	value
Source concentration [mg/L]	1
Total source concentration [mg/kg]	50
Depth of contaminated layer [cm]	40
Depth to water table [cm]	1000
Bulk density [kg/L]	1.5
Fraction of organic carbon f_{oc} [%]	1
Van Genuchten parameters:	
θ_r [-], θ_s [-],α [1/cm], n [-]	0.0464, 0.3476, 0.0358, 3.1562
k_s [cm/d], l [-]	473.22, 0.5
Diffusivity in Air [cm²/d]	7077
Diffusivity in Water [cm²/d]	0.864

Highly uncertain parameters are the partitioning coefficient K_d, which can be approximated from the partitioning coefficient between water and organic carbon K_{oc} and the organic fraction of the soil, the half life, the infiltration rate, the dispersivity and the Henry constant. Literature values from Montgomery (1996), Wiedemeier et al. (1999), Spitz and Moreno (1990), and Howard et al. (1991) for the parameters K_{oc} and Henry constants, show the ranges

given in Table 2. Field biodegradation half-life is almost impossible to predict. Experiments are usually conducted in the laboratory and the transfer of these values to the field is questionable. Therefore, the maximum half life expected for aerobic conditions is taken as the minimum half life and the maximum half life expected for anaerobic conditions is taken as the maximum half life. The biodegradation rates for aerobic and anaerobic conditions can be found in Howard et al. (1991).

For the dispersivity values between 0.01 and 0.1 of the transport length seem reasonable. The infiltration rate into the sand varies between 100 and 300 mm/a. The distribution of the input parameters is assumed to be uniform, which means that all values between the minimum and maximum values are equally probable.

Table 2 – Uncertain parameters with minimum and maximum values

Parameter	min value	max value
log K_{oc} [log(L/kg)]	1.279	1.76
K_d [L/kg]	0.19	0.575
Half life [d]	200	720
Infiltration rate [cm/d]	0.0274	0.0822
Dispersivity [cm]	10	100
Henry constant [-]	0.02	0.06

3.2 Best and Worst Case Estimates

Using all possible 32 (2^5) combinations of minimum and maximum values from Table 2, the highest concentration that will reach the point of compliance is 26 µg/L. All possible concentrations using the minimum and maximum values are shown in Figure 1.

In many cases it will not be obvious which combination of minimum and maximum values will lead to the highest respectively lowest maximum concentration at the point of compliance. In Table 3 the combination of input parameters giving the highest and lowest concentration are listed. With these calculated highest and lowest concentrations it is not possible to determine whether the contamination is a threat the groundwater or not.

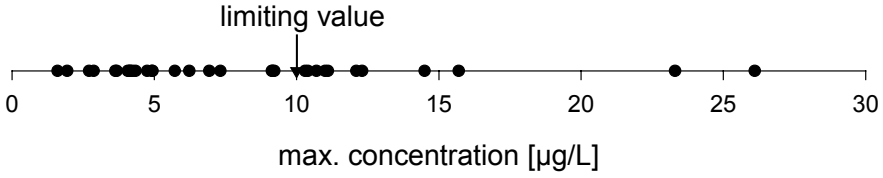

Figure 1: Evaluation of max. concentrations using appropriate values from Table 2.

Table 3 – Parameters for highest and lowest concentrations at point of compliance

Parameter	highest c_{max}	lowest c_{max}
K_d	min	max
Half life [d]	max	min
Infiltration rate [cm/d]	max	min
Dispersivity [cm]	max	min
Henry constant	min	min

3.3 Results of the Uncertainty Analysis

Figure 2 shows the results of the Monte Carlo uncertainty analysis. The histogram of the output values follows a log normal distribution as can also be seen from Figure 3, where the output values are shown as their logarithmic values. The more simulation runs are conducted the better is the agreement between simulated relative frequencies and the theoretical log normal distribution.

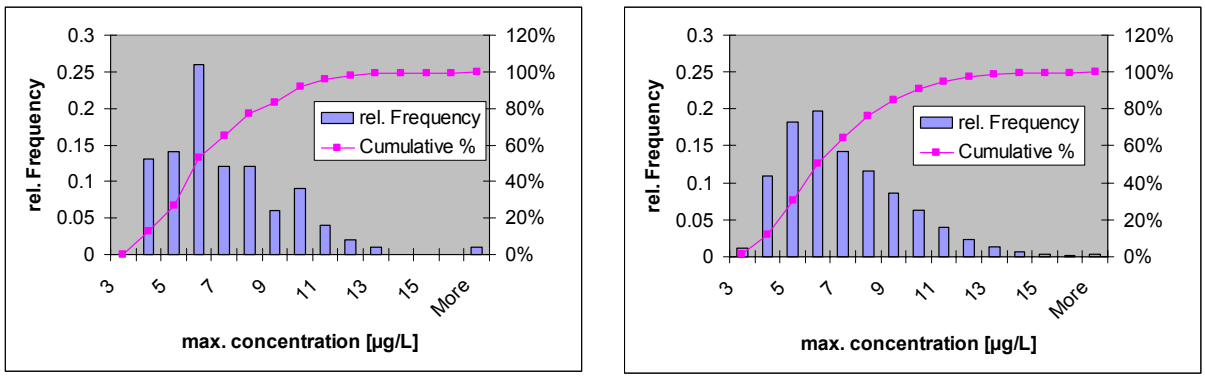

Figure 2: Histogram of output parameters for 100 respectively 2000 simulation runs.

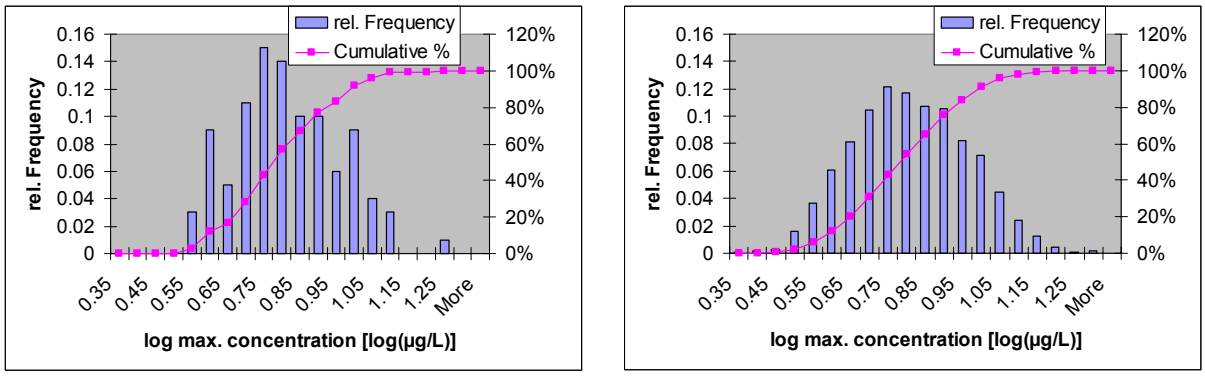

Figure 3: Histogram of output parameters in log scale for 100 respectively 2000 simulation runs.

Exposure and risk analysis often examine the probability of the 95th percentile (James and Oldenburg 1997). If the 95th percentile is the desired quantity a reasonable number of Monte Carlo runs is obtained when the addition of more runs does not change the value which belongs to the 95th percentile. Figure 4 shows the development of some statistical quantities versus number of Monte Carlo simulation runs. Assuming that the 95th percentile is the desired quantity at least 100 runs are needed.

The value belonging to the 95th percentile is 11 µg/L. This value slightly exceeds the limiting value. The percentile belonging to 10 µg/L is the 90th. This means that with a probability of 90% the maximum concentration at the point of compliance falls below the limiting value.

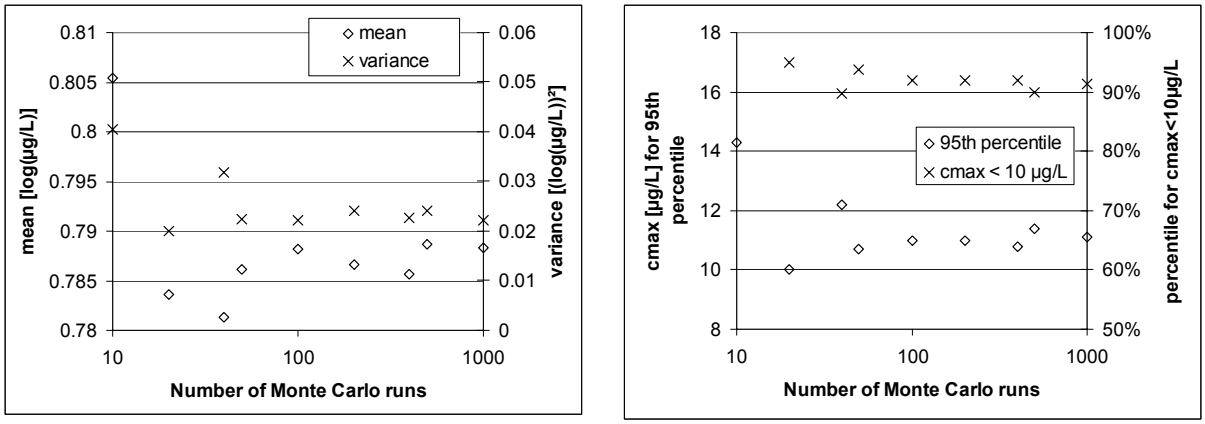

Figure 4: Development of the statistical characteristics of the output for different numbers of Monte Carlo simulation runs.

4. Conclusions

As many other researchers stated before, it appears desirable that a probabilistic framework accounting for uncertainty should be integrated into the groundwater risk assessment procedure. Using only minimum and maximum values for the evaluation of contaminations will, in many cases not lead to an answer, because many parameters are uncertain or even unknown in early stages of site investigations. The next step should be a global sensitivity analysis which would show the influence of the different input parameters on the variance of the output. The parameter with the greatest influence on the output should be the one to examine in more detail.

Acknowledgements

The research presented in this paper is supported by the German Federal Ministry for Education, Science, Research, and Technology (BMBF) under grant number 02WP0220.

References

BBodSchV (Bundesbodenschutz- und Altlastenverordnung vom 16. Juli 1999), 1999. Bundesgesetzblatt Jahrgang 1999 I. (36), 1554-1682.

Fuller, E.N., Schettler, P.D., and Giddings, J.C., 1966. A new method for prediction of binary gas-phase diffusion coefficient. Ind. Eng. Chem., 58: 19-27.

Helton, J.C. and Davis, F.J., 2000. Sampling-Based Methods. In: Saltelli, A., Chan, K., and Scott, E.M. (Editors) Sensitivity Analysis. Wiley Series in Probability and Statistics. John Wiley & Sons Ltd. Chichester, UK, p. 101- 153.

Howard, P.H., Boethling, R.S., Jarvis, W.F. and Michalenko, E.M., 1991. Handbook of environmental degradation rates. Lewis Publishers, Inc., Chelsea, 725 pp.

James, A.L. and Oldenburg, C.M., 1997. Linear and Monte Carlo uncertainty analysis for subsurface contaminant transport simulation. Water Resources Research, 33(11): 2495-2508.

McKay, M.D., Conover, W.J., and Beckmann, R.J., 1979. A comparison of three methods for selecting values of input variables in the analysis of output from a computer code. Technometrics, 21: 239-245.

Montgomery, J.H., 1996. Groundwater Chemicals Desk Reference. Lewis Publishers, Boca Raton, 1345 pp.

SimLab, 2000. Software for Uncertainty and Sensitivity Analysis, Version 1.1 Developed by the Joint Research Centre, Ispra

Simunek, J., Sejna, M. and van Genuchten, M.T., 1998. The HYDRUS-1D Software Package for Simulating the One-Dimensional Movement of Water, Heat, and Multiple Solutes in Variably-Saturated Media Version 2.0, U.S. Salinity Laboratory Agricultural Research Service U.S. Department of Agriculture, Riverside, California.

Spitz, K. and Moreno, J., 1996. A practical guide to groundwater and solute transport modeling. John Wiley & Sons, Inc., New York, 461 pp.

Tarantola, S., Giglioli, N., Jesinghaus, J. and Saltelli, A., 2002. Can global sensitivity analysis steer the implementation of models for environmental assessment and decision-making? Stochastic Environmental Research and Risk Assessment, 16: 63-76.

Wiedemeier, T.H., Rifai, H.S., Newell, C.J. and Wilson, J.T., 1999. Natural Attenuation of Fuels and Chlorinated Solvents in the Subsurface. John Wiley & Sons, Inc., New York, 617 pp.

KEY NOTE: Biodegradation of fuel vapours in the vadose zone at Airbase Værløse, Denmark

Peter Kjeldsen[1*], Mette Christophersen[1], Mette Broholm[1], Patrick Höhener[2], Ramon Aravena[3], and Daniel Hunkeler[4]

[1]*Environment & Resources DTU, Technical University of Denmark*
** Corresponding author: Bygningstorvet, DTU – Building 115, DK-2800 Kgs. Lyngby, Phone: (+45) 45251561, Fax: (+45) 45932850, E-Mail: pk@er.dtu.dk*
[2]*Swiss Federal Institute of Technology, ENAC-ISTE-LPE, Switzerland*
[3]*Department of Earth Sciences, University of Waterloo, Canada*
[4]*Centre for Hydrogeology, University of Neuchâtel, Switzerland*

Abstract: A jet fuel source zone has been installed in the vadose zone at Airbase Værløse by burying 12 L of artificial kerosene. This field experiment was conducted to investigate the natural attenuation of volatile organic compounds (VOCs) in order to obtain a better evaluation of the risk for groundwater contamination. The migration of the hydrocarbon vapors has been monitored with high spatial resolution within 20 m distance of the source zone during 12 months. Also monitored were the hydrocarbon concentrations in the pore water and in the groundwater. The field data and calculations of mass in the pore air indicated a large loss within a short period of time. Laboratory experiments and isotopic analysis proved that biodegradation was occurring. The results indicated that for most compounds degradation was significantly reducing the concentrations. Natural attenuation as a remediation technology appears promising.

1. Introduction

Pollution of groundwater as a result of contaminated soils is the major concern in risk assessment at contaminated sites throughout Europe. At many sites fuel has been spilled in the vadose zone. The volatile compounds of the fuel are released from the spill by vaporization and spread by gas migration in the unsaturated zone. The volatile contaminants cause contamination of the subsurface environment including the groundwater both in lateral and vertical directions.

Field experiments have been conducted to provide detailed analysis of the transport behavior of solvent vapors (TCE) within the unsaturated zone and found that temperature, organic matter content and soil moisture content were the important parameters controlling contaminant migration (Conant et al., 1996). Lahvis et al. (1999) investigated aerobic biodegradation and volatilization rates at a gasoline spill site in five vapor wells in the vadose zone and found the highest degradation rates in the capillary fringe. Hers et al. (2000) investigated biodegradation of BTEX vapors in soil above a hydrocarbon pollution in the groundwater and observed significant vadose zone biodegradation over a relatively small depth interval. Several researchers have conducted laboratory experiments to prove that biodegradation of hydrocarbons is occurring in the unsaturated zone (Ostendorf et al., 1996, Franzmann et al., 1999, Höhener et al., 2003).

Processes contributing to natural attenuation include volatilization, sorption and biodegradation. The ultimate goal for remediation is the complete conversion of contaminants to end-products as carbon dioxide and water. However in the field it can be difficult to distinguish between the different processes. Isotopic analysis can be a way to elucidate biodegradation. The bacteria prefer to consume the lighter isotopes leaving the residual

contaminants enriched in the heavier isotopes. Furthermore, CO_2 with a characteristic isotopic signature is produced. Measurements of isotope ratios of individual contaminants has recently been used to demonstrate biodegradation of fuel compounds in the saturated zone of aquifers (Stehmeier et al., 1999, Mancini et al., 2002).

The field experiment conducted at Airbase Værløse was designed especially to investigate and prove the natural attenuation potential in the vadose zone in order to obtain better evaluations of the risk for groundwater contamination from vadose zone fuel contamination. Different techniques to measure biodegradation in the field and the laboratory were compared.

2. Materials and methods

The field experiment was conducted at Airbase Værløse. The geology was investigated prior to the experiment by use of geophysical measurements and boreholes. These investigations showed that the site has a relatively thin vadose zone (3-4 meters). Sandy dark brown topsoil of app. 50 cm thickness was overlying a layer of 2 - 3.3 m of homogeneous glacial melt water sand, followed by a thin layer of moraine sand/gravel (0.5 – 1 m). The moraine sand/gravel was underlain by moraine clay (up to 50 m). The secondary groundwater aquifer had a thickness of 0.5-1 m. The organic carbon content in the upper 50 cm was 0.1-1.5% and 0.03% in the melt water sand.

The field experiment was conducted from July 2001 to July 2002. A circular source consisting of sand from the site mixed with the NAPL was placed 0.8-1.3 m below surface. The NAPL was an artificial hydrocarbon mixture consisting of volatile and semi-volatile compounds (BTX, n-, iso and cyclo-alkanes) similar to jet-fuel – see Table 1. Evolution of the composition of the source is described in another paper (Broholm et al. 2003). The halocarbon 1,1,2-trichloro-1,2,2-trifluoroethane (CFC113) was used as a conservative tracer.

The oil phase was mixed with sand from the site in a concrete mixer in five shifts and packed in a hole with a diameter of 0.70 m to form a source of hydrocarbons. The source was covered with a lid to prevent rainwater from infiltrating the source.

Table 1. Composition of the oil phase after installation, and 1st order degradation rates measured on day 12 in the laboratory column experiment at 26°C.

Compound	Amount (wt%)	1st order rate (day^{-1})	Compound	Amount (wt%)	1st order rate (day^{-1})
Benzene	1.02	0.25	Dodecane	9.50	n.m.
Toluene	2.93	0.8	3-Methylpentane	7.45	0.07
m-Xylene	4.57	1.95	Isooctane	15.36	0.2
1,2,4 Trimethylbenzene	10.99	3.7	Cyclopentane	1.59	0.05
Hexane	7.26	0.12	Methylcyclopentane	5.79	0.15
Octane	7.16	1.2	Methylcyclohexane	10.23	0.35
Decane	15.99	5.2	CFC113	0.16	<0.02

The monitoring network, which was developed based on modeling of the site and the source, consisted of 107 soil gas probes made of stainless steel, 7 multi-level water samplers each with 9 levels, and 6 porous cups for sampling water from the unsaturated zone. The installations was mainly placed in one radial transect with control points in other directions.

In the main radial the hydrocarbons in the pore gas was monitored to a distance of 20 m from the center of the source. The sampling is further described in Christophersen et al. (2002).

The experiment included one year monitoring of hydrocarbons and tracer (CFC113) migration from the fuel source in the unsaturated zone in soil gas, pore water, and capillary groundwater and of soil gasses sensitive to hydrocarbon degradation (oxygen, carbon dioxide, methane). Other parameters, which were measured, are among others: soil moisture content, soil temperature, meteorological parameters, and the direction of the secondary groundwater flow.

Selected sampling points were used for an isotope study. They included two vertical profiles at different distances from the source and a horizontal profile at the depth of the source with sampling points out to 5 m from the source. The carbon isotopic composition of nine of the source compounds was determined over a time period of 295 days using a method similar as described in Hunkeler & Aravena (2000). In addition, the carbon isotopic composition of CO_2 and the oxygen isotopic composition of O_2 were measured. (Hunkeler et al., 2003).

Sand from the field site was used for column experiments in the laboratory. A one-dimensional column experiment was carried out during 44 days at room temperature. The laboratory column was homogeneously packed with moist sand. The sand and its indigenous microflora were left undisturbed during 20 days to acclimatize after packing. At day 0 the column was connected to a reservoir containing fuel mixture. The column was equipped with 15 sampling points positioned every 5 or 10 cm. (Höhener et al., 2003).

3. Results and discussion

3.1 Field experiment

Figure 2 shows the migration of one of the compounds in the source: methylcyclohexane (MCH) at selected sampling dates during the experiment.

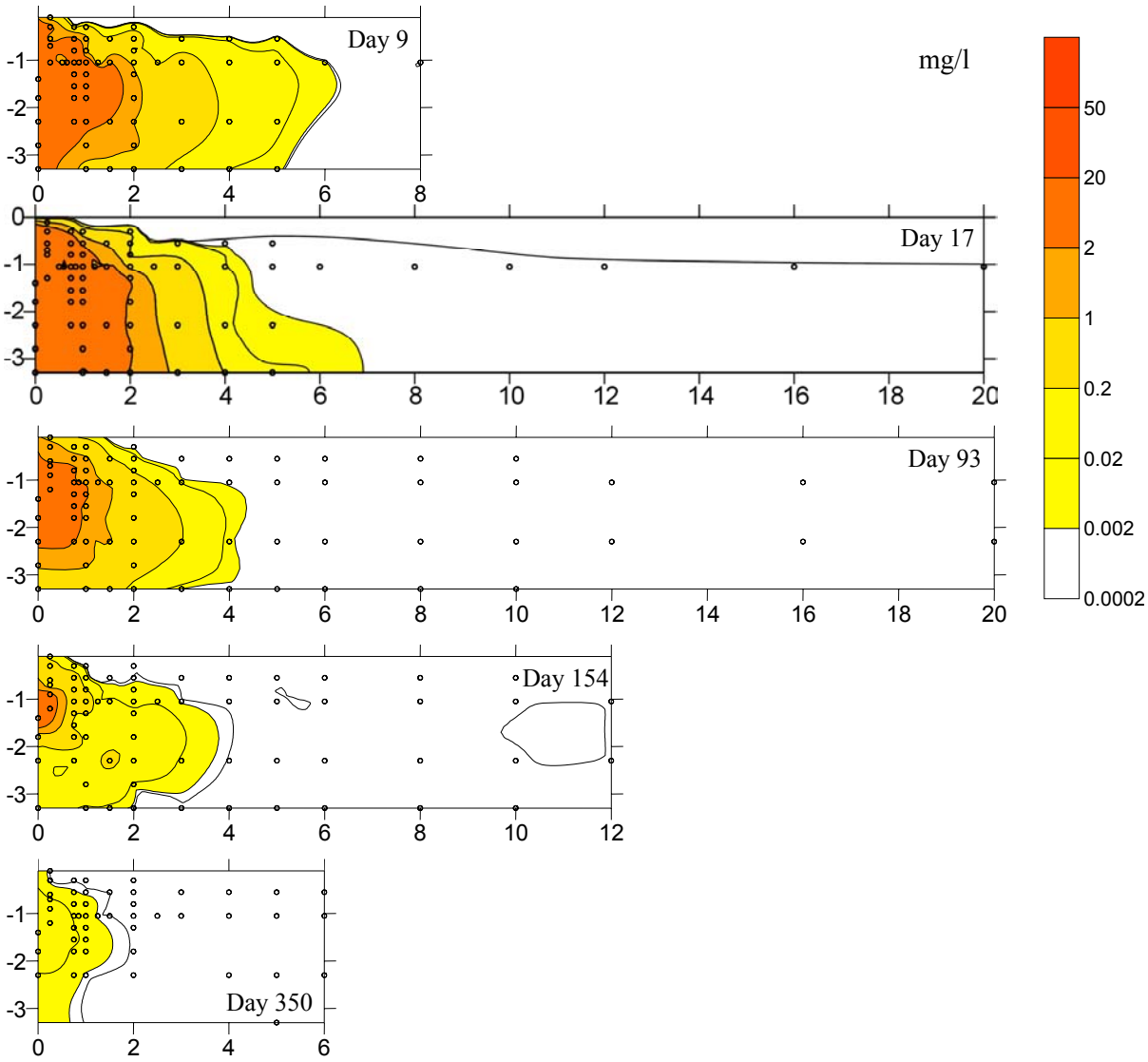

Figure 1. Cross-section of the main monitoring. Radial concentrations of methylcyclohexane in mg/l on day 9, 17, 93, 154 and 350 respectively. Dots represent points, which have been sampled.

From figure 1 it can be seen that MCH migrated fast and was monitored 6 m from the source on day 9. The maximal spreading of MCH occurred at day 17, where MCH was monitored in low concentrations out to 20 m from the source. Soon after the MCH plume stabilized at around 4 m from the center of the source. The concentration in the source was stable and high until around day 154. Hereafter the concentration in the center decreased and so did the MCH plume. However at the end of the experiment there were still considerable amounts of MCH left in the pore air. Similar behavior was observed for other compounds.

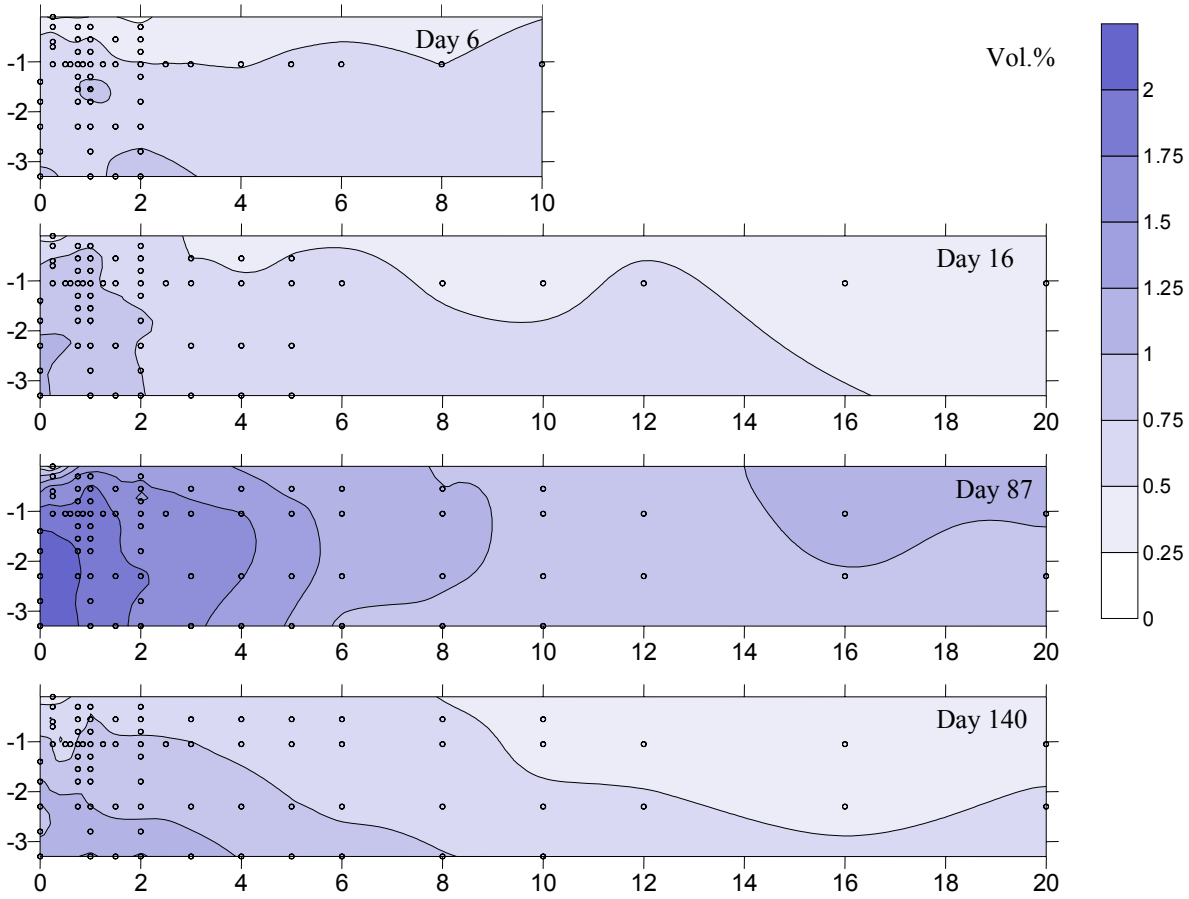

Figure 2. Carbon dioxide concentrations in vol% at selected sampling dates. Dots represent points, which have been sampled.

At day 6 the contour plot of the carbon dioxide concentrations looked similar to the background concentrations. However, from day 16 and forward carbon dioxide production and oxygen consumption (data not shown) was clearly observed out to 4-6 m from the source and especially beneath the source. Figure 2 shows examples of the CO_2 concentrations. The carbon dioxide production and oxygen consumption was however quite small and there has never been more than 2.5 % carbon dioxide and less than 17 % oxygen in the pore air at all depths at all times.

The stabilization of the MCH (and some of the other compounds) plume at a distance closer to the source than the maximal migration distance combined with the stable high concentrations in the center of the source and carbon dioxide production indicate that biodegradation was occurring. Degradation started soon after installation of the source.

The total mass of the 14 compounds in the pore air was calculated by dividing the field site into pieces of cylinders each with a representative sampling point. The volumes of the cylinders were then multiplied with the measured concentrations and summed up. The results for the less volatile compounds are shown in Figure 3. The mass of the different compounds in the pore air was increasing fast and then decreasing at rates depending on the properties of the compounds and availability for biodegradation. It is evident that the heavier compounds (m-xylene, trimethylbenzene, decane and dodecane) had maximum of mass in the pore air much later than the most volatile. The increase in mass for the heavier compounds continued until around day 100. At day 250, where almost all of the volatile compounds had

disappeared, the mass of the heavier compounds increased again. The increase could also be partly caused by the increase in temperature.

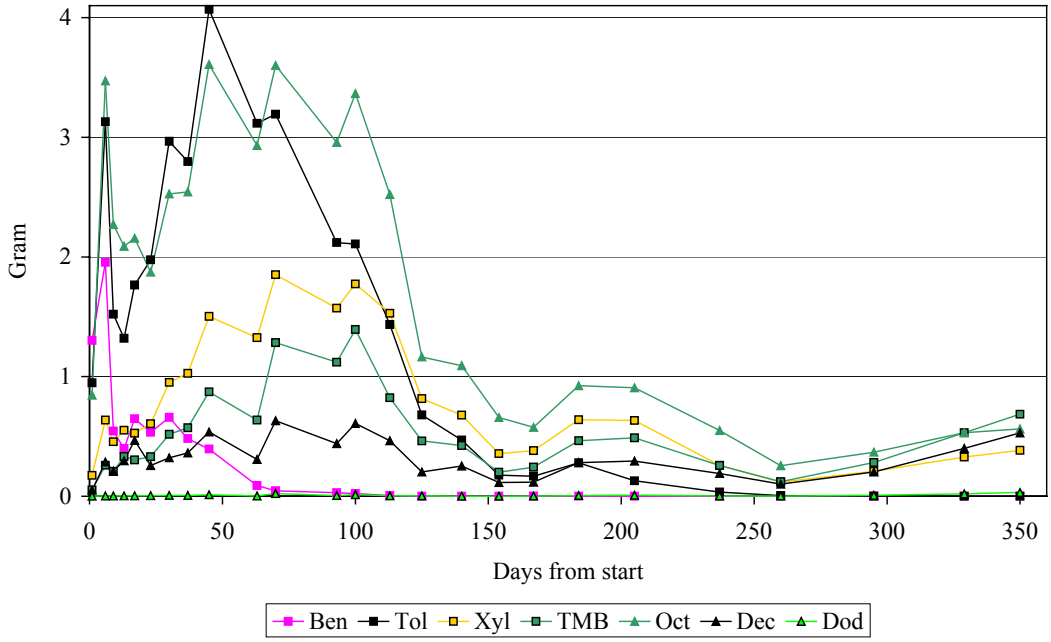

Figure 3. The total calculated mass in the pore air of the source compounds with the lowest concentrations as a function of time. Calculated based on the measurements.

At day 1 the total sum of mass in the pore air was 109 g. The mass increased to almost 450 g at day 17 and then decreased to 2 g at day 350. The initial amount of source was 7500 g and the analysis showed that the heavier compounds were still present in the source at the end of the experiment (1000 g). This showed that a considerable amount of the initial source has disappeared within the one-year experiment. Seven of the most volatile compounds were neither found in the pore air nor in the source at the end of the experiment. The soil had relatively low organic matter content so sorption is not significant. Some of the compounds were found in the upper secondary groundwater but only for a short period and some of the compounds were also found in the pore water. However, the total amount of compounds in the water phase was limited. The rest of the mass must have disappeared either by emission to the atmosphere or by biodegradation. However it can be difficult to distinguish between these two processes.

3.2 Laboratory column experiment

The temporal evolution of VOC concentration profiles along the length axis in the laboratory column experiment was monitored for 44 days. Concentration versus distance profiles for two selected VOC's are shown on day 12 at Figure 4. This day was chosen because CO_2 and O_2 profiles suggested that biodegradation rates were maximal around that day, and because VOC migration data suggested that steady state profiles were achieved. For all the VOC, except CFC-113, curved profiles were observed and these were reasonable well represented by a first-order biodegradation model (Höhener et al. 2003). The first-order degradation rates obtained by fitting the data are shown in Table 1. It was not possible to get reliable results for dodecane due to the low vapor pressure.

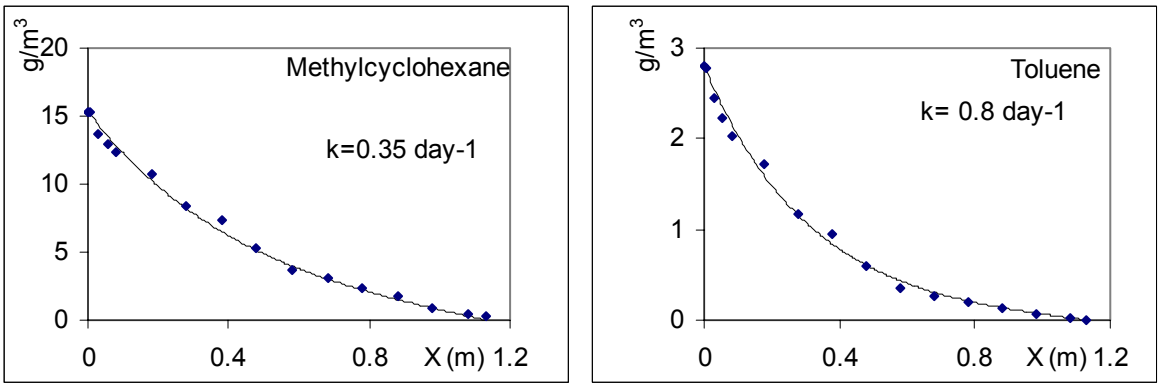

Figure 4. Vapor concentration profiles (symbols) measured on day 12. Solid lines represent best fit of the first-order decay model described elsewhere (Höhener et al., 2003), where k is apparent first-order rate applied to gaseous phase.

3.3 Isotopic analysis

Pore air samples were taken out during the field experiment and sent for isotopic analysis. In general, similar spatial and temporal trends of the $\delta^{13}C$ values were observed for the different compounds, although the magnitude of variations was different depending on the compounds. At day 3, $\delta^{13}C$ values of most of the compounds were more negative with increasing distance from the source as can be seen for methylcyclopentane in Figure 5. Then the $\delta^{13}C$ values leveled off again and started to become enriched in ^{13}C, first at locations further away from the source and later on also at locations closer to the source (Figure 5). The trend towards enriched $\delta^{13}C$ values was observed for all compounds except 1,2,4-TMB. The largest ^{13}C changes could be observed for 3 -methylpentane (-30 to -19 ‰), hexane (-31 to -21‰) and methylcyclopentane (-35 to -27‰). Methylcyclohexane, toluene and iso-octane showed an enrichment of ^{13}C of about 3-4 ‰ within 26 weeks, m-xylene of about 2 ‰.

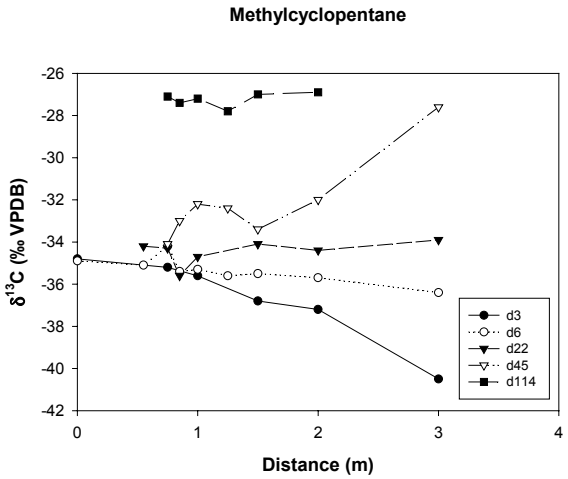

Figure 5. Carbon isotope ratio $\delta^{13}C$ of Methylcyclopentane along a horizontal profile at the depth of the source for different times given in days after emplacement of the source.

The processes that have likely the largest effect on isotope ratios are diffusion and biodegradation. Regarding diffusion, molecules with lighter isotopes generally diffuse slightly faster than molecules with heavier isotopes. Regarding biodegradation, several studies under saturated conditions have shown that biodegradation of monoaromatic compounds under aerobic conditions leads to significant carbon isotope fractionation with isotopic enrichment factors in the range of –1 to –4 ‰. At the field site the observed variations in isotope ratios are likely the result of combination of diffusion and biodegradation. The initial decrease in $\delta^{13}C$ with increasing distance from the source could be due to the faster diffusion of molecules with light isotopes compared to those with heavy isotopes away from the source after its emplacement. The subsequent shift of isotope ratios to more positive $\delta^{13}C$ compared to the initial value is likely due to biodegradation of the compound. This conclusion is consistent with the $\delta^{13}C$ values of CO_2, which shifted from –22 ‰ to more negative $\delta^{13}C$ values confirming biodegradation of the fuel compounds.

4. Conclusions

The field data and the isotopic date indicated that degradation started soon after installation of the source. Laboratory experiments confirmed that the compounds can be degraded in the Værløse soil.

The calculation of the total mass in the pore air at the field site showed that the maximum mass in the pore air was measured at day 17 and that only a small amount of mass was left in the pore air after one year.

In general the results indicated that for most of the compounds degradation significantly decreased the concentrations. Therefore natural attenuation as a remediation technology looks promising for this type of contaminations.

5. References

Broholm, M., Christophersen, M. & Kjeldsen, P. 2003. Evolution of the composition of the emplaced source in the field experiment at Airbase Værløse, Denmark. Proceedings of the 2nd International Workshop on Groundwater Risk Assesment at Contaminated Sites and Integrated Soil and Water Protection, 20-21 March 2003, Tübingen, Germany.

Christophersen,M., Broholm,M.M. & Kjeldsen,P. 2002. Migration and degradation of fuel vapours in the vadose zone. Field experiment at airbase Værløse. In: Vintermøde om jord- og grundvandsforurening, Vingstedcentret 5-6 marts, pp. 147-155. ATV-fonden for Jord og Grundvand, Kgs. Lyngby, Denmark.

Conant, B.H., Gillham, R.W. and Mendoza, C.A., 1996. Vapor transport of trichloroethylene in the unsaturated zone: Field and numerical modeling investigations. *Water Resources Research* 32 (1), 9-22

Franzmann, P.D., Zappia, L.R., Power, T.R., Davis, G.D. and Patterson, B.M., 1999. Microbial mineralisation of benzene and characterisation of microbial biomass in soil above hydrocarbon-contaminated groundwater. *Fems Microbiology Ecology* 30 (1):67-76.

Hers, I., Atwater, J., Li, L. and Zapf-Gilje, R., 2000. Evaluation of vadose zone biodegradation of BTX vapours. *Journal Of Contaminant Hydrology* 46 (3-4):233-264.

Hunkeler and Aravena, 2000. Determination of compound-specific carbon isotope ratios of chlorinated methanes, ethanes and ethenes in aqueous samples. Environmental Science and Technology, 34 (13), 2839-2844.

Hunkeler, D., Aravena, R., Diao, X., Christophersen, M., Broholm, M., Kjeldsen, P., 2003. Application of isotopes analysis to evaluate biodegradation of hydrocarbons in the vadose zone. Extended abstract for ConSoil 2003, 12-16 May 2003, ICC Gent, Belgium

Höhener, P., Duwig, C., Pasteris, G., Kaufmann, K., Dakhel, N., and Harms, H., 2003. Biodegradation of petroleum hydrocarbon vapors: laboratory studies on rates and kinetics in unsaturated alluvial sand. Accepted for publication in *Journal of Contaminant Hydrology*

Lahvis, M.A., Baehr, A.L. and Baker, R.J., 1999. Quantification of aerobic biodegradation and volatilization rates of gasoline hydrocarbons near the water table under natural attenuation conditions. *Water Resources Research* 35 (3), 753-765.

Mancini, S.A., Lacrampe-Couloume, G., Jonker, H., van Breukelen, B.M., Groen, J., Volkering, F. and Sherwood Lollar, B., 2002. Hydrogen Isotopic Enrichment: An Indicator of Biodegradation at a Petroleum Hydrocarbon Contaminated Field Site. *Environmental Science and Technology* 36 (11), 2464-2470.

Ostendorf, D.W., Long, S.C., Schoenberg II, T.H. and Pollock, S.J., 1996. Aerobic Biodegradation of Petroleum-Contaminated Soil: Simulations from Soil Microcosms. *Transportation Research Record* (1546):121-130.

Pasteris, G., Werner, D., Kaufmann, K. and Hohener, P. 2002. Vapor phase transport and biodegradation of volatile fuel compounds in the unsaturated zone: A large scale lysimeter experiment. *Environmental Science & Technology* 36 (1):30-39.

Stehmeier, L.G., Francis, M.M., Jack, T.R., Diegor, E., Winsor, L. and Abrajano, T.A., 1999. Field and in vitro evidence for in-situ bioremediation using compound-specific C-13/C-12 ratio monitoring. *Organic Geochemistry* 30 (8A):821-833.

Compositional evolution of the emplaced source in the field experiment at Airbase Værløse, Denmark

Mette M. Broholm, Mette Christophersen, & Peter Kjeldsen,

Environment & Resources DTU, Technical University of Denmark,Bygningstorvet B115, DK-2800 Kgs. Lyngby, Denmark. Phone +45 45251475, Fax +45 45932850, E-Mail mmb@er.dtu.dk.

Abstract: A field experiment with an emplaced fuel-NAPL source in the vadose zone was conducted. A large part of the source evaporated in the first month of the experiment after which source depletion slowed down. The evolution in the source composition corresponded well with expectations based on Raoults Law. Comparison of hydrocarbon concentration in pore-air within the source with estimates from the source NAPL composition based on Raoults Law indicated activity coefficients different from 1. The spatial distribution of the NAPL composition was very uniform, except for the compound being depleted, for which lower mole fractions were observed at the top and the perimeter of the source. Preliminary evaluation suggests that the more soluble aromatic hydrocarbons were depleted slightly faster than aliphatic hydrocarbons of similar volatility.

1. Introduction

Fuel (jet-fuel, gasoline, diesel, etc.) spills resulting in a water immiscible liquid phase of fuel (also known as a Non-Aqueous Phase Liquid or NAPL) in the unsaturated zone commonly occur. Fuel is a NAPL consisting of a large number of compounds, dominated by aliphatic and aromatic hydrocarbons. The NAPL constitutes a source for contamination of pore-air and groundwater, as the volatile and soluble compounds in the NAPL are released by evaporation and dissolution, respectively. The evaporation of the volatile compounds in the NAPL results in changing composition of the NAPL, which in turn leads to changing concentrations of the compounds in the pore-air. The concentration of the individual compounds in air (C_i) in equilibrium with the NAPL is frequently estimated by use of Raoults Law:

$$C_i = \gamma \cdot x_i \cdot C_{i,sat}$$

Where γ is the activity coefficient, x_i is the mole fraction of compound i in the NAPL, and $C_{i,sat}$ is the saturation concentration for compound i in air. For NAPLs with simple compound mixtures it has been shown that Raoults Law with $\gamma=1$ applies.

A field experiment with an emplaced fuel-NAPL source in the vadose zone was conducted at Airbase Værløse, Denmark.

The scope of the part of the field experiment presented here is to: investigate the evolution of the composition of the emplaced source and resulting compound concentrations in the pore-air, investigate the spatial distribution of NAPL in the source, evaluate the applicability of Raoults law, and - if possible - evaluate whether the effect of hydrocarbon degradation in the vadose zone pore-water (or –air) is reflected in the source composition.

Other aspects of the field experiment are discussed in Christophersen et al. (2003, this workshop proceeding).

2. Experimental

The field experiment was conducted from July 2001 to July 2002. The field site at Airbase Værløse has a relative thin vadose zone (3-4 meters) consisting of melt water sand with 50 cm sandy mould topsoil. An artificial hydrocarbon mixture consisting of volatile and semi-volatile compounds similar to jet-fuel (see Table 1) was mixed with sand and emplaced in the vadose zone to form a source of hydrocarbons (0.8 to 1.3 m bgs.). Since loss of very volatile compounds during installation can not be avoided, greater volumes of the most volatile compounds than aimed for in source was added. Freon 113 was added as non-degradable tracer, and Sudan IV, a hydrophobic dye, was added to make the NAPL phase visually observable during mixing, installation and subsequent excavation. A large circular tub was placed on pillars over the source area to prevent rainwater infiltration directly above the source and hence, to prevent depletion of the most water-soluble compounds in percolating water. Sodium bromide mixed with sand was placed immediately below the emplaced NAPL-source to reveal any percolation of the source to the groundwater.

Pore-air hydrocarbon concentrations were monitored in 3 points within the source. Probe installation, pore-air hydrocarbon sampling and analysis were described by Christophersen et al. (2002). The source material was sampled during and immediately after installation, 4 times during the field experiment, and in connection with removal of the remaining source by excavation at the end of the experiment. During the experiment the source material was sampled from soil-cores abstracted from the source. The hole was then filled with a bentonite cement mixture. The source material was immediately transferred to vials with pentane for extraction. The extracts were analyzed for the hydrocarbons by gas chromatography with flame ionization detection (GC-FID). Freon, cyclopentane and 3-methylpentane were not included in the analysis, as they elute concomitantly with the pentane extract.

3. Results and discussion

The installation of the source was completed successfully in 25 minutes. Initial NAPL and resulting source-NAPL composition is given in Table 1.

Table 1: NAPL composition prior to (A) and immediately after installation (B)

Compound	A Volume (L)	A Mole %	B Volume (L)	B Mole %
Benzene	0.140	1.65	0.090	1.45
Toluene	0.310	3.06	0.253	3.49
m-Xylene	0.465	3.97	0.399	4.80
1,2,4-Trimethylbenzene	1.020	7.79	0.939	10.11
Hexane	1.440	11.56	0.870	9.95
Octane	0.935	6.03	0.784	7.20
Decane	1.750	9.41	1.638	12.48
Dodecane	1.000	4.61	1.000	6.48
3-Methylpentane[1]	1.600	12.93	0.757	7.91
Iso-octane	2.250	14.28	1.702	14.98
Cyclopentane[1]	0.385	4.29	0.128	1.80
Methyl-cyclopentane	1.015	9.46	0.597	7.66
Methyl-cyclohexane	1.315	10.80	1.009	11.61
Freon 113 (tracer)[1]	0.019	0.17	0.006	0.07
Total	13.644	100.00	10.172	100.00

[1]: Compounds not included in analysis, B-values are estimated from expected loss during installation based on compound vapor pressures and actual loss of compounds included in analysis during installation.

The loss of volatiles was close to the loss expected (slightly lower – 10 L total NAPL was aimed for), resulting in near the composition aimed for.

A large part of the NAPL evaporated during the first month of the experiment and the rate of depletion of the source then gradually decreased (total volume in liters, day after start in brackets): 10.2(0), 2.8(23), 2.2(113), 1.5(225), 1.3(352).

The evolution of the source composition is illustrated in Figure 1. The compounds are listed (top to bottom) in order of increasing vapor pressure. As expected, greater loss of the most volatile compounds was observed.

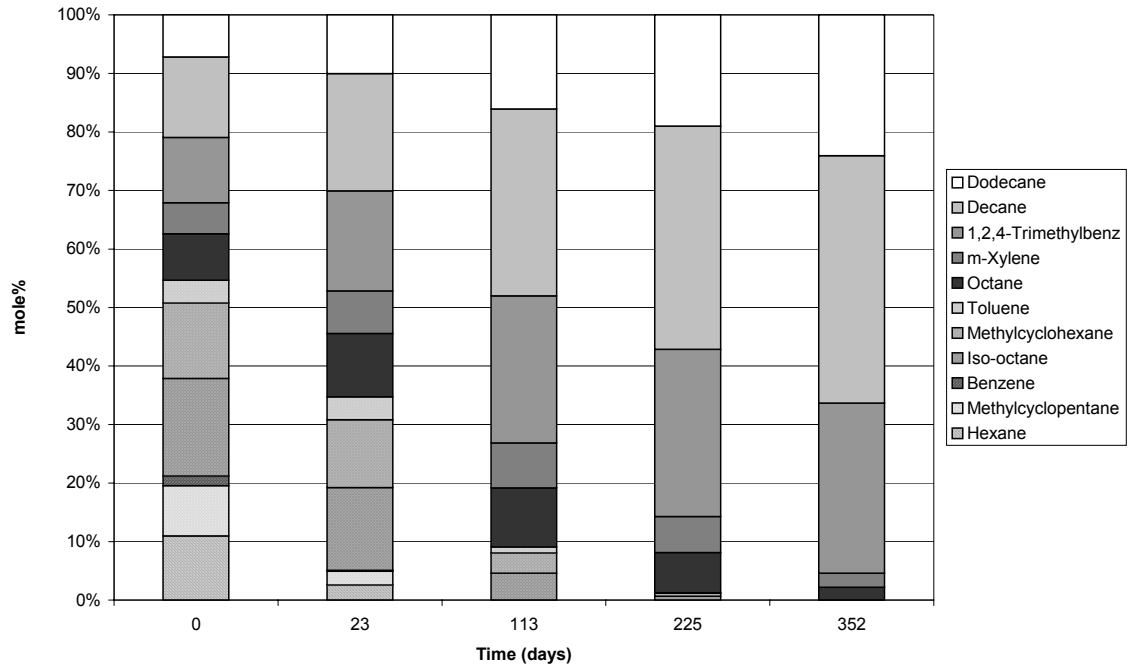

Figure 1: Evolution in source composition.

The results appear to be in correspondence with the expected behavior based on Raoults law.

The compound concentrations in air in equilibrium with the NAPL was calculated from the source composition at the days sampled by use of Raoults Law under the assumption of $\gamma = 1$. The source composition (mole-fractions) used are the averages based on 10 samples from different depths within the source, standard deviations reflect the standard deviations on these averages.

The calculated concentrations are compared to measured pore-air concentrations in the source for 3 selected compounds in Figure 2a-c. The samples of hydrocarbons in pore-air collected within the source on day 0 to 9 were biased typically by overloading of the sorption tubes and therefore, measured concentrations are too low, particularly for the most volatile compounds. There is some scatter in the measured pore-air hydrocarbon concentrations. Therefore, evaluations are based on the trend of a series of data points.

The most volatile compounds are exemplified by methylcyclopentane in 2a. For these compounds the measured concentrations are typically higher than the calculated concentrations, implying that γ may be >1.

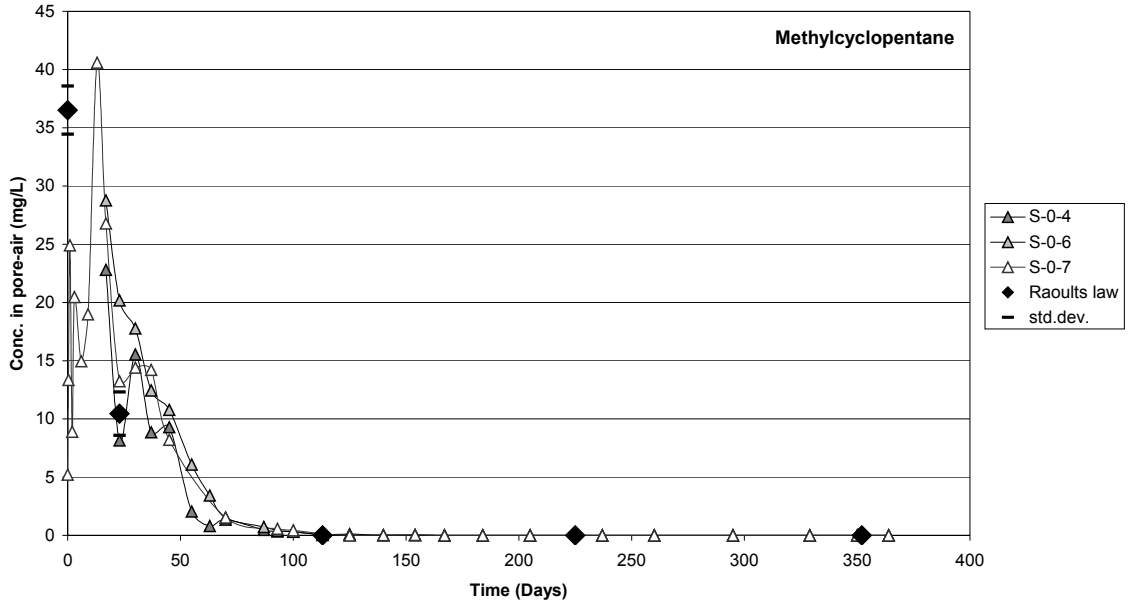

Figure 2a: Methylcyclopentane concentrations calculated from source composition by use of Raoults Law assuming γ = 1 compared with measured concentrations in pore-air in 3 sampling points within the source.

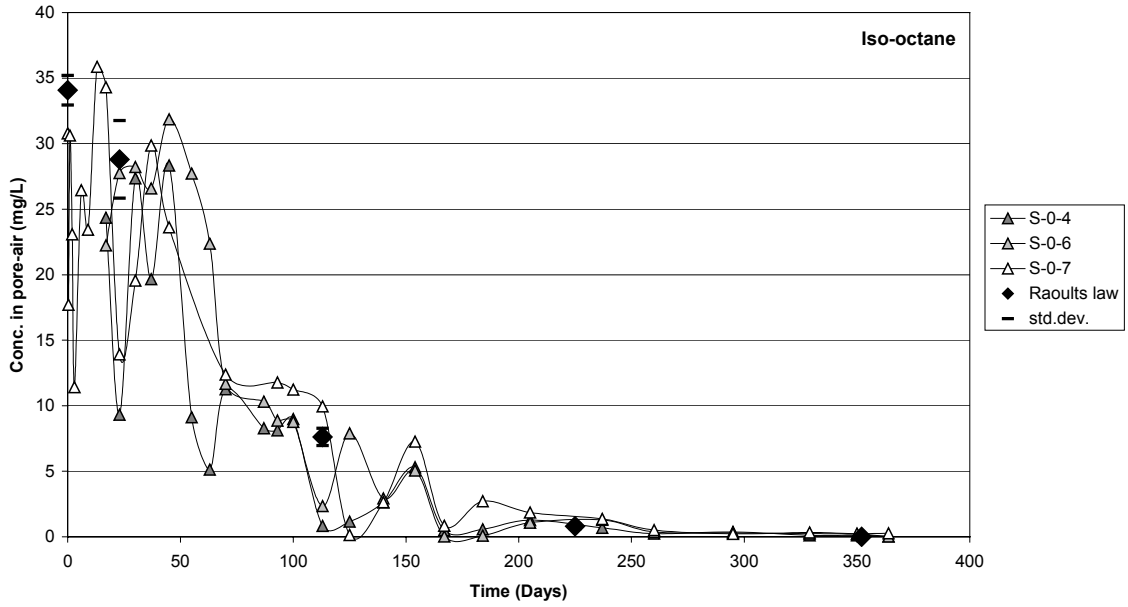

Figure 2b: Iso-octane concentrations calculated from source composition by use of Raoults Law assuming γ = 1 compared with measured concentrations in pore-air in 3 sampling points within the source.

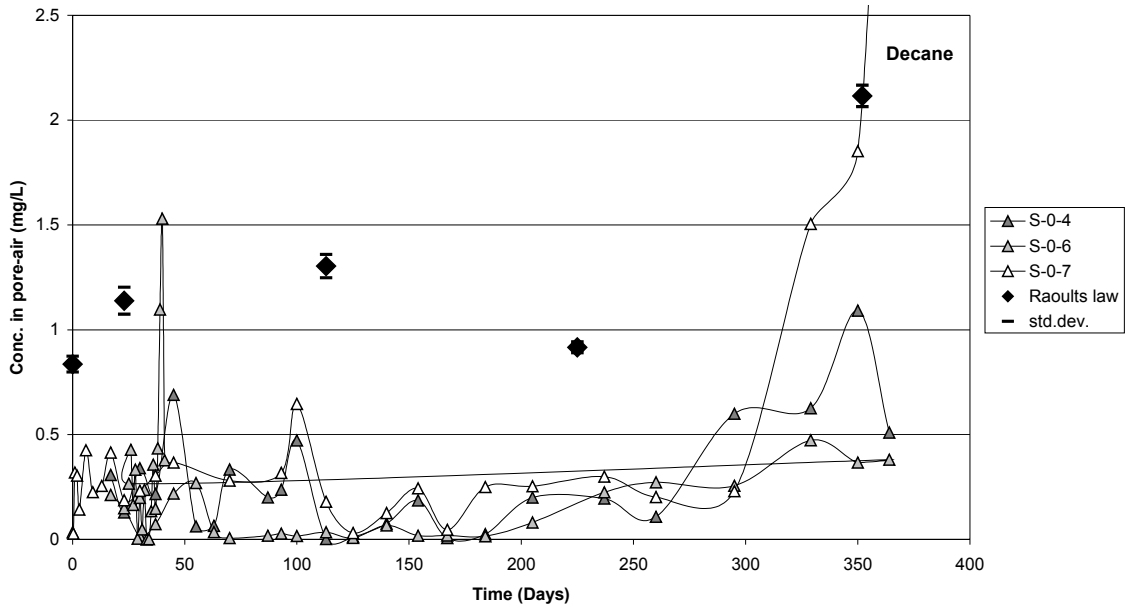

Figure 2c: Decane concentrations calculated from source composition by use of Raoults Law assuming γ = 1 compared with measured concentrations in pore-air in 3 sampling points within the source.

The compounds of intermediate volatility are exemplified by iso-octane in 2b. For these compounds initial concentrations correspond relatively well for γ = 1. However, as the initially most volatile compounds are depleted and these compounds become the most volatile of the remaining compounds, the measured concentrations become greater than calculated concentrations, suggesting increasing γ.

The least volatile compounds are exemplified by decane in 2c. The low calculated value for day 225 is an effect of low soil temperature (winter) on the vapor pressure, the mole fraction of decane in the source generally increases (see Figure 1). For these compounds the measured concentrations are typically lower than the calculated concentrations, suggesting that γ may be less than 1. However, as all other compounds are depleted, the measured concentrations appear to approach the calculated concentrations for γ = 1 for the now much simpler source composition. Unifac modeling of activity coefficients for the NAPL composition of the source is planned to evaluate the observations.

The distribution in NAPL composition with depth within the source was very uniform for most compounds. Except, as a compound was being depleted, its mole fraction would first decrease at the top of the source. Likewise, it is expected that it would first decrease at the perimeter of the source relative to the center. This was verified by the special distribution of xylene, trimethylbenzene and dodecane in the source-NAPL at the end of the experiment.

Excavation of the source revealed that some NAPL had migrated into the sand below the source around the pipe with the pore-air samplers and in one additional location to a depth of approximately 1.8 m bgs. No bromide was found in the groundwater, suggesting that rainwater did not percolate through the source.

Preliminary evaluation suggests that the aromatic hydrocarbons (particularly benzene and toluene) were depleted slightly faster than aliphatic hydrocarbons of similar boiling point. These aromatic compounds are much more soluble in water than the aliphatic compounds. Attempts (by modeling) will be made to evaluate if this may suggest an effect of degradation of the aromatic compounds, as degradation is predominantly expected to occur in pore-water.

4. Preliminary conclusions

The source installation was completed successfully with near expected loss of volatiles. Some migration of NAPL into the sand underlying the source occurred.

A large part of the source evaporated in the first month of the experiment after which source depletion slowed down.

The evolution in source composition appear to correspond well with expectations based on Raoults Law. Comparison of hydrocarbon concentration in pore-air within the source with estimates from the source NAPL composition based on Raoults Law indicate activity coefficients different from 1 for the compounds of the complex NAPL compositions.

The spatial distribution of NAPL composition was very uniform, except for the compound being depleted, for which lower mole fractions were observed at the top and the perimeter of the source.

5. References

Christophersen, M., Broholm, M.M., Kjeldsen, P., 2002. Migration and degradation of fuel vapours in the vadose zone. Field experiment at Værløse Airforce Base, Denmark. Proceedings of the 1st International Workshop on Groundwater Risk Assesment at Contaminated Sites, 2002, Tübingen, Germany.

Christophersen, M., Broholm, M.M.,Höhener, P., Aravena, R., Hunkeler, D., and Kjeldsen, P., 2003. Biodegradation of fuel vapours in the vadose zone at Airbase Værløse, Denmark. Proceedings of the 2nd International Workshop on Groundwater Risk Assesment at Contaminated Sites and Integrated Soil and Water Protection, 2003, Tübingen, Germany.

Modelling transport and natural attenuation of fuel compounds in the vadose zone at the emplaced fuel source experiment, Airbase Værløse, Denmark

Uli Maier[1], Uli Mayer[2] and Peter Grathwohl[1]

[1]*University of Tübingen, Department of Applied Geology, Sigwartstr. 10, D-72076 Tübingen*
[2] *Department of Earth and Ocean Sciences, University of British Columbia, 6339 Stores Road, Vancouver V6T 1Z4, Canada, Phone: +49-7071-2977452, Fax:+49-7071-5059, Email:uli.maier@uni-tuebingen.de*

Abstract:Numerical simulations were performed in order to assess the diffusive spreading of volatile fuel constituents and their biodegradation in the unsaturated zone for the Værløse field test site, Denmark. The measured field data of 14 NAPL compounds, oxygen and reaction products can be reproduced by the model MIN3P. Modelling results illustrate that the attenuation rates depend mainly on distribution parameters such as Henry's Law constant of the fuel constituents, on the biological degradation rate constant, on soil water content and temperature. The measured field data were reproduced well with the model. The emission into groundwater could be estimated after the processes in the unsaturated zone were quantified.

Introduction

Contaminated land in Europe poses a serious problem with respect to soil quality and the risk of spreading of pollutants into other compartments of the environment. The major concern at most contaminated sites is the risk of groundwater pollution by organic and inorganic compounds. Since the remediation of all of the contaminated sites in Europe is economically not feasible, groundwater risk assessment procedures are needed for the ranking of sites, decision making on further use and remedial actions. Of special interest is the inexpensive method of Monitored Natural Attenuation (Wiedemeyer, 1999).

At sites where petroleum products are handled or stored, contamination of the unsaturated soil zone is frequently found. Volatile organic compounds (VOC) can reach the groundwater by transport with percolating water and by spreading in the soil gas. Degradation processes can limit the spreading in the unsaturated soil zone and - in the best case - restrict the contamination to the unsaturated zone. At the Værløse Airforce Base, Denmark, a well controlled field experiment on the diffusive spreading of volatile fuel constituents and their biodegradation was conducted. Numerical simulations were performed in order to describe these processes for the field site. The objective of this study was to validate the model MIN3P with the field data to allow future predictions for groundwater risk assessment at a variety of other sites.

Conceptual Model

The numerical model MIN3P (Mayer, 1999) uses a finite volume algorithm and allows for the calculation of vapour phase transport and unsaturated flow in the vadose zone. Groundwater transport processes and mass transfer across the capillary fringe can be simulated as well and a variable number of geochemical reactions such as biodegradation processes can be handled (Mayer, 1999).

Site characterisation with respect to grain size distribution, geochemistry, permeability, etc. was implemented in the model as precisely as possible. The experimental setup and sampling

network was designed according to previous numerical simulations. The site has a vadose zone of 3.5 meters thickness, consisting of sandy and not too heterogeneous material. The source was emplaced in the subsurface at 1 m depth on July 2nd, 2001. It contained 10 kg (13.6 l, respectively) of a synthetic hydrocarbon mixture consisting of 13 volatile to semi-volatile kerosene compounds and one tracer (freon). The soil surface at the field site was not sealed but a 2 m^2 roof was placed directly above the source to prevent leaching. Monitoring of the contaminant spreading in soil air and groundwater samples in a one-year measurement campaign allowed a comparison to modelled data. After termination of the measurement campaign the source was excavated in August 2002. Even though it was calculated to be at residual saturation, it had migrated downward by about 50 cm. A vertical cross section of the model domain is given in Fig. 1. To reduce computational time, several sensitivity analyses were performed in 1D and 2D, whereas a 3D model was used to reproduce field data.

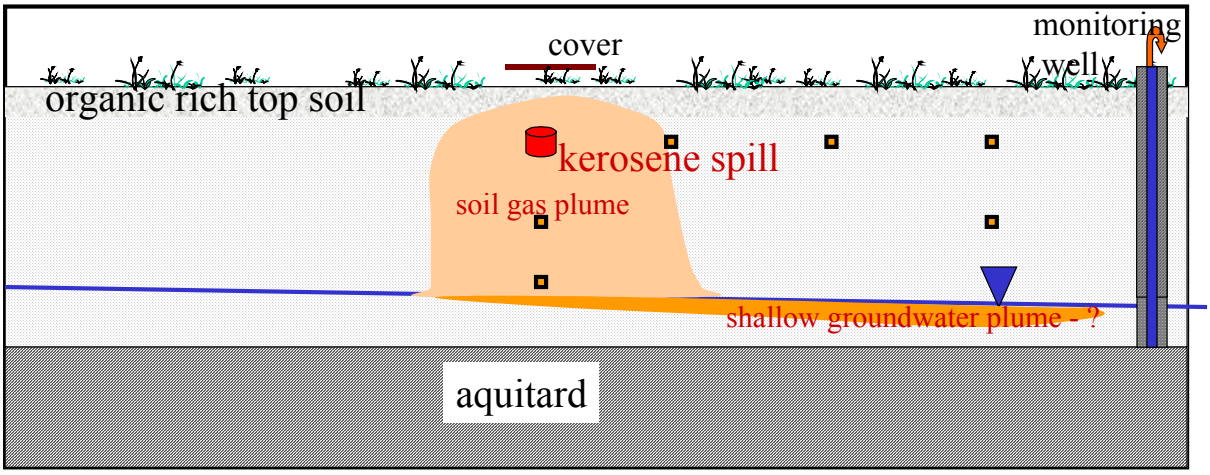

Fig. 1 Conceptual model for the Værløse field site, Denmark.

Daily measured temperature and precipitation data from a weather station at the site were implemented in the model. Approximately 50 cm of organic rich top soil showed generally higher water contents that the underlying sand. Infiltration and soil water contents were calculated using a Van-Genuchten module in MIN3P. The hydraulic conductivity of the aquifer was $1.2 \cdot 10^{-4}$ m s^{-1} which results in groundwater flow velocities of 0.2 to 0.3 m day^{-1}. Diffusion coefficients were $8 \cdot 10^{-10}$ m^2 s^{-1} in the aqueous phase and $7.3 \cdot 10^{-6}$ m^2 s^{-1} in the gaseous phase.

Results - field site model

The contaminant spreading at the field site and the interactions of 13 kerosene compounds and the tracer could be reproduced well by the model. No depletion of O_2 was observed even at the source location, which coincides as well with the field measurements.

An ageing of the NAPL source can be observed as the enrichment of the lower volatile compounds on the expense of the components with higher vapour pressure escaping. The transient evolution of the composition of the NAPL source is given in Fig. 2, which can be regarded as a typical example of kerosene ageing during one year after spill. A fast depletion due to higher temperatures in the summer months can be observed in the early times followed by slower volatilisation during the winter. After the duration of the measurement campaign of 1 year (350 days) only 5 compounds remained in the phase in significant amounts: xylene, tri-methyl-benzene, n-octane, n-decane, n-dodecane and methyl-cyclo-hexane.

To evaluate the importance of soil and meteorological parameters for the contaminant behaviour, sensitivity analyses conducted in 1D and 2D. As an important result, depletion of

the NAPL phase can be accelerated by rapid biodegradation. This is because the dissolution of the NAPL-phase will be enhanced by higher biodegradation rates which produce steeper concentration gradients around the source. As well, a low Henry's law constant H of a compound was found to favour biodegradation even at low rate constants λ compared to high H compounds. If H is low, a greater amount of the contanminant will be present in the aqueous phase where biodegradation actually takes place. High soil moisture decreases degassing to the atmosphere and thus slightly increases the biodegraded fraction as long as there is no oxygen limitation. Higher temperatures increase both, volatilisation and biodegradation (Maier et al., 2002).

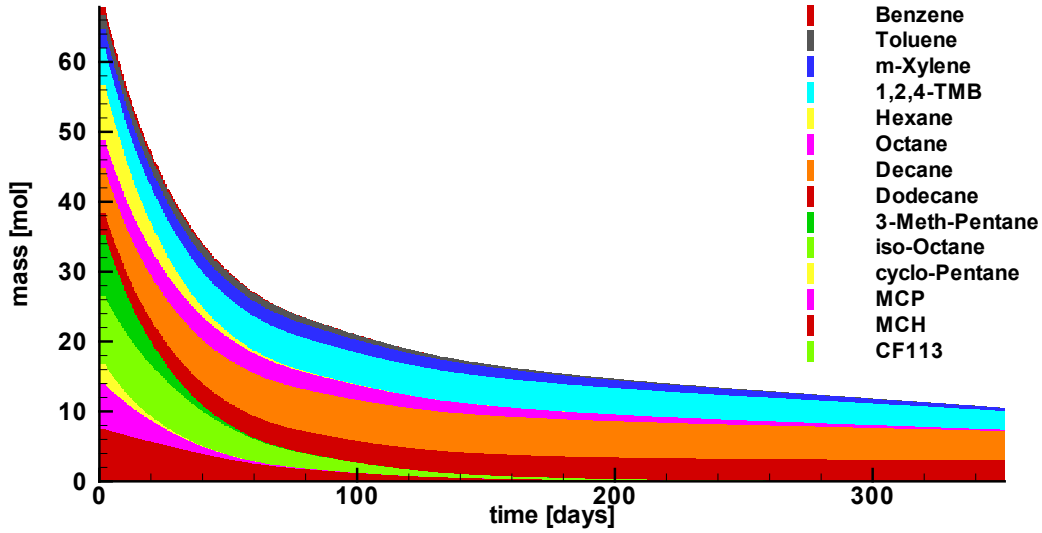

Fig. 2 The mass of the kerosene compounds remaining in the NAPL during the first year in a 3D model (in moles). Sorted in compound classes, from top to bottom: Benzene, Toluene, 1,2,4-Tri-Methyl-Benzene, Hexane, Octane, Decane, 3-Methyl-Pentane, iso-Octane, Cyclo-Pentane, Methyl-Cyclo-Pentane, Methyl-Cyclo-Hexane, and the tracer freon CF113 (only in very small fraction).

A view of a vertical cross-section through a 2D model domain is shown in Fig. 3 for the concentration of iso-octane, which is initially the main compound in the NAPL source, at the time of its maximum concentration at the source location.

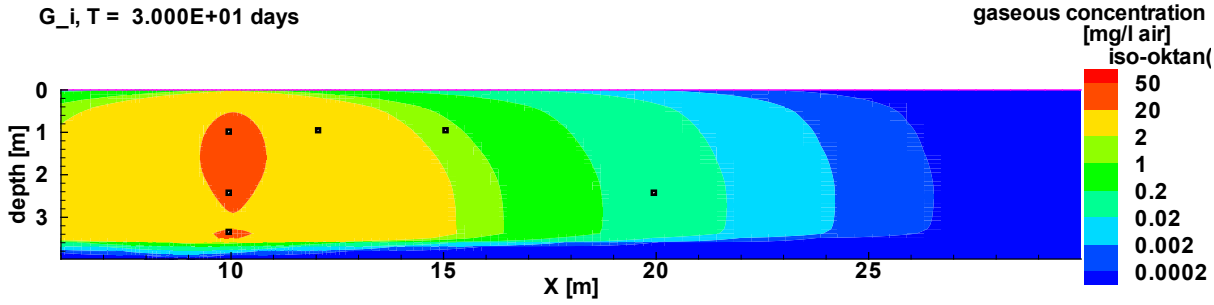

Fig. 3 A vertical cross section through the model domain for a 2D scenario and the compound iso-octane 30 days after source installation (time of maximum concentration at the source).

As shown by the simulations above, the greatest amount of VOC mass will remain in the unsaturated zone, either be transported to the atmosphere and be subject to biodegradation and

only a very small amount will reach the groundwater. Groundwater recharge is a significant contaminant pathway only in soils with high water content and for compounds with low Henry's Law constants (e.g. MTBE in silt or clay). This was already observed in previous studies (Klenk, 2000, (Pasteris et al., 2002). Thus, the main parameters, which cannot be measured directly and have to be adjusted in the model to reproduce field data is the biodegradation rate constants in the unsaturated zone. Then, after the contaminant behaviour for the vadose zone was quantified, the mass transfer to groundwater could be evaluated by realistic estimates of transverse vertical dispersion and diffusion in the capillary fringe.

To take the first step in this procedure, measured and simulated data were compared as 'breakthrough curves' at four different sampling locations (at the source location, 1 m below, 1 & 2 m laterally, respectively). Modelled concentrations and the measured field data show good agreement for the sampling ports in the vicinity of the NAPL source (see Fig. 4 for four compounds 1 m below the centre of the NAPL source). The model misses high concentration peaks at early times during the first 3 –5 days. A possible explanation is a lag time of microbial growth, as evidence of microbial activity (CO_2-production) in the field was observed only 2 weeks after the start of the experiment.

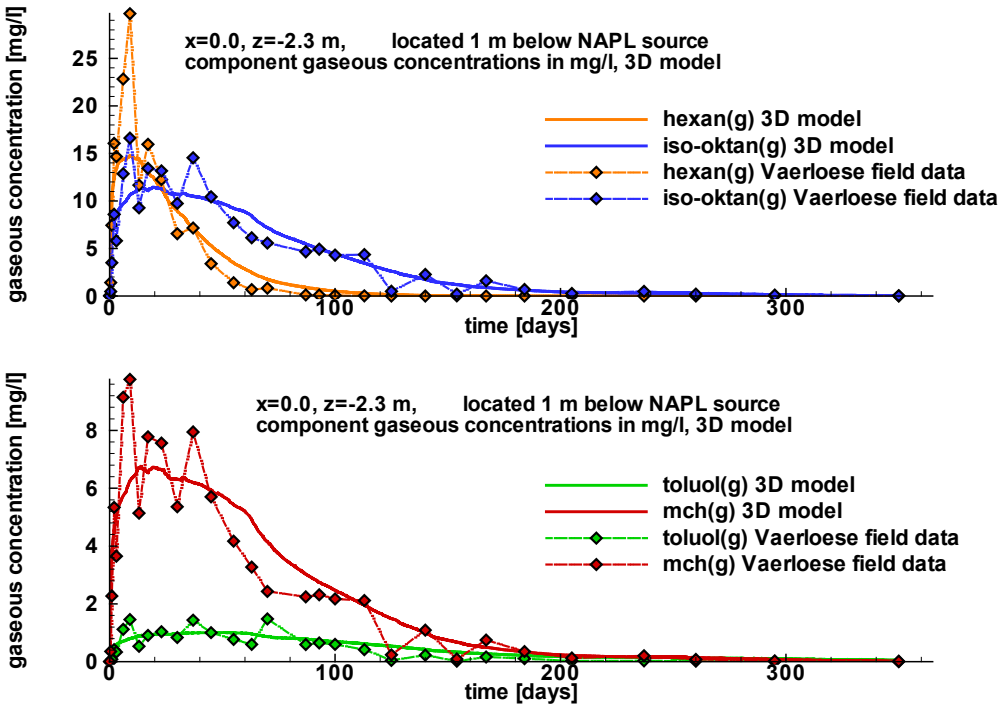

Fig. 4 Comparison of measured and simulated concentrations at a sampling port 1 m below the centre of the kerosene source for four selected compounds.

The maximum transport to groundwater was found for the most volatile and soluble compounds toluene, CF113 and cyclo-pentane and comprised little more than 3 % of the total mass for toluene (Tab. 2). The flux to the atmosphere was pronounced for the tracer freon 113 (99%), the light alkanes due to their low to mediate biodegradation rate constants. Biodegradation was most important for the aromatic compounds (low Henry's law constant) and the heavier n-alkanes (very high biodegradation rate constants). The model calculated that a total mass of 5 kg O_2 was consumed during one year of the experiment and a little less CO_2 was produced (oxygen is also being used up for oxidation of hydrogen of the hydrocarbons). The biodegradation rate constants in the aqueous phase (pseudo first order) applied to the field site model are as well given in Tab 2.

Compound	Flux to groundwater [%]	rate constant [day^{-1}],
Benzene	0.01%	0.43
Toluene	3.12%	0.069
m-Xylene	0.01%	0.43
1,2,4-TMB	0.00%	0.69
Hexane	0.08%	0.26
Octane	0.00%	130
Decane	0.00%	691
Dodecane	0.00%	(1037)
3-Meth-Pent.	0.05%	0.43
iso-Octane	0.02%	1.73
Cyclo-Pent.	0.40%	0.173
MCP	0.01%	2.59
MCH	0.03%	1.73
CF113	0.64%	0

Tab. 2. Mass outflux from groundwater for the best fit run in % of mass volatilised from the source. Also shown biodegradation rate constants (pseudo first order) in s^{-1} (aqueous phase) used for modelling soil gas plume spreading at Værløse field site.

Implementing a depth and time-dependent temperature field, that accounts for the lower vapour pressures in the winter months, enhances the agreement to the measured data significantly compared to constant temperatures. A temporally variable unsaturated flow field due to infiltration events, however, does not affect the kerosene vapour concentrations remarkably, but helps to reproduce the elevated concentrations of CO_2 during longer precipitation periods. This can be explained by higher pore water saturation in the top soil which diminishes the diffusive transport of the biodegradation product to the atmosphere (Fig. 5).

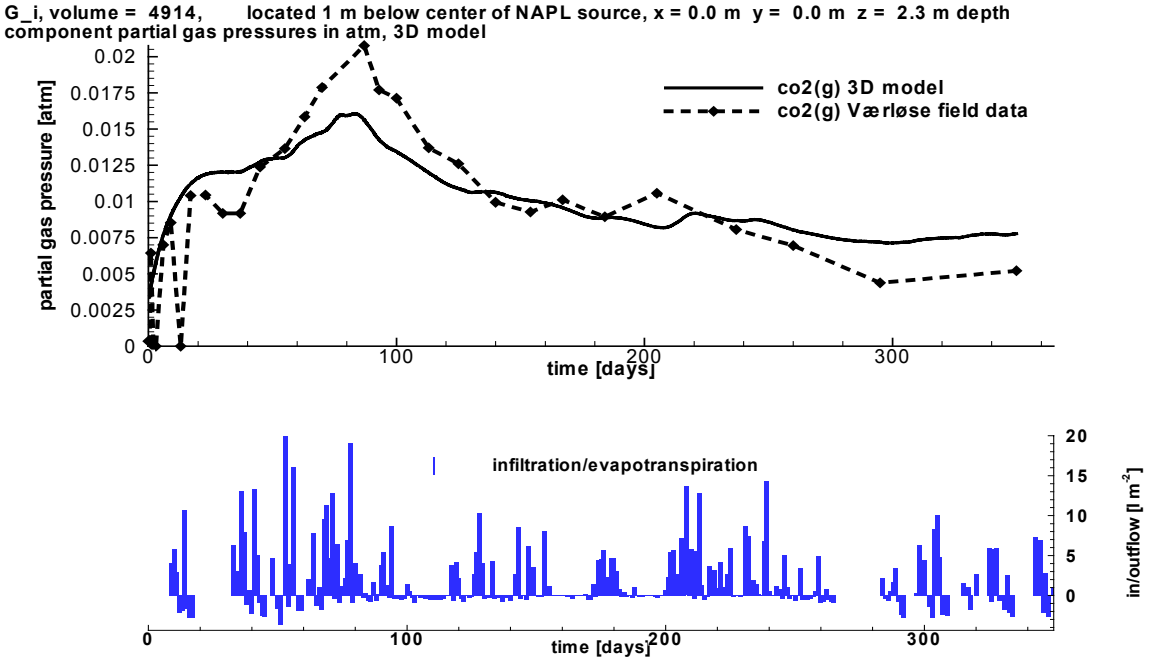

Fig. 5 Comparison of measured and simulated CO_2 concentrations at a sampling port 1 m below the centre of the kerosene source and its correlation to measured infiltration and evapotranspiration.

The mass transfer from the unsaturated zone to groundwater across the capillary fringe is governed by the two processes dispersion and diffusion (McCarthy et al., 1993). Reproduction of measured groundwater concentrations by the model is subject to a greater uncertainty than in the unsaturated zone. The best fit to match measured concentrations of VOC in groundwater could be achieved applying a transverse vertical dispersivity α_t of 2 cm.

Conclusions

Modelling results provided an identification of the main parameters that govern the behaviour of VOC in the unsaturated. The mass balance shows that highly volatile organic contaminants mainly degas to the atmosphere, water soluble compounds are mainly degraded and only small a fraction to groundwater (which could still mean that the legal limit can be locally exceeded). Temporal changes of temperature and infiltration can affect VOC behaviour significantly. The validation of the model also implies that Henry's and Raoult's law are valid (local equilibrium in air/water partitioning and activity coefficients = 1 in the mixture).

Measured data at the well controlled field experiment of a kerosene spill in the unsaturated zone at Værløse site can be reproduced with the numerical model MIN3P. The emission into groundwater can be determined once the processes in the unsaturated zone are quantified. This field investigation used for the validation of the model will allow to quantify the risk of groundwater contamination for a variety of other scenarios.

References

Klenk, I.D., 2000. Transport of volatile organic compounds (VOC's) from soil-gas to groundwater. PhD Dissertation, TGA, C55, Geological Institute, Tübingen

Mayer, K.U. 1999. A multicomponent reactive transport model for variably saturated media. PhD-Thesis at the University of Waterloo, Department of Earth Sciences, Waterloo, Ontario, Canada.

Maier U., Maier. U. Grathwohl. P. (2002). Natural Attenuation of volatile hydrocarbons in the unsaturated zone - modelling for the Værløse field site. 1st international workshop on Groundwater Risk Assessment at COntaminated Sites (Gracos), Tübingen.

McCarthy, K. A. J., R.L. (1993). "Transport of volatile organic compounds across the capillary fringe." Water Resource Research 29(6): 1675 - 1683.

Pasteris, G., Werner, D., Kaufmann, K. Höhener, P. (2002). "Vapor phase transport and biodegradation of volatile fuel compounds in the unsaturated zone: a large scale lysimeter experiment." Environmental Science & Technology 36((1)): 30-39.

Wiedemeier, T.H., Rifai, H.S., Newell, C.J., Wilson, J.T. (1999): Natural Attenuation of Fuels and Chlorinated Solvents in the Subsurface. John Wiley and Sons, New York.

Cost-effective modelling of fuel mixture transport in the vadose zone: Application to a field experiment, Airbase Værløse, Denmark

Petros Gaganis[1], Peter Kjeldsen[2], Vasilis N. Burganos[1]

[1] *Institute of Chemical Engineering and High Temperature Chemical Processes – Foundation for Research and Technology, Hellas (ICE/HT-FORTH), Patras, Greece.*
[2] *Environment & Resources DTU, Technical University of Denmark, Kgs. Lyngby, Denmark.*

Abstract: The constituent averaging technique is applied to a large-scale field experiment at Airbase Værløse, Denmark. A target fuel component is simulated as individual constituent while the effect of mixture composition on its transport process is approximated by defining a small number of pseudospecies. All parameters, except biodegradation, used in the calculations are assigned values either measured at the site or obtained from the literature or calculated from other related properties. The values for the biodegradation constants of the simulated compounds are adjusted through a model calibration process that involved integration of the equations and matching the experimentally determined concentration profiles. These adjusted values lie within the range of probable biodegradation rate values reported in similar studies. The applicability of this approach to large-scale contamination problems is demonstrated through a number of simulations performed using different fuel components as target contaminants. In all cases, simulation results are in close agreement with the gas concentration profiles observed in the field. Compared to the case of simulating all organics as individual compounds, the constituent averaging technique offers the advantage of a greatly reduced computational cost, reduced data requirements, as well as a smaller impact of the uncertainty in the compound properties on modelling results because effective values are used for each composite constituent, which follow a pdf with reduced variance compared to that of the individual values.

1. Introduction - background

Treatment of a large number of components in a model of attenuation of VOC mixtures is a formidable task, as a multitude of processes must be taken into account for each component, involving a whole set of parameters that are usually difficult to estimate. An additional difficulty that is typically encountered is the often large number of constituents in an actual VOC mixture compared to the number of species that can be handled numerically.

An approach to overcome these problems is recently suggested by Gaganis et al., 2002. This approach to a cost-effective prediction of the fate of VOC mixtures (constituent averaging technique) consists of simulating few mixture components (target contaminants) as individual constituents while, in order to account for the effect of the mixture composition on the transport process of the selected target contaminants, simulate the rest of the mixture hydrocarbons using a small number of pseudospecies (composite constituents). A composite constituent is defined to have the following concentration at all times:

$$C_a^c = \sum_{i=1}^{k} C_a^i, \qquad a = o, w, g \tag{1}$$

where C_a^c is the concentration of the composite constituent in phase a (o = organic phase, w = aqueous phase and g = gas phase) and C_a^i is the concentration of member component i in phase a.

In contrast to the case of individual compounds, the thermodynamic properties of composite constituents may be time dependent due to temporal composition changes. In Gaganis et al. (2002), an objective function is introduced for minimizing their time dependence through a selection of an optimal grouping criterion. The procedure for selecting the optimal grouping criterion includes:

1) Randomly select *n* different sets of *m* individual hydrocarbons (*m* = maximum number of constituents that can be handled by the numerical code) from the actual organic mixture.

2) Simulate the temporal evolution of the mole fraction of individual compounds in each set.

3) Investigate the change with time of the composition of composite constituents for alternative grouping schemes and select, as a grouping criterion, the property that minimizes the following objective function:

$$J(p) = \frac{\sum_{j=1}^{n}\left[\sum_{t=0}^{t_{\max}}\left[\sum_{i=1}^{k}\left(R_i^o - R_i^t\right)^2\right]\right]}{n} \quad (2)$$

where *p* is the property used to form the composite constituents, $j = 1,\ldots, n$ represents a set of *m* individual hydrocarbons, *t* is the time, $i = 1,\ldots, k$ represents a composite constituent that consists of two individual components a_i and b_i, R_i^o and R_i^t are the mole fraction ratios of a_i and b_i ($R_i = x_{a_i} / x_{b_i}$) at time equal to zero and *t*, respectively.

Furthermore, Gaganis et al. (2002) suggested an algorithm to relate the effective thermodynamic properties of composite constituents to the properties of individual member. Based on data from Pasteris et al. (2001), they have shown that the effective aqueous solubility and Henry's law constant of a composite constituent are best approximated as the mole fraction-weighted geometric and arithmetic weighted averages of solubility and Henry's law constant values of its individual components, respectively. They also demonstrated that the values of the sorption distribution coefficients and the biodegradation rate coefficients of the least sorbing and least biodegradable member hydrocarbons represent the values of these properties that should be assigned to the composite constituents.

The objectives of this study is (i) to test the applicability and validate the above methodology to the large-scale emplaced fuel source experiment, Airbase Værløse, Denmark, and (ii) to explore its potential and usefulness in predictive modeling.

2. Emplaced fuel source experiment

The hydrologic cross-section of the site includes a sandy dark brown top soil of approximately 50 cm thickness overlying a layer of 2-3.3 m of homogeneous glacial melt water sand, which, in turn, overlies a thin layer (0.5-1 m) of moraine sand/gravel. Beneath the moraine sand/gravel lies a thick moraine clay layer (up to 50 m). The water table ranges from 2.5-3.5 m below ground surface while the secondary unconfined aquifer has a thickness of 0.5-1 m. The field experiment was started in the beginning of July 2001. A circular source (diameter of 0.75 m) consisting of sand from the site mixed with the oil phase was placed between 0.8-1.3 below ground surface.

Table 1 – Fuel mixture composition after source installation (Christophersen et al., 2002)

Compound	Weight fraction (%)	Compound	Weight fraction (%)
Benzene	1.02	Dodecane	9.50
Toluene	2.93	3-Methyl-pentane	7.45
m-Xylene	4.57	Iso-octane	15.36
1,2,4 Trimethylbenzene	10.99	Cyclo-pentane	1.59
Hexane	7.26	Methyl-cyclo-pentane	5.79
Octane	7.16	Methyl-cyclo-hexane	10.23
Decane	15.99	CFC113	0.16

The oil phase is an artificial hydrocarbon mixture consisting of volatile and semi-volatile compounds (BTX's, n-, iso- and cyclo-alcanes) similar to jet fuel (Table 1). The monitoring network of the site and the source consists of 107 soil gas probes, 7 multi-level water samplers (9 levels), and 6 porous caps for sampling water from the unsaturated zone. The monitoring devices were placed mainly in one radial transect with control monitoring points in the other directions. In the main radial transect, the hydrocarbons in the pore gas was monitored to a distance of 20 m from the center of the source. The migration of the hydrocarbons and tracers in the soil gas, pore water and groundwater was monitored till July 2002, when the source was removed and the site was remediated. For more details the reader is referenced to Christophersen et al. (2002).

3. Hydrogeological model

The field experiment is simulated using the numerical code MOFAT (Katyal et al., 1991). This code, which has a number of coding features that facilitate simulation of field-scale multicomponent transport (up to 5 components) in two dimensions, uses a finite element technique to solve the governing flow equations in the three phases and transport equations in the gas and aqueous phases. MOFAT allows for a fairly flexible mathematical description of the boundary conditions and processes involved in the field experiment. The main features of the hydrogeological simulation model include (i) the relationships between phase permeabilities, saturations and pressures are described by a three phase extension of the van Genuchten model (Kaluarachchi and Parker, 1992), (ii) flow due to density differences and advective transport in the gas phase are incorporated in the model, (iii) the partitioning between the gas-aqueous, gas-NAPL, and aqueous-solid phases is assumed to be at equilibrium, and (iv) biodegradation, which takes place only in the aqueous phase, is modeled as a 1st order process. In addition to those features, in order to deal with the large seasonal temperature variations at the site, an external module was used with the code that takes advantage of its restart option for updating the thermodynamic properties of the fuel mixture components at selected times based on equations of their temperature dependence selected form the literature.

A two-dimensional model domain (20m x 5m) and radial coordinates are used for the simulations. Thus, groundwater flow was not incorporated in the model. However, as indicated by field measurements, ignoring the influence of flowing groundwater does not have a significant impact on the transport process in this case. The model domain consists of 24 grid-blocks in the horizontal direction and 16 in the vertical direction and is composed of 5 horizontal homogeneous layers of different soil characteristics. In both directions, the model domain is discretized using a variable nodal spacing of 15-20 cm near the source zone (highest concentration gradient) that gradually increases up to 2 m at the outer boundaries. The boundary conditions for fluid flow and contaminant transport are (i) atmospheric

pressure, groundwater recharge and constant concentration at the upper boundary (C = 0), which allow for mass loss to the atmosphere, (ii) specified temporarily varying water table (as measured in the field) and zero concentration gradient along the left and right boundary, and (iii) no flow and zero concentration gradient at the lower boundary. The flow model is calibrated to measured temporal variations of soil moisture profile by adjusting the recharge rate. Following the constituent averaging technique, a target fuel component is simulated as individual constituent while the effect of mixture composition on its transport process is approximated by defining a small number of composite constituents. The composite constituents are selected based on equation (2), which indicated the aqueous solubility as the optimal grouping criterion. All other parameters, except biodegradation rates, are assigned values either measured at the site or obtained from the literature (individual constituents) or calculated from member compound property values using the algorithm described above (composite constituents). The values for biodegradation rate constants of the simulated compounds are adjusted through a calibration of the transport model. All parameters sensitive to temperature variations are updated at specified times according their temperature dependence functions.

4. Results and discussion

A number of simulations are performed using different fuel components as target contaminants to demonstrate the applicability of this approach to large-scale contamination problems. In the simulation results shown in Figure 1, toluene is selected as the target contaminant. The rest of the compounds are grouped into four composite constituents: (i) benzene, CFC113, m-xylene and cyclopentane (composite constituent 1), (ii) 1,2,4 trimethylbenzene, methylcyclopentane, methylcyclohexane, 3-methylpentane and hexane (composite constituent 2), isooctane and octane (composite constituent 3), and decane and dodecane (composite constituent 4). The modeling results for CFC113 and hexane as target contaminants are shown in Figure 2. The 1st order biodegradation rates associated with the best match of modeling results and experimental data are also shown in Figure 1 and Figure 2.

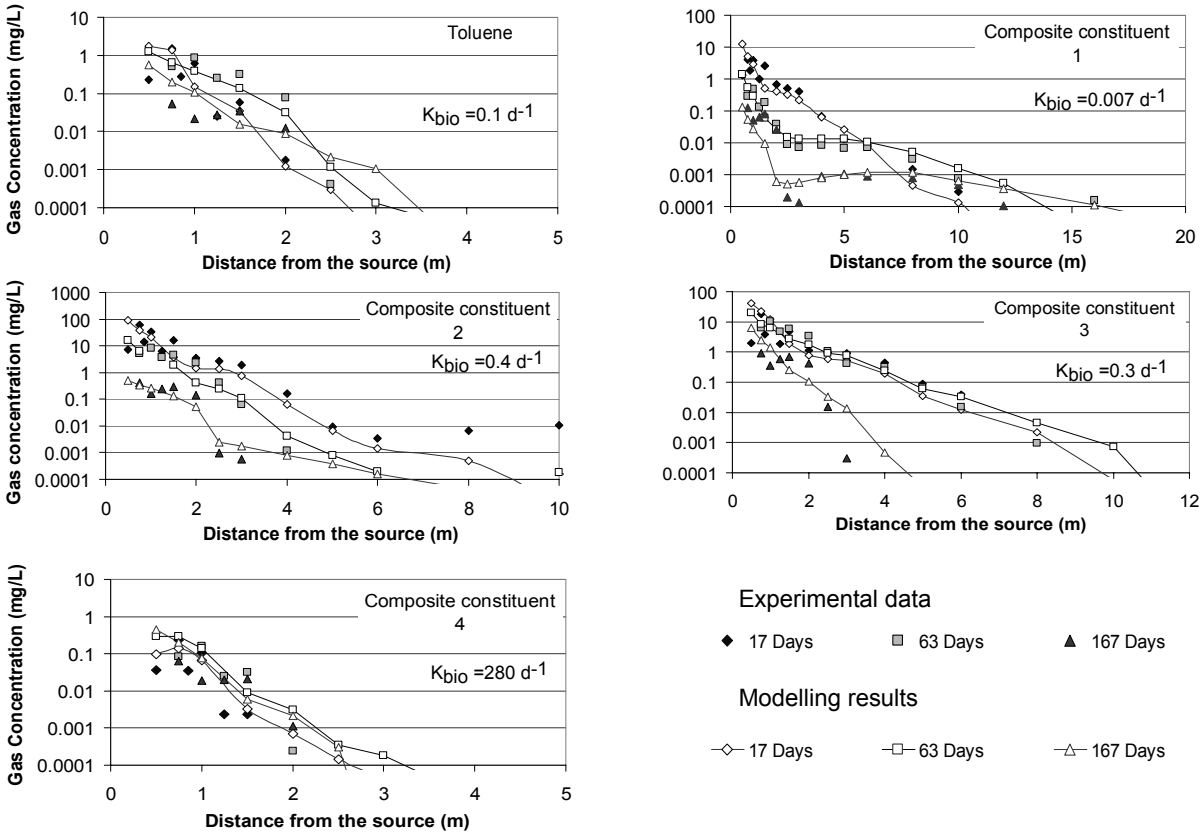

Figure 1: Reproduction of experimental data for the five simulated constituents in terms of gas concentration at depth 1.05 m below the ground surface.

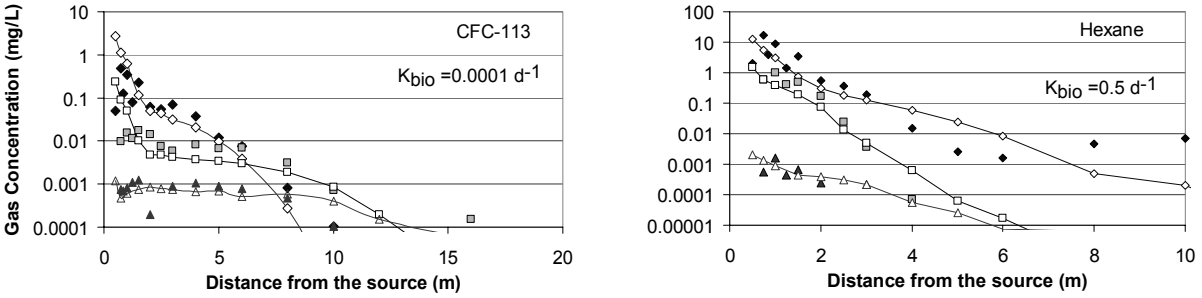

Figure 2: Reproduction of experimental data for CFC-113 and hexane as target contaminants in terms of gas concentration at depth 1.05 m below the ground surface.

In all cases, simulation results are in close agreement with the gas concentration profiles measured in the field, although gas concentrations range over several orders of magnitude. These results indicate that 1st order kinetics to describe biodegradation may represent a good approximation for VOCs in the vadose zone. Biodegradation rates that provided the best match to experimental data in this study lie within the range of probable values reported in the literature and close to the lower bound of the rates estimated from batch and column experiments (i.e. 0.12±0.06 d^{-1} for toluene and 2±1.23 d^{-1} for hexane) for the soils of the Værløse site. The evolution of the source composition with time as measured experimentally is also satisfactorily matched indicating that all the important processes are taken into account in the model. In this field study, advective transport in the gas phase is proved to be an

important process with significant impact on the spreading of the VOCs in the vadose zone. Practically all contaminant mass that is dissolving or volatilising ends up in the atmosphere rather than in groundwater. Accounting only diffusion for VOC transport in the gas phase was not sufficient to explain the travel distances of many fuel mixture compounds. There are limited data, therefore, large uncertainty regarding the temperature dependence of thermodynamic properties of several compounds. In the constituent averaging technique, when individual compounds are grouped into composite constituents, this uncertainty in the property values has a smaller impact on modelling results because effective values are used for each composite constituent, which follow a probability density function (pdf) with reduced variance compared to that of the individual values.

5. Conclusions

The constituent averaging technique may provide the means for a rapid low-cost assessment of contamination when dealing with complex VOC mixtures in the vadose zone. The applicability and potential of this approach was demonstrated in this study using data from the large-scale field experiment at the Værløse site. It resulted in simulation results in close agreement with the gas concentration profiles observed in the field. When compared to the case of simulating all organics as individual compounds, the constituent averaging technique offers the advantage of greatly reduced computational cost with minimum loss in accuracy, reduced data requirements, as well as a smaller impact of the uncertainty in the compound properties on modelling results. The latter is of particular significance in this type of problems and is due to the fact that effective values are used for each composite constituent, which follow a pdf with reduced variance compared to that of the individual values. Biodegradation is one of the most important but uncertain parameters when modelling VOC transport in the vadose zone. In the absence of reliable site-specific data, it may be appropriate to be treated as stochastic parameter.

References

Christophersen, M., M. Broholm M. and P. Kjeldsen. 2002. Migration and Degradation of Fuel Vapours in the Vadose Zone. Field Experiment at the Airforce Base, Denmark. *Proceedings of the 1st International Workshop on groundwater Risk Assessment at Contaminated Sites*, Tübingen, Germany,83-87.

Gaganis, P., H. K. Karapanagioti and V. P. Burganos. 2002. Modeling Multicomponent NAPL Transport in the Unsaturated zone with the Constituent Averaging Technique. *Advances in Water Resources*, 25, 723-732.

Kaluarachchi JJ, Parker JC. 1992. Multiphase flow with simplified model for oil entrapment. Trans Porous Media; 7:1-14.

Katyal, A.K., Kaluarachchi, J.J., Parker, J.C., 1991. MOFAT: A two-dimensional finite element program for multiphase flow and multicomponent transport, EPA/600/2-91/020.

Pasteris, G., Werner, D., Kaufmann, K., Hoehener, P., 2002. Vapor Phase Transport and Biodegradation of Volatile Fuel Compounds in the Unsaturated Zone: A Large Scale Lysimeter Experiment, *Environ Sci Technol*, 36, 30-39.

Fate and transport of dissolved jet fuel contaminants in the unsaturated zone: effect of soil heterogeneity

Gijs D. Breedveld [1], Eli Alfnes [2], Per Aagaard [2], Sjoerd E.A.T.M. van der Zee [3]

[1]*Corresponding author: Norwegian Geotechnical Institute, P.O. Box 3930 US, N-0806 Oslo, Norway*
Phone: +47-22023000, Fax:+47-22230448, E-Mail:gbr@ngi.no
[2] *Department of Geology, University of Oslo, P.O. Box 1047 Blindern, N-0316 Oslo, Norway*
[3] *Dep. of Env. Sciences, Wageningen University, PO Box 8005, 6700 EC Wageningen, The Netherlands*

Abstract: The effect of soil heterogeneity on the fate and transport of dissolved jet fuel contaminants has been studied using laboratory and field experiments at the Gardermoen experimental station. The sedimentary layered structures and textural changes had a profound influence on contaminant transport and observed residence time. Based on the geological structure at the site, 2-D simulations of water and solute transport in variable saturated media were carried out. These showed that the observed preferential flow was related to the infiltration rate and water saturation level. Under the used experimental conditions with relative high infiltration rates, anisotropy dominated the transport direction. Incorporation of coupled multispecies transport, sorption, biodegradation and gas diffusion in the model revealed that both oxygen diffusion and the initial biomass present in the unsaturated zone were limiting the observed biodegradation of the dissolved jet fuel contaminants. The results of our study indicate that the attenuation capacity of the unsaturated zone might be "short-circuited" during episodic snow-melting events when high pollution loads can be expected. This has serious implication for groundwater risk assessment in cold climates.

1. Introduction

The unsaturated zone has an important role in the attenuation of organic contaminants. Processes such as sorption, evaporation and degradation can prevent contaminants from reaching the groundwater. Quantification of these processes for the purpose of risk assessment is usually based on the assumption of homogeneity with regard to soil processes. This assumption can lead to a serious overestimation of the natural attenuation potential, since small textural changes can create preferential flow that result in rapid flow through a small part of the soil matrix and reduced residence times in the unsaturated zone.

The Gardermoen project has focused on these processes during the last ten years. The Gardermoen delta is a glaciomarine deposit and contains the largest unconfined aquifer in Norway (Tuttle, 1997). This is also the site of Oslo international airport, giving rise to numerous conflicts between airport operation and groundwater quality. Both airport de-icers and jet fuel related hydrocarbons are effectively attenuated in the unsaturated zone provided that the residence time is sufficient (French et al., 2001; Breedveld et al., 1997). However the clear depositional structure at Gardermoen has been shown to result in large variations in contaminant transport (Kitterød, 1997).

2. Moreppen field station

The Moreppen field station was established in 1992 and consisted originally of one lysimeter trench down to 2,5 m depth in upper part of the unsaturated zone with mainly horizontally orientated layers of fine to medium and coarse sand. This trench has been used to study fate and transport of de-icing chemicals under natural infiltration conditions (French et al., 2001).

A second lysimeter trench penetrating the complete unsaturated zone down to 3.5 m depth was established in 1997 (Figure 1). This trench covered both the horizontally orientated top set units (down to 1.8 m) as well as the dipping fore set unit of alternating fine and coarse sand (Søvik et al, 2002). This trench has been used to study the fate and transport of jet fuel related hydrocarbons (toluene and o-xylene) under artificial high irrigation conditions (100 mm/d) which might occur during snow melting along the airport runways.

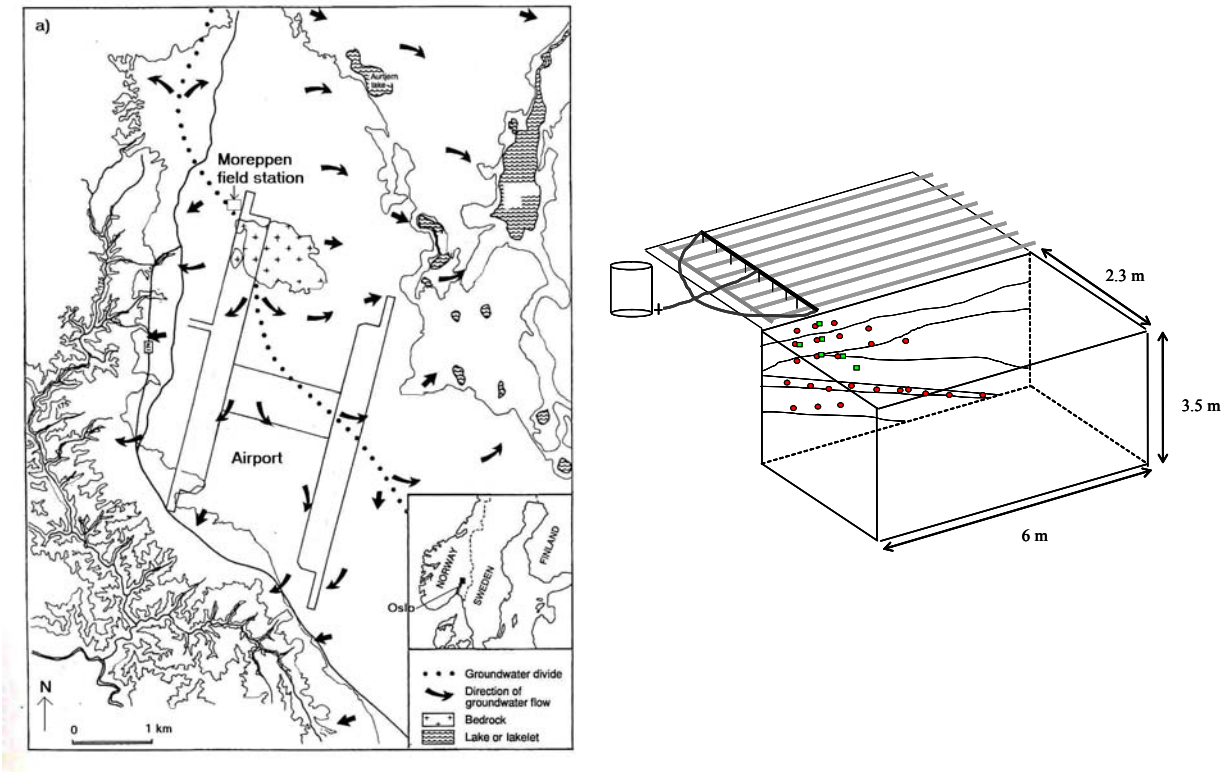

Figure 1: Location of Moreppen field station on the Gardermoen delta and details of the second trench, the irrigation lines and the position of the soil moisture and gas probes are indicated.

Field observation indicated a strong influence of the dipping fore set beds, resulting in a preferential flow path. A 4 m depth a horizontal displacement of more than 4 m was observed for the non-reactive tracer (bromide) and the dissolved hydrocarbons (Søvik et al., 2002). Despite this preferential flow the hydrocarbons were nearly completely degraded before reaching the saturated zone.

3. Modeling

To get a better understanding of the dominating processes in the unsaturated zone resulting in the observed preferential flow, numerical simulation tools have been used. The numerical code for transport in the unsaturated zone SWMS-3D has been extended with coupled multispecies transport, microbial degradation following Monod kinetics and diffusive gas transport of oxygen and hydrocarbons (Alfnes, 2002). Based on the soil grain size distribution the necessary soil physical model parameters could be estimated. To be able to reproduce the general flow pattern satisfactorily the textural changes in itself were not sufficiently pronounced at the applied infiltration rate. Anisotropy (directional variation in hydraulic conductivity) as a result of particle orientation during sedimentation had to be included to capture the general flow features (Figure 2). To be able to describe the reactive hydrocarbon transport properly sorption had to be reduced compared to laboratory determined values. The

observed lag phase in biodegradation could be captured by adjusting the initial amount of biomass and the maximum utilization rate. The simulation results indicated local oxygen depletion, which was not observed in the field (Søvik et al., 2002). This might be a result of small scale heterogeneity within the sedimentary layers.

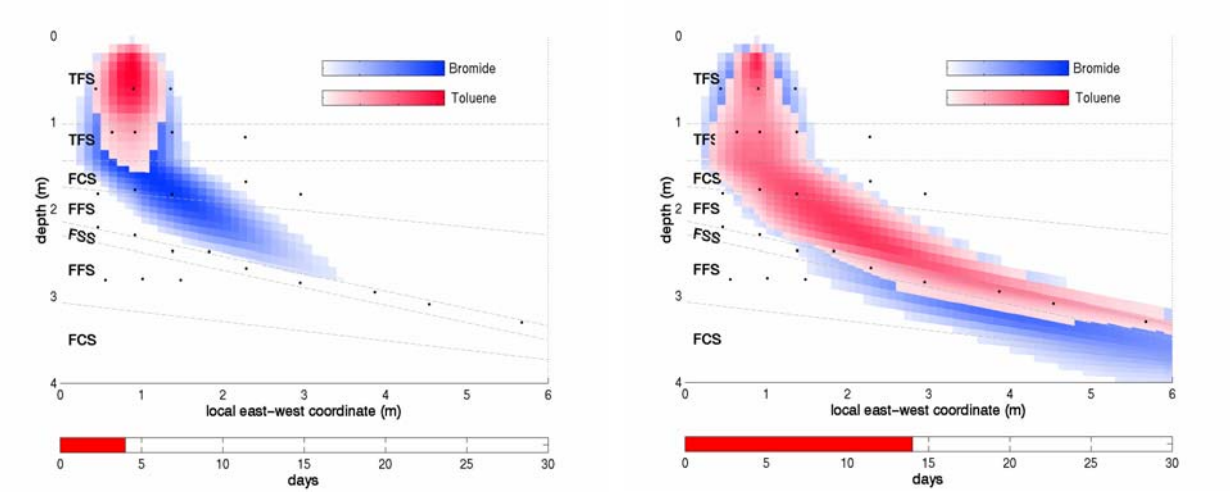

Figure 2: Simulation of the flow pattern of a non-reactive tracer and toluene after 4 and 14 days of infiltration (Alfnes, 2002).

Based on the modeling results and the general geological structure of the Gardermoen aquifer, areas can be identified where rapid transport through the unsaturated zone can be expected (Wong, 2003). The attenuation capacity of the unsaturated zone might there be "short-circuited" especially at high infiltration rates like episodic snow-melting events. These events often coincide with the release of high pollution loads accumulated in the snow cover. This has serious implication for groundwater risk assessment in cold climates.

4. References

Alfnes, E. 2002. Coupled modeling of contaminant transport and microbial degradation in the unsaturated zone of a structured delta deposit. PhD Thesis, Dep. of Geology, University of Oslo, Norway.

Breedveld, G.D., G. Olstad and P. Aagaard. 1997. Treatment of jet fuel-contaminated runoff water by subsurface infiltration. Bioremed. J. 1:77-88.

French, H.K., S.E.A.T.M. van der Zee and A. Leijnse. 2001. Transport and degradation of propyleneglycol and potassium acetate in the unsaturated zone. J. Contam. Hydrol. 49:23-48.

Kitterød, N.-O. 1997. Stochastic estimation and simulation of heterogeneities important for transport of contaminants in the unsaturated zone. PhD thesis, Dep. of Geophysics, University of Oslo, Norway.

Søvik, A.K., E. Alfnes, G.D. Breedveld, H.K. French, T.S. Pedersen and P. Aagaard. 2002. Transport and degradation of toluene and o-xylene in an unsaturated soil with dipping sedimentary layers. J. Environ, Qual. 31:1809-1823.

Tuttle, K. 1997. Sedimentological and hydrological characterisation of a raised ice-contact delta - the Preboreal delta-complex at Gardermoen, South Eastern Norway. PhD Thesis, Dep. of Geology, University of Oslo, Norway.

Wong, W.K. 2003. Contaminant migration and its risk mapping in the subsurface – the case of Gardermoen, Norway. PhD thesis, Dep. of Geophysics, University of Oslo, Norway.

In situ method for the determination of apparent gas-phase diffusion coefficients in the unsaturated zone

David Werner[1] and Patrick Höhener[2]

[1]*Corresponding author, present address: Department of Civil and Environmental Engineering, Stanford University, Phone: 650 725 0315, Fax: 650 725 3164, E-mail: dwerner@stanford.edu*
[2]*Swiss Federal Institute of Technology Lausanne (EPFL), ENAC-ISTE-LPE, CH-1015 Lausanne, Switzerland*

Abstract: Knowledge of gas-phase diffusion coefficients is crucial for both modelling of vapor migration and risk assessment at sites, where the subsurface has been contaminated with volatile organic chemicals (VOCs). The theory and its practical application are presented of an in situ method for the determination of both effective and sorption-affected diffusion coefficients in the vadose zone. A small volume of gas containing two or more gaseous compounds is injected into soil. One compound is a conservative tracer, while the remainings are the compounds of interest. As all the compounds diffuse away, small soil gas samples are withdrawn from the injection point through the sampling capillary. The measured data are interpreted with an equation for gas-phase diffusion in a homogeneous unsaturated medium. The air-filled porosity is determined independently. The tortuosity factor and mass fraction in the gas phase are obtained for the compounds of interest. From these parameters the apparent gas-phase diffusion coefficients can be calculated. Results are reported for the sandy soil at the GRACOS field site near Værløse, Denmark.

1. Introduction

Gas-phase diffusion dominates the migration of natural gases and volatile pollutants in the unsaturated zone in the absence of pressure gradients. It is crucial for vapor migration of volatile organic chemicals at contaminated site for the supply of molecular oxygen to soil organism or for ^{222}Rn migration from soil to houses. The molecular diffusion coefficients in free air can be measured or estimated from empirical relationships (1). For gas-phase diffusion in a porous medium, coefficients are defined with proportionality factors accounting for the effects of the physical reduction and/or partitioning (2). Effective diffusion coefficients D_e are used to calculate gas fluxes from Fick's first law or for the interpretation of steady state vapor concentration profiles. They account for the reduced cross-sectional area and increased mean path length in soils. Sorption-affected diffusion coefficients D_s account for the effect of increased mean path length and partitioning into stationary phases. They describe transient diffusion under non steady state conditions such as the change of concentration profiles as a function of time.

Large differences between values for the effective diffusion coefficients obtained from the various existing empirical relationships (3), in laboratory tests (4), and field experiments explain the need for accurate in situ measurements of the parameters affecting the gas-phase diffusion in soils. A recently developed method quantifies the effect of the tortuosity factor as well as the overall effect of processes, which slow the diffusive spreading of compounds such as air-water and air-solid partitioning and adsorption to interfaces (5). The gaseous compound of interest is injected into the vadose zone together with a conservative tracer to form an instantaneous point source, and the concentration decline is monitored at the injection point. The air-filled porosity is determined independently. The tortuosity factor is obtained from the conservative tracer data. The mass fraction in the soil gas is determined from the ratio of the

concentration of the compound of interest relative to that of the conservative tracer. Both the effective and the sorption-affected diffusion coefficient can be calculated from these parameters. In this study, CFC-12 was used as a conservative tracer to determine the effective diffusion coefficient in a sandy soil near Værløse, Denmark. The mass fraction in the soil gas phase was determined in a separate experiment for toluene relative to hexane.

2. Theory

The theory of instantaneous point source diffusion experiments in an unsaturated porous medium, as described in (5), is based on the following assumptions: The soil can be described as a homogeneous porous medium with uniform and constant properties consisting of soil air, soil water, and the solid matrix. The partitioning of the gaseous compounds between those phases can be described by an instantaneous, reversible linear equilibrium. Gas-phase diffusion is the only relevant transport mechanism, and degradation is negligible over the timescale of the experiment.

A small gas volume V_{in} containing the gaseous compound at concentration C_{in} is injected into the soil. The decline in $C_r=C_a/C_{in}$ at the injection point as a function of time t can be described by

$$C_r(0,t) = \frac{V_{in} f_a}{8\theta_a (f_a \tau D_m \pi)^{1.5}} \cdot \frac{1}{t^{1.5}} \ , \qquad (1)$$

where C_a denotes the soil air concentration, f_a the mass fraction in the soil gas, θ_a the air-filled porosity, D_m the molecular diffusion coefficient in air, and τ the tortuosity factor. Equation 1 leads to

$$\tau = \frac{V_{in}^{2/3}}{4\pi\theta_a^{2/3} C_r(0,t)^{2/3} f_a^{1/3} D_m} \cdot \frac{1}{t} \ . \qquad (2)$$

For a conservative tracer f_a equals one and τ can be obtained from the measured $C_r(0,t)$ if θ_a is known or can be estimated. For two simultaneously injected compounds, one finds

$$\frac{f_{a,1}}{f_{a,2}} = \left[\frac{C_{r,2}(0,t)}{C_{r,1}(0,t)}\right]^2 \cdot \left[\frac{D_{m,2}}{D_{m,1}}\right]^3 . \qquad (3)$$

Thus if compound 2 is a conservative tracer with $f_{a,2}=1$, one can obtain $f_{a,1}$ from eq 3. The effective diffusion coefficient D_e and the sorption-affected diffusion coefficient D_s are defined as

$$D_e = \theta_a \tau D_m \qquad (4) \ , \qquad D_s = f_a \tau D_m \ . \qquad (5)$$

3. Materials and Methods

The geology of the field site near Værløse, Denmark is shown schematically in Figure 1. The total porosity θ_t of the sand layer is 0.37 and the fraction of organic carbon f_{oc} 0.02% of the dry weight (6). A controlled hydrocarbon spill experiment was conducted at this site by the Danish Technical University (DTU) to investigate the natural attenuation of volatile

hydrocarbons in the vadose zone (7). Artificial fuel was mixed with sand from the site and packed into a cylindrical hole with a diameter of 70 cm at a depth between 0.8 and 1.3 m below the surface to form a source of hydrocarbons. The temperature and water content at the field site were monitored with thermometers and TDR probes.

The tortuosity factor τ and the effective diffusion coefficient D_e were determined at 1 m depth in the glacial sand deposit in the center of the contaminated sand and in 0.73 m, 2.35 m and 9.5 m distance from the center (Figure 1). Soil gas probes with a low dead volume were used as described in (5). A volume of 5 mL gas containing CFC-12 was sucked into a gastight sample lock syringe. The concentration of CFC-12 in the syringe was determined by withdrawing three samples of 20 µL, which were diluted and stocked in air-filled 64 mL flasks. The gas was then injected into the soil followed by 1 mL of clean air. Two to four soil gas samples (100 µL) were taken from the injection point at times >40 min after the injection and stocked in gastight sample lock syringes until analysis. Before sampling 2.5 mL of soil gas was withdrawn to flush the sampling capillary. Samples were analysed on a GC equipped with an ECD and an FID connected to the same column. These experiments were performed 102 days after the installation of the hydrocarbon source. The temperature at 1 m depth was 13°C and the water-filled porosity θ_w determined from TDR measurements was 0.10.

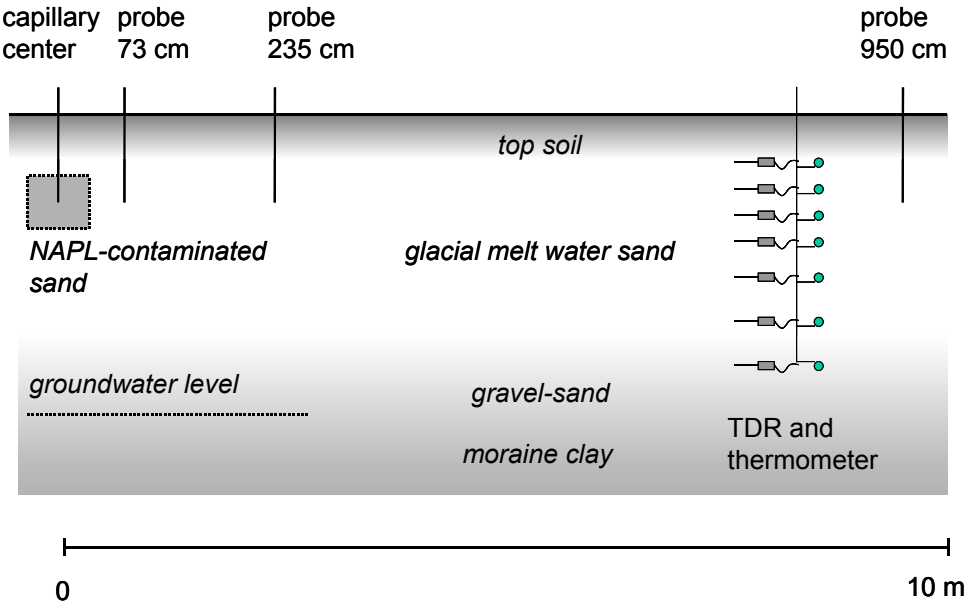

Figure 1: Profile of the subsurface at the Værløse field site and instrumentation used in this study.

Toluene and hexane were present in the vapors emanating from the hydrocarbon source and experiments with these compounds could only be performed after toluene and hexane concentrations in the soil gas had declined below the detection limit (360 days after the installation of the hydrocarbon source). Three probes were installed at 10 m distance from the source zone in the corners of a triangle with sidelines of 25 cm. The tips of the soil gas probes were at a depth of 1.2 m. A gas volume of 10 ml containing hexane and toluene as gaseous compounds was injected through one probe to form a point source. Hexane was one of the most volatile and hydrophobic tracers reliably retained in the sorption tubes and chosen to be the conservative tracer. After 30 min 10 ml of soil gas were sucked from each of the probes onto sorption tubes. Sampling was repeated every 30 min for a total of 6 hours thereafter. The

sorption tubes and analytical system are described in (8). The temperature at the 1.2 m depth was 14.5°C and the water-filled porosity θ_w determined from TDR measurements was 0.10.

4. Results and Discussion

The tortuosity factor τ and the effective diffusion coefficient D_e were calculated from the measured CFC-12 concentrations according to eqs 2 and 4 with the assumption $f_{a,CFC-12}=1$. The air-filled porosity $\theta_a=0.27$ was determined from the volumetric water content measured with TDR probes at 1 m depth ($\theta_t=0.37$, $\theta_w=0.10$). The tortuosity factor τ and the ratio between effective and molecular diffusion coefficient D_e/D_m reported in Table 1 are the average of measurements at 2-4 different times t during the experiment. The error is given as the standard deviation. The differences between the measured values are probably the result of heterogeneities such as a local variation in the soil water content. The average ratio D_e/D_m for the four locations is 0.125±0.031. This agrees best with the value predicted by the empirical relationship proposed by Moldrup, et al. (9) $D_e/D_m= \theta_a^{2.5}/\theta_t$, which predicts a value of 0.102. The Penman relationship (10) $D_e/D_m= 0.66\theta_a$ predicts a value of 0.178 and the Millington and Quirk relationship (11) predicts a value of 0.093.

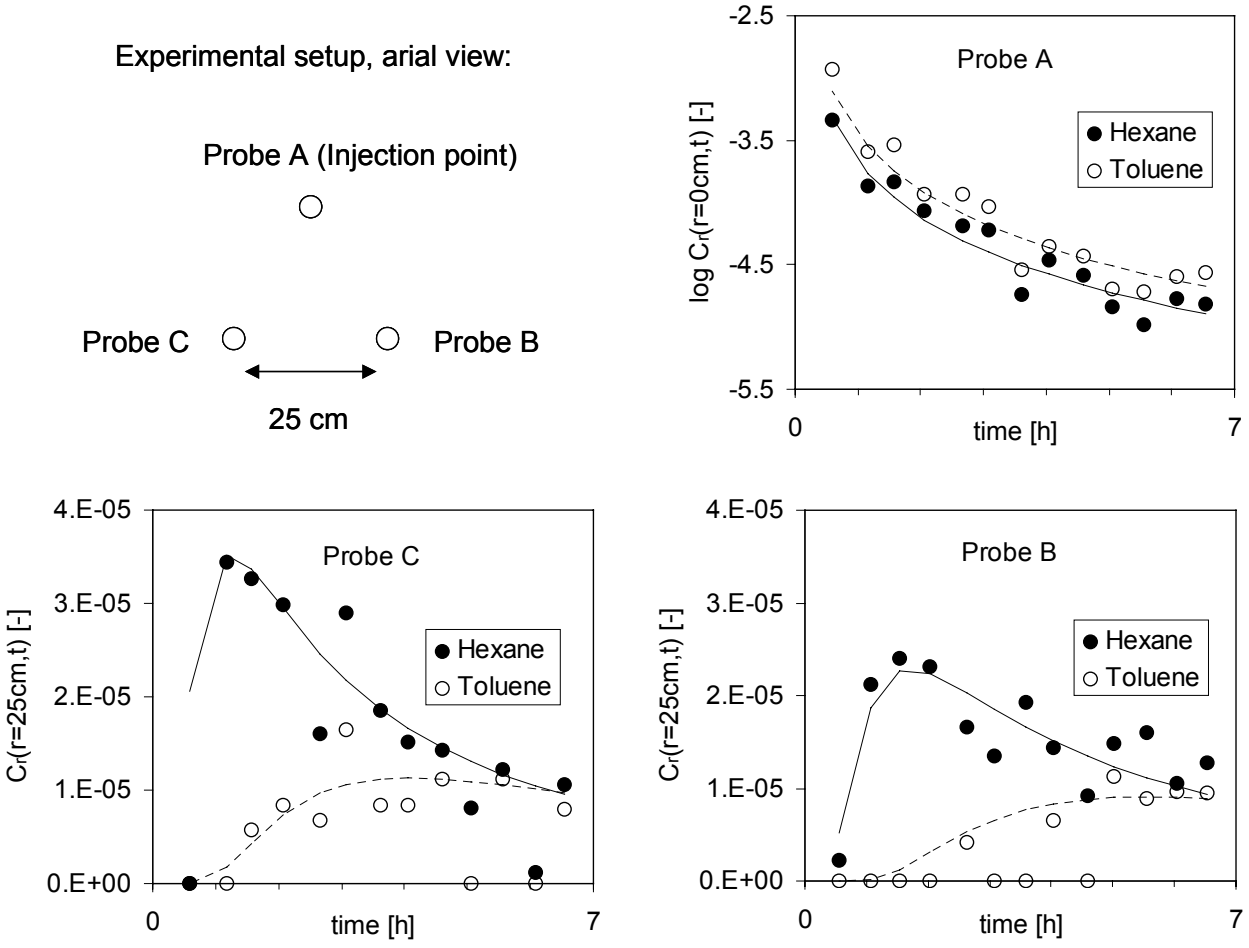

Figure 2: Measured relative concentrations for toluene and hexane at the injection point (Probe A) and two measured diffusive breakthrough curves in 25 cm distance (Probe B and C). Lines represent the fitted equations for diffusion in a homogeneous medium.

Table 1 - Tortuosity factor, effective diffusion coefficient, and VOC concentrations at different locations on day 102 after the source installation.

Distance from contamination [cm]	0	73	235	950
τ [-]	0.52±0.04	0.30±0.05	0.48±0.04	0.56±0.04
D_e/D_m [-]	0.14±0.01	0.08±0.01	0.13±0.01	0.15±0.01
Methyl-pentane [µg/ml]	0.08	0.029	n.d.	n.d.
n-Hexane [µg/ml]	0.15	0.059	0.003	n.d.
Methyl-cyclopentane [µg/ml]	0.30	0.115	0.017	n.d.
Isooctane [µg/ml]	9.1	3.22	0.12	n.d.

Volatile organic chemicals in the soil air samples could be detected simultaneously with the injected tracer CFC-12, because the GC column was connected both to an ECD and an FID. The concentrations of four VOCs, which emanate from the artificially embedded contamination, are reported in Table 1. It is worthwhile noting that the proposed method has the potential to quantify diffusive contaminant fluxes in the unsaturated zone by simultaneously measuring both the background soil gas concentrations and the effective diffusion coefficient in situ.

Toluene and hexane were injected into the glacial melt water sand at 10 m distance from the embedded contamination on day 360 through probe A. The measured concentration decline at the injection point (Probe A) is shown in Figure 2. From the measured relative concentrations $C_r(0,t)$ the mass fraction ratio $f_{a,toluene}/f_{a,hexane}$ can be calculated according to eq 3. As an average for the measurements at different times t one can obtain $f_{a,toluene}/f_{a,hexane}$ = 0.30±0.10. Measured diffusive breakthrough curves in 25 cm distance from the injection point are shown in Figure 2 for Probes B and C. The more volatile and hydrophobic compound hexane arrives before toluene. For the latter, gas-phase diffusion in the soil is slowed by partitioning into the soil water. Both compounds arrive at lower concentrations and later times at Probe B as compared to at Probe C. This suggests that the distance to the injection point was not exactly equivalent. It is possible that the probes were not emplaced perfectly vertically. As a result the distance between the tip of the probes may deviated from the 25 cm measured above ground. For each diffusive breakthrough curve the concentration maximum was determined by fitting the equation $(a/t^{1.5})\exp(-b/t)$ with a least square root procedure to the measured data, where a and b are the fitting parameters. From the times of the concentration maxima the ratio $f_{a,toluene}/f_{a,hexane}$ can also be obtained as described in (5), with $f_{a,toluene}/f_{a,hexane}$=0.29 for Probe B and $f_{a,toluene}/f_{a,hexane}$=0.28 for Probe C in good agreement with measurements at the injection point (Probe A).

Assuming negligible sorption for hexane ($f_{a,hexane}$=1), the mass fraction of toluene in the soil gas phase of the glacial melt water sand is estimated to be $f_{a,toluene}$=0.29 for a water-filled porosity θ_w of 0.10. This reduction in the mass fraction in the soil gas can almost entirely be explained by partitioning into the soil water. Sorption to the solids seems to be less important. This agrees with the findings of Wang, et al. (12) and Bjerre, et al. (6), who both report small K_d values of 0.02 and 0.04 [l/kg], respectively for toluene in the glacial melt water sand. Combining the measured f_a with an average tortuosity factor of 0.47, one calculates D_s/D_m= 0.14 for the ratio between the sorption-affected and the molecular diffusion coefficient of toluene at 15°C in the glacial melt water sand with θ_w=0.10.

In conclusion, the in situ measurements reported in this study confirm two findings of a laboratory column study (12): The effective diffusion coefficient D_e in the melt water sand is best described by the empirical relationship proposed by Moldrup et al. (9) and the sorption of toluene to the solids is less important than its partitioning into the water phase.

Acknowledgments

Financial support was provided by the Board of the Federal Institutes of Technology, and by the Swiss Federal Office for Education and Science (BBW No. 99.0412). The study was part of the European project *Groundwater risk assessment at contaminated sites GRACOS*, EVK1-CT-1999-00029. The authors thank Lone E. Holtegaard for assisting the field work and all other GRACOS partners for a pleasant cooperation.

References

E. N. Fuller, P. D. Schettler, J. C. Giddings, *Ind. Eng. Chem.* **58**, 19-27 (1966).

P. Grathwohl, *Diffusion in natural porous media : contaminant transport, sorption/desorption and dissolution kinetics* (Kluwer, Boston, 1998).

B. R. Scanlon, J. P. Nicot, J. M. Massmann, in *Handbook of soil sciences* M. E. Sumner, Ed. (CRC Press, Boca Raton, Florida, 2000) pp. A277-A319.

S. Batterman, I. Padmanagham, P. Milne, *Environmental Science and Technology* **30**, 770-778 (1996).

D. Werner , Swiss Federal Institute of Technology Lausanne, Ph. D. Thesis No. 2625 (2002).

T. Bjerre, L. E. Holtegaard, Masterthesis, Danish Technical University (2002).

M. Christophersen, M. Broholm, P. Kjeldsen, in *Proceedings of the 1st International Workshop on Groundwater Risk Assessment at Contaminated Sites (GRACOS)* D. Halm, Ed. (Tuebingen, 2002).

M. Christophersen, M. Broholm, H. Mosbaek, P. Kjeldsen, *Vadose Zone Journal* **in prep** (2003).

P. Moldrup, et al., *Soil Sci. Soc. Am. J.* **64**, 1588-1594 (2000).

H. L. Penman, *J. Agr. Sci.* **30**, 570-581 (1940).

R. J. Millington, J. P. Quirk, *Trans. Faraday Soc.* **57**, 1200-1207 (1961).

G. Wang, S. Brederode , P. Grathwohl, *Vadose Zone Journal* **submitted** (2003).

Method evaluation of soil pore-water concentration estimates of some volatile organic compounds and Phenanthrene

H. de Jonge[1], P. Moldrup[2], M. Kjærgaard[3], K. Dahlstrøm[4]

[1]*Danish Institute of Agricultural Sciences, Research Centre Foulum, Blichers Allé 20, 8830 Tjele, Denmark, Hubert.deJonge@agrsci.dk;*
[2]*Aalborg University, Dept. of Environmental Engineering, Sohngaardsholmsvej 57, 9000 Aalborg;*
[3]*GEO, Danish Geotechnical Institute, Saralyst Allé 52, 8270 Højbjerg, Denmark;*
[4]*Danish Environmental Protection Agency (Danish EPA),Ministery of Environment, Strandgade 29, 1401 København K.*

1. Introduction

Leaching risk from contaminated soils has traditionally been estimated from soil concentrations derived from soil samples in combination with phase exchange equilibrium (PEEQ) calculations (e.g. Danish EPA, 2002). Simple and robust methods are a prerequisite for regulatory purposes, and validation/improvements to the current methodologies are needed. The main objective of the present project was to compare a range of existing operational methods for estimating pore water concentrations (PWCs): soil sampling and soil concentrations (after pentane-extraction), pore-water sampling, pore-gas sampling, and a batch leaching test. These methods were compared under steady state conditions in laboratory column experiments, and in large outdoor lysimeters with different flow regimes. With respect to practical application of the different methodologies we will recommend some of them in order to improve risk assessment of contaminated sites.

2. Methods and materials

Three soil types were used, a sandy subsoil from Voldby, Denmark; a sandy loam subsoil from Røgen, Denmark; and a sandy subsoil from Tylstrup, Denmark (Table 1). Soil water retention curves of the three soils are shown in Fig 1. For the laboratory experiment, intact Voldby sandy subsoil columns (20 cm diameter × 40 cm height, steel) were collected by pushing the columns into the sediment using hydraulic pressure. For the lysimeter experiments, two large intact cores of the loamy, macroporous Røgen subsoil were collected in steel lysimeters (60 cm diameter × 100 cm height, steel) and placed on stainless steel funnels filled with coarse drain sand. In addition, two lysimeters were manually filled with Voldby subsoil.

Laboratory experiments
Two identical column flow systems were constructed. Constant input concentrations were maintained by mixing a saturated solution with a solute-free solution (Fig. 2). The saturated solution contained either free phase trichloroethylene (TCE) or free phase gasoline and an excess amount of phenanthrene. The calculated input concentrations for TCE and gasoline were 5% and 50% of the maximum solubility, respectively. The background electrolyte was 3 mM $CaCl_2$. Columns were irrigated at a constant rate of 10 mm/hr. Pilot experiments, without pore-water samplers, showed that steady state was reached in about 48 hr (data not shown).
Two sets of five column experiments, five TCE, five gasoline/phenanthrene, were irrigated at a constant flow rate of 10 mm/hr for 72 hr. In the first three experiments, a PTFE/quartz pore-water sampler was installed, and a stainless steel porous pore water sampler was installed in the final two experiments. After 72 hr irrigation, 100 ml input and output solution were sampled from closed loops

(Fig 2) into a 100 ml sample flask, 100 ml sample was obtained with the pore-water sampler into a 100 ml sample flask, and pore-gas was sampled through a small hole in the column wall at the bottom of the column. Then the soil columns were destructively sampled for pentane-extraction and a batch leaching test (Table 2).

Table 1. Soil physical parameters.

		Voldby sand	Tylstrup sand	Røgen sandy loam
Sand [g/g]		n.d.[1/]	0.81	0.65
Silt [g/g]		n.d.	0.15	0.17
Clay [g/g]		n.d.	0.04	0.15
Fraction organic C [g/g]		0.001	0.003	0.002
Ks [mm/day]		5902	1740	3.02 (matrix)
Retention curve: van Genuchten parameters[2/]	θ_s	0.400	0.424	0.328
	α	$3.13 \cdot 10^{-2}$	$1.06 \cdot 10^{-2}$	$6.88 \cdot 10^{-2}$
	n	2.72	2.399	1.194
Bulk density [g/cm^3]		1.59	1.40	1.70
Porosity [cm^3/cm^3]		0.40	0.47	0.36 ± 0.01

[1/] n.d. not determined, [2/] Van Genuchten, 1980.

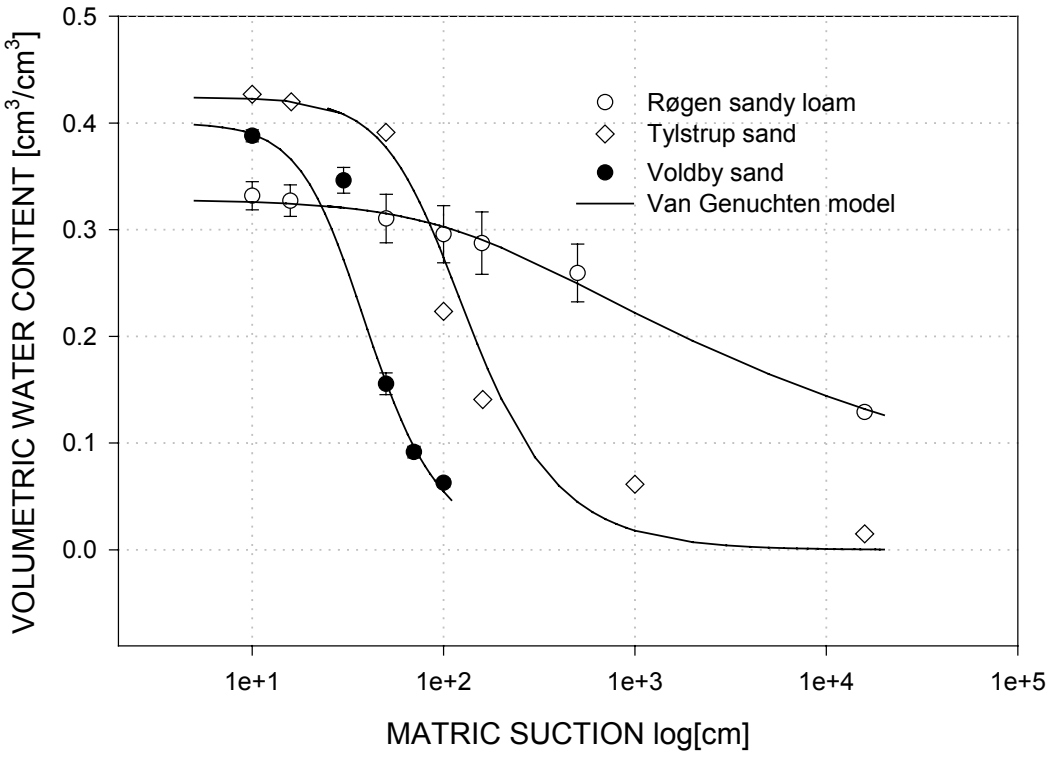

Figure 1. Soil water retention curves of the three soils used in the present study.

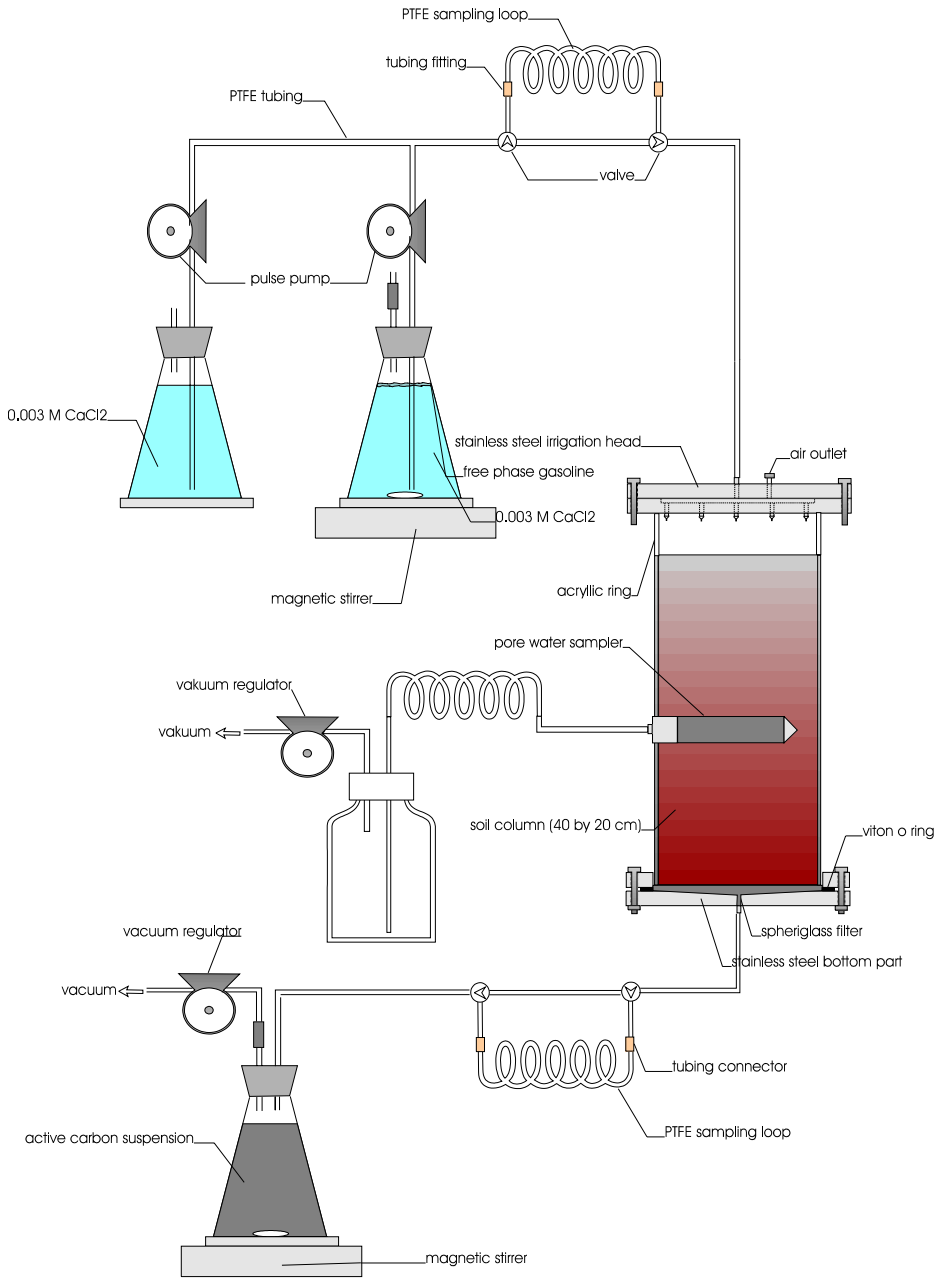

Figure 2. Column flow system used in the laboratory experiments. One system was used for TCE, one system was used for gasoline/phenanthrene leaching experiments.

Lysimeter experiments, first spiking

The top 40 cm of the two lysimeters filled with intact Røgen subsoil (R1, R2) was removed and repacked with Voldby sand (10-40 cm depth, bulk density 1.59 kg/dm^3). Two other identical steel lysimeters were packed with Voldby sand (10-100 cm depth, V1, V2, bulk density 1.62 kg/dm^3). The soils were covered with a 2 cm thick layer of pelleted active carbon, and a 10 cm thick layer with grass was placed on top. The lysimeters were spiked on September 3, 2001, by injecting either TCE or gasoline liquids at a depth of approximately 15 cm, at 26 gridpoints. The spiked amounts are shown in Table 3. The lysimeters were irrigated manually at weekdays and shielded from natural rainfall by an automated mobile roof construction equipped with rain detectors. A water balance was updated with weekly summed potential evapotranspiration, in order to attain a net water flux of 3 mm/day. Immediately after collection of the first effluent water, three pore-water samplers were installed at 90

cm depth (two steel, one PTFE). The soil from the boreholes was used for batch leaching tests. Effluent and pore-water samples were then collected at intervals of approximately 21 days. Three days before sampling of effluent, the funnel was closed. The last effluent sample before the second spiking was collected on the December 3, 2001.

Table 2. The tested methods for porewater concentration measurements.

Method	Description	Extraction	Analytical Detection
Reference	Direct sampling of influent (column experiments) and effluent solution (column and lysimeter experiments)	Pentane (liquid/liquid) or purge and trap	GC-FID (total hydrocarbons); GC-ECD (TCE), GC-MS (phenanthrene, BTX, MTBE, TCE)
Soil Pentane-extraction + PEEQ calculation	Soil sampling with auger (ca. 60-100 gr.). Mass balance calculation from soil-water-air phase equilibrium.	Pentane	Same as reference samples
Pore-water samplers	Constant vacuum method, PTFE and stainless steel lysimeters.	Pentane (liquid/liquid) or purge and trap	Same as reference samples
batch leaching test + PEEQ calculations	Soil sampling with auger (ca. 500 g), 4 hr shaking with 3 mM $CaCl_2$, soil:water 1:2 (w/w), colloid separation by 18 hr flocculation (0.1M $CaCl_2$). Mass balance calculation from soil-water-air phase equilibrium.	Pentane (liquid/liquid) or purge and trap	Same as reference samples
Pore-gas sampling + PEEQ calculations	Sampling of pore-gas with vacuum pump over active carbon tubes. Mass balance calculation from soil-water-air phase equilibrium.	Carbondisulfide	Same as reference samples

Lysimeter experiments, second spiking

The upper 40 cm of the four lysimeters was removed and repacked with Tylstrup sand, having a much higher water holding capacity than the Voldby sand (Fig. 1). This enabled us to create starting conditions with a high water content, thus reducing excessive volatilisation of spiked solutes from the surface. Before spiking, the soil was wetted up by three repeated manual irrigations of 50 mm each at 6, 5, and 4 days before the second spiking, respectively. The second spiking procedure (12 march, 2002) was similar as described above, except also methyl t-butyl ether (MTBE) was included (Table 3). Directly after spiking, all lysimeters received 50 mm water during a 6 hr time period. Twenty-four hr after spiking, the lysimeters were again irrigated with 50 mm water. Effluent and pore water samples were taken at intervals of approximately 10 and 20 mm outflow, respectively. However, the sampling frequency of the PTFE pore-water samplers was limited by the sampling rate at the applied vacuum (0.8 bar). After 72 hr, draining from the columns stopped. Three soil samples were taken from the lysimeters at 90 cm depth, and used for batch leaching tests.

Table 3. Lysimeter spiking levels and anticipated/measured effluent concentrations.

Lysimeter	Year /intensity	Parameter	TCE	Gasoline	MTBE
R1	2001/low	Spiked amount (g)	0	208	0
		PWC estimate (mg/L)[1/]	0	2144	0
		Concentration (mg/L)[2/]	0	0.93	0
	2002/high	Spiked amount (g)	0.43	208	0.43
		PWC estimate (mg/L) [1/]	3.31	2144	5.81
		Concentration (mg/L) [2/]	0.63	n.d.[3/]	11
R2	2001/low	Spiked amount (g)	4.37	0	0
		PWC estimate (mg/L) [1/]	33.1	0	0
		Concentration (mg/L) [2/]	0.59	0	0
	2002/high	Spiked amount (g)	4.37	20.8	4.37
		PWC estimate (mg/L) [1/]	33.1	214.4	58.1
		Concentration (mg/L) [2/]	2.94	n.d.	50
V1	2001/low	Spiked amount (g)	0	208	0
		PWC estimate (mg/L) [1/]	0	2843	0
		Concentration (mg/L) [2/]	0	0.64	0
	2002/high	Spiked amount (g)	0.43	208	0.43
		PWC estimate (mg/L) [1/]	4.49	2843	8.28
		Concentration (mg/L) [2/]	0.162	n.d.	0.56
V2	2001/low	Spiked amount (g)	4.37	0	0
		PWC estimate (mg/L) [1/]	44.9	0	0
		Concentration (mg/L) [2/]	0.02	0	0
	2002/high	Spiked amount (g)	4.37	20.8	4.37
		PWC estimate (mg/L) [1/]	44.9	284.3	82.8
		Concentration (mg/L) [2/]	2.47	n.d.	0.009

[1/] Estimation of pore-water concentration, assuming mixture of the compound over 0-100 cm depth, and using PEEQ calculations for phase distribution. Pentane was assumed to represent the PEEQ parameters of the gasoline mixture.

[2/] Heighest measured concentration, either in effluent, from suction cells or from batch leaching tests (dilution calculations).

[3/] Not determined. In the high flow campaign, FID total gasoline amount was not determined, instead individual BTX compounds were quantified.

Table 4. Solute parameter values used for PEEQ calculations.

Solute	Molar mass	Vapour pressure	Aqueous solubility	Log Kow	Koc[1/]
	[g/mol]	Pa	g/l		
Benzene	78.1	12700	1.76	2.1	22.1
Gasoline[2/]	72.2	70000	$4.1 \cdot 10^{-2}$	3.62	$8.41 \cdot 10^{2}$
MTBE	88.2	245	51.0	.94	1.37
phenanthrene	178.2	0.016	$1.2 \cdot 10^{-3}$	4.57	$8.18 \cdot 10^{3}$
TCE	131.4	9900	1.40	2.53	61.8

[1/] After Abdul et al. (1987).

[2/] The parameters of n-pentane were used as an approximation for the gasoline mixture.

Phase exchange equilibrium (PEEQ) calculations

PEEQ principles were used to estimate pore-water concentrations from soil concentrations, batch leaching tests and pore-gas concentrations. The worksheet program JAGG vers. 1.5 from the Danish EPA was used for this purpose. It is assumed that phase exchange between soil, pore-water, and air-filled pores is at equilibrium. Water-gas equilibrium is controlled by Henry law, and water-soil equilibrium is controlled by linear partitioning via K_{oc}. Solute parameters values used in these calculations are shown in Table 4. Also, bulk density, water content and total porosity are needed in such calculations. For the soil concentrations, we assumed that the concentrations represent mass retrieved from all the three phases (total soil). This concentration was distributed over the three phases, using PEEQ calculations and mass balance assumptions. For the concentration in the pore-gas samples it was assumed that all the mass retained on the sorbent tube was coming from the soil gas phase. This mass, together with the total volume of air sampled, was then used to approximate the PWC. For the batch leaching tests, PEEQ calculations must be performed twice. First, the total mass in the batch system was calculated from the eluate concentration. This mass was subsequently, analogue to the soil concentration, distributed over the three soil phases. Alternatively, we used a simple dilution approach were it is assumed that no mass exchange between different phases occurs during the sample handling and batch leaching test. A pore-water estimate can then be deducted from the soil:solute ratio, the concentration in the batch eluate and the soil water content.

3. Results and Discussion

Laboratory column experiments

The laboratory experiments represent "ideal" sampling conditions: steady state solute and water flow, a sandy soil without macropores, a low organic carbon content, and easy access for sampling. This was done to eliminate flow heterogeneity, sorption non-equilibrium and colloidal transport. All the tested methodologies underestimated the "true" PWC concentrations, as represented by the effluent concentrations from the soil columns (Fig. 3).

Steel pore-water samplers performed best under these conditions. Apparently, the porous steel was non-reactive with respect to all the tested solutes. By contrast, phenanthrene was not recovered with the PTFE/quartz pore-water samplers at all. We believe the porous material was reactive to highly non-polar substances such as phenanthrene. Also, the recovery of TCE and gasoline with PTFE/quartz samplers was relatively low with PTFE/quartz samplers.

PWCs from batch leaching tests were in the same order of magnitude for TCE and gasoline, however with a tendency to under-predict the pore-water concentration. For gasoline and TCE, the simple dilution approach yielded more close approximations than the PEEQ calculations. Phenanthrene PWC estimates from the batch leaching tests were highly inaccurate (Figure 3). PWC estimates from PEEQ calculations strongly under-predicted the effluent concentrations. This is the either caused by a misprediction of K_{oc}, or equilibrium conditions were not met during the batch leaching test. For phenanthrene, simple dilution calculations do not seem to be a useful alternative for PEEQ calculations. Our results are in line with other studies reporting that batch leaching prediction errors for PAHs (including phenanthrene) were generally higher than for volatiles (Danish EPA, 2001).

PWC estimates from soil pentane-extractions were very poor for gasoline and phenanthrene (Fig 3). By contrast, PWCs for TCE were quite well predicted with this method. We believe that soil pentane-extraction has a low recovery for gasoline and phenanthrene, causing the poor PWC estimates for these solutes. If volatilisation would have been the main course for under-prediction, TCE would have been affected to a similar extent, but this was not the case.

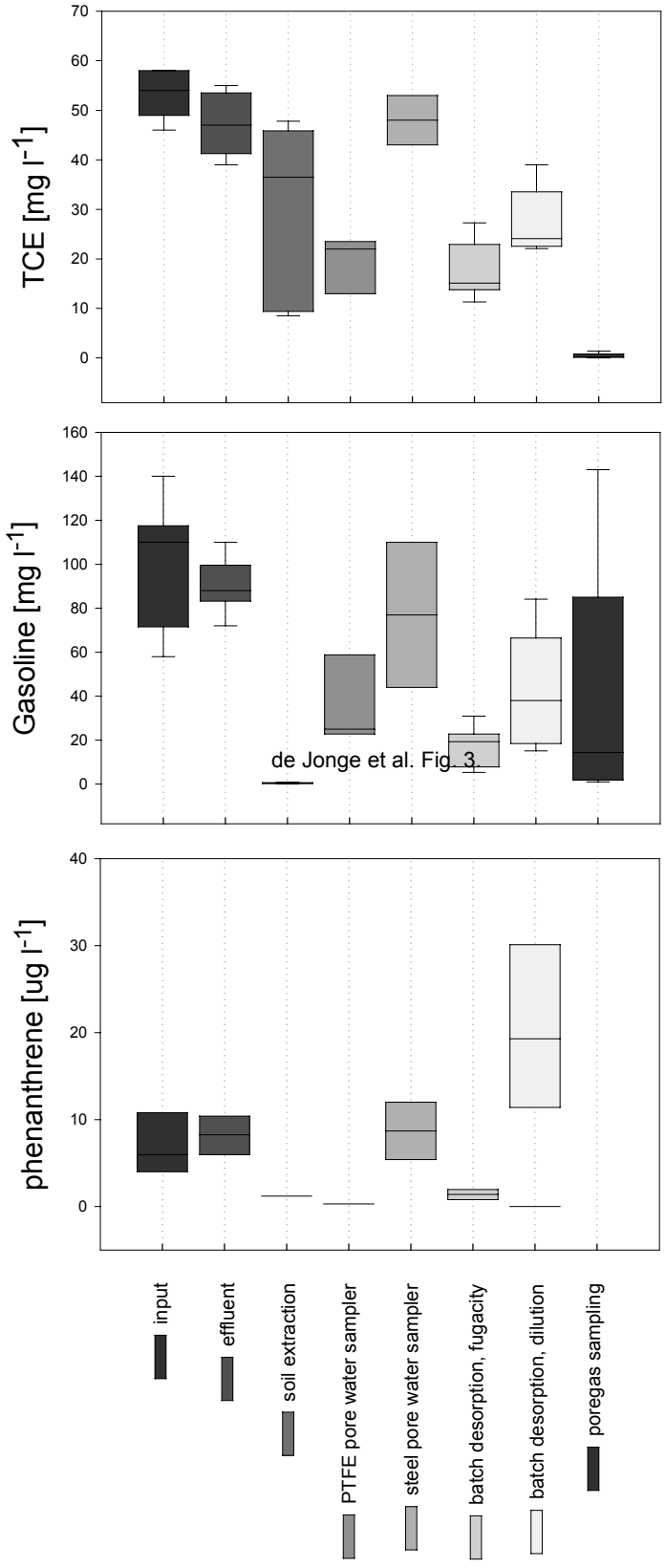

Figure 3. Results from laboratory column experiments. A direct comparison between influent/effluent concentrations and methods for PWC estimates.

Pore-gas sampling strongly underestimated TCE concentrations, while the gasoline PWC estimates varied over more than two orders of magnitude. The cause of this poor performance remains unknown. At present it is our speculation that the wet sampling conditions affected both the actual sampling volume, due to low air-filled pore connectivity, and also affected the sorption and/or recovery of the gas on the carbon tubes. Pore-gas sampling was therefore not included in the lysimeter experiments.

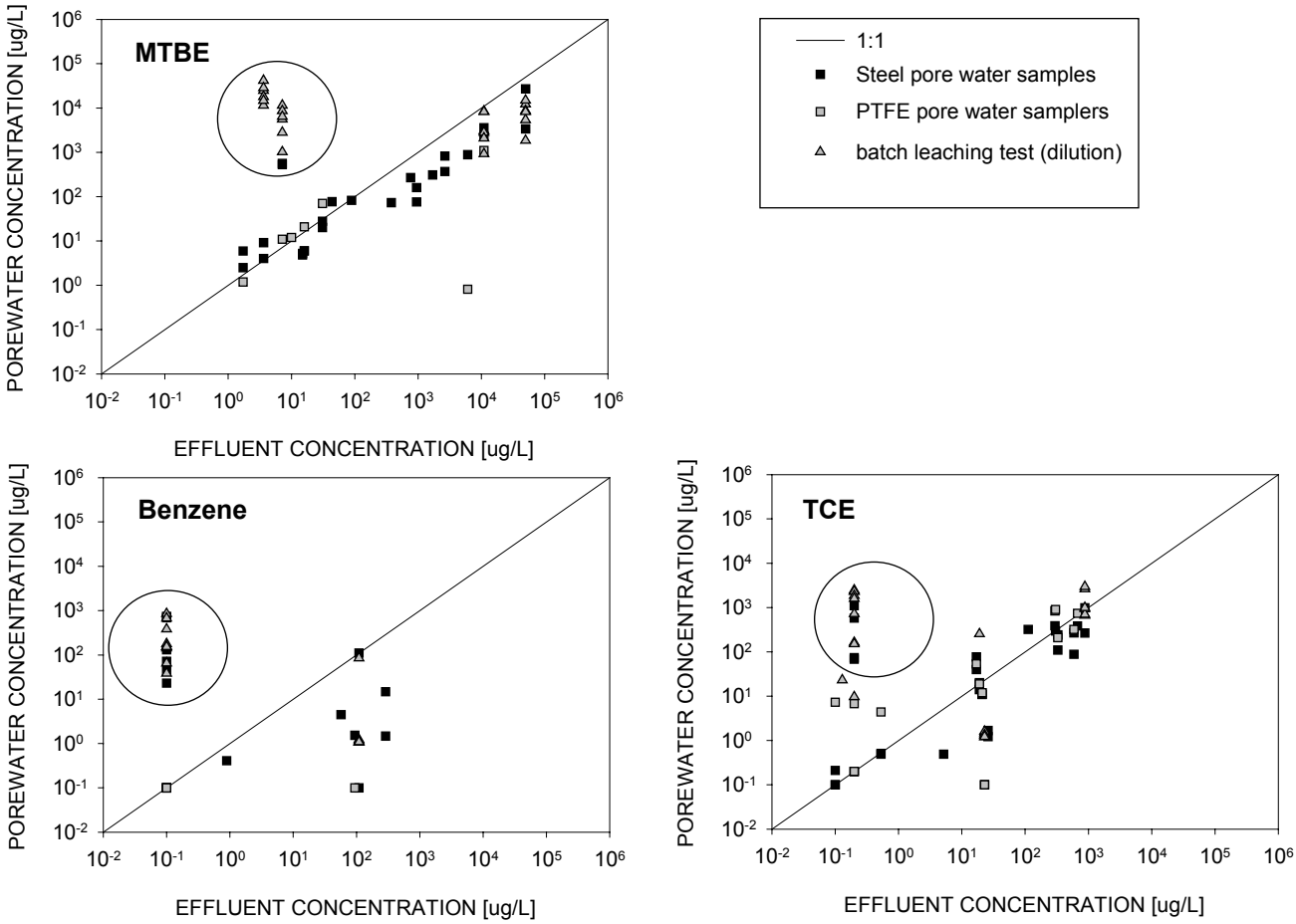

Figure 4. Results from lysimeter experiments for MTBE, benzene, and TCE, showing scatterplots of PWC estimates versus measured lysimeter effluent concentrations. The encircled data points refer to sampling events close to a steep concentration gradient in the sandy soil.

Lysimeter experiments

A priori calculated PWC estimates, using the spiked amounts for each solute and subsequent PEEQ calculations, were much higher than measured effluent concentrations (Table 3). The only exception was MTBE, the least volatile of the spiked test compounds (Table 4). The PEEQ calculations considered an instantaneous equilibrium distribution of the spiked solutes over the full depth of the lysimeter. In reality, transport of volatile compounds occurred both in the upward direction, leading to volatilisation loss, and in the downward direction, as combined gaseous diffusion and solute transport. Modelling exercises showed that under the first spiking conditions in 2001, 99% of spiked TCE mass might be lost by volatilisation within 200 to 1600 hr (data not shown).

Table 3 shows that the leaching rates were dependent on soil type and flow scenario. As may be expected, high flow conditions resulted in higher effluent concentrations. Perhaps more surprising, the

Røgen sandy loam subsoil leached at higher rates than the sandy subsoil (Voldby soil). We believe this was due to the higher water content in the clayey subsoil (≈30 vol%) than in the sandy soil (5-20 vol%), so that volatilisation losses were lower. Moreover, preferential transport in macropores occurred in the Røgen soil, because solutes were recovered in the first effluent collected after spiking.
Figure 4 shows scatter plots comparing PWC estimates with directly measured lysimeter effluent concentrations. Large deviations did occur, however, this was to be expected because macropore flow and dynamic temporal flow of both water and solutes affected the PWC estimates. Some of the very pronounced over-estimations (circled in the graph) were due to the high flow spiking and sampling scenario in the Voldby soil. Apparently, a steep solute front had reached the 90 cm depth from which the pore-water and the soil samples were taken, while this front had not yet reached the bottom of the lysimeters. This demonstrates, that in real site evaluations it may be difficult to estimate a representative flux concentration when steep concentration gradients occur.
MTBE concentrations were relatively closely approximated with pore water samplers and batch leaching tests. Both methods tended to under-predict MTBE concentrations in the Røgen soil, especially at higher concentrations. This may possibly be explained by higher flow velocity in macropores. However, such under-predictions were not observed for TCE (Fig 4). For TCE, the pattern was more erratic, especially under the high flow conditions of the second spiking event. This was partly due to steep concentration gradients in the sandy soils as discussed above. PTFE/quartz and steel pore-water samplers gave comparable results, in contrast to results from laboratory tests. Possibly, sorption to PTFE/quartz is dependent on the concentration levels of TCE. The batch leaching tests quite closely predicted TCE concentrations in the Røgen soil, and PEEQ calculations did not improve this prediction. The predictions for benzene (Fig 3) and other aromatics (data not shown) were very poor for both pore water samplers and batch leaching tests. Benzene has a higher vapour pressure than TCE and MTBE, and has a low aqueous solubility. This combination may have caused multi-phase flow rather than combined solute transport and gas diffusion.

4. Conclusion and recommendations

It has long been recognized that is difficult to calculate/measure the flux concentration in contaminated soils with respect to groundwater contamination risk. Provisionary results from the present study show that soil samples extracted for TCE and MTBE, in combination with PEEQ calculations, gave useful PWC predictions. By contrast, soil sampling followed by pentane- extraction for hydrocarbons (gasoline, PAHs) were found unsuitable due to low recovery.
Batch leaching tests gave useful results for volatiles (TCE, MTBE), with a tendency to under-predict the PWC. Much attention should be paid to avoid volatilisation during soil sampling. Batch leaching tests with phenanthrene, in combination with PEEQ calculations, resulted in strong under-predictions of the PWC. The method is very sensitive to the attainment of sorption equilibrium, both in the soil and in the batch system. The degree in which the contaminated soil system in accordance with the PEEQ assumptions, will depend on soil type, flow regime and contamination history.
Pore-gas sampling for TCE and gasoline is not recommended for risk analysis in field-moist soils, as the method is both imprecise and irreproducible, even under ideal test conditions such as in the present study.
Steel pore-water samplers gave consistent and accurate results for phenanthrene, gasoline, TCE and MTBE. Teflon/quartz samplers can be used for TCE and MTBE, and gasoline compounds, but this technique was not found suitable for phenanthrene due to strong sorption to the sampler material. If precise and longer-term monitoring results are needed, pore-water samplers are recommended. However, for practical purposes the method is labour intensive. During dry periods, long sampling periods are foreseen. Many samples may be required when temporal dynamics are anticipated close to a hot spot source area in order to collect representative data. For other solutes than the ones tested in the presents work, a test for sorption to the pore-water sampler should always be made beforehand.

It is important to recognise, that the methods that were not recommended (soil analysis for gasoline, phenanthrene, pore-gas analysis) may yield under-predictions by several order of magnitude. The recommended methods (pore-water samplers, batch leaching test, soil pentane-extraction for TCE) will yield at best "order of magnitude" estimates. Both under- and over-predictions must be anticipated, depending on spatial variation, flow regime, sorptive strength of the contaminant, and contamination history. More precise determination of a long-term pore water concentration would require a large number of chemical analyses and a higher survey budget.

5. References

Abdul, A.S., T.L. Gibson, and D.N. Rai, 1987. Statistical correlations for predicting the partition coefficient for nonpolar organic contaminants between aquifer carbon and water. Hazard. Waste and Waste Mater. 4: 211-222.

Danish EPA, 2002. Guidelines on Remediation of Contaminated Sites. Environmental Guidelines No. 7, Copenhagen, Denmark.

Van Genuchten, M.T., 1980. A closed-form equation for predicting the hydraulic conductivity of unsaturated soils. Soil Sci. Soc. Am. J. 44 (5): 892-898.

Danish EPA, 2001. Miljøprojekt, 579; Teknologiudviklingsprogrammet for jord- og grundvandsforurening . Udvikling af metode til testning af udvaskning af organiske stoffer fra jord og restprodukter (In Danish).

Acknowledgements

The Danish EPA, Technology Programme for Soil and Groundwater Contamination, financed this study. Technical support from Finn Christensen, Palle Jørgensen, Stig Rasmussen, Finn Gade, and Grethe Pedersen is gratefully acknowledged.

Using a passive multi-layer sampler (MLS) for measuring detailed profiles of gas-phase VOCs in the unsaturated zone

Ellen R. Graber[1], Yael Laor[2], Daniel Ronen[3]

[1]*Corresponding author: Institute of Soil, Water and Environmental Sciences, The Volcani Center, Agricultural Research Organization, P.O.B 6, Bet-Dagan, Israel, 50250; tel. 972-3-968-3307; fax. 972-3-960-4017; E-Mail: ergraber@volcani.agri.gov.il.*

[2] *Institute of Soil, Water and Environmental Sciences, Agricultural Research Organization, Newe Ya'ar Research Center, P.O.B. 1021 Ramat Yishay 30095, Israel. Tel. 972-4-953-9539; E-mail: laor@volcani.agri.gov.il*

[3]*Water Quality Division, The Water Commission, Rehov HaMasger 14, Tel Aviv 61203, Israel, and Ben Gurion University, Israel; danronen@bgumail.bgu.ac.il*

Abstract: The purpose of this study was to test in the laboratory and the field the performance of a passive multi-layer sampler (MLS) for obtaining detailed profiles of gas-phase volatile organic compounds (VOCs) in unsaturated sediments. The sampling principle is based on passive equilibration of the unsaturated zone gas phase with water in dialysis cells. After testing the required equilibration time in the laboratory (about 50h), results of a large container (210L) experiment show that trichloroethene (TCE) concentrations obtained by the MLS deployed inside a well screen corresponded very well to the profile obtained by dialysis cells buried in the sediment. A field profile taken at the saturated-unsaturated interface region (SUIR) of a VOC-contaminated area using the MLS shows steep TCE concentration gradients (1,119 μg TCE/L-air/cm) in the gas phase of the unsaturated zone just above the water table. Such details and gradients can only be detected under passive sampling conditions. This unique feature makes the MLS an especially useful tool for exploring vapor transport behavior during water table fluctuations and for measuring with great detail VOCs in the saturated and unsaturated zones simultaneously in one borehole.

1. Introduction

Volatile organic compounds (VOCs) introduced into the unsaturated zone of an aquifer via spills or by volatilization from contaminated groundwater may be transported as vapors, creating widespread gas plumes (e.g., *1-6*). In general, vapor phase transport may be an important cause of subsurface contamination for any VOC having a Henry's constant (K_H) of at least 50 Pa-m^3/mol and a vapor pressure ≥130 Pa at ambient temperature (*7*). To correctly estimate vapor fluxes across the soil/atmosphere and saturated zone/unsaturated zone interfaces, it is important to know the concentration distribution of VOC vapors in the unsaturated zone and to understand the mechanisms controlling vapor transport through it and across both interfaces.

A passive multilayer sampler (MLS) developed for obtaining detailed chemical profiles in groundwater at a vertical resolution of less than 3 cm (*8, 9*) was evaluated in this study for obtaining gas phase VOC profiles in porous media. The express purpose was to test the accuracy at which the VOC profile obtained with the MLS inside a monitoring well represents the VOC profile in the gas phase of the surrounding sediment. This was tested using trichloroethene (TCE) as a model VOC. VOC profiles through the saturated/unsaturated interface region (SUIR) at a VOC-contaminated site were then obtained using the MLS. This extended abstract summarizes the results of Laor et al. (2003; *10*).

2. Experimental Methodology

Multi Layer Sampler (MLS). The MLS used in the present study consists of individual units that can be attached in a modular fashion (Fig. 1). Each unit has a stainless steel frame into which stainless steel dialysis cells are inserted at right angles to each other. Flexible Teflon-lined Viton seals that fit the inner diameter of the well screen separate between consecutive cells. For obtaining a groundwater profile or a profile of gases from the unsaturated zone, the cells are filled with distilled water and are closed at both ends with a dialysis membrane. The sampler is lowered into an observation well and retrieved from it after a given time interval (usually several weeks), and the chemical composition of the water in each dialysis cell is then determined.

In the unsaturated zone, gases will partition between the gas phase of the nearby sediment, and water inside the dialysis cell. After equilibration, concentrations of VOCs measured in the water of each dialysis cell are used to calculate concentrations in the gas phase of the unsaturated zone according to Henry's law.

General Experimental Framework. The rate of attainment of equilibrium between TCE vapor and water in the dialysis cells was studied in closed glass jars. Two jar setups were used: (i) dialysis cells emplaced in jars without any porous matrix, and (ii) dialysis cells embedded in air-dry packed sand. Gas phase profiles of TCE in granular sediments were then obtained using dialysis cells embedded in open glass cylinders packed with various porous media. A TCE gas profile was also obtained inside a large container to test the performance of the MLS inside a screened pipe for obtaining a vapor phase profile that accurately represents the TCE gas-phase profile of the surrounding unsaturated porous media. After these laboratory tests, the MLS was deployed in a monitoring well to measure a TCE gas profile in the region of the saturated-unsaturated interface (SUIR) at a site contaminated with chlorinated solvents.

3. Results and Discussion

Equilibration of dialysis cells with VOC vapors in jar experiments. The results of equilibration experiments are presented in Fig. 2. Average equilibrium concentration of TCE in the cells was 1,349 mg/L-water (st.dev. = 43.8 mg/L-water for the last 4 data points in Fig. 4a), corresponding to 540 (±17.5) mg/L-air, using an average K_H* of 0.40. According to Fig. 2a, equilibrium between gas and water phase TCE (ratio of concentration at time t (C_t) to concentration at equilibrium (C_e) of unity; C_t/C_e =1) was achieved after about 50 hr, whereas a value of C_t/C_e = 0.95 was reached after 24 hr (Fig. 2a inset). A similar equilibration period for TCE vapors was observed in the dry sand-filled jar as compared with the air-filled jar (Fig. 2b). The results of these experiments show that the dialysis cells are suitable for evaluating gas-phase concentrations of VOCs after an appropriate equilibration period is determined empirically in the laboratory.

Diffusion profiles in sand-packed open cylinders. Data obtained in the experiments conducted in sand-packed open glass cylinders are presented in Fig. 3 with aqueous TCE concentrations in the dialysis cells on the lower x-axis and gas phase concentrations on the upper x-axis. As shown in Fig. 3a, TCE gradients obtained between 47.5 and 117h were quite similar. Since attainment of equilibrium between the gas phase and the water in the dialysis cell required about 50 hours (Fig. 2a), we can assume that steady state gas profiles were developed in the cylinders relatively fast. The profiles presented in Fig. 3a are linear (r^2>0.99), as expected according to Fick's first law.

Figures 3b and 3c depict TCE profiles obtained in open cylinders packed with heterogeneous porous media. The TCE concentration gradient was slightly changed when a 3.5 cm layer of

wet coarse sand (θ_{gr} = 4.0%; 74% of field capacity) was located between two layers of dry coarse sand. In contrast, an abrupt change in the gas phase TCE profile was observed when the cylinder was packed with a wet sandy-loam soil layer (θ_{gr} = 17.5%; 83.7% of field capacity) located between two dry coarse sand layers (Fig. 3c). Adopting the theoretical approach taken by Millington (*13*) for the relationship between τ_g, total porosity (θ_T) and average gas-filled porosity (θ_g; $\tau_g = \theta_g^{(7/3)}/\theta_T^2$), we estimated tortuosity factors of 0.73 for the dry coarse sand ($\theta_g = \theta_T = 0.39$), 0.48 for the wet coarse sand ($\theta_g = 0.33$; $\theta_T = 0.40$), and 0.037 for the wet sandy-loam ($\theta_g = 0.11$; $\theta_T = 0.41$). As such, the effective diffusion coefficient (D_{eff}) through porous media, $D_{eff} = D_{air}\ \tau_g$, (where D_{air} is the free-air diffusion coefficient) for the dry coarse sand is calculated to be about 1.5 times greater than D_{eff} of wet sand, and about 20 times greater than D_{eff} of the wet sandy-loam layer.

The profiles presented in Fig. 3 demonstrate the suitability of dialysis cells embedded in unsaturated porous media to capture abrupt changes in concentration gradients of VOC vapors on a scale of centimeters.

Large container experiment. The results of the container experiment are presented in Fig. 4. Open squares represent average TCE concentrations in air obtained for triplicate cells buried in the sediment at the same depth. The vapor phase TCE profile obtained with the MLS (filled squares) is seen to be in good agreement with the profile obtained from the buried dialysis cells. As in the open glass cylinder experiment depicted in Fig. 3c, the wet sandy-loam layer in the middle of the container (θ_{gr} = 16.8%; 80% of field capacity) created an abrupt change in the TCE gas phase concentration gradient. Note that in the container experiment one of the MLS dialysis cells was located at the depth of the sandy-loam layer. TCE concentration in this cell reflects the expected TCE trend and clearly demonstrates the sensitivity and suitability of the MLS for obtaining detailed and accurate gas profiles. Results show that the gas profile obtained with the MLS inside the well reflects the gas profile in the surrounding porous media (Fig. 4).

*Field profile***.** A field profile of the SUIR obtained at the contaminated Coastal Plain aquifer of Israel in the Tel-Aviv area is depicted in Fig. 5. Above the water table, the concentrations of TCE are given both for TCE dissolved in water of the dialysis cells and for the corresponding calculated gas phase concentrations. The highest TCE concentrations (310,000 μg/L-water, corresponding to 124,000 μg/L-air) were detected 14 cm above the water table, decreasing with distance from the water table both in the unsaturated zone (to 150,000 μg/L-water; 60,000 μg/L-air, 72 cm above the water table) and in the saturated zone (to 43,000 μg/L-water, 304 cm below the water table). Fig. 5 is shown as an example to illustrate the type of detailed information that might be obtained with the MLS.

4. Conclusions

The exclusive feature of the MLS for measuring vapor phase VOC concentrations relies on its suitability for measuring with great detail VOCs in the saturated and unsaturated zones simultaneously in one borehole. Using the MLS, each dialysis cell is a continuous passive sampling system where the concentration will change according to the concentration in both the gas and liquid phases in the cell vicinity. In the example presented in Fig. 5 note the possibility of: (1) detecting steep TCE concentration gradients in the gas phase of the unsaturated zone (1,119 μg TCE/L-air/cm) within a vertical distance of only 57 cm, and (2) obtaining a continuous TCE profile across the SUIR and into both the unsaturated and saturated zones. Such details and gradients can only be detected under passive sampling conditions. This unique feature makes the MLS an especially useful tool for exploring vapor

transport behavior during water table fluctuations, and for measuring VOC concentrations simulataneously in the saturated and unsaturated zones in a single borehole.

5. Figures

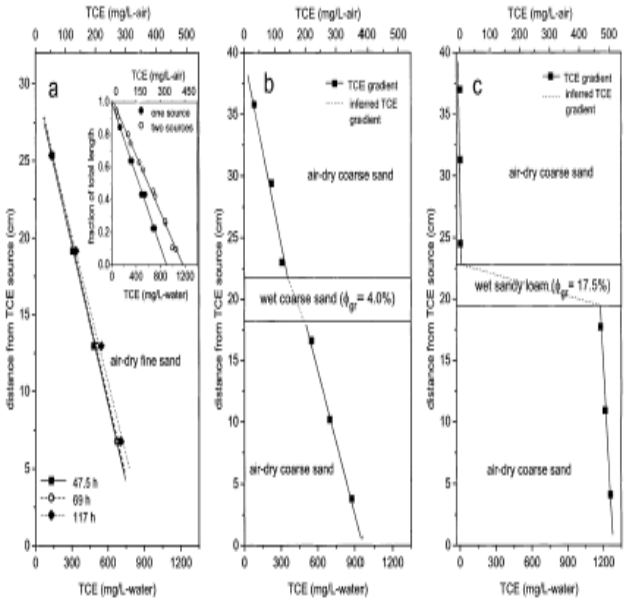

Fig. 3. Profiles of vapor phase TCE obtained in sand-packed open glass cylinders. (a) Profiles obtained after 47.5h, 69h and 117h in fine air-dry (b) Wet coarse sand layer between two layers of coarse air-dry sand; (c) Wet sandy-loam lay between layers of coarse air-dry sand.

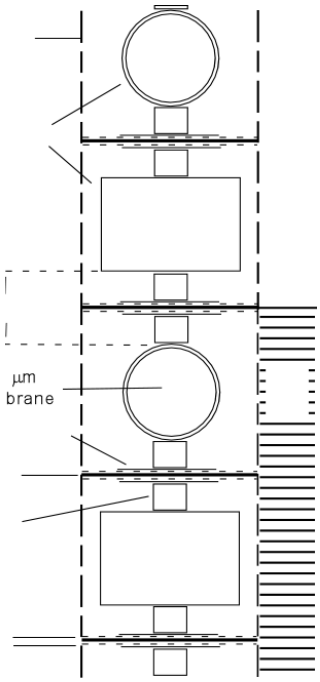

Fig. 1. Schematic representation of a section of a multilayer sampler (MLS

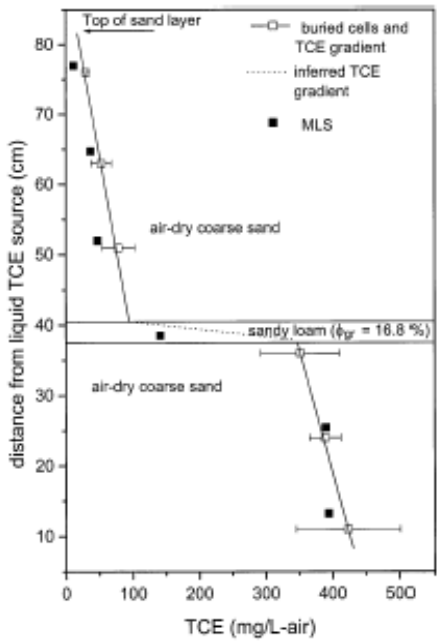

Fig. 4. TCE profile obtained in large container experiment. Bold squares denote results of double-cells located inside the well screen (MLS). Empty squares and horizontal bars denote average concentration and standard deviation of three cells embedded at the same depth in the container.

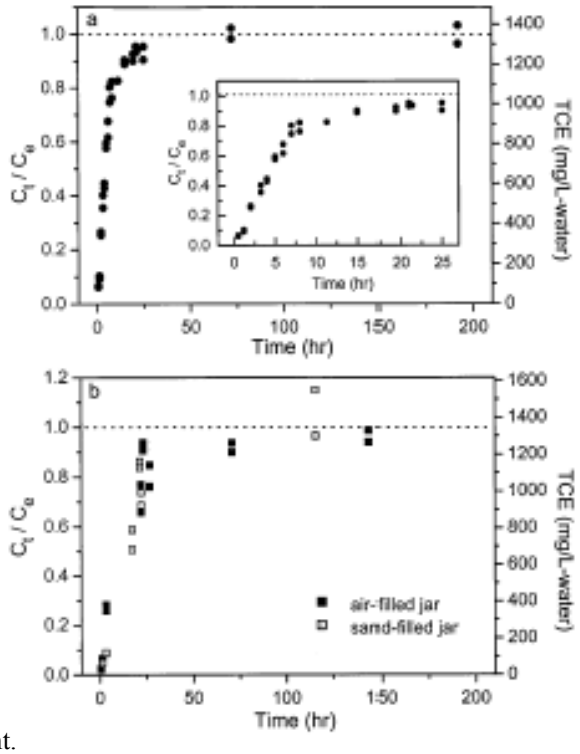

Fig. 2. Equilibration of dialysis cells with TCE and naphthalene vapors (a) TCE-Air-filled jars; (b) TCE-Sand-filled jars.

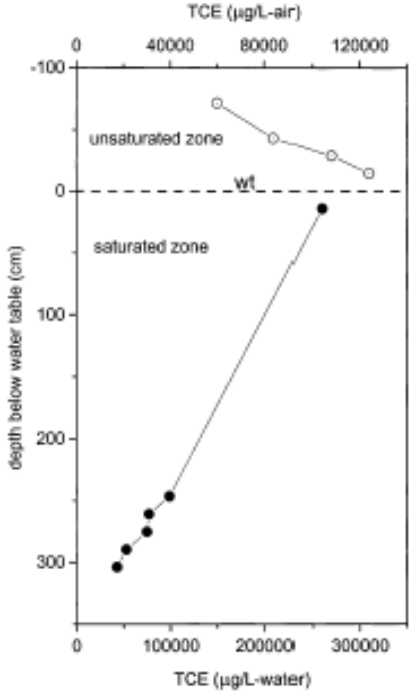

Fig. 5. TCE profile obtained with a MLS at the SUIR of the Coastal Plain aquifer of Israel in the Tel-Aviv area. The bold circles represent TCE concentrations (µg/L-water) obtained below the water table (wt). The open circles depict concentrations above the water table and the upper horizontal scale shows the corresponding TCE gas-phase concentrations (µg/L-air) in equilibrium with the dialysis cells in the unsaturated zone.

6. References

1. Marrin, D.L.; Thompson, G.M. *Ground Water* **1987,** *25*, 21-27.
2. Mendoza, C.A.; McAlary, T.A. *Ground Water* **1990,** *28*, 199-206.
3. Pouisen, M.M.; Kueper, B.H. *Environ. Sci. Technol* **1992,** *26*, 889-895.
4. McCarthy, K.A.; Johnson, R.L. *Water Resour. Res.* **1993,** *29*, 1675-1683.
5. Amali, S.; Rolston, D.E.; Yamaguchi, T. *J. Environ. Qual*. **1996,** *25*, 1041-1047.
6. Conant, B.H.; Gillham, R.W.; Mendoza, C.A. *Water Resour. Res*. **1996,** *32*, 9-22.
7. Marrin, D.L. *Ground Water Monitoring Rev.* **1988,** *8,* 51-54..
8. Ronen, D.; Magaritz, M.; Levy, I. *Water. Res*. **1986,** *20,* 311-315.
9. Kaplan, E.; Banerjee, S.; Ronen, D.; Magaritz, M.; Machlin, A.; Sosnow, M.; Koglin, E. *Ground Water*. **1991,** *29,* 191-198.
10. Laor, Y. Ronen, D, Graber, E.R. **2003**, *37*, 352-360.
11. Graber, E.R.; Ronen, D.; Elhanany, S. Assesment of aquifer contamination in the Nahalat Itzhak Area – Tel Aviv, Interim Report I, March, **2000**.
12. Graber, E.R.; Ronen, D; Elhanany, S. Assesment of aquifer contamination in the Nahalat Itzhak Area – Tel Aviv, Interim Report II, Sept, **2000**.
13. **Millington, R.J. *Science*, 1959, 130, 100-102.**

KEY NOTE: Estimation of the multiphase transport coefficients of fractures from transient experimental data of immiscible and miscible displacement

C. D. Tsakiroglou*, M. Theodoropoulou, V. Karoutsos, D. Papanicolaou

*Corresponding author: Institute of Chamical Engineering and High Temperature Chemical Processes - Foundation for Research and Technology Hellas
Stadiou Street, Platani, P.O.Box 1414, GR-26504 Patras, Greece
Phone: 30 2610 965212; Fax: 30 2610 96522; E-Mail: ctsakir@iceht.forth.gr

Abstract: The multiphase transport coefficients of porous and fractured media (e.g. relative permeabilities, hydrodynamic dispersion coefficients) are complex functions of the pore space morphology, dimensionelss flow parameters (e.g. capillary number, Peclet number, etc) and fluid properties (e.g. rheology, wettability, etc). The determination of reliable values for these coefficients is a prerequisite for running the macroscopic contaminant transport simulators, which are used as predictive tools in the risk assessment of contaminated soils and aquifers. Experimental data of the immiscible displacement of a wetting aqueous phase by a non-wetting NAPL of Newtonian or non-Newtonian rheology are introduced into a history matching scheme for the numerical estimation of the capillary pressure and relative permeability curves of artificial fractures as functions of the capillary number and NAPL rheology. The temporal evolution of the solute concentration profiles measured in different types of solute dispersion experiments, performed on artificial fractures, are fitted with analytical models for the estimation of the longitudinal and transverse dispersion coefficients as functions of Peclet number.

1. Introduction

Immiscible displacement experiments performed on artificial porous media (Lenormand et al., 1988; Avraam and Payatakes, 1995) as well as pore network simulations (Blunt and King, 1991; Vizika et al., 1994; Aker et al., 1998) have revealed that relative permeability and capillary pressure functions depend not only on the specific characteristics of the pore space morphology but also on a variety of dimensionless parameters such as the capillary number, viscosity ratio, wettability, etc. The estimation of relative permeability and capillary pressure functions from laboratory measurements may be based on steady-state experiments of the simultaneous flow of two phases through the porous medium or unsteady-state experiments of the immiscible displacement of the one fluid by the other. Although accurate and explicit, the steady-state methods are time consuming and expensive. In unsteady-state methods, the effective transport coefficients are estimated either explicitly from measured data (Johnson et al., 1959) or implicitly from the history-matching of the temporal evolution of pressure drop / fluid production / fluid saturation profile (Jennings et al., 1988; Chardaire-Riviere et al., 1992; Kulkarni et al., 1998). Although it is well-known that the transient displacement patterns in a porous medium are strongly correlated with the capillary number, the dependence of the implicitly estimated multiphase flow coefficients (history matching) on the flow rates have been overlooked.

A great deal of experimental work has been focused on the determination of the hydrodynamic dispersion coefficients as function of the Peclet number by using a variety of techniques (acoustic, NMR, CT-Scan, radioactive tracers, etc) for the measurement of the transient changes of solute concentration (Ding and Candela, 1996; Peters et al., 1996; Drazer et al., 1999; Manz et al., 1999). The dispersion of dissolved contaminants in fractured rocks

and soils (Adler and Thovert, 1999) depends strongly on the variability of the fracture aperture, and large fracture aperture regions result in significant channelling of the fluid flow. Visualization dispersion experiments performed on transparent model porous media of regular morphology (Charlaix et al., 1987; Didierjean et al.,1997) and artificial fractures (Detwiller et al., 2000) are useful not only for the quantification of the dispersion coefficients as functions of Peclet number and structural properties of the pore space, but also for the identification of the dispersion flow regimes, the understanding of small-scale effects on the macroscopic coefficients and the evaluation of models and numerical simulators.

In the present work, visualization experiments of the immiscible or miscible displacement, performed on artificial glass-etched single fractures, provide data concerning the transient changes of the fluid saturation or the solute concentration distribution across a fracture. Numerical codes based on non-linear (Bayesian) estimation, are used to fit the experimental data to numerical or analytical models and estimate the relative permeability / capillary pressure curves or the hydrodynamic dispersion coefficients as functions of pertinent parameters.

2. Methods and materials

Artificial single fractures were fabricated by etching mirror image patterns of two different pore networks, M-1 (of narrow pore width distribution) and M-2 (of wide pore width distribution), on two glass plates with hydrofluoric acid, and sintering the pre-aligned etched plates in a programmable furnace. The cross-sections of pores have elliptical shape and the statistics of the pore major and minor axis length was estimated from the input distribution functions of the original pattern and experimental values of absolute permeability (Theodoropoulou et al., 2001).

Paraffin oil was used as a non-wetting Newtonian NAPL. Synthetic inelastic and time-independent non-Newtonian NAPLs were prepared by dissolving ozokerite (natural mineral wax) at varying concentrations in paraffin oil. The shear viscosity of NAPLs was measured as a function of the shear stress with a Dynamic Stress Rheometer (SR-200, Rheometrics Inc.) and was fitted to a mixed Meter-and-power law fluid model (Tsakiroglou, 2002). Drainage experiments were performed on artificial fracture M-1 under controlled values of the capillary number ($Ca = \mu_{nw} u_{nw} / \gamma_{ow}$) and viscosity ratio (Theodoropoulou et al., 2001) by using Newtonian (paraffin oil) and non-Newtonian NAPLs as well. At each experiment, the transient flow patterns, namely the spatial and temporal evolution of the NAPL distribution within a central region of the pore network was analyzed by recording short-cuts of the displacement and measuring the NAPL saturation distribution across the pore network at various times with the aid of ScanPro 5.0 image analysis software. For the non-Newtonian NAPLs, an apparent viscosity, $\mu_{nw,app}$, was determined from Darcy's law, and used in the calculation of the capillary number.

A technique was developed for the measurement of the transient changes of the solute concentration distribution throughout the pore network (Tsakiroglou et al., 2002a; Theodoropoulou et al., 2003). The technique was based on the detection of color changes caused on a dilute HCl aqueous solution during its mixing with a dense HCl solution. The color of indicators contained in traces in both solutions was so sensitive to the pH of the solution that even a small change in solute concentration caused detectable changes in the color intensity of solution. Regarding the resolution of the technique, it's worthwhile noting that eighteen colours were able to be distinguished within the full range of solute concentrations used in experiments. An efficient algorithm was developed in the environment

of Scan Pro 5.0 (SPSS) for the automatic identification of the pore space and solid matrix, recognition of the boundaries of unit cells and measurement of the intrinsic average colour intensity of each unit cell over each region. Afterwards, with the aid of calibration curves, the colour intensities were converted to solute (HCl) concentrations. The contours of equal solute concentration were determined for miscible displacement experiments (where the low solute concentration solution initially occupying the pore space was being displaced by the high solute concentration solution), performed on fracture M-2, and single source-solute transport experiments (where a high solute concentration solution was being injected at a very flow rate through a hole into a low solute concentration solution flowing steadily through the pore network), performed on fracture M-1, under varying values of Peclet number.

3. Parameter estimation

The fractional flow equations describing the one-dimensional immiscible displacement of a wetting aqueous phase by a non-wetting NAPL in a porous medium (Sahimi, 1995) were properly adapted to non-Newtonian NAPLs by extending a single-phase flow non-Darcian model (Tsakiroglou, 2002) to two-phase flow (Tsakiroglou et al., 2002b). Corey type parameteric models were used to represent the capillary pressure, $P_c(S_{nw})$

$$P_c = P_c^0\left(1-\frac{S_{nw}}{1-S_{wi}}\right)^{-m} \tag{1}$$

and relative permeability curves, $k_{rw}(S_{nw})$ and $k_{rnw}(S_{nw})$

$$k_{rw} = k_{rw}^0\left(\frac{1-S_{nw}-S_{wi}}{1-S_{wi}}\right)^{n} \qquad k_{rnw} = k_{rnw}^0\left(\frac{S_{nw}}{1-S_{wi}}\right)^{l} \tag{2}$$

The two-phase immiscible displacement is an initial-boundary value problem, and the macroscopic fractional flow equations constitute a mixed system of algebraic and partial differential equations. For the numerical solution of this system, the PDAPLUS solver of ATHENA (Caracotsios and Stewart, 1995) software package was used by selecting a finite difference discretization scheme for the space coordinate. For the estimation of the parameters of relative permeability and capillary pressure functions, the stochastic Bayesian estimator of GREGPLUS solver of ATHENA software (Stewart and Caracotsios, 1992) was used by fitting the numerical predictions of PDAPLUS to the experimental transient saturation profiles (Tsakiroglou et al., 2003).

The transient evolution of the spatial distribution of the solute concentration in the pore network of a single fracture is expressed by the convection-dispersion equation by assuming one-dimensional flow at constant velocity. A generalized analytic solution of this equation was obtained for solute transport from multiple sources in a porous medium extending to infinity along flow direction and having impervious lateral boundaries (Theodoropoulou et al., 2003). The dispersion coefficients were estimated separately for miscible displacement and single source-solute transport experiments by fitting the transient solute concentration profiles measured on one or two regions of the pore network to the corresponding analytic solution with the aid of GREGPLUS solver of ATHENA software. In this code, a minimization problem is finally solved with quadratic programming by using a modified Gauss-Jordan algorithm (Bard, 1974), and interval estimates of parameters are computed by a posterior density function constructed from the final quadratic expansion of the objective function.

3. Results and discussion

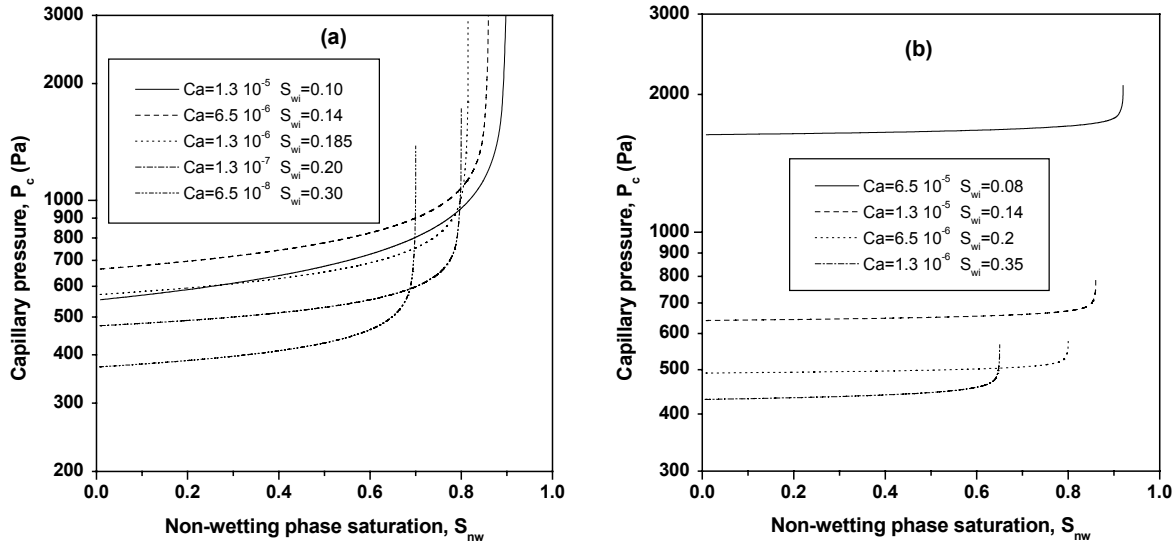

Figure 1: Estimated capillary pressure curves for various values of the capillary number. (a) Newtonian NAPL. (b) Non-Newtonian NAPL

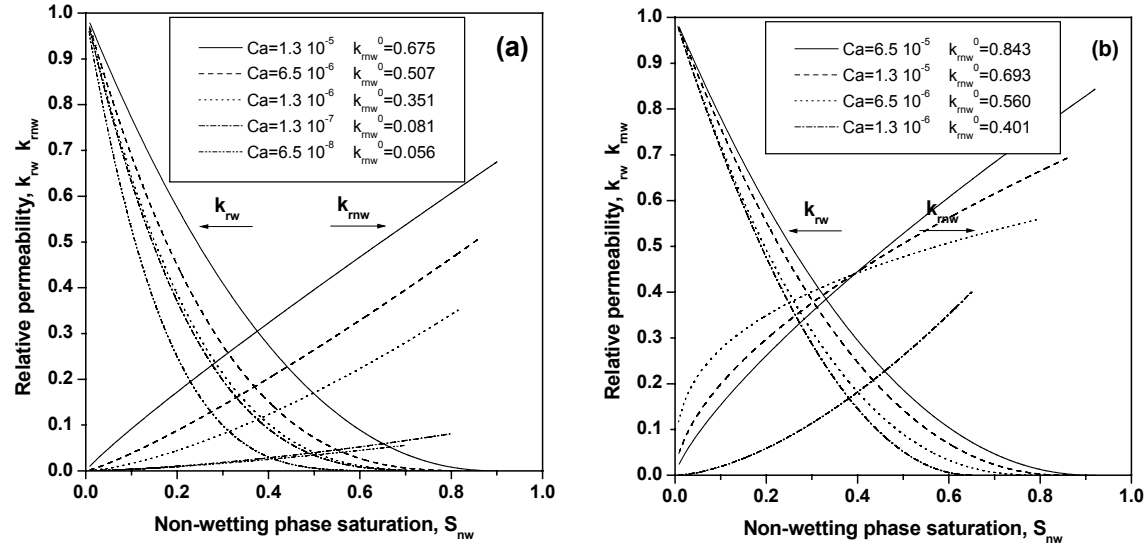

Figure 2: Estimated relative permeability curves for various values of the capillary number. (a) Newtonian NAPL. (b) Non-Newtonian NAPL

Dynamic capillary pressure and relative permeability curves, estimated from unsteady axial NAPL saturation distributions, measured on artificial fracture M-1, are shown in Figs.1 and respectively. The parameter values as functions of the capillary number are also given in Table 1. In general, the capillary pressure is an increasing function of the capillary number (Fig.1, Table 1). Although, in Newtonian NAPLs $P_c(S_{nw})$ has the tendency to be stabilized at high Ca values (Fig.1a), where the displacement pattern at the network is dominated by frontal drive (Tsakiroglou et al., 2003) no such asymptotic behavior occurs in non-Newtonian NAPLs (Fig.1b) because of the non-linear dependence of the pressure drop across the displacing phase on the flow rate. Likewise, the relative permeability curves are increasing functions of the capillary number for both cases (Fig.2a,b, Table 1) with the parameters of $k_{rnw}(S_{nw})$ varying non-linearly with Ca for non-Newtonian NAPLs (Fig.2b, Table 1).

Table 1: Estimated parameter values

Ca	P_c^0 *(Pa)*		*m*		*n*		*l*	
	Newt NAPL	*Non-Newt. NAPL*	*Newt NAPL*	*Non-Newt NAPL*	*Newt NAPL*	*Non-Newt. NAPL*	*Newt NAPL*	*Non-Newt. NAPL*
$6.55\ 10^{-5}$		*1633.6*		*0.0215*		*2.141*		*0.767*
$1.31\ 10^{-5}$	*553.1*	*640.9*	*0.248*	*0.0181*	*2.20*	*2.237*	*0.91*	*0.5797*
$6.55\ 10^{-6}$	*664.1*	*491.7*	*0.181*	*0.0142*	*3.02*	*2.460*	*1.20*	*0.340*
$1.31\ 10^{-6}$	*571.2*	*430.5*	*0.142*	*0.0239*	*3.38*	*2.019*	*1.47*	*1.628*
$1.31\ 10^{-7}$	*474.6*		*0.112*		*3.45*		*1.51*	
$6.55\ 10^{-8}$	*371.0*		*0.114*		*4.13*		*1.43*	

Dispersion coefficients estimated from miscible displacement experiments performed on artificial fracture M-2, are shown in Fig. 3a. At high Pe values, convective transport dominates, and solute dispersion is affected more drastically by details of the flow field and initial positions of solute molecules (Adler and Thovert, 1999). Consequently, the approximate analytical model developed may fit satisfactorily to experimental solute concentration measurements, at low and intermediate Pe values, but deviates sensibly from observed data at high Pe values (Theodoropoulou et al., 2003). D_L follows a power law of the form $D_L \propto Pe^{\beta_L}$ with $\beta_L = 1.006$ (Fig.3a) and this behaviour is in agreement with earlier experimental results (Sahimi, 1995; Whitaker, 1999). Specifically, at intermediate Pe values, macrodispersion induced by the variability of pore sizes dominates, and $D_L \propto Pe$, while at high Pe values Taylor dispersion induced by velocity variations across the pore network dominates and $D_L \propto Pe^2$ (Detwiller et al., 2000). The transverse dispersion coefficient has the tendency to become constant at increasing Pe values (Fig.3a) in agreement with earlier theoretical studies (Souto and Moyne, 1997).

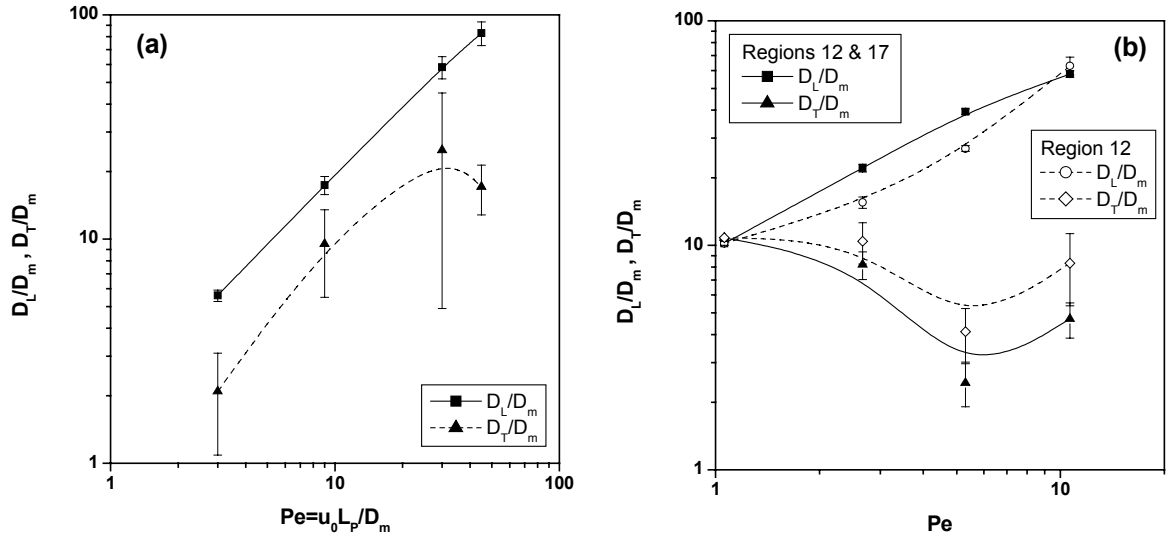

Figure 3: Longitudinal and transverse dispersion coefficients estimated by fitting analytic models of the convection-dispersion equation to transient data of (a) miscible displacement experiments performed on fracture model M-2, (b) single source-solute transport experiments performed on fracture model M-1.

Dispersion coefficients estimated from single source-solute transport experiments performed on artificial fracture M-1 are shown in Fig.3b. D_T is comparable to D_L at very low Pe values, takes on a local minimum at a low Pe value, and becomes an increasing function of Pe at higher values of this parameter. This behavior can be explained with reference to the steady-state solute concentration distribution within the pore network and using arguments of the volume averaging method as applied to solute dispersion processes (Theodoropoulou et al., 2003).

Acknowledgements

This work was performed under Energy Environment and Sustainable Development (EESD) contract number EVK1-CT1999-00013 (project acronym: TRACe-Fracture) supported by the European Commission.

References

Adler, P.M. and J.-F. Thovert, "Fractures and Fracture Networks: Theory and Applications of Transport in Porous Media" Kluwer Academic Press, Dordrecht, Netherlands (1999).

Aker, E., K.J. Maloy, A. Hansen, and G.G. Batrouni, A two-dimensional network simulator for two-phase flow in porous media. *Transp. Porous Media*, **32**, 163-186 (1998).

Avraam, D.G. and A.C. Payatakes, "Flow regimes and relative permeabilities during steady-state two-phase flow in porous media" *J. Fluid Mech.*, **293**, 207-236 (1995).

Bard, Y., "Nonlinear Parameter Estimation" Academic Press, London (1974).

Blunt M. and P. King, "Relative permeabilities from two- and three-dimensional pore-scale network modeling", *Transp. Porous Media*, **6**,407- (1991)

Caracotsios, M., and W.E. Stewart, "Sensitivity analysis of initial-boundary-value problems with mixed PDEs and algebraic equation; applications to chemical and biochemical systems", *Computers & Chemical Engineering*, **19**,1019 (1995).

Chardaire-Riviere, C., G. Chavent, J. Jaffre, J. Liu and B.J. Bourbiaux, "Simultaneous estimation of relative permeabilities and capillary pressure", *SPE Form. Eval.*, **December**, 283-289 (1992).

Charlaix, E., J.-P. Hulin, C. Leroy, and C. Zarconne, "Experimental study of tracer dispersion in flow through two-dimensional networks of etched capillaries" *J. Phys. D: Appl. Phys.* **21**, 1727-1732 (1988).

Detwiller, R.L., H. Rajaram, and R.J. Glass, "Solute transport in variable-aperture fractures: An investigation of the relative importance of Taylor dispersion and macrodispersion" *Water Resour. Res.* **36**, 1611-1625 (2000).

Didierjean, S., H.P.A. Souto, R. Delannay, and C. Moyne, "Dispersion in periodic porous media. Experience versus theory for two-dimensional systems" *Chem. Eng. Sci.* **52**, 1861-1874 (1997).

Ding, A. and D. Candela, "Probing non-local tracer dispersion in flows through porous media" *Phys. Rev. E* **54**, 656-660 (1996).

Drazer, G., Chertcoff, R., Bruno, L., Rosen, M. and Hulin, J.P., 1999. Tracer dispersion in packings of porous activated carbon grains. Chem. Eng. Sci. 54, 4137-4144 (1999).

Jennings, J.W., D.S. McGregor, and R.A. Morso, "Simultaneous determination of capillary pressure and relative permeability by automatic history matching", *SPE Form. Eval.*, **June**, 322-328 (1988).

Johnson, E.F., D.P. Bossler and V.O. Naumann, "Calculation of relative permeability from displacement experiments", *J. Pet. Tech.*, **January**, 61-63 (1959).

Kulkarni, R., A.T. Watson, J.-E. Norttvedt and A. Sylte, "Two-phase flow in porous media: property identification and model validation", *AIChE J.*, **44**, 2337-2350 (1998).

Lenormand, R., E. Touboul, and C. Zarcone, "Numerical models and experiments on immiscible displacement in porous media", *J. Fluid Mech.*, **189**, 165-187 (1988).

Manz, B., P. Alexander, and L.F. Gladen, "Correlations between dispersion and structure in porous media probed by nuclear magnetic resonance" *Phys. Fluids* **11**, 259-267 (1999).

Peters, E.J., R. Gharbi, and N. Afzal, "A look at dispersion in porous media through computed tomography imaging" *J. Petr. Sci. Eng.* **15**, 23-31 (1996).

Sahimi M., "Flow and Transport in Porous Media and Fractured Rock**:** From Classical Methods to Modern Approaches", VCH, Weinheim, Germany (1995)..

Souto, H.P.A. and C. Moyne, "Dispersion in two-dimensional periodic porous media. Part II. Dispersion tensor" *Phys. Fluids* **9**, 2253-2263 (1997).

Stewart, W.E., M. Caracotsios, and J.P. Sorensen, "Parameter estimation from multiresponse data", *AIChE J.*, **38**, 641 (1992).

Theodoropoulou, M., V. Karoutsos and C. Tsakiroglou, "Investigation of the Contamination of Fractured Formations by Non-Newtonian Oil Pollutants", *J. Environmental Forensics*, **2**, 321-334 (2001).

Theodoropoulou, M., V. Karoutsos, C. Kaspiris, and C.D. Tsakiroglou, "A new visualization technique for the study of solute dispersion in model porous media" *J. Hydrology*, in press (2003).

Tsakiroglou, C.D., "A methodology for the derivation of non-Darcian models for the flow of generalized Newtonian fluids in porous media", *J. Non-Newtonian Fluid Mechanics* , **105**, 79-110 (2002).

Tsakiroglou, C.D., M. Theodoropoulou, V. Karoutsos, K. Kaspiris and D. Tsovolou "Visualization studies of pollutant dispersion in fractured porous media", Proceedings *6th International Conference on the Protection and Restoration of the Environment,* 1-5 July 2002, Skiathos Island, Greece, A.G. Kungolos et al. (eds.), pp.335-343 (2002a).

Tsakiroglou, C.D., M. Theodoropoulou, V. Karoutsos and D.G. Avraam, "Use of history matching for the estimation of the relative permeability functions of single fractures for two-phase immiscible displacement processes including non-Newtonian NAPLs", Proceedings of the *14th International Conference on Computational Methods in Water Resources (CMWR)*, 23-27 June 2002, Delft, The Netherlands, M. Hassanizadeh et al. (eds.), Vol.1, pp.327-334 (2002b).

Tsakiroglou, C.D., M. Theodoropoulou, and V. Karoutsos, "Non-equilibrium capillary pressure and relative permeability curves of porous media", submitted (2003).

Vizika, O., D.G. Avraam, and A.C. Payatakes, "On the role of the viscosity ratio during low-capillary number forced imbibition in porous media", *J. Colloid Interface Sci.*, **165**, 386-401 (1994).

Whitaker, S., "The Method of Volume Averaging", Kluwer Academic Publ., Dordrecht, Netherlands (1999).

Contaminant transport in fractured fine-grained glacigene sediments

C. D. Tsakiroglou[1], K.E.S. Klint [2], P. Gravesen[2]., C. Laroche[3], P. Le Thiez[3]

[1]*Corresponding author: Institute of Chamical Engineering and High Temperature Chemical Processes - Foundation for Research and Technology Hellas*
Stadiou Street, Platani, P.O.Box 1414, GR-26504 Patras, Greece
Phone: 30 2610 965212; Fax: 30 2610 96522; E-Mail: ctsakir@iceht.forth.gr
[2]*Geological Survey of Denmark and Greenland, Østervoldgade 10, 1350 Copenhagen K, Denmark*
[3]*Institut Français du Pétrole, 1-4 Avenue de Bois-Préau, 92852 Rueil-Malmaison, France*

Abstract: In this study, multi-scale geological information was collected during extensive fieldwork on a fractured clay-till site situated in Denmark (Ringe site). Meso-scale field data such as fracture spacing/connectivity and hydraulic "in situ" tests were combined with micro-scale laboratory studies of mechanical fracture apertures and pore network geometry of fractures and matrix so that a conceptual macro-pore model was established. At the small scale, pore network modeling approach was used to simulate the two-phase flow in single fractures and fracture networks, in the capillary dominated regime. Up-scaling from the pore to the fracture network allowed the estimation of average transport properties and their introduction into a macroscopic simulator of contaminant transport in dual porosity media (SIMUSCOPP). This macroscopic simulator is used for the long-term forecasting of the spatial and temporal evolution of the distribution of a typical LNAPL (creosote) over an extended area around the contaminated site

1. Introduction

Fractures are widespread in the upper part of the Earth's crust. They exist in all types of rocks and soils in different scales ranging from micro fractures to regional crystal scale features. Their size, density connectivity and morphology affects substantially the short- and long-term transport of non-aqueous phase liquid (NAPL) pollutants in both the unsaturated and saturated zones of the subsurface. The design and installation of any remediation scheme on a contaminated fractured site, requires information about the distribution of pollutants throughout the subsurface. Such information is provided either by field-scale studies or by numerical predictive codes that solve the macroscopic transport equations in fractured reservoirs (Adler and Thovert, 1999).

The role of fractures as hydraulic highways contributing substantially to the spreading of pollutants in aquifers has been widely recognized during the last decade (Fredericia, 1990; Jakobsen and Klint, 1999). The need for the introduction of high quality fracture properties into contaminant transport models has accordingly become more evident (Klint and Tsakiroglou, 2000). Most fracture models need accurate input data concerning the fracture orientation, the length and spatial distribution (connectivity) of fractures, the fracture density and the statistics of fracture aperture in a given area.

The mechanical and hydraulic properties of the host rock influence strongly the nature and hydraulic behavior of fractures. In tight crystaline rocks, such as granite and gneiss, the rock permeability is negligible, and fractures form the only significant pathways for fluid migration. On the other hand, in highly porous rocks, like clay or limestone, the capacity of the microporosity for fluid storage is pronounced, while the permeability is still controlled by

fractures. In these cases, except for fracture characterization, methods used for the determination of the properties of the micro-porous matrix may be necessary, as well.

2. Site description

The "Ringe site" is situated in Funen Island, Denmark (Fig.1); its subsurface consists of fractured clay till overlaying a primary sandy aquifer. The site was strongly contaminated by leaking storage tanks of a creosote and asphalt factory (1930-1960) as well as by waste oils of automobile workshops (1960-1988).

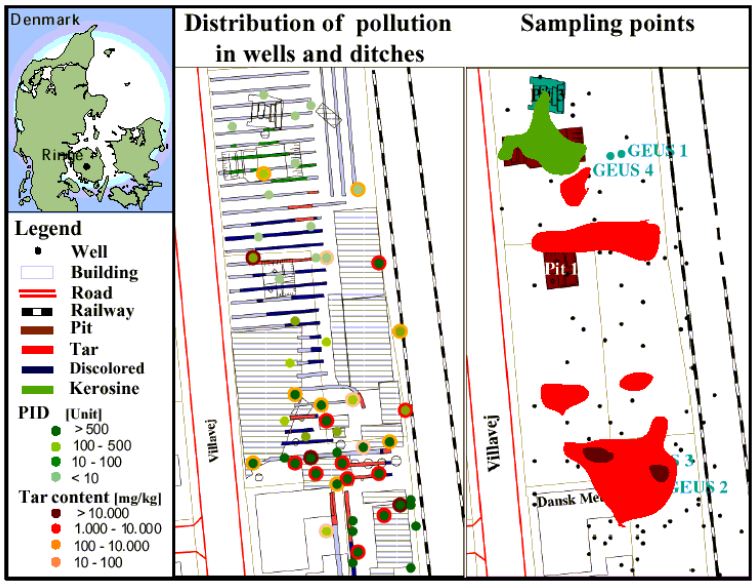

Figure 1: Spatial distribution of NAPL on the Ringe site

3. Methods

Discrete fracture models need information concerning the *position*, *orientation, size*, *density (connectivity)* and *aperture* of single fractures. The *fracture density* may be quantified by the total fracture area per unit volume (which is very difficult to measure) or by the fracture trace-length per unit area, which is measurable, but its value is biased. Another approach is to measure or calculate the average distance between fractures in each fracture system (*fracture spacing*), or the number of fractures per unit volume (*fracture intensity*). Finally the *connectivity* of fractures is extremely important for the bulk hydraulic properties of the area, and good outcrop maps are therefore important in order to evaluate the spatial distribution of fractures.

3.1 Fracture classification

Fractures in clay till originate from a certain stress situation either as systematic sets of parallel fractures with a distinct orientation formed by the loading and shearing of advancing glaciers, or in some cases as more irregular non systematic fractures with an overall random orientation (dessication or freeze/thaw fractures). Systematic fractures form "families" of fractures with special characteristics. Once fractures have been classified as systematic or non-systematic, their properties may be estimated, whereas a more detailed classification may be based on other characteristics such as the fracture shape and size.

3.2 Field measurement technique

The analysis of fractures in clay tills were carried out in large freshly excavated pits in order to avoid the formation of additional fractures caused by stress release, weathering and

desiccation processes (Klint and Tsakiroglou, 2000; Klint et al., 2001a,b). The pits were up to 5.5 meters deep and constructed in order to study the fractures on vertical and horizontal sections in three dimensions. Horizontal reference lines were attached to the profiles, and the position, orientation, minimum size, shape, roughness and the precipitation of all 1st and 2nd order fractures were measured and described (Klint et al., 2001a; Rosenbom and Klint, 2001). The sediments from excavations were described and characterized according to Larsen et al. (1995) with respect to composition, colour, structure and texture. Samples of fractures were collected from selected sections. A small monolith of till containing one fracture was captured in a steel box. The orientation and position of the box and fracture were measured, before removing the box from the wall.

3.3 Laboratory work

Preparation of the samples for image-analysis requires thus three basic operations: (i) removal of the water from the sample; (ii) resin impregnation / solidification in the void space of the sample; (iii) selection of the fractures, cutting and grinding of thin and/or thick sections for SEM analyses. Scanning Electron Microscope (SEM) images of the selected fracture were captured with the Back-scattered Electron detector (BSE) utilising a Phillips XL-40 Scanning Electron Microscope (SEM). The methodology of using thick-sections instead of thin sections, allows the cutting of the sample in multiple sections, thus facilitating the analysis of the pores in three dimensions. The stored 2-D images of resin-impregnated till samples were analysed, in order to measure some geometrical parameters of fracture apertures, with the aid of the Sigma ScanPro-5 image analysis software. The 2-D features of the fractures were analysed using the SEM-images

4. Conceptual macropore model

The geological model is divided into three parts: (1) the upper part consists of 5-8 meter fractured clay till, (2) the central part consists of 8-11 m deformed glacigene, clay till and sand, and (3) the lower part is a sandy aquifer (Klint et al., 2001a). Fracture intensity / spacing were measured and calculated for the uppermost 5 m of the till (Table 1) and from these values a conceptual fracture model was established (Fig.2).

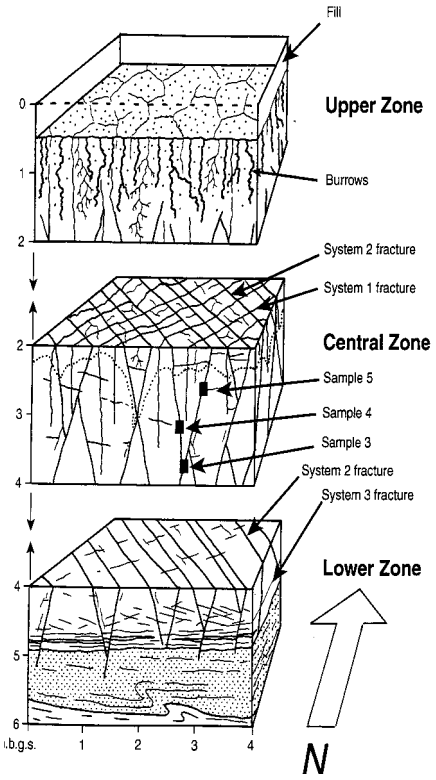

Figure 2. Conceptual geological macropore model.

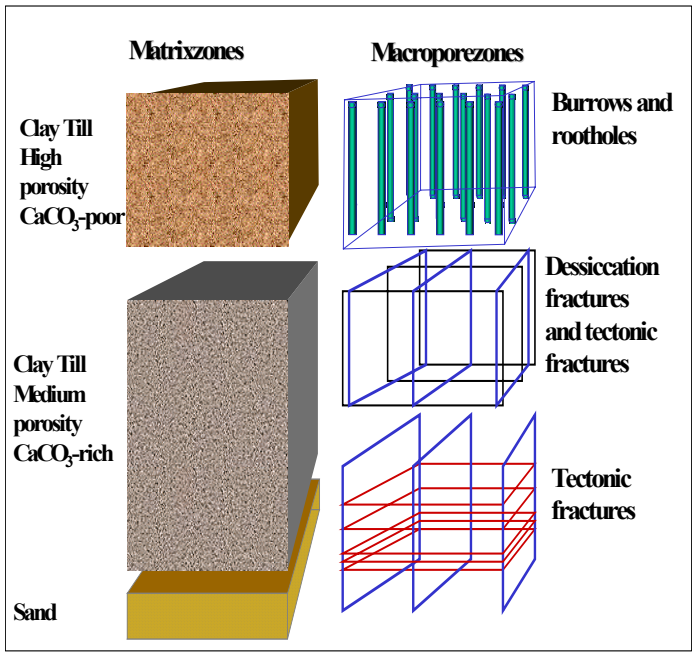

Figure 3 Conceptual dual model: macropore zones (fractures) and matrix zone

The upper zone is dominated by bio-pores, dessication fractures and high porous matrix. The dominant flow system over this zone consists of biopores that form vertical channels with a diameter ~ 2-5mm. The central zone is dominated by well connected desiccation (system 1) and glaciotectonic (system 2) shear-fractures. The lower zone is dominated by glaciotectonic shear-fractures (system 2).

5. Derivation of phenomenological models

Experiments performed on artificial fractures aimed at identifying the transient two-phase flow patterns (Theodoropoulou et al., 2001) and solute dispersion regimes (Theodoropoulou et al., 2003), and estimating the dynamic relative pemeability & capillary pressure curves (Tsakiroglou et al., 2002, 2003) and the hydrodynamic dispersion coefficients (Theodoropoulou et al., 2003), all in dependence on pertinent parameters (capillary number, NAPL rheology, Peclet number). With the aid of critical path analysis analytical equations were described for the determination of the electrical formation factor and absolute permeability of single fractures from geometrical / topological properties of their aperture (Tsakiroglou, 2002). Fracture network models were developed to represent the morphology of the various fracture systems identified on the site. These models were evaluated with respect to field hydraulic data obtained with infiltration, column and slug tests. An existing pore network simulator of the immiscible displacement of a wetting by a non-wetting fluid, was properly updated to dual pore networks (representing a single fracture / matrix porosity system) and its results were used as input data to determine the upscaled capillary pressure and relative permeability functions of fracture systems bounded within a block of the macroscopic numerical grid (Bekri et al., 2002).

6. Macroscopic numerical simulation

The macroscopic simulator SIMUSCOPP was updated to dual porosity / dual permeability media (Laroche et al., 2003) in order to account for porous matrix / fracture interactions. The geological conceptual model of an area on Ringe Site (Fig.3) was translated into a numerical grid, by assigning porosity and permeability values to matrix and fracture grids, and the downward flow of pollutants was simulated for a specific scenario of pollution (Fig.4). The flow pathways were identified by ignoring and including rainfall precipitation in the simulations (Fig.4). In order to study the dissolution / dispersion of dissolved compounds at a large scale within the aquifer, a two-step procedure was adopted: (1) the macroscopic simulation of two-phase in a cross-section of the fractured (dual porosity) medium was used to determine the NAPL flux toward the aquifer; (2) the flux was used as boundary condition on the water table for the simulation of dissolution/dispersion of compounds (phenol, naphthalene) at large distances within the (simple porosity) aquifer (Fig.5). The concentrations of dissolved organic compounds detected on the field (Table 1) were found much lower than those obtained with simulations, and this discrepancy might be attributed to two factors (Laroche et al., 2003): (1) there is no field evidence that the NAPL pool reached the top of the aquifer, contrary to what the simulations predicted. (2) The composition of the NAPL may have changed, due to natural attenuation of some organic compounds (volatilization of the lighter compounds, biodegradation, etc) and the concentrations of naphthalene and phenol in the NAPL may be therefore much lower than the original ones.

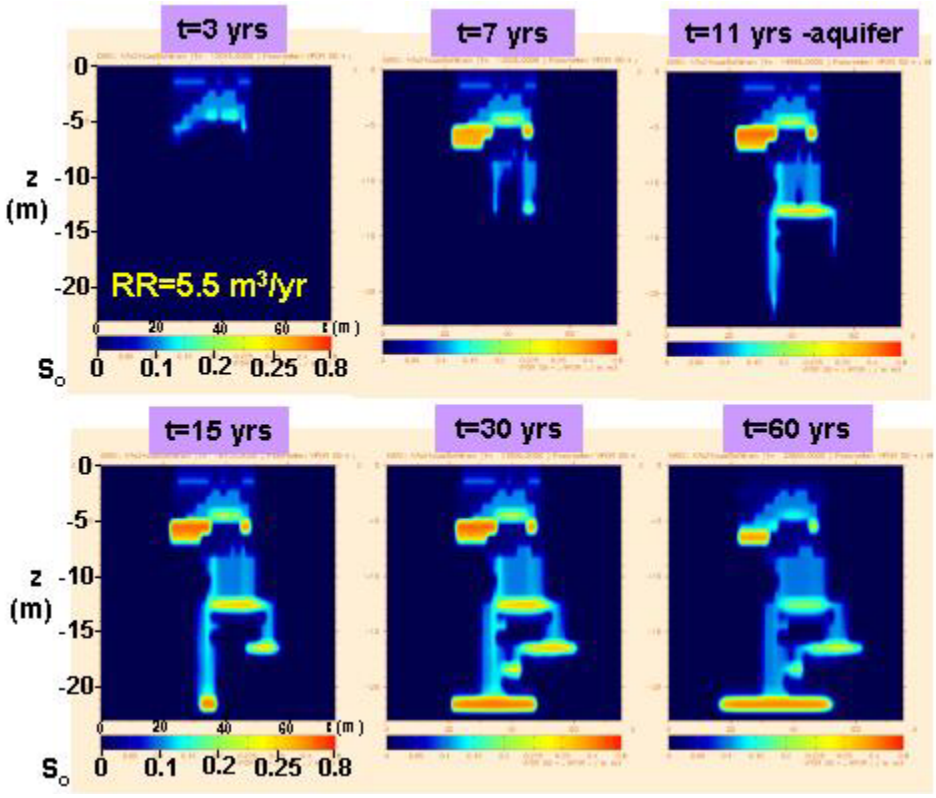

Figure 4: Simulation of NAPL pathways in the fractured Ringe Site (clay till) under wet conditions (the rainfall rate matches the annual rain precipitation in the regional area). Investigated scenario of contamination: creosote is leaking from the aboveground storage tanks of the tar factory on a surface of 25m^2 at a constant rate 5 10^{-3} m^3/d, for a period of 30 years; afterwards, the source of pollution is removed and the simulator is used to predict the pollutant migration over a total period of 60 years

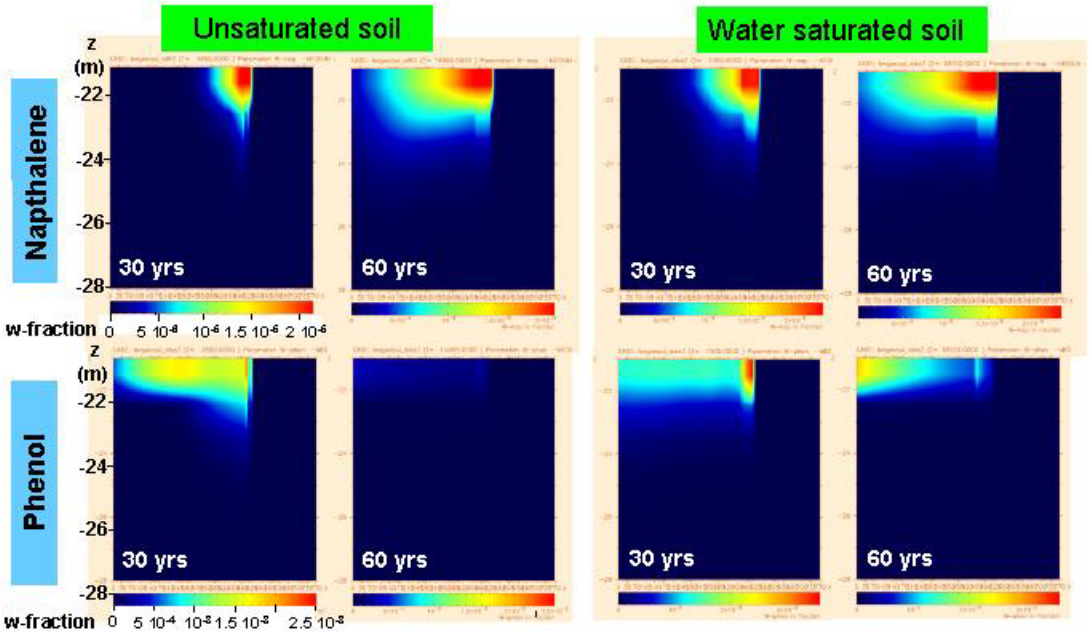

Fig.5: Simulation of naphthalene (concentration in NAPL: 70-90%) and phenol (concentration in NAPL: 10%) dispersion in the underlying sandy aquifer. The NAPL flux on the water-table is given by the two-phase flow simulations (Fig.4).

Table 1. Compounds detected in groundwater on Ringe Site

Concentration of different compounds in groundwater sample

compound	466664-01 9911B	466665-01 9911	466666-01 9811A	466667-01 9811	466668-01 1012
Benzen	0,19	1.800	0,39	244	0,26
Toluen	0,16	12	0,12	0,74	0,18
Xylener*	-	365	0,14	18	0,13
1,2,3-Trimethylbenzen	-	16	-	0,87	-
1,2,4-Trimethylbenzen	-	88	-	4,7	-
1,3,5-Trimethylbenzen	-	-	-	-	-
Naphthalen	-	254	-	12	-
1-Methyl-naphthalen	-	0,75	-	0,12	-
Phenol	-	34	-	7,9	-
o-Cresol	-	0,85	-	-	-
m/p-Cresol	-	1,0	-	-	-
2,6-Dimethylphenol	-	450	1,1	150	-
2,4- og 2,5-Dimethylphenol	-	39	-	0,38	-
2,3-Dimethylphenol	-	7,1	-	-	-
3,4-Dimethylphenol	-	12	-	1,4	-
3,5-Dimethylphenol	-	4,3	-	0,29	-
Carbazol	-	-	-	-	-
Quinolin	-	-	-	-	-
Thiophen	-	73	-	4,3	-
Benzothiophen	-	173	-	11	-
Benzofuran	-	3,7	-	0,56	-
Dibenzofuran	-	-	-	-	-

* : Ethylbenzen, m-, p- og o-xylen.

7. Risk assessment of contaminated groundwater

Existing data concerning the geology and chemical status of groundwater of the contaminated site (Fig.1, Table 1) were compiled and classified, primarily from earlier research projects on

the site. Additional monitoring wells were established on the site and new data concerning the spreading of the contamination into the groundwater aquifer facilitated the construction of a new extended hydro-geological model. New data concerning the spreading of contaminants in the groundwater aquifer showed that contamination has migrated along the floor of the aquifer and is now situated approximately 200 meters southwest of the site at a depth of 40 meter below ground-surface.

8. Conclusions

In this study, an integrated methodology is suggested and applied to a fractured clay-till site situated in Denmark (Ringe site) and contaminated by organic pollutants. Multi-scale geological information has been collected with extensive fieldwork: a complete geological characterization and identification of the dominant fracture systems were performed. At the small scale, lab-scale analysis was performed on SEM images of single fractures and then pore network modeling was used to simulate the one- & two-phase flow in single fractures and fracture networks. In this manner, the average transport properties were estimated and were introduced into an updated macroscopic dual-porosity simulator. The simulator was used to quantify the pollution over an extended area around the contaminated site. Simulated along with field data can be used for the risk assessment of the contaminated groundwater.

Acknowledgements

This work was performed under Energy Environment and Sustainable Development (EESD) contract number EVK1-CT1999-00013 (project acronym: TRACe-Fracture) supported by the European Commission.

References

Adler, P.M. and J.-F. Thovert, "Fractures and Fracture Networks, Theory and Applications of Transport in Porous Media", Kluwer Academic Press, Dordrecht, Netherlands (1999)

Bekri, S., C. Henrique, C. Laroche, P. LeThiez, L. Trenty, K.E. Klint, and C.D. Tsakiroglou, "From microscopic to macroscopic simulations: an integrated methodology applied to fractured contaminated sites", *Proceedings of the 1st Intern. Workshop on Groundwater Risk Assessment at Contaminated Sites (GRACOS)*, p.147-151, 21-22 February 2002, Tubingen, Germany (2002).

Fredericia, J., "Saturated hydraulic conductivity of clayey till and the role of fractures" *Nordic Hydrology*, **21**, 119-132 (1990).

Jakobsen, P.R. and K.E. Klint, "Fracture Distribution and Occurrence of DNAPL in a Clayey Lodgement Till", *Nordic Hydrology*, **30**, No, 4/5, 285-300 (1995).

Klint, K.E. and C.D. Tsakiroglou, "A new method of fracture aperture characterization" *Proc. Int. Conf. Protection and Restoration of the Environment V*, (eds. V.A. Tsihrintzis et al.), Thassos Island, Greece, 3-6 July 2000, pp.127-136 (2000).

Klint, K.E., A. Rosenbom, and P. Gravesen, "Geological setting and fracture distribution on a clay till site in Ringe, Denmark", In: *TRACe-Fracture – Toward an Improved Risk Assessment of the Contaminant Spreading in Fractured Underground Reservoirs*, Progress Report no 36, GEUS, Denmark (2001a).

Klint, K.E., A. Rosenbom and C.D. Tsakiroglou, "A new approach to analysis of mechanical fracture aperture in rocks", *Proceedings (CD) of the International Conference 'Fractured Rock 2001'*, March 26-28, 2001, Toronto, Ontario, Canada (2001b).

Laroche, C., C. Henrique, S. Békri, L. Trenty, and P. Le Thiez, "From microscopic to macroscopic simulations: an integrated methodology applied to a fractured clay-till

contaminated site", to appear in *Proc. of ConSoil Conference*, 12-16 May 2003, Gent, Belgium (2003).

Larsen, G., J. Frederiksen, A. Villumsen, J. Fredericia, P. Gravesen, N. Foged, B. Knudsen, and J. Baumann, "A guide to engineering geological soil description", *Bull. Danish Geotechnical Society,* 130p. (1995).

Rosenbom, A and K.E. Klint, "Image and SEM-analysis of fractures and pore structures in clay till, In: TRACe-Fracture – Toward an Improved Risk Assessment of the Contaminant Spreading in Fractured Underground Reservoirs", Progress Report no 37, GEUS, Denmark (2001).

Theodoropoulou, M., V. Karoutsos, V. and C.D. Tsakiroglou, "Investigation of the contamination of fractured formations by non-Newtonian oil pollutants", *J. Environmental Forensics*, **2**, 321-334 (2001).

Theodoropoulou, M., V. Karoutsos, C. Kaspiris, and C.D. Tsakiroglou, "A new visualization technique for the study of solute dispersion in model porous media" *J. Hydrology*, in press (2003)

Tsakiroglou, C.D., M. Theodoropoulou, V. Karoutsos, and D.G. Avraam, "Use of history matching for the estimation of the relative permeability functions of single fractures for two-phase immiscible displacement processes including non-Newtonian NAPLs", *Proceedings of the 14th International Conference on Computational Methods in Water Resources (CMWR)*, pp.327-334, 23-27 June 2002, Delft, The Netherlands (2002).

Tsakiroglou, C.D., "Determination of the transport properties of single fractures with the aid of critical path analysis", *Industrial & Engineering Chemistry Research*, **41**, 3462-3472 (2002).

LECTURES

LARGE SCALE DIFFUSE POLLUTION: INTEGRATED SOIL AND WATER PROTECTION (SOWA)

KEY NOTE: The discovery of emerging contaminants for soil and water protection

Damià Barceló, Mira Petrovic and Ethel Eljarrat

Department of Environmental Chemistry, IIQAB-CSIC, Jordi Girona 18-26, E-08034 Barcelona, Spain, e-mail: dbcqam@cid.csic.es

Abstract: A wide range of man-made chemicals designed for use in industry, agriculture and consumer goods and chemicals unintentionally formed, or produced as by-products of industrial processes or combustion are potentially of environmental concern. Beside recognized pollutants, numerous new chemicals are synthesized each year and released into environment with unforeseen consequences. This presentation will discuss the importance of so-called emerging contaminants in the environment, sources and pathways of contamination, and their behavior and fate in river-sediment-soil-groundwater system.

1. Introduction

During the last decades, large amounts of different chemicals are released to the environment through industrial waste, agricultural practice and through the urine of mammalians, and via wastewater treatment plant effluent discharges. This contamination can have a critical impact in the ecosystem due to their strong activity at low doses. For the last 40 years, substantial evidence of the adverse effects of pesticides and certain industrial chemicals (PAHs, PCBs, etc) have been demonstrated and are now considered as priority contaminants. Actually, a second wave of pollutants, the so-called **Emerging Contaminants** (Table 1) are suspicious of causing adverse effects in both humans and wildlife. Between them we can mention important intermediates and end products of the chemical and pharmaceutical (veterinary also) industry. Pentabromobiphenylether, 4-nonylphenol, C_{10}-C_{13} chloroalkanes and the di(2-ethylhexyl)phthalate (DEHP) have been listed as priority hazardous substances in the field of water policy by EC Water Directive 2000/60/EC and the final EU decision No. 2455/2001/EC. Active hormonal substances (natural hormones are active at levels of ng/l) are being widely used in medicine or veterinary such as estrogens, anti-inflammatory corticosteroids and anabolizant androgens.

One of the key issues with Emerging Contaminants is that although few of them have been recently introduced in the legislation, still many of such pollutants are not in the legislation and as a consequence no routine monitoring programmes exists. One of the key issues is the evaluation of risks of such non-regulated chemicals that are currently detected in water. In this presentation, the general problems associated with unexpected chemicals in water and soil will be discussed. The analytical methodology for different groups of emerging contaminants is still evolving and the lack of appropriate analytical methods is often an important obstacle for more intensive occurrence studies. In this presentation the current state-of-the-art in the analysis of several groups of emerging contaminants will be discussed.

Finally, tools and research needs for the evaluation of unexpectedly growing risks due to the presence of emerging contaminants in water and soil will also be given.

Table 1 - Emerging compound classes

Compound class	Examples
Pharmaceuticals	
Veterinary and human antibiotics	Trimethoprim, erytromycine, lincomycin, sulfamethaxozole
Analgesics, anti-inflammatory drugs	Codein, ibuprofene, acetaminophen, acetylsalicilyc acid, diclofenac, fenoprofen
Psychiatric drugs	Diazepam
Lipid regulators	Bezafibrate, clofibric acid, fenofibric acid
β-blockers	Metoprolol, propanolol, timolol
X-ray contrasts	Iopromide, iopamidol, diatrizoate
Steroids and hormones	Estradiol, estrone, estriol, diethylstilbestrol
Personal care products	
Fragrances	Nitro, polycyclic and macrocyclic musks,
Sun-screen agents	Benzophenone, methylbenzylidene camphor
Insect repellants	N,N-diethyltoluamide
Antiseptics	Triclosan, Chlorophene
Surfactants and surfactant metabolites	Alkylphenol ethoxylates, 4-nonylphnol, 4-octylphenol, alkylphenol carboxylates
Flame retardants	Polybrominated diphenyl ethers (PBDEs), Tetrabromo bisphenol A, C_{10}-C_{13} chloroalkanes Tris(2-chloroethyl)phosphate
Industrial additives and agents	Chelating agents (EDTA), aromatic sulfonates,
Gasoline additives	Dialkyl ethers, Methyl-*t*-butyl ether (MTBE)

2. Analysis of emerging contaminants

The diversity of chemical properties of emerging contaminants, complexity of environmental matrices and low detection limits required make their analysis very challenging and imply a need for a comprehensive approach for their quantitative determination. At the moment different methods, mainly based on LC-MS, or GC-MS are being developed for the analysis of emerging contaminants at trace levels in aquatic and terrestrial environments, however methodology continue to evolve in the lights of new data on their occurrence and health risks. The development of analytical methodology is one of priorities since without appropriate tools it will not be possible to investigate behaviour, fate and bioavailability of emerging pollutants and to conduct adequate monitoring. That is why there is a need to develop and accept when ready, standard procedures of determination of emerging contaminants, together with inter-comparison studies in order to validate the analytical protocols.

The objectives of current research are improvements of existing methods and development of new, more sensitive and efficient protocols. Great effort is going into the development of cost-effective sample handling techniques characterized by the efficiency and simplicity of operations and devices. Several prevailing trends could be distinguished: (i) application of highly specific tailored sorbents (i.e. molecular imprinted polymers, immunosorbents, restricted access materials) for solid phase extraction, (ii) integration of several sample preparation steps into one (i.e. application of passive samplers for simultaneous sampling, extraction and enrichment of pollutants from liquid and gaseous samples and (iii) automation through coupling of sample preparation units and detection systems.

Driven by the eco-toxicity (or estrogenicity at low ng/L level) of some compounds and their low environmental concentrations, the detection limits required for the monitoring of organic pollutants are being pushed from the microgram to the nanogram or even to below nanogram

per liter range. Such low detection limits are achievable mostly due to development of hyphenated chromatography-mass spectrometry techniques, which are today the methods of choice for the determination of trace organic analytes in environmental samples.

Currently the main breakthrough is observed in the application of LC-MS and LC-MS-MS techniques, especially for those compounds which are not amenable to GC analysis. Examples are alkylphenolic compounds, steroid sex hormones, bisphenolic compounds, polar pharmaceuticals, aromatic sulfonates.

3. Occurrence in the environment

Surface water contaminated by municipal and industrial sources, and diffuse pollution sources from urban and agricultural areas continue to build up pollution levels in the environment. Numerous field studies, designed to provide basic scientific information related to the occurrence and potential transport of contaminants in the environment are being continuously conducted with the aim to identify which contaminants enter the environment, at what concentrations, and in what combinations. A large body of literature exists on occurrence of specific groups of organic contaminants in the environment. However, for long time research priorities have been focused on priority pollutants, such as POPs, pesticides, toxic metals, radionuclides, and just recently attention of scientific community has started to shift to emerging contaminants.

The major sources of emerging contaminants in the environment are primarily wastewater treatment plant (WWTP) effluents and secondarily terrestrial run-offs. The characteristic of these contaminants is that they do not need to be persistent in the environment to cause negative effect since their high transformation/removal rates can be compensated by their continuous introduction into environment. For most of emerging contaminants occurrence, risk assessment and ecotoxicological data are not available and therefore it is difficult to predict what health effects they may have on humans and aquatic organisms. Table 2. summarizes the data regarding the occurrence of several emerging contaminants in the environment.

Another aspect is the use of sewage sludge for agriculture. With the implementation of the 91/271/EEC Directive on urban wastewater treatment, more than 40.000 sewage treatment plants will be needed in Europe till the year 2005. It has been estimated that the amount of sludge produced in Europe will increase from 6.5 to 11 millions tonnes in the year 2005. At present around 40 % of the sewage sludge produced in Europe is deposited in landfills and 40 % goes to land use, whereas the rest is directed to incineration and below 10% still is dumped to the sea. According to the EU the quantity of sludge re-used would represent around 53% of the total sludge produced. In general the EU considers that the re-use of sludge should be encouraged since it represents a long-term solution provided that the quality of the sludge re-used is compatible with public health and environmental protection requirements. A soil protection policy document ahs been recently released by the European Union e.g. as defined recently by DG ENV (*Towards a Thematic Strategy for Soil Protection*, COM(2002), 179 final) and the EC (IP/02/592; 19/04/2002) that points out the problems associated with soil issues, including sludge used for soil amendment. Many of the organic contaminants that are released from the sludge used for agriculture are not currently regulated. However, the new directive (Working Document on Sludge, 3rd Draft, 2000, unpublished) propose limit values for several organic pollutants in sludge added to agricultural soil (Fig. 1).

Table 2. Summary data for selected emerging contaminants

Compound	Origin	Persistence Bioaccumulation	Observed in environment	Concentration level
Nonylphenol	Degradation product of non ionic surfactants	Medium persistent Bioaccumulative	Soil Sediment Sludge Water	Low mg/kg* Low mg/kg Low-high mg/kg Low µg/L
Bisphenol A	Plastics	Not bioaccumulative	Surface water Groundwater	Low-high ng/L Low-high ng/L
Phthalates	Plastics	Low to medium persistent	Water Sediment Sludge	Low-medium µg/L Low µg/kg Low-medium µg/kg
PBDE	Flame retardant	Persistent/highly accumulative	Sediment Soil Sludge	Low-medium µg/kg Low-high ng/kg* Low-medium µg/kg
C_{10}-C_{13} chloroalkanes	Flame retardant	Persistent/highly accumulative	Surface water	Low-medium µg/L
Sulphonamides	Human and veterinary drug	Slightly-very persistent	Groundwater Surface water	Low µg/L Low µg/L
Tetracyclines	Human and veterinary drug	Moderately-very persistent	Groundwater Soil	Low µg/L Low-medium µg/kg*
Steroid sex hormones	Contraceptives	Moderately persistent	Water Sediment Sludge	Low ng/L Low µg/kg Low-medium µg/kg
MTBE	Gasoline additive	Persistent Not bioaccumulative	Groundwater	Very variable

* sludge amended soil

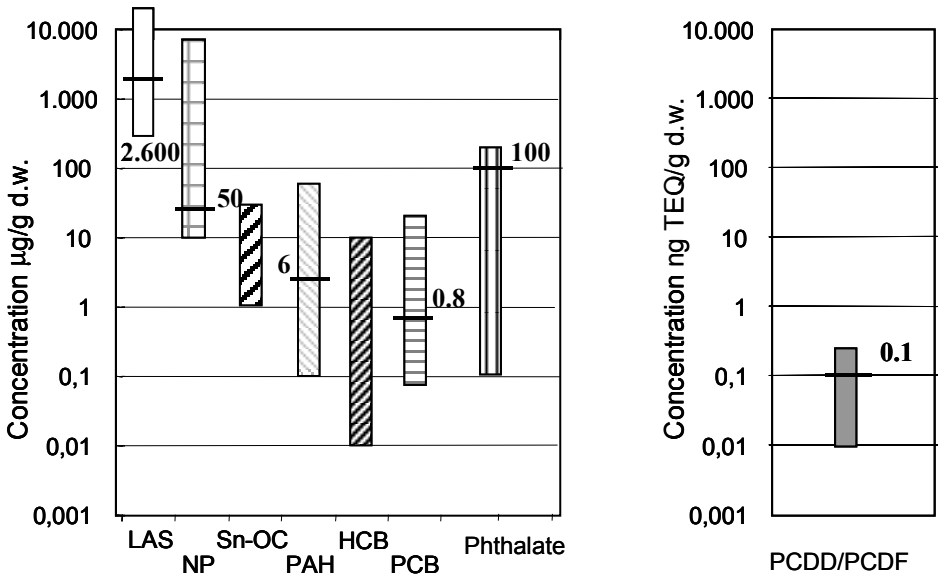

Figure 1. Levels of antrophogenic chemicals in sewage sludge and limit values for sludge to be applied onto soil (European Commission, 2000 draft proposal)

4. Executive summary including future research needs

Summarizing the different issues discussed during this lecture, the following research needs on the assessment of water/soil systems functioning in relation to emerging contaminants were identified:

1. There is an urgent need for a European list of emerging contaminants, as possible candidates for the introduction into the WFD list of priority substances. This list is amendable for revision and addition of new contaminants each four years and thus, based on surveys and on the results of further monitoring programs the lists of new pollutants could be integrated. To achieve this purpose, a systematic survey of emerging contaminants in waterways (especially those receiving WWTP or animal-farms) should be undertaken . The resulting combined list will represent an initial step towards a more detailed picture of environmental contamination and better understanding of soil-water-sediment functioning beyond priority pollution. Further features can be added – concentrations, frequency of finding, physico-chemical, environmental and ecotoxicological properties.
2. The development of additional analytical methods including improved preconcentration and clean-up techniques and more specific and selective detection would benefit the environmental monitoring community. Although analytical methods do exist for analyzing emerging compounds individually, the key issue is to develop multi-residue methods in which different compound classes can be determined by a single short analysis
3. The interaction between soil and water is a key issue. It is expected that the chemical composition (geochemical and man-made pollution) of the soil and the biological and chemical processes will determine the resulted water quality. Other aspects to be addressed are the mobility of contaminants within sediments and soil after once they have transferred there, their bioavailability, pore water concentrations or *in-situ* quality.
4. There is a lack of studies to assess the functioning of the water/soil system like investigations on the behavior of emerging contaminants at the surface water-groundwater during artificial recharge. In this way the river bed can serve as an attenuation barrier for groundwater pollution. A better understanding of contaminant transport and fate of emerging pollutants is a key issue for an efficient design, operation and optimisation of bank filtration that will reduce the amount of treatment needed at drinking water treatment plants

Acknowledgements: This work is part of the EU accompany measure on Integrated Soil and Water Protection (SOWA) EVK1-CT-2002-80022

Worldwide diffuse pollution of groundwater with anthropogenic chemicals: Lessons learned from freons

Patrick Höhener

Swiss Federal Institute of Technology (EPFL), ENAC, ISTE-LPE, CH-1015 Lausanne, Switzerland, Phone 0041 21 693 57 50, Fax 0041 21 693 28 59 E-Mail: patrick.hoehener@epfl.ch

Abstract: Freons, more precisely named as chlorofluorocarbons (CFCs), are synthetic halogenated volatile organic compounds that have been manufactured since 1930 and can be detected analytically in water in pg L^{-1} concentrations. The use as tracers for age-dating of pristine groundwater has been summarized by several review articles (Plummer and Busenberg, 1999; Plummer et al., 1993). Occasional failure of the CFC age-dating technique caused by local CFC contamination in excess of the equilibrium with modern air was reported (Oster et al., 1996). This presentation will present findings from a more recent review article focussing on pollution of groundwater with CFCs (Höhener et al., 2003). A global overview on the occurrence of CFCs in groundwater and the levels of contamination exceeding equilibrium with modern air is given. The following specific questions will be addressed:

1) In which concentration ranges do CFCs occur in groundwater, and how frequent is contamination exceeding atmospheric equilibrium?
2) Which sources release CFCs to groundwater?
3) Which factors determine the vulnerability of aquifers?

Introduction

Chlorofluorocarbons (CFCs) have been manufactured since the 1930s (Siegemund et al., 1988) and were used world-wide as aerosol propellants, refrigerants, foam blowing agents, solvents and intermediates for the synthesis of fluorinated polymers. CFCs were produced by several manufacturers and sold under many different trade names such as Freon, Flugene, or Frigen. HFCs and HCFCs contain at least one hydrogen atom in the molecule and are numbered similarly. The chemical characteristics of the important compounds on the world market reveal low boiling points, high vapor pressures, and moderate to low water solubility.

Records of production, sales and atmospheric releases have been published by the *Alternative Fluorocarbons Environmental Acceptability Study* (AFEAS), an organization grouping the 11 world leading manufacturers of volatile fluorinated compounds. Production of CFC-12 preceded those of CFC-11 and CFC-113 by ~ 10 and 30 years, respectively (Busenberg and Plummer, 1992; Cook and Solomon, 1995). Total world production of CFCs and HCFCs peaked in 1986 with ~ 10^6 metric tons per year (Key et al., 1997). CFC-11 and CFC-12 made up to 77 % of total global production of CFCs until 1994 (Key et al., 1997). Due to the release into the environment, the volatility and excellent chemical stability, CFCs accumulated in the atmosphere and were proven to be involved in the depletion of the stratospheric ozone and in global warming (Watson et al., 1990). Many governments thus signed the *Montreal protocol on substances that deplete the ozone layer* and decreased the production of CFCs in the 1990's coming to a ban in 1996. Only some medical applications are still allowed. It is predicted that CFC concentrations in the atmosphere will be significant for at least the next century because of the long atmospheric lifetimes and continuing emissions by long-lived applications such as in closed-cell insulation foams (Watson et al., 1990). As replacement products, HFCs and HCFCs are currently used, until they will be phased out toward 2020 and 2030 (AFEAS). A steep increase in production of HCFCs and HFC-134a has been observed since 1990.

Results

Data for the chlorofluorocarbons CFC-11 and CFC-12 in 24 aquifers and 2 regions on 4 continents were compiled (Höhener et al., 2003). In only 8 aquifers, all water samples had CFC concentrations at or below expected equilibrium concentrations with respect to local air. These 8 completely uncontaminated aquifers included volcanic hot springs, and porous aquifers in rural areas in Ontario, New Jersey, and Germany, and a fractured aquifer in South Africa. In 16 aquifers, 5% or more of the samples contain at least one CFC in a concentration exceeding significantly the equilibrium with modern air. No clear trend is evident whether CFC-11 or CFC-12 excess is more frequent. There is no obvious correlation furthermore between the location of partially contaminated aquifers and the population density. Contamination can be as high as three orders of magnitude over air equilibrium. Fractured aquifers are particularly affected by high numbers of contaminated samples. A number of aquifers showed anomalies in having lower CFC-11 concentrations than expected. The low CFC-11 concentrations are explained by degradation. Data of the CFC-113 concentrations in aquifers have been reported less frequently than for CFC-11 and CFC-12. Only in 4 out of 12 aquifers in Germany, Georgia, Florida and South Africa, all CFC-113 samples were not exceeding the equilibrium concentration in freshwater. In the other aquifers, some or all samples exceeded the equilibrium concentration. At the two landfill sites, the equilibrium was exceeded by 3 to 6 orders of magnitude. Pathways of CFC-input to groundwater such as local atmospheric pollution, river water infiltration, landfills, and industrial solvent spills will be discussed.

References

AFEAS, **A**lternative **F**luorocarbons **E**nvironmental **A**cceptability **S**tudy. www.afeas.org

Busenberg, E.; Plummer, L.N., 1992. Use of chlorofluorocarbons (CCl_3F and CCl_2F_2) as hydrologic tracers and age-dating tools: The alluvium and terrace system of central Oklahoma. Water Resources Research, 28: 2257-2283.

Cook, P.G.; Solomon, D.K., 1995. Transport of atmospheric tracer gases to the water table: Implication for groundwater dating with chlorofluorocarbons and krypton 85. Water Resources Research, 31: 263-270.

Höhener, P.; Werner, D.; Balsiger, C.; Pasteris, G., 2003. Worldwide occurrence and fate of chlorofluorocarbons in groundwater. Crit. Rev. Environ. Sci. Technol., 33: 1-29.

Key, B.D.; Howell, R.D.; Criddle, C.S., 1997. Fluorinated organics in the biosphere. Environmental Science and Technology, 31: 2245-2254.

Oster, H.; Sonntag, C.; Munnich, K.O., 1996. Groundwater age dating with chlorofluorocarbons. Water Resources Research, 32: 2989-3001.

Plummer, L.N.; Busenberg, E., 1999. Chlorofluorocarbons: tools for dating and tracing young groundwater. In: P. Cook and A. Herczeg (Editors), Environmental tracers in subsurface hydrogeology. Kluwer, Boston, pp. Chapter 15, pp 441-478.

Plummer, L.N.; Michel, R.L.; Thurman, E.M.; Glynn, P.D., 1993. Environmental tracers for age-dating yound groundwater. In: W.M. Alley (Editor), Regional groundwater quality. Van Nostrand, New York, Chapter 11, pp 255-294.

Siegemund, G.; Schwertfeger, W.; Feiring, A.; Smart, B.; Behr, F.; Vogel, H.; McKusick, B., 1988. Organic fluorine compounds. In: W. Gerhartz, Y.S. Yamamoto, B. Evers and J.F. Rounsaville (Editors), Ullmann's Encyclopedia of Industrial Chemistry. VCH Verlagsgesellschaft, Weinheim, pp. 349-392.

Watson, R.T.; Rodhe, H.; Oeschger, H.; Siegenthaler, U., 1990. Greenhouse gases and aerosols. In: J.T. Houghton, G.J. Jenkins and J.J. Ephraums (Editors), Climate change - the IPCC scientific assessment. Cambridge University Press, Cambridge, pp. 4-40.

Determination of PAH fluxes at the catchment scale: A mass balance approach

Tilman Gocht[1] and Peter Grathwohl[1]

[1] *Centre for Applied Geosciences, Sigwartstr. 10, 72076 Tuebingen, Germany*
Phone: : +49-7071-2977452, Fax: +49-7071-5059; e-mail: tilman.gocht@uni-tuebingen.de

Abstract: A mass balance of polycyclic aromatic hydrocarbons was calculated for a hydrologically closed, rural catchment based on measurements of the atmospheric deposition rates (input) as well as concentrations in soil (storage) and water (output) of these persistent pollutants. The results indicate, that more than 90% of the deposited PAHs remain in the soils and tend to accumulate especially in the organic top layers, where concentrations up to 5.5 mg kg^{-1} were observed. Intercompartment fluxes of PAHs occur mainly in connection with stormy weather periods and are presumably limited to interflow on preferential pathways and particle carried transport.

1. Introduction

Polycyclic aromatic hydrocarbons are one group of compounds including persistent organic pollutants (POP), which are introduced into the environment due to combustion of fossil fuels from point (e. g. power stations) or diffuse sources (traffic). Emission inventories indicate that most of the contaminants are released into the environment by diffuse sources (Wild and Jones, 1995). Persistent PAHs tend to accumulate in environmental compartments such as soils and sediments (Jones et al., 1989). In contrary to point sources, diffuse contamination of soils cannot be removed and therefore are likely to persist over very long time periods (years - centuries) and this can pose a long-term risk of transfer of the pollution to other environmental compartments such as groundwater.

The aim of this study was to determine quantitatively the long-term input of PAHs into soils from atmospheric deposition (using passive samplers) and their transport in surface and seepage water as well as in groundwater at the micro-catchment scale, which spatially integrates all processes involved. This "mass balance" approach is illustrated in a small catchment, which is well characterized concerning the hydrological and pedological properties. The example catchment is located in a rural area in the Northern Black Forest, Germany. The basic principle is to subdivide the catchment into compartments and to determine fluxes and internal storage of pollutants in the system.

2. Materials and Methods

The catchment (Seebach, 4.3 km^2) is located in the northern part of the Black Forest, Germany (Fig. 2) between 680 m and 1000 m (a.s.l.). This area is well characterized concerning hydrogeological properties, spatial distribution of soils, acidification and inorganic compounds (Hinderer, 1995). Rocks of the Bunter Sandstone Formation geologically characterize the catchment. The crystalline basement prevents further penetration of seepage water (Fig. 1). Thus, the catchment acts as a hydrological closed system. Most of the hills are covered by periglacial debris, which influences the overall water fluxes. Most of the surface area is covered by forest woods, which consists mainly of spruce.

The bulk atmospheric deposition of PAHs was collected with a passive sampling device. The system was extensively tested in the field and is already validated (a national draft of a

standard already exists) (Martin and Grathwohl, 2002). The passive sampling system consists of a glass-funnel connected to an adsorption cartridge packed with a suitable solid phase, for PAHs Amberlite® IRA-743 is used. The cartridges trap both, the wet and dry deposition either by adsorption and/or filtration (particles), respectively. The samplers were distributed over the catchment with respect to expected heterogeneities of atmospheric deposition of PAHs. Topographical differences as well as differences between open field and forest deposition were taken into account. The funnel of the bulk samplers in the forest were equipped with a 0.5 mm sieve (stainless steel) in order to separate the litterfall (spruce needles) from the throughfall. After sampling, the cartridges were solvent-extracted with acetone. The PAHs were measured with a Hewlett-Packard 5890 gas chromatograph equipped with a 7673 automatic sampler and coupled to a 5972A mass spectrometer.

In addition to this precipitation samples were collected in 2 l bottles under a funnel. The precipitation samples were filtered with solvent soluble membrane filters (pore size 0.05 µm). Then the filters were dissolved in acetone and the particles were embedded in acrylic resin and studied under a Leica DMRX photometer microscope. This was done to separate and characterize the atmospheric particles, which are assumed to be an important carrier for the PAHs.

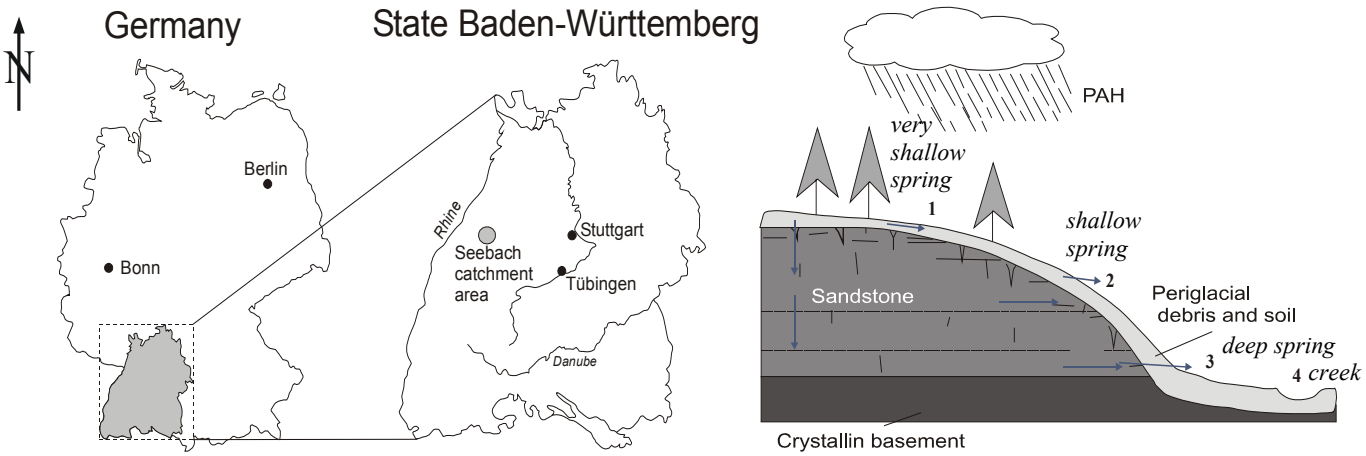

Figure 1: Map of the location (left) and schematic cross section of the Seebach catchment (Hinderer, 1995, modified).

Soil samples were taken horizontically from typical soil profiles in the catchment. 10 litre metal buckets were filled with soils from each horizon using stainless steel shovels and spoons. They were then air dried (room temperature), passed through a 2 mm sieve (stainless steel) and well homogenized. The samples were sequentially extracted using an Accelerated Solvent Extractor (ASE 300, Dionex), first with acetone (100°C, static time 10 min), then with toluene (150°C, static time 10 min). The extracts were conditioned using column chromatography with coupled polar (Al_2O_3) and non-polar (SiO_2) adsorbents and PAHs were measured with GC-MS. Furthermore, the content of organic carbon was determined using pulverised samples of each horizon, dried at 75°C for 48 hours using elemental analysis (Elementar, Germany).

Water samples were taken from springs with respect to different hydrogeological situations (Fig. 1): (1) A very shallow spring close to the top of the hill representing surface runoff and/or drainage of the periglacial debris (depending on weather conditions in the days before sampling); (2) a shallow spring representing drainage of periglacial debris and/or shallow

parts of the sandstone aquifer; (3) a deep spring representing drainage of the deeper part of the sandstone aquifer. Situations at point (1) and (2) depend on precipitation events at the days before the sampling campaign. During wet periods point 1 is dominated by surface runoff and point 2 by discharge from the periglacial debris, respectively. During dry periods point 1 is dominated by discharge from the periglacial debris (or it runs dry) and point 2 by the shallow parts of the sandstone aquifer. The sampling of the different springs provides information about internal inter-compartment PAH-fluxes in the catchment. Finally, water samples from the Seebach creek (4) were taken at the outlet of the catchment in order to determine the PAH flux leaving the investigation area. The water samples were taken in 1 l brown-glass bottles, which were covered with a 0.5 mm sieve (stainless steel) to retain coarse particles like needles. Two bottles were filled at each sampling point. Furthermore two blanks (bottles containing millipore water) were carried along and analysed during each sampling campaign. The PAHs were liquid-liquid extracted by adding 3 ml of cyclohexane to the bottles. Again PAHs were measured using GC-MS.

3. Results and discussion

Fig. 2 shows the seasonal variation of the PAH bulk deposition rates as average values of the different sampling stations (sum of litterfall and throughfall for the samplers in the forest) with higher values during winter and spring and lower ones during summer and autumn. The seasonal variations as well as the deposition rates are in good agreement with previously reported values from rural/semi-rural areas (Brorström-Lunden and Löfgren, 1998). Generally during winter the emission rates of diffuse sources increase (e.g. domestic heat) (Guidotti et al., 2000) and on the other hand snow can act as a very efficient scavenger for atmospheric pollutants (Franz and Eisenreich, 1998). Because of the absence of any point source of pollution (e.g. power plants or incinerators) in or in the vicinity of the catchment, this region is only affected by long-range transport of PAHs. Main sources for such diffuse pollution of rural areas are domestic heat and traffic (Wild and Jones, 1995).

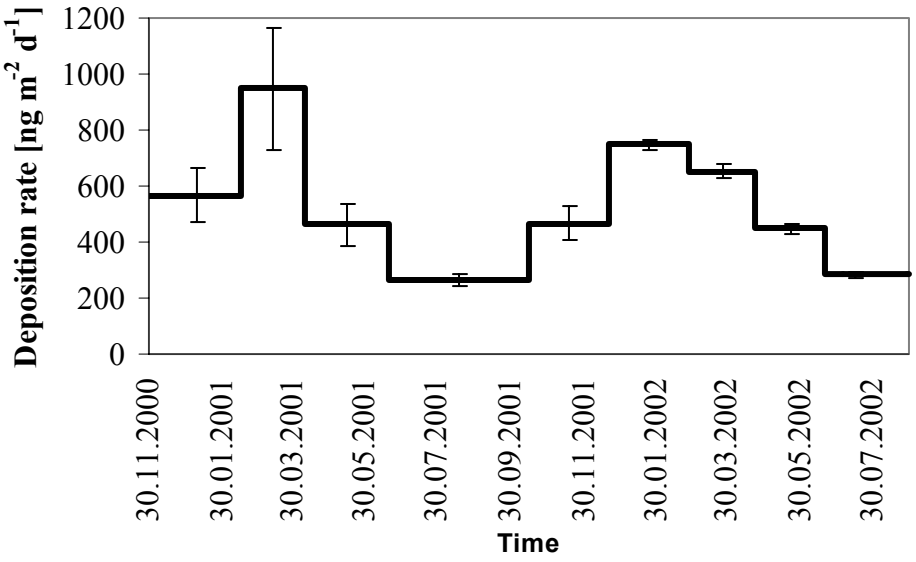

Figure 2: Deposition rates of PAHs in the Seebach catchment during a 2 a monitoring period. Error bars represent one standard deviation (n = 4).

The deposition samplers were placed in different topographical positions: In the valley of the Seebach creek (approximately 700 m a.s.l) and uphill close to the watershed (approximately 1000 m a.s.l.). Furthermore differences between open field and forested areas were considered. Surprisingly, only little influence on the average deposition rates was observed using the time-integrated passive sampler technique within sampling periods of 2 - 4 months (see error bars in Fig. 2). At this time interval the spatial heterogeneity of the atmospheric deposition on a micro-catchment scale seems to be negligible. Therefore, the obtained values were assumed to be representative for the overall catchment.

The PAH concentrations in the soil samples are presented in Tab. 1. The highest concentrations of PAHs were obtained from the organic layers (Oe and Oa) in coincidence with the highest organic carbon content. The concentrations increased with depth from Oe to Oa. A steep decrease in concentrations occurred from the Oa to the AE horizons. The PAH-storages of each horizon were calculated based on the horizon thickness and the bulk density of that layer. Even if the concentrations between the horizons of the different soil profile locations disagree, the storages over the entire profiles matched quite well. This supports the findings of similar time-integrated deposition rates at various locations in the catchments (if deposition is homogeneous in the catchment then an equally distributed storage is expected). The results are in line with investigations by other authors, who also reported high concentrations in the organic top layers (up to 18 mg kg^{-1}) and much lower ones in the mineral horizons (Krauss et al., 2000). Since the distribution of PAHs between soil solution and solid compounds is related to the organic matter content of the soils, the organic layers of the forest soils act as the main sink/reservoir in forested environments.

Table 1 Soil properties, PAH concentrations and calculation of PAH storage in two representative soil profiles of the Seebach catchment.

Spodosol						Stagnic Luvisol					
Horizon	Thick-ness [m]	Bulk density [g cm^{-3}]*	Organic carbon [%]	PAH Conc. [µg kg^{-1}]	PAH Storage [µg m^{-2}]	Horizon	Thick-ness [m]	Bulk density [g cm^{-3}]*	Organic carbon [%]	PAH Conc. [µg kg^{-1}]	PAH Storage [µg m^{-2}]
Oe	0.06	0.10	48.2	4803	28820	Oe	0.03	0.10	47.1	1283	3849
Oa	0.05	0.20	36.7	5488	54880	AeOa	0.4	0.50	22.3	3497	69940
AE	0.07	1.20	4.4	236	19820	Ae	0.02	1.00	3.6	164	3280
Bh	0.17	1.40	1.2	26	6188	Swh	0.10	1.70	0.4	50	8500
Bs	0.56	1.40	1.0	5	3920	Sw	0.21	1.70	0.3	22	7854
						Sd	0.42	1.50	0.3	13	8190
Sum					113630						101613

* estimated

In the water samples highest concentrations were measured in very shallow springs mixed with surface runoff (maximum value 25 ng l^{-1}). These springs sometimes run dry. In the deep spring water PAH concentrations were always in the range of the blanks (3 ng l^{-1})or below the detection limit of 0.5 ng l^{-1} for each compound. The concentrations in water samples of the Seebach creek, reflecting a mixture of the different water discharges, were only slightly above the blank values (maximum 9 ng l^{-1}). In the shallow springs the PAHs could be detected only after long rain periods, which is consistent to previous reported results (Schrimpff, 1984). This indicates that drainage of the periglacial debris predominate the discharge.

Using the data on atmospheric deposition rates as input and water discharge and concentration as output, a mass balance was calculated for the whole catchment area (4.34 km^2) for the year 2001. For calculation of the output flux an averaged annual concentration of 10 ng l^{-1} for the

PAH_{15} was assumed (worst case scenario). The result of the mass balance (Tab. 2) shows, that more than 90% of the atmospheric PAH influx remains in the catchment and persistent compounds accumulate in the soil. This is consistent with previously reported results (Schrimpff, 1984; Simmleit and Herrmann, 1987).

Table :2 Mass balance (input – output) of PAHs in the Seebach catchment for the year 2001.

Discharge	PAH Input	PAH Output		PAH Remaining in the soils	
[m^3]	[kg]	[kg]	[% of input]	[kg]	[% of input]
7 559 000	0,9817	0,0756	7,7	0,9061	92,3

The results of the mass balance show that the top soils act as a buffer for the contaminants. Internal PAH-fluxes in the catchment seem to be limited to special meteorological conditions, e.g. if preferential flow occurs and a small fraction of contaminants bypasses the unsaturated zone.

If atmospheric deposition rates remain on a high level in the future and if the PAHs in the soils are stable, then the question of maximum sorption or filter capacity of the soils arises (maximum load). Under this perspective it is of importance, that most of the PAHs (e.g. benzo(a)pyrene) are sorbed onto particles (e.g. soot, chars, charcoals) during atmospheric transport and the deposition process. Fig. 3 shows carbonaceous particles separated from precipitation and soil samples. It is obvious that the deposition of such particles will influence the long-term sorption capacity of the soils because of their extremely high sorption coefficients (Kleineidam et al., 1999). In order to assess the risk of a possible groundwater contamination from atmospheric deposition of organic compounds at regional scale, future research has to focus on the behaviour of atmospherically derived carbonaceous particles in the soils (e.g. time scale of weathering) and their associated pollutants.

Figure 3:Organic particles (char) in precipitation (left hand side) and soil (right hand side) with a size of about 10 µm.

4. Conclusions

Currently most of the PAHs which reach the investigated catchment by atmospheric deposition are stored in the soil. Soil profiles in various locations in the catchment show similar PAH-storage over the entire profile of about 100 000 µg m^{-2} which agrees with the findings from the time-integrated monitoring of the deposition rates which are similar throughout the catchment. Up to now the soils act as a barrier for migration of PAHs through the unsaturated zone, indicated by the very low PAH concentrations measured in the water samples from the different springs. Internal PAH fluxes after their deposition seem to be limited to short-term preferential flow and/or surface runoff. Organic particles were found in

precipitation and soil samples as well. These particles are assumed to play a key role in the long-term fate of PAHs in the soils (bioavailability, leaching behaviour etc.).

References

Brorström-Lunden E. and Löfgren C. (1998): Atmospheric fluxes of persistent semivolatile organic pollutants to a forest ecological system at the Swedish west coast and accumulation in spruce needles.- Environ. Poll. 102: 139-149.

Franz T. and Eisenreich S. (1998): Snow scavenging of polychlorinated biphenyls and polycyclic aromatic hydrocarbons in Minnesota.- Environ. Sci. Technol., 32: 1771-1778.

Guidotti M., Giovinazzo R., Cedrone O. and Vitali M. (2000): Determination of organic micropollutants in rain water for laboratory screening of air quality in urban environment.- Environ. Intern., 26: 23-28.

Hinderer M. (1995): Simulation langfristiger Trends der Boden- und Grundwasserversauerung im Buntsandstein-Schwarzwald.- Z. dt. geol. Ges., 146: 83-97.

Jones K. C., Stratford J. A., Waterhouse K. S., Furlong E. T., Giger W., Hites R. A., Schaffner C. and Johnston A. E. (1989): Increases in the polynuclear aromatic hydrocarbon content of an agricultural soil over the last century.- Environ. Sci. Technol., 23: 95-101.

Kleineidam S., Rügner H., Ligouis B. and Grathwohl P. (1999): Organic matter facies and equilibrium sorption of phenanthrene.- Environ. Sci. Technol., 33: 1637-1644.

Krauss M., Wilcke W. and Zech W. (2000): Polycyclic aromatic hydrocarbons and polychlorinated biphenyls in forest soils: Depth distribution as indication of different fate.- Environ. Poll., 110: 79-88.

Martin H. and Grathwohl P. (2002): Entwicklung von Adsorberkartuschen als Passivsammler zum zeitlich integrierenden Depositionsmonitoring für Polyzyklische Aromatische Kohlenwasserstoffe.- Bodenschutz 7: 18-22.

Simmleit N. and Herrmann R. (1987): The behaviour of hydrophobic, organic micropollutants in different karst water systems.- Water, Air, and Soil Poll., 34: 79-95.

Schrimpff E. (1984): Organic micropollutants balances in watersheds of northeastern Bavaria.- Fresenius Z. Anal. Chem., 319: 147-151.

Wild S. and Jones K. C. (1995): Polynuclear aromatic hydrocarbons in the United Kingdom environment: A preliminary source inventory and budget.- Environ. Poll., 88: 91-108.

Magnetic proxy mapping as a tool for outlining contaminated areas

E. Appel, V. Hoffmann, W. Rösler, and L. Schibler

Institut für Geowissenschaften, Sigwartstraße 10, D-72076 Tübingen, Phone: +49(0)7071-297-4132, Fax: +49(0)7071-295-842, erwin.appel@uni-tuebingen.de

Abstract:. Iron and iron oxides constitute a significant part of the atmospheric aerosols. These magnetic particles can have common sources and transport paths as pollutants and partly also serve as carriers of various contaminants such as heavy metals (HM). In situ measurements of soil surface magnetic susceptibility (MS) allow to map the spatial distribution of atmospherically deposited dust. In combination with shallow vertical MS profiles (30 cm), the discrimination between geogenic/pedogenic and anthropogenic contributions to the measured MS values is facilitated. Due to fast acquisition of a high number of data points in the field and data interpretation during the field campaign, the method is especially suitable as a first step of site investigation. The resulting map of MS serves as a proxy for contaminations and allows a specific selection of optimum sampling points for further analyses (e.g. chemical analyses for HM or PAH) at indicated pollution hot spots.

Introduction

In recent time, the need for new, fast, and cost effective environmental screening and monitoring methods has grown significantly. The European Water Framework Directive (WFD) regulates by law to control all impacts - physical, polluting and otherwise - on the water environment with the aim of achieving 'good' ecological status for rivers and water systems. In addition to former approaches in water quality management it addresses also the impacts of diffuse pollution to entire water systems, including subsurface water and soil. As diffuse pollution comes from a large number of small sources, probably comprising a variety of different pollutants, affecting large areas far distant from individual pollution sources, new strategies for assessing the pollution state are needed. Traditional screening and monitoring methods like geochemical analyses or biomonitoring methods generally do not allow to investigate a large number of data points within short time at reasonably low costs. Here a cost-effective, fast and easy to use screening scheme using proxy parameters for estimating and outlining the extent of pollution, in combination with traditional analysis methods at selected sites, could solve the problem.

Magnetic proxy mapping

All materials possess magnetic properties, which are mainly controlled by iron and a group of iron-bearing minerals. Magnetic susceptibility (MS) is a very sensitive parameter for classification of materials and for identifying even trace amounts of highly magnetic minerals like magnetite (Dearing, 1994). In addition to the natural content of iron bearing minerals, the accumulation of magnetite-rich anthropogenic ferri(o)magnetic particles in soils gives a significant contribution to topsoil magnetic susceptibility values (Hunt et al., 1984; Heller et al., 1998; Kapička et al. 1999).

Within the EU funded RTD project MAGPROX - Screening and Monitoring of Anthropogenic Pollution over Central Europe by using MAGnetic PROXies (5th FP, project No. EVK2-CT-1999-00019), a fast and cost-effective environmental screening scheme was developed and tested on different scales, on different geological backgrounds, and with different amounts of environmental pollution. Top soil magnetic susceptibility was measured

on forest soils in a grid of 10 km by 10 km over large parts of Central Europe, covering areas with long term industrial activities with known environmental pollution as well as presumably clean areas without major industrial activities. For data acquisition, a Bartington MS2B susceptibility meter was used in combination with a GPS system for geographic positioning. Standardized procedures for site selection, recording of site-relevant information, and for the measurement process were developed and tested to guarantee repeatable and comparable results of individual measurements (Schibler et al., 2000). The resulting large scale map (Fig. 1) clearly delineates areas with major anthropogenic impact, such as the so-called "black triangle" industrial area at the borders of Eastern Germany, Czech Republic, and Poland or the Upper Silesian industrial region in South Poland.

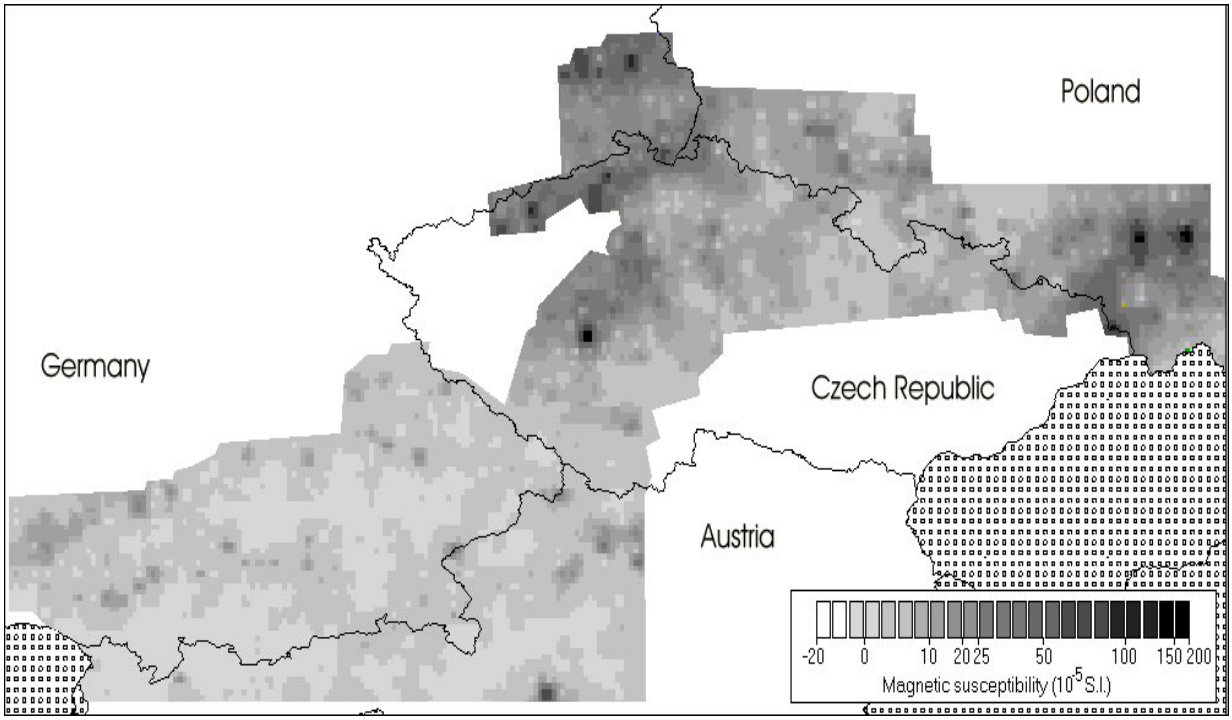

Figure 1: Magnetic susceptibility values of forest top soils in a 10 km by 10 km grid over Central Europe. EU RTD project MAGPROX, field mapping campaigns 2000, 2001.

To discriminate effects of anthropogenic pollution from natural background values, shallow soil cores of 30 cm length and 3.5 cm diameter were taken using a Humax soil corer. Magnetic susceptibility depth profiles were measured at these cores. Enhanced MS values close to soil surface (in O and Ah horizons) indicate anthropogenic (atmospheric) input whereas MS values increasing with depth indicate natural (lithogenic, pedogenic) origin. For a faster discrimination of anthropogenic and geogenic contributions to the MS, an instrument for in situ measurements of high resolution MS profiles in shallow boreholes was developed. The MAGPROX SM400 downhole susceptibility meter (Fig. 2) allows to record MS depth profiles within few minutes at selected sampling points. Together with the results of the MS mapping, a three-dimensiaonal distribution of MS can be obtained (e.g. Fig. 3).

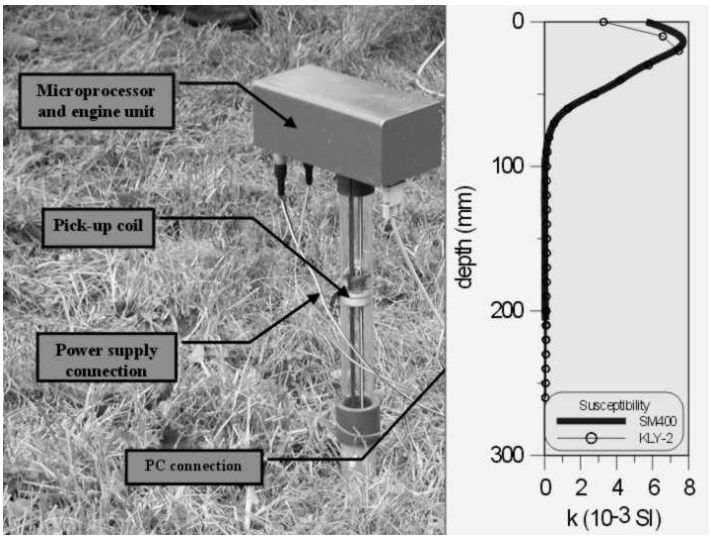

Figure 2: Magprox SM400 susceptibility meter with downhole susceptibility curves obtained in situ (SM400; thick line) and in laboratory on subsamples of the extracted soil core (KLY-2, dots). The curve shows a distribution of MS values with a maximum close to the soil surface and lower values with increasing depth, which is typical for anthropogenic origin of the MS signal.

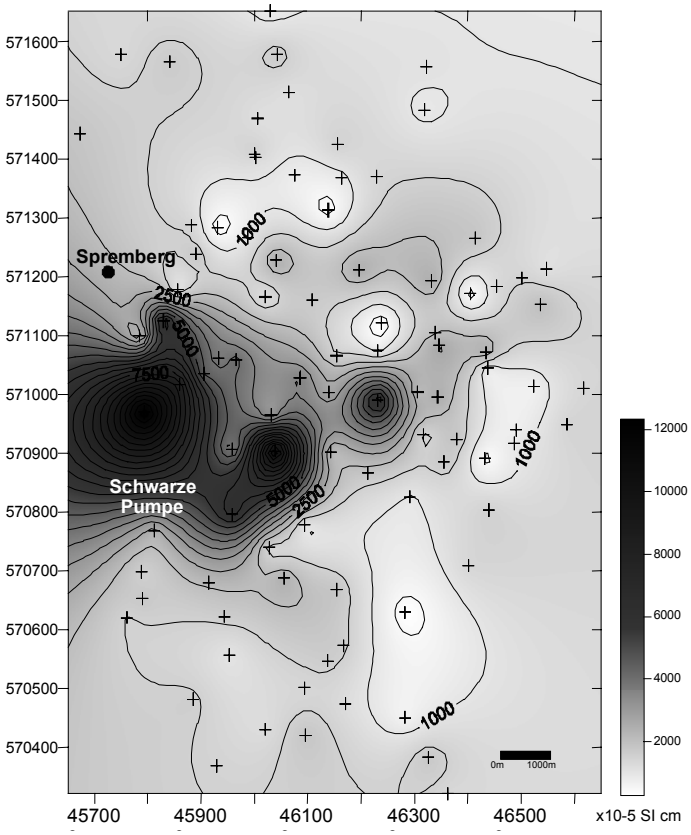

Figure 3: Map of local MS distribution near Schwarze Pumpe brown coal power plant, Lausitz, Eastern Germany. The image shows an "integrated" MS values with depth, combination of lateral and depth distribution of MS values. The highest values can be found close to the powerplant location, distributed along the main wind direction.

Correlation of magnetic susceptibility and pollutants

Magnetic minerals themselves are not hazardeous to human health or to ecosystem functioning. But where natural sources are unlikely, the anomalous presence of magnetic minerals may indicate anthropogenic impacts like deposition of atmospheric aerosols generated by industrial processes. A case study, based on the results of the large scale MS map (Fig. 1) was carried out in the Lausitz region, Eastern Germany, in order to investigate the regional and local distributions of MS and heavy metal contents in the area and along shallow vertical soil profiles (Kalinski, 2002; Spiteri, 2002). Strong positive correlations

between MS values and HM concentrations are found for Fe, Mn, Pb, Zn, Cu, and Cd within the studied soil profiles (Fig. 4).

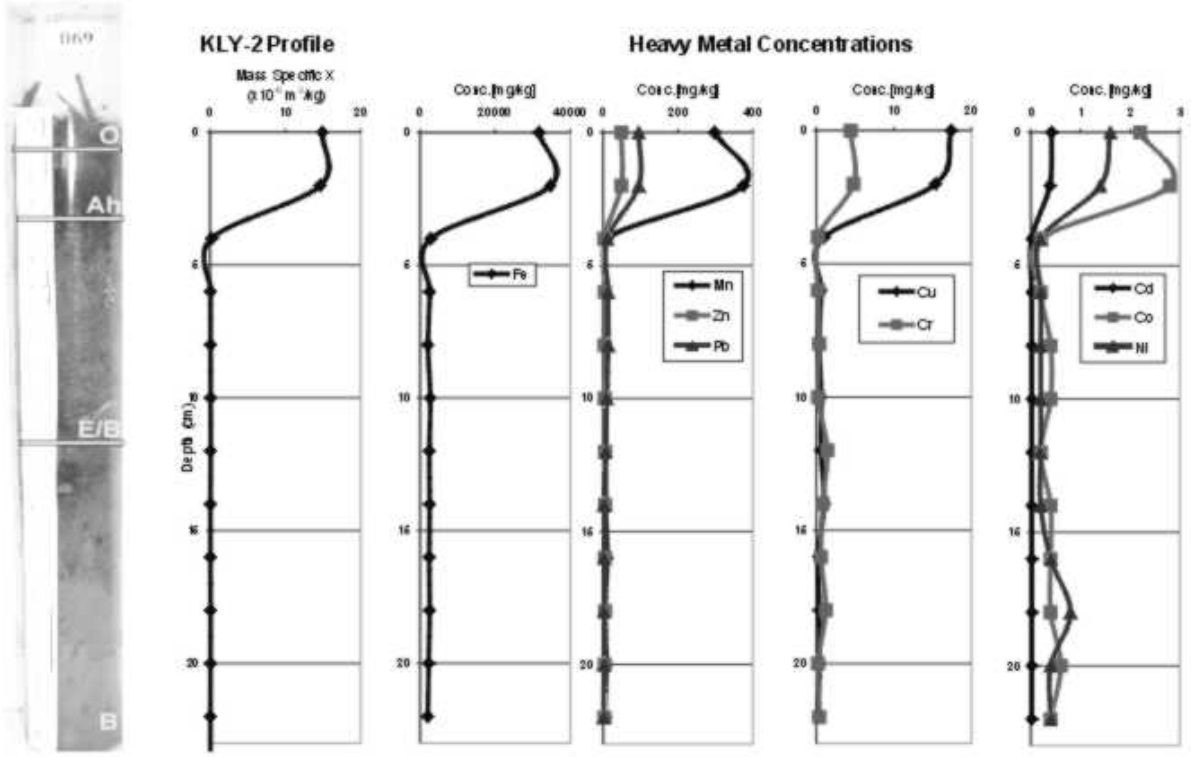

Figure 4: Distributions of magnetic susceptibility and heavy metal contents (Fe, Mn, Zn, Pb, Cd, Cu, Ni, Cr and Co) along a soil core profile from Lausitz area.

References

Dearing J. (1994): Environmental Magnetic Susceptibility; Using the Bartington MS2 System – Chi Publishing, England, 104pp

Heller, F., Strzyszcz, Z., Magiera, T., 1998. Magnetic record of industrial pollution in forest soils of Upper Silesia, Poland. *J. Geophys. Res.,* **103, B8**, 17767-17774.

Hunt, A., Jones, J., Oldfield, F., 1984. Magnetic measurements and heavy metals in atmospheric particulates of anthropogenic origin. *Sci. Total Environ.*, **33**, 129-139.

Kalinski V., 2002. Environmental Hotspot Screening/Monitoring in Spremberg and Weißwasser Area, Germany; Detailed Surface/Soil Profile Magnetics – Unpublished M.Sc. thesis, University of Tübingen, Germany

Spiteri, C., 2002. Environmental Hotspot Screening/Monitoring in Spremberg and Weißwasser Area: Correlation Analysis between Magnetic Proxies and Heavy Metal Contamination in Polluted Soils - Unpublished M.Sc. thesis, University of Tübingen, Germany

Kapička A., Jordonova N., Petrovskỳ E. and Ustjak S. (1999): Magnetic stability of power-plant fly ash in different soil solutions – Phys. Chem. Earth (A), **25, 5**, 431-436

Schibler L., Boyko T., Ferdyn M., Gajda B., Höll S., Jordonova N., Rösler W. and MAGPROX team (2000): Topsoil magnetic susceptibility mapping: Data reproducibility and compatibility, measurement strategy- Stud. Geophys. Geod., **46**, 43-57

"Hot spots" on the map of magnetic susceptibility of soils in Poland" as potential areas of soil and groundwater contamination

Tadeusz Magiera, Zygmunt Strzyszcz, Marianna Czaplicka,

Institute of Environmental Engineering, Polish Academy of Sciences , ul. M. Sklodowskiej-Curie 34, tel. +48 32271 64 81, fax.. +48 32271 69 50, E-mail: magiera@ipis.zabrze.pl

Abstract: Magnetic mapping based on the measurement of soil magnetic susceptibility as a result of industrial dust deposition is fast, inexpensive and accurate tool for assessing the state of soil contamination. In many cases, the proper interpretation of the magnetic susceptibility distribution in study area could (1) substitute for direct chemical analysis of soil samples polluted by various heavy metals and organic pollutants and (2) provide an easy means identifying the source(s) of contaminants. Observed "hot spots" of the topsoil magnetic susceptibility on the map of Poland suggests that observed anomalies are result of mostly anthropogenic pollution. The largest areas of magnetic anomalies as well as the highest values measured during the study are located in urban and industrial areas (Upper Silesia, Walbrzych, Turoszow – "black triangle", Krakow, Gdansk, Wroclaw, Lodz,). The map illustrates the spreading of dust emissions produced by many branches of industry using the coal as a source of energy. Also the urban sources of emission, as a result of coal burning for heating, play an important role in producing the magnetic particles of anthropogenic origin. The same sources emit also many organic pollutants as: PAH, VOC etc. The concentration of some heavy metal (Pb, Zn, Cd) and organic pollutants (PAH, VOC) in soil of selected "hot spots" in Upper Silesia was studied to find the potential hazard of such areas for pollution mobilization and transport.

1. Introduction

The fast development of industry in the 19th and 20th centuries has caused a degradation of the natural environment in many parts of the world. Industrial emissions of toxic substances have produced widespread soil contamination in some areas. Industrial gases, dusts and aerosols emitted to the atmosphere contain many substances potentially dangerous for humans. They are transported by winds and air currents and finally deposited on the soil surface. Than they can migrate down to the soil profile and reach the groundwater level. In many industrial and urban areas the concentration of contaminants in topsoil is considerable high. Such abnormally high concentration exemplify so called "ecological bomb" that can "explode" suddenly in case of even minimal changes of physical or chemical conditions of soil environment. Such areas can influence the groundwater slowly but permanently for long time by infiltration processes causing the contamination of groundwater. It is urgent need to identification such areas and permanent monitoring to observe the pollution pathway and soil – water interaction.

The new method of such fast and cost-effective can became the soil magnetometry based on magnetic susceptibility measurement that is result of anthropogenic magnetic particle concentration in topsoil. Iron oxides are components of many industrial dusts deposited on the soil surface. The magnetic particles are tracers of many pollutants contained in industrial and urban dusts and aerosols, mostly inorganic (heavy metals) but also some indirect correlation between some organic pollutants has been reported (Morris et al. 1994). In many cases, the proper interpretation of the magnetic susceptibility distribution in areas of magnetic "hot spots" (1) substitute for direct chemical analysis of soil samples polluted by various heavy metals and (2) provides an easy means identifying the source(s) of contaminants.

2. Methods

Topsoil magnetic susceptibility map of Poland was based on laboratory measurement of 10 800 topsoil archival samples Polish Geological Institute that was used for geochemical prospecting (Lis et al. 1995). For the susceptibility measurement MS2B "Bartington" susceptibility meter was used. The measured volume susceptibility was recalculated for specific (mass) susceptibility. From the whole Polish territory the area of the largest magnetic "hot spot" was selected to detailed chemical study for heavy metals and organic compounds. The selected area covers 9800 km^2 of Upper Silesian Industrial Region (USIR) and surroundings. Geostatistic data concerning heavy metals were calculated on the base of 593 topsoil samples chemical analysis obtained by Lis (Lis et al. 1995) during the geochemical prospecting. Samples for analysis of organic compounds from USIR were collected in industrial areas influenced by coking and chemical industry and determined with application of gas chromatography using standard methodology (Kubica et al. 1998, Czaplicka et al. 2000).

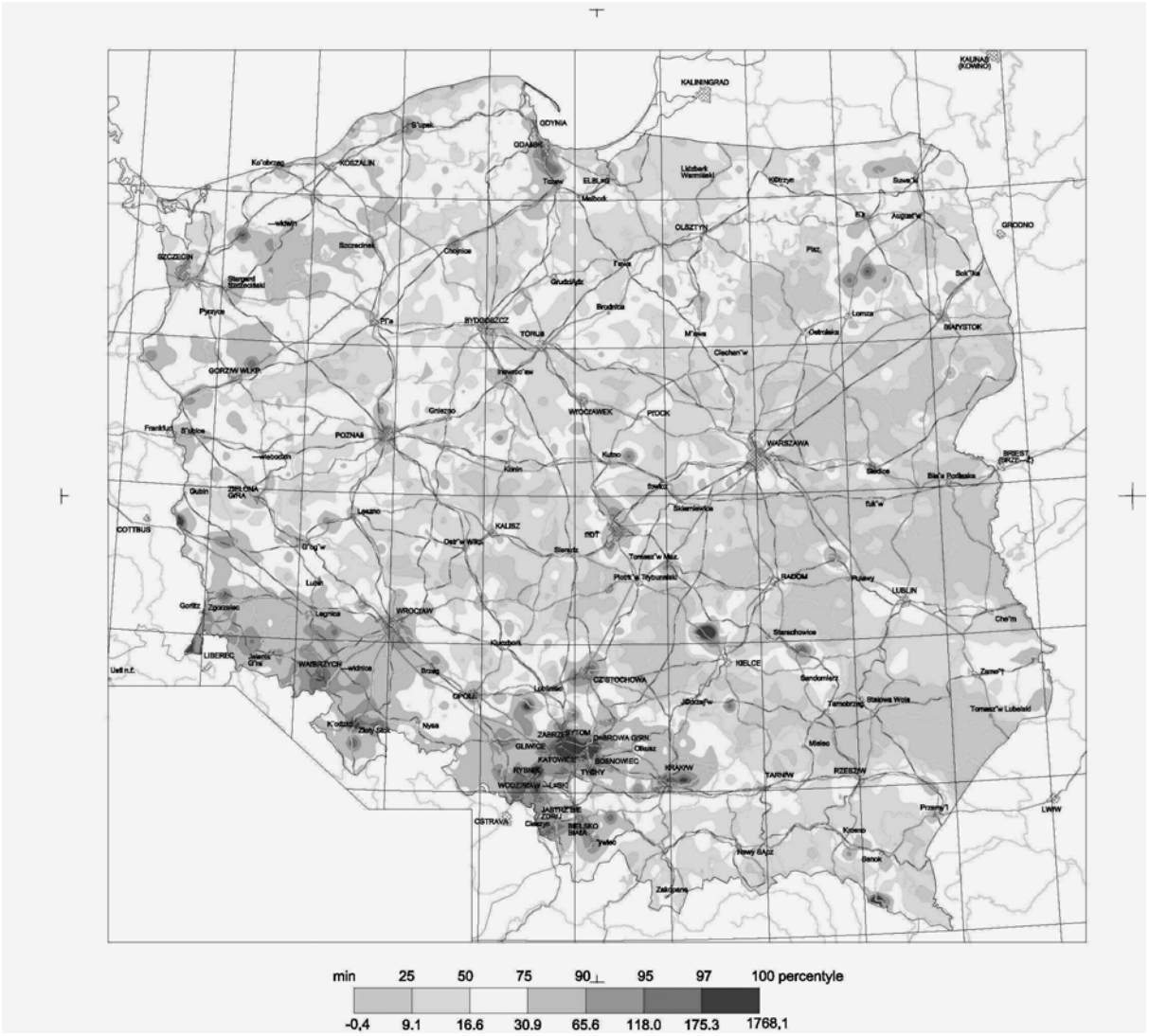

Figure 1: Topsoil magnetic susceptibility map of Poland with some black "hot spots".

3. Results and discussion

Distribution of topsoil magnetic susceptibility "hot spots" on the map of Poland (Fig. 1) suggests that observed anomalies are result of mostly anthropogenic pollution. The largest areas of magnetic anomalies as well as the highest values measured during the study are located in urban and industrial areas (Upper Silesia, Wałbrzych, Turoszów – "black triangle", Kraków, Gdańsk, Wrocław, Szczecin, Łódź, Częstochowa). The exception is only "hot spot" located NW from Kielce. That is connected with local bog iron ore exploration in XIX century. Generally the map illustrates the spreading of dust emissions produced by many branches of industry using the coal as a source of energy.

The urban sources of emission using the coal burning for heating play an important role in producing the magnetic particles of anthropogenic origin. According to statistical data given in Table 1, which, suggest the strong relationship between the magnetic susceptibility and character of land development, the urban source of magnetic topsoil anomaly is even more important. In residential areas the average (dispersed development) values of susceptibility is 3.30 higher than in uninhabited areas and in urban areas with compact development the susceptibility is over 4 times higher then in uninhibited or rural areas and the both are even higher than in industrial areas (enrichment factor 2.61).

The magnetic particles emitted from high stocks of industrial plants are transported in longer distance from the source in contrary to these produces by urban sources, which are accumulated in topsoil close to emission sources. The role of so-called "low emission" is very often neglected. Thousands of small urban boilers and millions of home hearths contribute to the high dust pollution at urban sites. Construction of high smoke stacks and installation of more efficient electrofilters in modern power plants as well as partially elimination of environmentally harmful technologies in metallurgical and cement plants causes decreasing and spatial dispersion of emissions therefore the high anomalies close to the relatively new power plants as Połaniec, Kozienice and Konin was not observed on the map (Magiera et al. 2002)

Table 1 – Enrichment factor for magnetic susceptibility (κ) and selected heavy metals in relation to land development.

Land use	κ	Cr	Cu	Ni	Sr	Pb	Zn
uninhabited areas	1.00	1.00	1.00	1.00	1.00	1.00	1.00
rural areas	1.20	1.25	1.50	1.67	1.66	1.17	1.52
residential areas	3.30	1.50	3.00	2.00	3.17	2.25	2.59
urban areas	4.35	1.75	3.50	2.30	3.83	2.92	3.48
industrial areas	2.61	1.25	1.25	1.67	2.17	2.08	2.10

The "hot spot" areas are usually enriched in organic and inorganic pollutants. In urban and industrial areas the enrichment factors are the highest for Zn, Pb, Cu and Sr (tab. 1). In many cases the high correlation between magnetic susceptibility and some heavy metal content (mostly Pb, Zn and Cd) were observed in areas influenced by high industrial and urban dust fall (Strzyszcz and Magiera 1998). Two kinds of relationship between the magnetic susceptibility and dust pollutants concentration in soil are observed. The first, direct relationship is connected with geochemical and mineralogical properties of fly ashes, where the first row transition elements - V, Cr, Mn, Co, Ni, Zn and Cu are mostly connected with magnetic mineral phases and occur usually in the form of substituted spinels $Fe_{3-x}M_xO_4$.

(Hansen et al. 1982). If the elements are incorporated inside the mineral lattice they are quite stable and potential hazard of their mobilisation in soil environment are low. However in many cases they are connected with the mineral surface only by adsorption forces (Hullet et al 1980) that can be easily mobilized in acid soil (especially forest soil) condition. The defects or imperfection of surface structure of anthropogenic ferrimagnetic minerals can favour also the presence of many easily mobilised impurities in the lattice close to the mineral surface (Vaughan et al. 2002).

The second, indirect relationship is a result of common emission sources for anthropogenic magnetic particles and many pollutants (including also organic pollutants). The magnetic particles can serve in this case as easily detected tracers of potentially contaminated sites.

Table 2 presents the enrichment factor of some heavy metals and organic pollutants in the area of the largest and most intensive "hot spot" in Poland connected with Upper Silesian Industrial Region "hot spot", in relation to the national average in topsoil. The highest enrichment is observed for the most hazardous element as Cd (6.25) and Pb (6.46). On the almost whole area of USIR "hot spot" the Cd content is over 4 mg/kg, Pb > 100 mg/kg and Zn > 300 mg/kg. Also in case of organic pollutants, particularly PAH's the enrichment factor is high, particularly for semi-volatile hydrocarbons (naphthtalene, phenanthrene, anthracene, fluoranthene) and benzo(a)pyrene in topsoil of former coking plant areas. The high enrichment factors in samples form coking plant - coking battery are result of direct influence of technological process on environment (Tab. 3).

The high enrichment factor of susceptibility (3.46) can serve as a tracer of this contamination. The Pb, Zn and Cd contents in large areas of the studied region exceed national limits for agriculture, forest and urban areas and some percentage of this territory has the Pb concentration even over limits for industrial and mining areas (Tab. 2). It is obvious that such areas are thread also for groundwater by soil-water interaction.

Table 2 – Enrichment factor of some heavy metals in USIR "hot spot"in relation to the national average in topsoil. 1) in $x10^{-8}m^3kg^{-1}$, 2) in mg/kg 3) in %

Pollutant	USIR average	Enrichment factor in relation to national average	USIR maximal values	National limits for topsoil (gropuB/groupC)*	Area of USIR with concentration over national limits B/C (%)
$\kappa^{1)}$	121	3.46	1768	-	-
$As^{2)}$	9	2.25	238	20/60	7/1
$Cd^{2)}$	5	6.25	160	4/15	32/6
$Co^{2)}$	3	1.20	21	20/200	0.2/0.0
$Cr^{2)}$	7	1.17	95	150/500	0/0
$Cu^{2)}$	17	1.70	805	150/600	0.8/0.2
$Fe^{3)}$	1	1.49	3.57	-	-
$Mn^{2)}$	380	1.42	7000	-	-
$Ni^{2)}$	7	1.17	89	100/300	0/0
$Pb^{2)}$	226	6.46	16972	100/600	45/6
$Zn^{2)}$	504	5.73	11899	300/1000	38/11

**) group B - arable forest and urban areas; group C – industrial, mining and communication areas*

Table 3 - Enrichment factor of PAHs for selected area

Compound	coking plant (coking battery)	coking plant (coke-quenching tower)	heavy industrial plant -processing of tar	heavy industrial plant - processing of benzene
naphthalene	357.8	26.2	31.8	9.8
phenanthrene	299.8	4.0	27.7	2.3
anthracene	79.9	2.8	15.0	1.5
fluoranthene	92.1	1.0	11.8	1.1
chrysene	14.7	14.9	1.8	1.8
benzo(a)anthracene	13.3	3.8	1.6	1.7
benzo(a)pyrene	53.5	9.0	8.0	7.5
benzo(g,h,i)perylene	1.2	1.0	1.0	1.1
total PAHs	61.58	5.55	9.25	1.97

4. Conclusions

1. The analysis of magnetic susceptibility map of Polish topsoil reveals existing of many areas of magnetic “hot spots” closely connected with industrial and urban areas mostly in south and south-western Poland.
2. Areas of magnetic susceptibility “hot spots” are enriched in heavy metals and organic compounds of anthropogenic origin.
3. The magnetic susceptibility as an easily detected parameter can serve as an indictor of presence inorganic and organic soil pollutants being the result of urban and industrial dust deposition. These areas can be also the potential source-areas for groundwater contamination.

References

Czaplicka M., Weglarz A., Klejnowski K., Analysis of organic contaminants adsorbed on particulate matter from motor vehicles. Anal. Chem. (Warsaw) 45, 23-30, 2001.

Hansen L. D., Silberman D., Fisher G. L.,1981. Crystalline components of stack-collected, size-fractionated coal fly ash. Environ. Sci. Technol., 15, 1057-1062.

Hulett L. D., Weinberger A., J., Northcutt K., J., Ferguson M., 1980. Chemical species in fly ash from coal-burnning power plant., Science, 210, 1356-1358.

Kubica K., Czaplicka M., Kordas T., 1998. Determination of organic contaminates in soil from coking plant. Anal. Chem. (Warsaw), 43, 57.

Lis J., Pasieczna A., 1995. Geochemical Atlas of Poland. PGI. Warszawa.

Magiera T., Lis J., Nawrocki J., Strzyszcz Z., 2002. Magnetic Susceptibility of Silos In Poland. PIG Warszawa.

Morris W. A. Versteeg J. K., Marvin C. H., McCarry B. E., Rukavina N. A., 1994. Preliminary comparisons between magnetic susceptibility and polycyclic aromatic hydrocarbon content in sediments from Hamilton Harbour, western Lake Ontario. The Science of the Total Environment, 152, 153-160.

Strzyszcz Z., Magiera T., 1998. Heavy Metal Contamination and Magnetic Susceptibility in Soils of Southern Poland. Physics and Chemistry of the Earth, Vol. 23, No 9-10, 1127-1131.

Vaughan D. J., Pattrick R.A.D., Wogelius R.A., 2002. Minerals, metals, and molecules: ore and environmental mineralogy in the new millennium. Mineralogical Magazine, 66(5), 653-676.

Real-time/in-situ determination of pollutants in soil and water systems: FTIR spectroscopy combined with fiberoptics or membranes

Shaviv Avi[1], Shmulevitch[1], I. , Katzir[2], A., Kenny[1], A. and Linker[1], R.

[1]*Civil and Environmental Engineering, Technion-IIT,Haifa 3200, Israel, phone: 972-4-8292602, Fax: 972-4-8221529, E-Mail: agshaviv@tx.technion.ac.il*
[2] *Dept. Applied Physics, Tel-Aviv University, Israel*

Abstract: The development of new silver halide ($AgCl_x Br_{1-x}$) fibers that transmit with minimal loss into the mid-IR, paved the way to their successful utilization as effective *in-situ* ATR elements promoting the implementation of Fiberoptic Evanescent Wave Spectroscopy (FEWS) for monitoring soil pollutants such as nitrate. This work focuses on the *in-situ*, remote and online detection of nitrate and other pollutants in soil or water using FTIR-FEWS systems. Spectra of soil pastes, suspensions and phosphate, carbonate, sulphate, ammonium and those of organic constituents were isolated from soil spectra in order to study possible interference with nitrate determination.
Standard error of estimate (SEE) and R^2 values obtained with flat fibers under the single point correlation method, were superior to those obtained for cylindrical FEWS and ZnSe ATR crystals in pure water. Significant improvement in the SEE and R^2 was achieved in most soil pastes by applying the simple mode of the Cross Correlation method and more sophisticated methods. Direct transmission of MIR radiation through ion-exchange membranes, partially loaded with nitrate or carbonate, was found an effective alternative for FTIR determination of these ions. This can be further modified to combine membranes with ATR devices or FEWS for detection of ionic or organic pollutants.

1. Introduction

Direct and real-time monitoring of nitrate and MIR absorbing solutes in soils would be extremely useful for managing application of fertilizers and agrochemicals. Such monitoring would allow adjusting agrochemical levels to 'local' field requirements (precision farming), thus reducing both agrochemical costs and pollution. However, due to technological limitations, real time monitoring of solutes/pollutants is not common.

MIR spectroscopy, and more particularly Attenuated Total Reflection (ATR) with Fourrier Transform Infra-Red (FTIR) spectrometers, has been used for the study of liquids, pastes and powders, in which intense scattering of absorption precludes the use of transmission spectroscopy (e.g., Johnson and Aochi, 1996). Shaviv et al. (2002) demonstrated the usefulness of the FTIR/ATR technique for the determination of nitrate concentration in soil solution. Shaviv et al. (2002) also investigated the use of new optic fibers with high transmittance in the MIR range (Fiberoptic Evanescent Wave Spectroscopy – FEWS, Messica et al. (1991,1996)). A typical FEWS system (Figure 1) consists of a fiber-optic based ATR sensor connected to the IR source and sensor via long fiberoptic cables. Such a configuration would enable both continuous and remote monitoring as required for precision agriculture and environmental protection. However, as indicated by the results of Shaviv et al. (2002), further improvements of this FTIR/ATR approach are required, especially with regard to the data processing, and more sophisticated sensing elements (e.g. combination of FEWS or ATR devices and membranes. These are under current investigation.

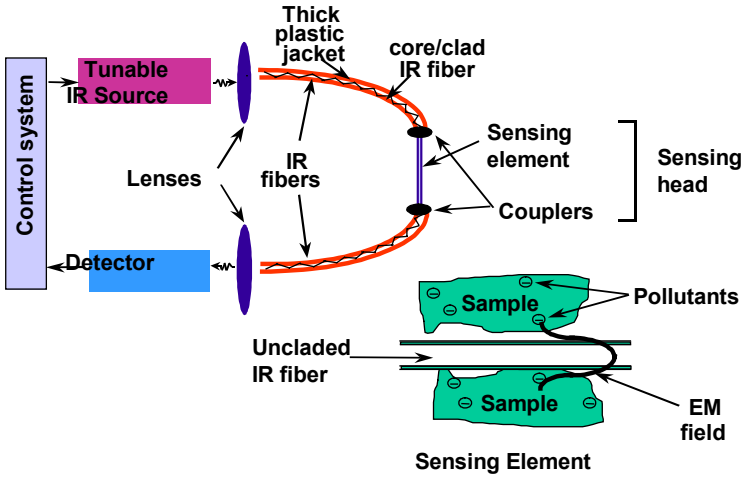

Figure 1: Scheme of the experimental system consisting of an IR source (tunable IR source or FTIR source), silver halide fibers as wave-guides, FEWS or ATR sensing element and detector

2. Experimental Methods

Several types of experiments and data processing approaches were used:

i. Spectral measurements were performed using a FTIR/ATR spectrometer (Bruker Vector 22) equipped with a ZnSe horizontal crystal and a DGTS detector. Experiments with the FEWS were with either cylindrical or flat fibers, dipped in solutions or pastes and connected to the spectrometer with special optical connectors. The spectra were taken in the range of 800 -2000 cm^{-1} with a precision of 2 cm^{-1}.

ii. Comparison of the ATR (ZnSE) common crystal vs. the new cylindrical and flat FEWS;

iii. Comparison of spectra obtained in pure solution with those obtained in soil pastes or for reclaimed effluents;

iv. Identify possible interferences of ionic compounds such as bi-carbonate, phosphate, ammonium, organic compounds and soil constituents with nitrate.

v. Use of direct transmission of MIR via anion-exchange membranes loaded with nitrate, carbonate or sulphate;

vi. Assessment of several options for improving data processing and thus increasing accuracy. These include: noise reduction and removal of interference with the water spectrum (Powell et al., 1986; Libnau et al., 1994); use of the cross-correlation method (Smith, 1997); use of the PCA (principle component analysis) method; use of the Nitrate peak-area at a given interval to correlate with nitrate concentration; perform soil-specific calibration curves based on soil identification using soil-specific MIR peaks.

3. Results Summary

i. Nitrate has a MIR absorption peak around 1350-1390 cm^{-1} that can be used for its determination in water based systems (solutions, effluents, soil pastes/slurries).

ii. Flat fibers act as good as and even better than the ATR/ZnSe crystal as nitrate sensors in water.

iii. Bicarbonate, ammonium, soil organic and mineral constituents interfere with nitrate determination in soil pastes and thus more sophisticated data processing methods are required to improve accuracy of the determination;

iv. Anion exchange membranes offer the potential to serve as sensors for MIR absorbing substances either via direct transmission or in combination with ATR/FEWS.

v. Spectra of soil pastes display special features, showing two distinct areas of absorption in the range of 900 to 1200 cm^{-1} and in the range of 1300 to 1600 cm^{-1}. These can be used for identifying the soil type and for the construction of soil-specific calibration curves, which significantly increase the accuracy of nitrate determination.

vi. Special treatment of the water peak around 1600 cm^{-1} and reduction of its interference with that of Nitrate provides significant improvement in the calibration curve.

vii. Methods such as: cross-correlation; PCA (principle component analysis); can be successfully used for improving the accuracy of determination being applied directly on a data set or for a specific soil after its identification and creation of a soil-specific calibration curve (as in section iv).

viii. The best results obtained with the ATR systems so far are with SEE around 10-20 ppm $N\text{-}NO_3$ in soil pastes, which translates to 3 to 10 ppm $N\text{-}NO_3$ on dry soil basis. The results obtained with membranes offer at least one order of magnitude improvement but the standardization of the concept needs further elaboration and modification.

ix. The results were obtained with a DGTS detector and it is anticipated that the use of an MCT detector with proper filters may further improve the accuracy!

x. The findings regarding nitrate can be modified/extended and implemented for other ions and solutes absorbing in the MIR .

References

1. Johnston, C. T. and Aochi, Y. O. 1996. Fourrier transform infrared and Raman spectroscopy. *In* Methods of soil analysis, Part 3. Bartels, J.M. and Bigham, J.M. (Eds). Soil Science Society of America Inc., Madison, USA.
2. Jolliffe, I.T., Principal Component Analysis, New York: Springer-Verlag, 1986.
3. Libnau, F. O., Kvalheim, O. M., Christy A. A. and Toft, J. 1994. Spectra of water in the near- and mid-infrared region. Vibrational spectroscopy 7:243-254.
4. Messica,A., A.Katzir, U.Schiessl, M.Tacke, "Fiber Optic Evanescent Wave Spectroscopy of Liquids and Gases using Tunable diode Lasers," Proc. SPIE, 1420 (1991)
5. Messica, A.; Greenstein, A.; Katzir, A. *Appl.Opt.* 1996, 35, 2284.
6. Powell, J. R., Wasacz, F. F. and Jakobsen, R. J. 1986. An algorithm for the reproducible spectral subtraction of water from the FT-IR spectra of proteins in dilute solutions and absorbed monolayrers. Applied Spectroscopy 40(3): 339-344.
7. Shaviv A., Kenny, A., Shmulevich, I., Singher, L., Reichlin, Y. and Katzir, A.2002. Real Time and Remote Monitoring of Soil and Water Nitrate by FTIR Based FEWS or Membrane Systems. In review of Env. Sci. & Tech
8. Smith, S. W. 1997. The Scientist and Engineer's Guide to Digital Signal Prossecing; California Technical Publishing.

Solute transfer in natural porous media : Concepts and modeling approaches

Michel Jauzein

Université Henri Poincaré Nancy 1, Faculté des Sciences et Techniques, LIMOS, BP289, F-54506 Vandoeuvre-lès-Nancy Cedex; Phone : +33.383684763; Fax : +33.383684765; E-Mail : michel.jauzein@lss.uhp-nancy.fr

Abstract: Solute transfer in natural porous media is mainly due to water transfer and related phenomena. Transport by water or advection, hydrodynamic dispersion, biogeochemical interactions and mass transfer limitations are the main types of mechanisms. The deterministic flow of water in porous media can be described, in a preliminary approach, as a set of independent stream tubes. Each tube is characterized by specific parameters such as the residence time of water, the distribution of interactive constituents and the characteristic times of interactions. This one-dimensional problem can be studied on the basis of models developed for column experimentation. These models couple the advective-dispersive solute transfer equations with geochemical equilibrium constraints and kinetic concept formulations (Parkhurst and Appelo, 1999; Jauzein and al., 1989). The integration of results is than obtained from the latest mixing of solute breakthrough at the outlet of each stream tube. For sufficiently homogeneous systems and linear processes (linear partition, first order kinetics, …), this simplified approach is quite efficient. In the case of strongly non-linear processes or heterogeneous distribution of interaction properties, complementary concepts must be added to describe and couple the effect of known processes. As a matter of fact, the existing stream tubes are not totally segregated and they interact through lateral mixing phenomena. In addition, the heterogeneity of dispersion and interaction mechanisms along a stream line can significantly modify the solute breakthrough. Here, we try to demonstrate the importance of these complementary concepts and propose an alternative modeling approach to study their effects. Defining ideal extreme conditions, it will be possible to place real systems between them and follow a better predictive approach for the integrated management of soil and water quality.

1. Introduction

The integrated management of soil and water quality needs effective tools to identify, understand, and predict the predominant mechanisms involved in the transfer of contaminant from soil to surface water systems (Bear, 1994; Young, Mohamed and Warkentin, 1992). The fundamental knowledge of potential mechanisms is more and more developed and a lot of models have been created, and partially validated for the simulation of contaminant transfer in soils, unsaturated zones and groundwater systems. The modeling of water transfer in natural porous media, even in the unsaturated zone, is well established (Bear, 1972). The description of geochemical equilibria constraints is also quite well understood (Sposito and Mattigold, 1979). The knowledge about biological interactions and physico-chemical kinetics is continuously progressing (Parkhurst and Appelo, 1999). But the integrated approach of all these phenomena is still a bottleneck, especially when a bottom-up strategy is applied, trying to combine existing individual models within a single global one. A research effort is necessary to analyze available parameters at the laboratory or field level and follow a top–down strategy to derive systemic models of natural systems taking into account all the existing knowledge about individual processes involved. As an example, at the water catchment scale, the residence time distribution of water, RTD_w, can be studied using rain-flow correlation, water balance calculations and water tracer experiments. Precise water transfer models can be validated at the ten square meters scale in the unsaturated zone and at the ten square kilometers scale in the shallow aquifer domain. But the coupling of both, in the context of an heterogeneous distribution of soil properties, of potential preferential flow and

of uncertainties in the description of the groundwater system, is generally too complex. Even a water transfer model could be developed and validated at this scale, the good representation of rain-flow correlation, water balance calculations and water tracer breakthrough will be used to check the concept. Thus, the concept of mass balances and RTD_w are placed at the convergence between detailed models and field measurements. Consequently, is it possible to study contaminant transfer from this information only, as an alternative to the coupling between detailed models of water transfer and detailed models of solute dispersion and biogeochemical interactions ?

2. Ideal extreme behavior concepts

Three main behavior concepts can be used to study solute transfer in natural porous media. The first one is the segregated parallel plug flow reactors and is based on the representation of the RTD_w by a series of parallel stream tubes R_k with a fixed residence time τ_k and a negligible longitudinal dispersion. Mixing of upstream and downstream aqueous solutions never occur in this conceptual vision. The uniform inlet solution react in parallel and are mixed at the latest time at the outlet of all the stream tubes. The two other concepts are considering maximal internal mixing of the aqueous solution. The heterogeneity of water residence time is represented by the existence of a minimal number of mixing zones of maximal size. Consequently the mixing of upstream and downstream aqueous solutions occurs with a maximal effect. The uniform inlet solution can react in parallel streams but are mixed during their residence time in the system. This maximal mixing can occur at the earliest time or at the latest. In the case of earliest time mixing, the effect of interactions influenced by the mixing of upstream and downstream aqueous solutions takes place rapidly in the system compared to the effect of retardation by heterogeneous reactions. In the case of latest time mixing, the inverse occurs and can modify interaction effects on the breakthrough of solutes. These dispersive phenomena interact with non linear processes, enhancing the apparent dispersion of transfered solutes (Garabedian, 1987; Dagan, 1989; Kabala and Sposito, 1991; Haley, Sudicky and Naff, 1994).

The segregated parallel plug flow reactors (SPPFR) :

The RTD_w can be described by the function E(t). In the concept of parallel stream tubes, each reactive tube R_k in fed with a flow rate dQ equal to $(Q.E(\tau_k).d\tau)$. The modeling of solute transfer in each tube is possible through the use of one dimensional numerical approaches. In the case of non linear processes and local equilibrium assumption without dispersion, the pioneer approach of Helfferich (1967) is still available and developed (Schweich, Sardin and Jauzein, 1993) for the theoretical calculation of breakthrough curves (BTC_s). In the other situations, with dispersion or non linear kinetics, more classic numerical approaches simultaneously solving partial derivative equations and algebraic non-linear constraints can be proposed. Whatever the method selected, the results are the BTC_s of solutes at the outlet of each reactor characterized by its specific water residence time τ_k. The integrated result for the system is obtained by the conventional instantaneous mixing of individual fluxes at each time t taking into account geochemical equilibrium constraints on initial concentrations calculated by :

$$C(t) = \int_{\tau=0,\infty} C_k(t)\, E(\tau_k).d\tau$$

The limits of this concept are :

- The segregation between stream tubes. In real system, mixing occurs at different stage of the water transfer between upstream fluxes which are characterized by different histories and downstream fluxes which will have different futures. Upstream water with the same age can come from different sources, e.g. different initial stream tubes.
- The non dispersive transfer inside stream tubes. In real system, even at the pore size scale, dispersion phenomena occurs due to molecular diffusion and heterogeneity of the water velocity field.
- The homogeneity of transfer parameters along the stream tubes. In real system, dispersion and interactions depends on distributed parameters and the effect of space distribution is generally neglected.

The two last points can be studied on the basis of the same concept including space dependent dispersion and interaction parameters in numerical models. But the first one necessitates complementary conceptual approaches taking into account potential mixing zones.

The maximal mixing reactor concepts (LMMR and EMMR) :

The effect of a mixing zone is theoretically known. On an ideal point of view, the residence time of water in this zone has a maximal variance compared to its mean residence time. In this case the RTD_w function E(t) is a decreasing exponential function : $\tau^{-1}e^{-t/\tau}$ where τ is the mean residence time of water. For solutes and stationary phases, the concentrations are considered as strictly homogeneous within the mixing zone. In a plug flow reactor, the residence time variance is equal to zero and the concentrations are distributed along the reactor tube. In the parallel stream tube concept, the residence time variance is generated by the parallel distribution of plug flow reactors with fixed residence times and zero variance. In the maximum mixing concept, the residence time variance will be represented by the existence of a minimal number of mixing zones generating maximum variance. If all the variance is generated by the mixing zones, the other part of the system must be a plug flow system connected in series or in parallel with them. But depending on the placement of mixing zones from the inlet to the outlet, the effect of non-linear interactions will be different. Placed at the earliest time or the latest time, the coupling of non-linear interactions between upstream and downstream aqueous solutions (mixing effects) and non-linear interactions between the aqueous solution and the stationary phases (retardation effects) can differ significantly. Consequently two ideal extreme concepts must be used : the earliest maximum mixing reactor (EMMR) and the latest maximum mixing reactor (LMMR) concept. The modeling of solute transfer with respect to these two concepts can be obtained with networks of ideal reactors (ideal mixing reactors and plug flow reactors), derived from the RTD_w of the studied system. In this type of models, numerical approaches simultaneously solving partial derivative equations and algebraic non-linear constraints are generally used (Villermaux, 1985). Micromixing concepts have been developed by Zwietering (1959) using a single plug flow reactor with a staged inlet for earliest mixing (maximal effect) or staged outlet for latest mixing (minimal effect) but these concepts are intermediate situations of the internal mixing phenomena.

The limits of these concepts are :

- The maximal mixing. In real system, mixing occurs all along the pathway of water in the environment and the space distribution of mixing zones is generally unknown.
- The homogeneity of concentrations in mixing zones. If it can be discussed for the aqueous solution, it cannot be extended to the stationary phases due to the heterogeneous properties of natural media.
- The homogeneity of transfer parameters in the different zones. In real system, the space distribution of dispersion and interaction parameters can modify the global behavior of the system.

The last point can be studied on the basis of the same concept including space dependent dispersion and interaction parameters in numerical models. The first two points must be studied comparing the results obtained from the different concepts and trying to place a real system between them from experimental or monitoring data. The following figure gives a schematic view of this three ideal extreme behavior concept :

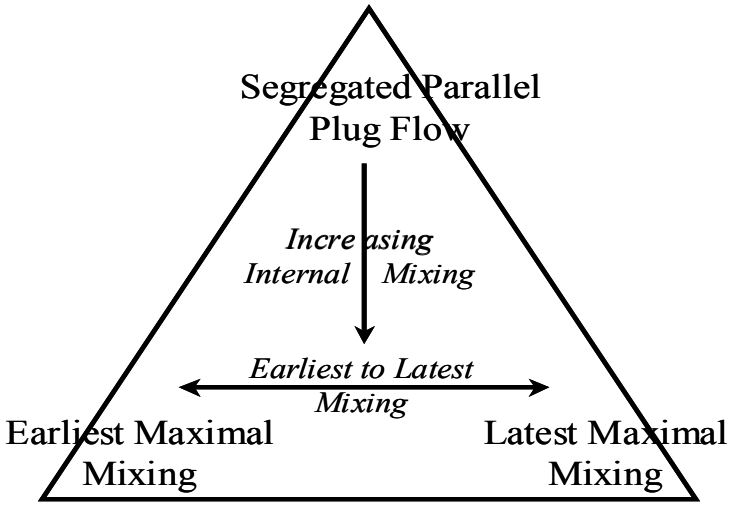

Figure 1: The three ideal extreme behavior concepts

3. Simulation example

To give an idea of the potential application of this conceptual approach, a theoretical case has been selected for illustrating extreme behaviors of solutes in complex systems. The selected example, is the transfer of a solute submitted to non-linear adsorption in a system where the RTD_w is an exponential function delayed in time (example from Danckwerts in Villermaux, 1985):

$$E(t) = 0 \text{ for } t < (\tau - \sigma) \text{ and } E(t) = \sigma^{-1} e^{-(t-\tau+\sigma)/\sigma} \text{ for } t > (\tau - \sigma) \quad \text{with } \sigma = \tau / 2$$

The non linear adsorption of the solute is described by the equation :

$$C_s = 100 \, . \, C_l^2$$

The figures 2 and 3 illustrates the selected residence time distribution and adsorption isotherm. It can be noticed that the non linearity of the interaction is not really strong.

The inlet signal is a step injection from 0 to 10^{-2} mol/l of solute inducing a progressive saturation of the porous media from 0 to 10^{-2} mol/l with a non linear partition of the solute

varying from 0 to 1 depending on solute concentration. The slope of the adsorption isotherm is given by :

$dC_s / dC_l = 200. C_l$

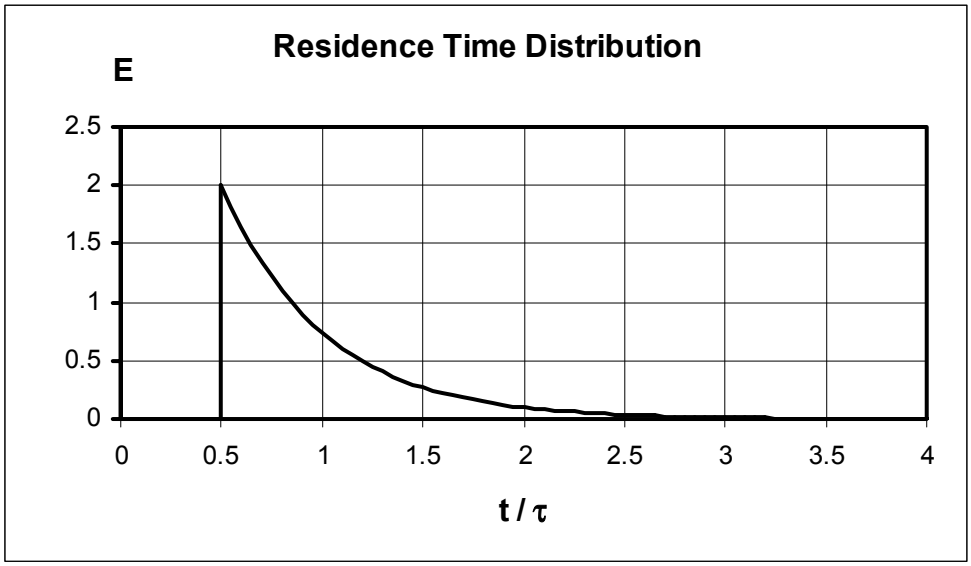

Figure 2 : Residence time distribution E(t) of water in the system

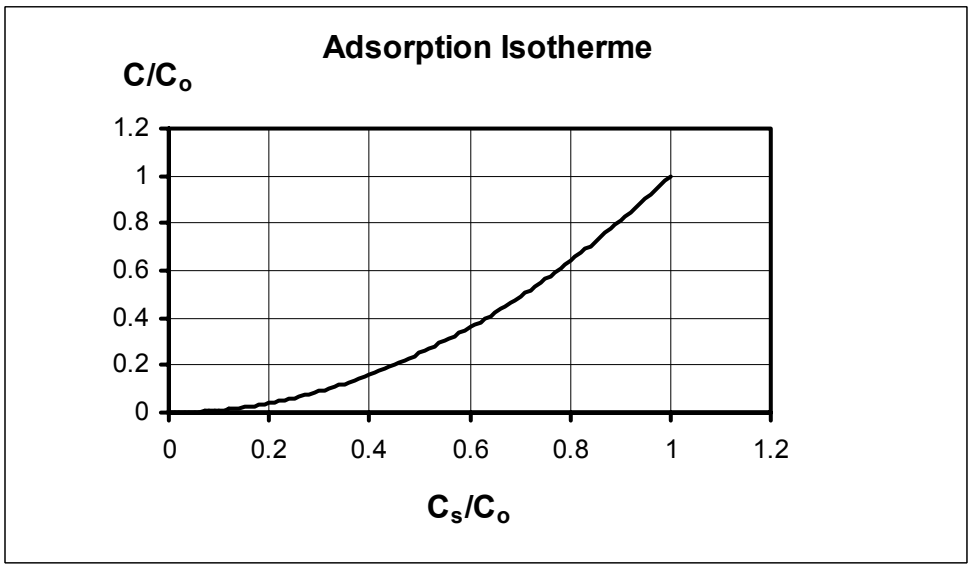

Figure 3 : Adsorption isotherm of the solute

Consequently, the apparent velocity of each concentration in the non dispersive, local equilibrium assumption can be calculated as :

$\upsilon(C_l) = \upsilon_w . 1/(1+200\ C_l)$ where υ_w is the velocity of water

For the calculation of the breakthrough curve with respect to the SPPFR concept, the characteristic BTC of a plug flow reactor is firstly derived from the function $\upsilon(C_l)$. The breakthrough time of the concentration is given by : $\tau_k . (1+200\ C_l)$ where τ_k is the residence

time in the reactor. Then, this BTC is submitted to a convolution with the RTD_w to obtain the final result.

In the case of LMMR, the BTC from a plug flow reactor with a residence time equal to $\tau / 2$, is used as inlet flux for an ideal mixing reactor with a mean residence time equal to $\tau / 2$. A numerical integration of the mass balance equation and coupled non-linear isotherm allows to estimate the final result.

In the case of EMMR, the numerical integration of the mass balance equation and coupled non-linear isotherm is performed for an ideal mixing reactor with a mean residence time equal to $\tau / 2$. The outlet result is used as inlet flux for a plug flow reactor with a residence time equal to $\tau / 2$ using the apparent velocity of concentrations.

The figures 4a and 4b illustrates the simulation results. The non linearity generates BTCs apparently more dispersed than the BTCs of a linear partitioning solute. At the begining of BTCs, concentrations are low and the solute is less retarded. The differences between extreme situations are significative and, even if the breakthrough occurs simultaneously for the three concepts ($t = \tau / 2$), it is more important for the EMMR, then for the LMMR and lastly for the SPPFR ideal case. In the final part of BTCs, differences are reduced by the tailing of curves but they are still significative with increasing tailing from SPPFR to EMMR result. The LMMR concept seems to give intermediate results with respect to the dispersive effect of the non-linear process.

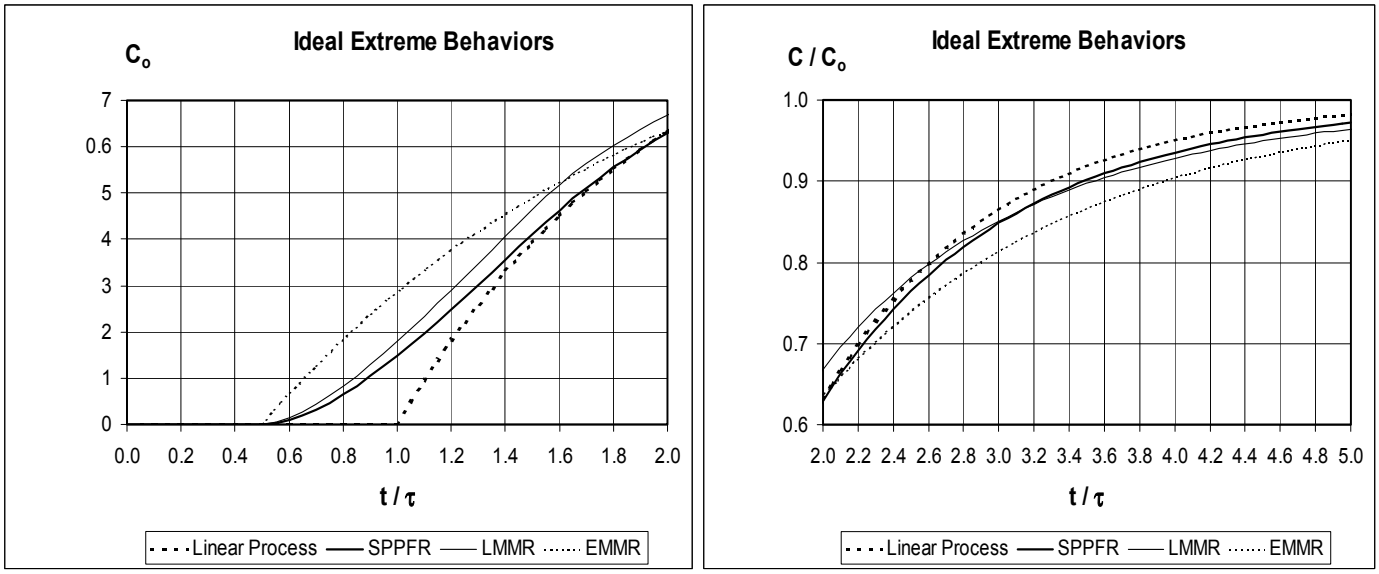

Figure 4 : Breakthrough curves of the non-linear interacting solute compared to a linear interacting one (linear partition adimentional coefficient equal to 1) for the three ideal extreme behavior concepts. (a) reduced time from 0 to 2, (b) reduced time from 2 to 5.

Here, it is important to remind that all calculations have been done with the local equilibrium assumption. The obtained dispersive effect is similar to kinetic effects. Thus it underlines the fact that non-linearities and kinetics can be confounded in the case of dispersive solute transfer.

4. Conclusions and application perspectives

The three developed concepts gives the opportunity to study the potential effect of dispersion on non-linear interactive solute transfer in natural porous media. Defining ideal extreme behaviors which significantly modify the breakthrough of solutes for the same residence time distribution of water (RTD_w), it seems possible to analyse the real state of natural dispersion phenomena. To obtain experimental or monitoring data allowing this analysis, tracer tests would be the best approach comparing a non-interactive tracer with a solute subjected to rapid non-linear interactions. The main problem will be to identify the combined effects of dispersion and kinetic limitations. This approach can be checked at different scale, from laboratory column experiments up to the water catchment scale if (i) the RTD_w can be evaluated, (ii) significant dispersion occurs and (iii) non-linear processes are involved in the studied solute transfer at the scale of interest. RTD_w evaluation is easy at the laboratory scale and can be performed with more or less technical limitations in lysimeters, drainage systems, aquifer zones or river portions. Dispersion is artificially reduced in laboratory columns but is generally important in natural systems. Non-linearity effects can be artificially increased in laboratory columns, but are generally reduced in natural environments due to rapid dilution of solutes. Consequently, the application perspectives are numerous but the opportunities must be checked carefully on a case by case basis.

5. References

J. Bear, 1972. Dynamics of fluids in porous media. *Elsevier*, Amsterdam, 764p.

J. Bear, 1994. Use of models in decision making. In T.H. Dracos and F. Stauffer editors. Transport and reactive processes in aquifers. *Balkema*, Rotterdam, 3-9.

G. Dagan, 1989. Flow and transport in porous formations. *Springer-Verlag*, 455 p.

S.P. Garabedian, 1987. Large-scale dispersive transport in aquifers : field experiments and reactive transport theory. PhD thesis, Dept. Civil Eng., *Massachussetts Institute of Technology*, Cambridge, 290 p.

D.F. Haley, E.A. Sudicky and R.L. Naff, 1994. Three-dimensional Monte Carlo analysis of spatial spreading during reactive solute transport by groundwater. In T.H. Dracos and F. Stauffer editors. Transport and reactive processes in aquifers. *Balkema*, Rotterdam, 437-443.

F. Helfferich, 1967. Multicomponent ion exchange in fixed bed. *Ind. Eng. Chem. Fundam.*, 6, 362-364.

M. Jauzein, C. Andre, R. Margrita, M. Sardin and D. Schweich, 1989. A flexible computer code for modelling transport in porous media : Impact. *Geoderma*, 44, 95-113.

Z.J. Kabala and G. Sposito, 1991. A stochastic model of reactive solute transport with at time-varying velocity in a heterogeneous aquifer. *Water Resour. Res.*, 27(3), p341-350.

D.L. Parkhurst and C.A.J. Appelo, 1999. User's guide to PHREEQC (version 2) : a computer program for speciation, batch-reaction, one-dimensional transport, and inverse geochemical calculations. Water-Resouces Investigations Report 99-4259, *U.S. Geological Survey*, Denver, Colorado.

D. Schweich, M. Sardin and M. Jauzein, 1993. Properties of concentration waves in presence of non linear sorption, precipitation/dissolution, and homogeneous reactions. 1-Fundamentals, 2-Illustrative examples. *Water Resour. Res.*, 29(3), p723-741

G. Sposito and S.V. Mattigold, 1979. GEOCHEM : a computer program for calculation of chemical equilibria in soil solutions and other natural water systems. *University of California*, Riverside.

J. Villermaux, 1985. Génie de la réaction chimique – Conception et fonctionnement des réacteurs. *Tec&Doc, Lavoisier*, Paris, 401p.

R.N. Young, A.M.O. Mohamed and B.P. Warkentin, 1992. Principle of contaminant transport in soils. *Elsevier*, Amsterdam, 327p.

T.N. Zwietering, 1959. *Chem. Eng. Sci.*, 11, 1.

Dual permeability modeling of variably saturated flow and solute transport in soils with preferential pathways

Tomas Vogel[1], Chittaranjan Ray[2], Milena Cislerova[1]

[1]*Faculty of Civil Engineering, Czech Technical University, Thakurova 7, 16629 Prague, Czech Republic, Phone +420 224 354 341, Fax +420 224 310 782, vogel@fsv.cvut.cz*

[2]*University of Hawaii at Manoa, Department of Civil and Environmental Engineering and Water Resources Research Center, Honolulu, HI 96822, USA*

Abstract: The basic concepts of dual-permeability modeling of water flow and solute transport in variably-saturated structured soils are briefly recapitulated. Two applications of the approach are presented. In the first application, the computer code S_1D_Dual was applied to simulate vertical transport of land-applied pesticide in macroporous soil. Several simulation scenarios were conducted to evaluate the combined effects of preferential flow and domain-specific sorption on the pesticide leaching in response to natural rainfall. Second application deals with the hillslope tracer experiment. In this case the computer code S_2D_Dual was used to simulate the solute transport in a hillslope segment conceptualized as a two-dimensional dual-permeability system. The tracer was applied continuously during a ponded infiltration experiment.

1. Introduction

When seeking a reasonably realistic description of the field scale movement of water and solutes, the assumption that soil is a single-continuum system is often inadequate. During the rainstorms or intensive irrigation events, water and chemicals can move at relatively large velocities in macropores or other structural features causing local non-equilibrium conditions in pressure heads and solute concentrations.

Preferential flow related to structure has been widely reported in soils containing wormholes, root channels, and inter-aggregate fissures (e.g. *Bouma*, 1981; *Beven and Germann*, 1982). Additional types of preferential flow have been linked to textural differences rather than structural effects. The evolution of finger-type preferential flow paths is associated with gravity-driven flow instability (*Raats*, 1973; *Parlange and Hill*, 1976). Fingering occurs in water repellent soils, when water percolates from a fine-textured into a coarse-textured layer, or when the air pressure increases ahead of infiltration front (e.g. *Bauters et al*., 1998).

In the last few decades, several two domain models (*e.g. Gerke and van Genuchten*, 1993a; *Ray et al*., 1997; *Vogel et al*., 2000) have been developed to simulate mobile water in soils conceptualized to have two pore systems, the matrix domain and the preferential flow domain (PF-domain). The models are commonly referred to as dual-permeability models. In these models, Darcian flow assumption for water movement and the advection-dispersion approach for solute transport have been assumed to be valid for each of the two pore domains separately, allowing local non-equilibrium between the domains.

2. Flow and transport equations

Using the concept of *Gerke and van Genuchten* (1993a) the variably saturated flow in a dual-permeability system can be described by means of two coupled Richards' equations:

$$C_f \frac{\partial h_f}{\partial t} = \nabla \cdot (\mathbf{K}_f \nabla h_f) + \nabla \cdot (\mathbf{K}_f \nabla z) - S_f - \frac{\Gamma_w}{w_f}$$
$$C_m \frac{\partial h_m}{\partial t} = \nabla \cdot (\mathbf{K}_m \nabla h_m) + \nabla \cdot (\mathbf{K}_m \nabla z) - S_m + \frac{\Gamma_w}{w_m} \quad (1)$$

where the subscripts *m* and *f* denote the matrix domain and the PF-domain, respectively. In the above equations: *h* is the pressure head (L), **K** is the hydraulic conductivity tensor (L/T), *C* is the differential water capacity (1/L), *z* is the vertical coordinate assumed to be positive upward (L), *S* is a sink term, here used to describe the local root water uptake (1/T), and Γ_w is the transfer term (1/T), which controls the exchange of water between the flow domains. The terms w_m and w_f are volume fractions of the matrix domain and PF-domain, respectively, with $w_m + w_f = 1$.

The water transfer between the matrix and the PF-domain is assumed to be proportional to the pressure head difference between the domains through the first-order transfer term:

$$\Gamma_w = \alpha_w (h_f - h_m) \quad (2)$$

where α_w is the water transfer coefficient. This coefficient was closely examined by *Gerke and van Genuchten* (1993b). Based on their evaluation, following formulation was suggested by *Ray et al*., (2002):

$$\alpha_w = \alpha_{ws} K_{ar} \quad (3)$$

where α_{ws} is the water transfer coefficient at saturation and K_{ar} is the relative unsaturated hydraulic conductivity of the interface between the matrix and the PF-domain. The value of K_{ar} fluctuates between 0 and 1 depending on the degree of saturation near the interface.

Similarly to the water flow, the dual-permeability solute transport can be described by means of two coupled advection-dispersion equations (*Gerke and van Genuchten*, 1993a; *Ray et al*., 2002):

$$\frac{\partial R_{1f}\theta_f c_f}{\partial t} + \nabla \cdot (\mathbf{q}_f c_f) - \nabla \cdot (\theta_f \mathbf{D}_f \nabla c_f) = -\lambda_{wf}\theta_f c_f - \rho_f \alpha_{2f}(\kappa_{2f} c_f - s_{2f}) - \frac{\Gamma_s}{w_f}$$
$$\frac{\partial R_{1m}\theta_m c_m}{\partial t} + \nabla \cdot (\mathbf{q}_m c_m) - \nabla \cdot (\theta_m \mathbf{D}_m \nabla c_m) = -\lambda_{wm}\theta_m c_m - \rho_m \alpha_{2m}(\kappa_{2m} c_m - s_{2m}) + \frac{\Gamma_s}{w_m} \quad (4)$$

where *c* is the solute concentration (M/L^3), θ is the soil water content (L^3/L^3), ρ is the soil bulk density (M/L^3), **D** is the tensor of hydrodynamic dispersion (L^2/T), **q** is the water flux (L/T) and λ_w is the solute decay rate (1/T). The subscripts 1 and 2 refer to equilibrium and kinetically-controlled sorption sites, respectively. The equilibrium sorption is incorporated through the retardation factor R_1. The symbol κ_2 refers to the kinetic sorption equilibrium coefficient, α_2 is the first-order kinetic sorption reaction rate, s_2 is the sorbed concentration at the kinetic site (M/M), Γ_s is the solute transfer term.

The kinetic sorption is governed by:

$$\frac{\partial s_{2i}}{\partial t} = \alpha_{2i}(\kappa_{2i} c_i - s_{2i}) \tag{5}$$

where i is equal to m for the matrix and f for the PF-domain.

The solute transfer term Γ_s is defined as the mass flux of solute being transported from one domain to the other, and is expressed as:

$$\Gamma_s = \Gamma_w c_i + \alpha_s (c_f - c_m) \tag{6}$$

In case that water flows from PF-domain to matrix: $c_i = c_f$, for flow in the opposite direction: $c_i = c_m$. The first term on the right hand side defines the advective exchange of solute due to movement of water, Γ_w, from one domain to the other because of water pressure difference between the two domains. The second term accounts for the diffusive exchange of solute due to a concentration difference. The rate of the diffusive exchange is controlled by the solute transfer coefficient, α_s.

In analogy to the water transfer coefficient, the solute transfer coefficient can be expressed as

$$\alpha_s = \alpha_{ss} \theta_{ar} \tag{7}$$

where α_{ss} is the solute transfer coefficient at saturation, and θ_{ar} is the relative degree of saturation near the interface between the matrix and the PF-domain.

3. Simulation of 1D pesticide transport problem

The dual permeability model (S_1D_Dual code) was used to study the transport of atrazine in an agricultural soil (Drummer glacial till silt loam, Champaign, Illinois, USA). The top boundary condition for water flow was natural rainfall recorded between May 15 and July 31, 1999. For solute transport, the applied pesticide was placed in the top 1cm depth of the profile as initial condition. The amount of pesticide was equivalent to the label application rate for one season. The bottom boundary was assumed to be a free-exit boundary condition (second-type boundary).

In addition to the reference single-permeability simulations, several dual-permeability simulation scenarios were considered: First, equilibrium sorption was invoked for both the matrix and the PF-domain. In the next model run, it was assumed that all sorption took place in the matrix domain and none in the PF-domain. Finally, the sorption process was considered to be rate controlled in the PF-domain and equilibrium controlled in the matrix domain.

The concentration profiles in the matrix and PF-domain, fluxes of chemicals in individual domains at the bottom of the profile and at several depths, and the exchange of chemical and water fluxes between the two domains at various depths and times were compared. For the last mentioned simulation scenario, the computed atrazine concentration history at the depth of 80 cm indicated that there was a single relatively short breakthrough episode, related to the intensive rainfall, which occurred in the middle of the simulated period of 75 days. Figure 1 shows the effect of different pesticide sorption half-lives applied in the PF-domain. It was confirmed that for progressively decreasing half-live the resulting concentration history would gradually converge to the scenario in which equilibrium sorption was applied in both domains

(leading to a negligible concentration peak), while increasing the sorption half-live would eventually converge to the scenario in which no sorption in PF-domain was considered (leading to a maximum relative concentration of about 0.010).

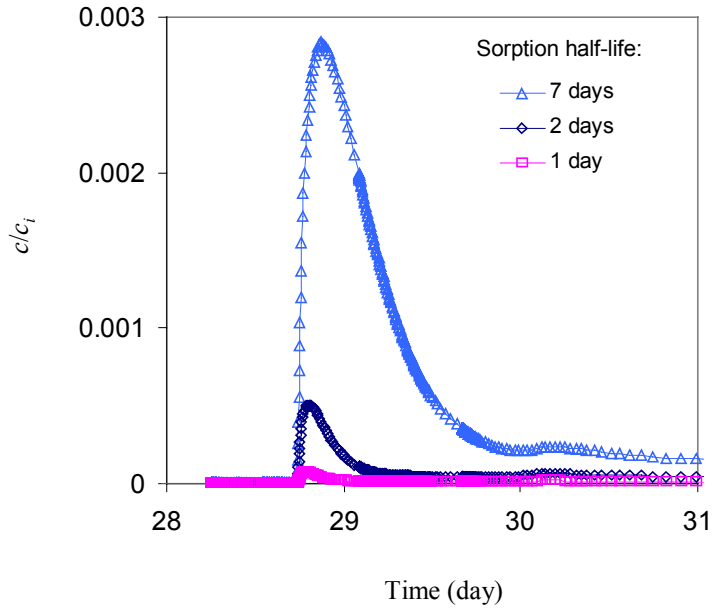

Figure 1: Simulated relative concentration history for atrazine at the depth of 80 cm in response to the rainstorm (simulation scenario: equilibrium sorption in the matrix, kinetic sorption in the PF-domain).

4. Evaluation of 2D field tracer experiment

The dual permeability model (S_2D_Dual code) was used to study transport of a tracer in a two-dimensional hillslope segment. The tracer was applied continuously during a ponded infiltration experiment performed on a relatively steep hillslope of a small headwater catchment (sandy-loam, Cambisol, Jizera Mountains, Czech Republic).

Figure 2 shows the tracer plume moving downhill in a dual-permeability system. Note the characteristic "ghost plume" in the matrix, resulting from the local mass transfer from the PF-domain to the matrix.

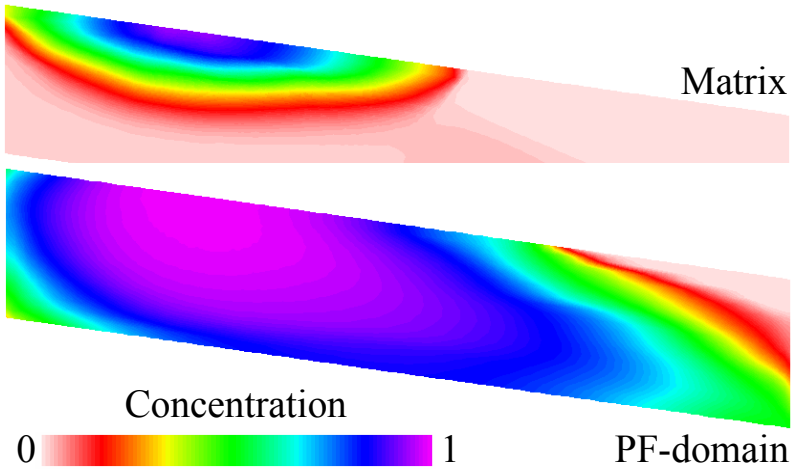

Figure 2: Simulated tracer plume at t = 0.1 as a result of continuous local application of the tracer during infiltration experiment. The segment is about 1m deep and 5m long. Dual-permeability system.

5. Acknowledgements

The research has been supported by the Grant Agency of the Czech Republic - grant A3060001, and Ministry of Education of the Czech Republic - research program MSM 211100002. Additional support for the international cooperation was provided by the National Research Council Program COBASE, and NATO Collaborative Linkage Grant EST974796.

6. References

Bauters, T.W.J., D.A. DiCarlo, T.S. Steenhuis, and J.-Y. Parlange, 1998. Preferential flow in water repellent sands. Soil Sci. Soc. Am. J., 62, 1185-1190.

Beven, K.J., and P. German, 1982. Macropores and water flow in soils. Water Resour. Res., 18, 1311-1325.

Bouma, J., 1981. Soil morphology and preferential flow along macropores. Agric Water Manage., 3, 235-250.

Gerke H.H. and van Genuchten, M.Th., 1993a. A dual-porosity model for simulating the preferential movement of water and solutes in structured porous media. Water Resour. Res., 29(2), 305-319.

Gerke H.H. and van Genuchten, M.Th., 1993b. Evaluation of a first-order water transfer term for variably saturated dual-porosity models. Water Resour. Res., 29(4), 1225-1238.

Parlange, J.-Y., and D.E. Hill, 1976, Theoretical analysis of weting front instability in soils. Soil Sci., 122, 236-239.

Raats, P.A.C., 1973. Unstable wetting fronts in uniform and nonuniform soils. Soil Sci. Soc. Am. Proc., 37, 681-685.

Ray, C., Ellsworth, T.R., Valocchi, A.J. and Boast, C.W., 1997. An improved dual porosity model for chemical transport in macroporous soils. J. Hydrol., 193: 270-292.

Ray, C., T. Vogel, and J. Dusek, 2002, Modeling depth-variant and domain-specific sorption and biodegradation in dual-permeability media, J. Contam. Hydrol. (submitted).

Vogel, T, Gerke, H. H., Zhang, R. and van Genuchten, M. Th., 2000. Modeling flow and transport in a two-dimensional dual-permeability system with spatially variable hydraulic properties, J. Hydrol., 238, 78-89.

Role of mobile organic sorbents for contaminant transport in natural porous media

Kai Uwe Totsche

Lehrstuhl für Bodenkunde, Department für Ökologie, Wissenschaftszentrum Weihenstephan, Technische Universität München, 85350 Freising-Weihenstephan, Germany, Phone +49 8161 713735, fax: +498161714466, totsche@wzw.tum.de

Abstract: Organic and inorganic colloids have been shown to affect the fate of nutrient and contaminants in soils and aquifer. They may act as carriers for strongly sorbing solutes and enhance or reduce solubility, mobility and availability due to complexation, solubilization, adsolubilization, association and solvophobic effect. Besides physicochemical processes, and mechanical perturbation, organic colloids are produced in large amounts by biological processes. In soils, the major amount of colloidal-size solution phase constituents are either of organic provenience (organic matter, including humic and non-humic substances), biocolloids, or inorganic particles with organic coatings. To estimate the effect of colloids on the fate of nutrients knowledge on the behavior of the colloids itself is required. Mobility and transport of colloids depends on the release rate and the sorption and deposition kinetics. The controlling factors are pH, ionic strength, type of elelctrolyte and charge of the colloids and the immobile sorbent. Under natural conditions, total amount and intensity distribution of precipitation and the moisture condition affect these factors. Thus colloid mobility and such the fate of strongly sorbing contaminants are strongly dependent on local climatological conditions.

1. Introduction

Colloids are small particles of variable geometry within the size range of 1 nm to 1000 nm (Figure 1). Once in solution, colloids are kept from sedimentation by Brownian motion of the solvent molecules. Field evidence reveals the large chemical and mineralogical diversity of mobile colloids, which comprise oxides and hydroxides of Fe and Mn, clay minerals, colloidal silica and carbonates and organic colloids. Within soils, the major amount of colloidal-size solution phase constituents are either of organic provenience (organic matter, including humic and non-humic substances), biocolloids, or inorganic particles with organic coatings. Organic colloids are produced in large amounts in organic carbon rich soil layers. Under forest vegetation, additional input comes from the forest floor and the canopy. The presence of colloids affect the solubility, mobility and availability of solutes due to complexation, solubilization, adsolubilization, carrier association and the solvophobic effect. Major processes between the solution and the solid phase, such as sorption, partitioning, speciation and ion-exchange are influenced by interactions with colloids. Organic colloids have been shown to affect contaminant fate in porous media (Kögel-Knabner and Totsche 1998) and facilitate the transport of radionuclides, pesticides and hydrophobic organic contaminants. However, carrier facilitated mobility of contaminants applies only to such environmental conditions where the organic colloids have to be considered a non-reactive mobile-phase constituent, i.e., neither sorption nor partitioning to immobile solid phase occurs. This is specifically the case for porous media which is either in sorptive equilibrium with the organic colloids or has unfavorable conditions for organic colloid sorption. The presence of organic colloids, however, may also lead to reduced contaminant mobility due to the immobilization of the organic colloids and thus of the associated contaminants (Totsche et al., 1997). In soils and the unsaturated zone organic colloid have to be considered reactive and

are subject to immobilization due to sorptive interactions with the bulk soil. In such environments, the colloid-associated pollutant will also be immobilized, resulting in reduced overall mobility. The underlying process has been described as co-sorption (Totsche et al., 1997). Colloid immobilization due to sorption/deposition can lead to an increase of the organic binding capacity of the bulk soil, thus increasing potential contaminant binding sites. This process, designated cumulative sorption, will lead to retardation of pollutants.

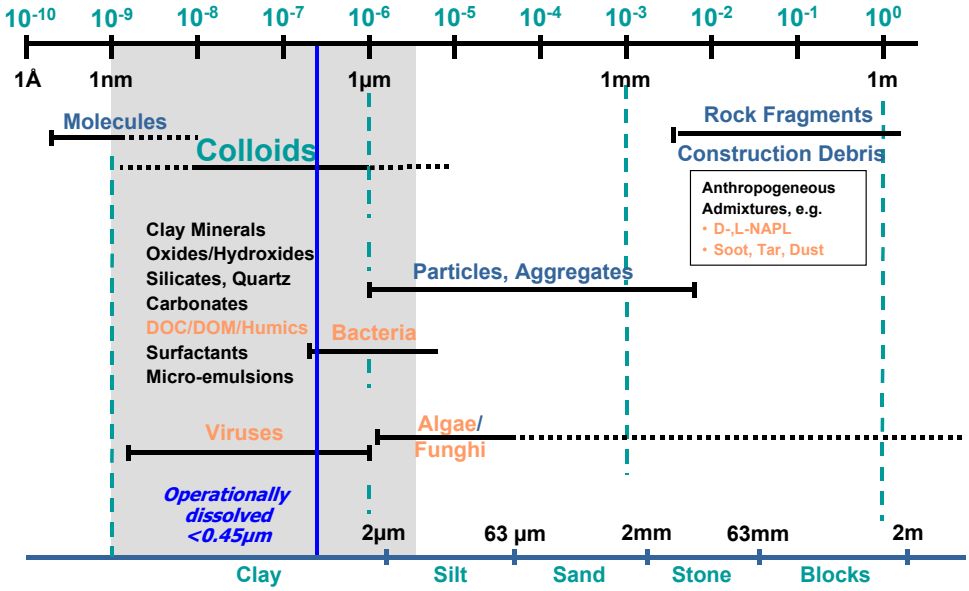

Figure 1: Size spectra of organic colloids. Note that the operationally defined "dissolved" phase obtained by 0.45µm filtration actually comprises a large part of the colloidal fraction.

As learned from column experiments and PAH depth profiles (Weigand et al. 1998, 2001; Totsche et al. 2002; Totsche et al 1997; Kögel-Knabner and Totsche, 1998), PAH migration within the unsaturated zone of contaminated sites is controlled by the transport of dissolved and colloidal phase substances, predominantly of organic provenience. Moreover, we learned, that both the flow regime and the infiltration of low-ionic strength solutions affect the release and transport of colloids in soils (Ryan & Elimelech 1996; Kretzschmar et al. 1997; Weigand and Totsche 1998; Münch et al. 2002). While the first results in release and transport due to increased shear forces and such leads to an increase of micro erosion and abrasion, the latter causes release by the expansion of the diffuse double layer and such in an outbalancing of the repulsive forces over the attractive forces. This, again, causes release and stabilization of colloids. To evaluate the relevance of these processes at the field site, we studied release and transport of PAH and colloids of organic provenience employing field lysimeters. Special consideration was thereby put on the effects of the distribution, intensity and duration of natural precipitation on the release and transport of soil borne colloids and such on the transport PAH.

2. Methods

The effect of the flow regime and natural rain events on the release and transport of colloids was studied with laboratory column and field lysimeter experiments. The lysimeters (surface area: 0.25 m2; Enclosed soil volume is 0,1 m3) were repacked with soil materials from a manufactured gas plant and covered with a layer (5 cm thickness) of the undisturbed A horizon material. Seepage water was sampled with glass bottles, sampling was done every fortnight, and additionally triggered by rain events with intensities high enough to cause recharge. Sample analysis comprised the determination of pH, el. conductivity, turbidity, DOC and the analysis of the 16 EPA priority PAH in the liquid and particulate/colloidal phase. To differentiate these two phases, seepage water samples were filtered with fibre glass-filters (Whatman GF/F; pore size < 0.45 µm). PAH determination measurement was done with a GC-MS.

3. Results and Discussion

3. 1 Effect on the export of colloids and suspended particles

Seepage water in autumn, winter and the early spring follow the precipitation rates. In the summer, evapo-transpiration reduces seepage water significantly. In general, the response of the lysimeters to precipitation was fast and dependent on the amount, intensity and moisture content prior to the rain event. In general, the mass of the sampled particles and colloids does not correlate with the cumulative precipitation distribution. However, two release situations were identified: (1) From June to August, strong rainfall events following extended dry periods result in colloid mobilisation and export from the lysimeters. (2) From September to October, at generally higher soil moisture contents, release of colloids is invoked at more uniform distributed precipitation. Micro-erosion and abrasion of particles and colloids is due to the increase of shear forces as a consequence of the high flow velocities. These processes are responsible for the high export of colloids reflected in situation 1. The dispersion of flocculated colloids due to the decrease of the ionic strength causes the increased release of colloidal material as observed in situation 2. The infiltrating low ionic strength rain water causes dilution of the soil solution and such an expansion of the diffuse double layer, which weakens the attractive forces in between individual colloids. This results in the dispersion and mobilisation of colloids and in the stabilisation of the colloidal solution.

3. 2 Effect on the export of PAH

For all rain events investigated, we measured concentration and pattern of the dissolved and colloidal phase PAH. The differentiation between the two phases was based on the operational fractions obtained by filtration with a 0.45µm glassfibre filter. The PAH passing the filter (filtrate), were defined as dissolved while the retentate resembles the colloidal/particulate fraction (Figure 2).

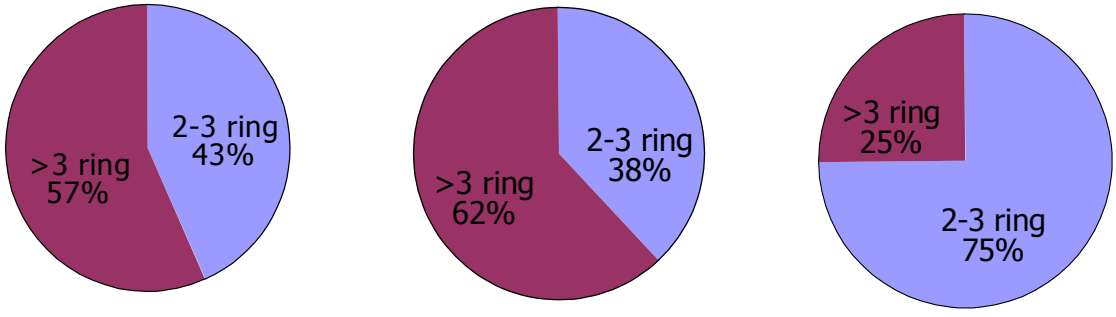

C_{soil}: 16.7 mg/kg Retentate: 12.4 mg/kg Filtrate 0.1 µg/l

Figure 2: Distribution of PAH on the dissolved (filtrate) and colloidal fractions (retentate)

For all sampling dates, the amount of PAH in the filtrate was negligible low (Figure 2). Dissolution of PAH from the source materials is not the dominating release process. This points to the fact that the transport of PAH in the dissolved phase is only marginal. The dominant PAH in the dissolved phase are the low molecular weight, fairly water soluble PAH with maximal 3 annealed aromatic rings. The dominant PAH in the retentate and in the soil are high molecular weight PAH with more than 3 annealed aromatic rings. The content of the PAH in the retentate (12.4 mg kg-1) is almost as high as in the soil (16.7 mg kg-1). This is also the case for the amount of 2-3 ring PAH. No change can be observed between the retentate and the soil. The PAH pattern does not change with depth. This can not be explained by dissolution processes driven by Raoults law. If dissolution would be the dominating process, we should expect a distribution of the PAH according to their aqueous solubility. We then should observe the more soluble PAH dominating the pattern. This obviously is not the case. In contrast, we believe that fractions of the source material itself are transported in colloidal or particulate form. Such a transport pathway would result in conservative PAH depth pattern without too much change compared to the source material.

Within the dissolved phase, the PAH seem to be not controlled by solubility, as well. When the dissolved PAH are scaled with their respective aqueous solubility, we even find that only the very insoluble PAH reach their theoretical water solubility. The low molecular weight PAH, which are fairly water soluble, do not even reach a thousandth part of their solubility. This, also, points to the fact that dissolution is of marginal importance at the site and that the attachment of PAH to colloids or small particles is the dominating process controlling PAH transport and redistribution in the unsaturated zone.

4. Concluding Remarks

In contaminated soils, processes seem to be active which effectively limit mass transfer of PAH into the soil solution. Dissolution according to Raoults Law from aged NAPL source materials is therefore not a relevant release process in the unsaturated soil zone. This might be because the mean residence time of the soil solution is not large enough to allow for equilibrium dissolution. In addition, the aged NAPL and tar source materials might serve as a mass transfer resistance which effectively prevents the release of tar and NAPL borne contaminants (Totsche et al. 2003). In summary, we found that

- PAH transport is controlled by the release and transport of soil borne colloids and particles.
- Amount and intensity of precipitation control the release of colloids/small particles and such of PAH.
- Both mechanical and physicochemical mobilisation processes account for colloid release.
- Dissolution of PAHs from source materials is of minor importance in the unsaturated zone.

5. References:

Kögel-Knabner I. & Totsche K.U. (1998). Influence of dissolved and colloidal phase humic substances on the transport of hydrophobic organic contaminants in soils. *Phys. Chem. Earth.23(2)*:179-185.

Kretzschmar, R. and Sticher, H. (1997): Transport of humic-coated iron oxide colloids in a sandy soil: influence of Ca2+ and trace metals.- Environ. Sci. Technol. 31: 3497-3504.

Münch, J.M., Totsche K.U., Kaiser K. (2002): Physicochemical factors controlling dissolved organic carbon release in forest subsois - a column study. *European J. Soil Sci.*, 53:311-320.

Ryan, J. N. and Elimelech, M. (1996): Colloid mobilisation and transport in groundwater.- *Coll. Surf.* A 107:1-56.

Totsche K. U., I. Kögel-Knabner, Scheibke R. , Geisen S. (2003): Evidence for Preferential Flow and Ageing of NAPL and NAPL borne Contaminants in the Unsaturated Soil Zone of a Creosote Contaminated Site: A Field Study. *J. Plant Nutr. Soil Sci.,* in press.

Totsche K.U., Kögel-Knabner I, Danzer J. (1997): Dissolved organic matter-enhanced retention of polycyclic aromatic hydrocarbons in soil miscible displacement experiments, *J. Environ. Qual.*, 26:1090-1100.

Totsche K. U., I. Kögel-Knabner and H. Weigand (2002) Modeling contaminant transport in anthropogenic soil: Reconstruction of spatial heterogeneity by analysing the relations of adjacent pedofacies. In: Schulz, H. D. and Teutsch, G. (Hrsg).Geochemical Processes: Conceptual Models for Reactive Transport in Soil and Groundwater. 1-18. Wiley VCH, Weinheim.

Weigand H. & Totsche K.U. (1998). Flow and reactivity effects on dissolved organic matter transport in soil columns. *Soil Sci. Soc. Am. J.* 62:1268-1274

Weigand H., Totsche K.U. & Kögel-Knabner I. (1998). Effect of Fluctuating Input of Dissolved Organic Matter (DOM) on Long-Term Mobility of Polycyclic Aromatic Hydrocarbons(PAH) in Soils. *Phys. Chem. Earth.23(2):*211-214.

Weigand H., Totsche K. U., Huwe B., Kögel-Knabner I. (2001): PAH mobility in contaminated industrial soils: a Markov chain approach to the spatial variability of soil properties and PAH levels. *Geoderma*, 102:371-389

Transport of colloid bound contaminants in the unsaturated zone

Alexandra Christ & Thilo Hofmann[1]

[1]*Corresponding author: Johannes Gutenberg Universität Mainz, Becherweg 21, 55099 Mainz Phone: +49-6131-3923771, Fax:+49-6131-3924769; E-Mail:thilo.hofmann@uni-mainz.de*

Abstract: Colloid bound transport may enhance contaminant relocation. Unsaturated column experiments show that the mobilization of colloid bound contaminants depends on hydraulic and hydrochemical boundary conditions and on the properties of the gas-water interface. Varying hydraulic and hydrochemical conditions in the unsaturated zone favor colloid mobilization. Neglecting this transport pathway in a risk assessment approach may lead to misinterpretation and thus a potential hazard for groundwater and other receptors. The complexity of the colloid facilitated relocation of pollutants determines a need for further research.

1. Background

According to the German soil protection law only the mobile amounts of contaminants in the seepage water are considered in a risk assessment approach (for the pathway soil-groundwater). Contaminant concentrations are assessed at the so called "point of compliance" which is located at the transition from the unsaturated to the saturated zone. In order to estimate the concentration of contaminants at the point of compliance all relevant transport pathways must be known and have to be quantified.

Sorption of contaminants at a mobile colloidal phase often remains unconsidered regarding the migration of organic and inorganic contaminants. Due to their high surface to volume ratio colloids represent important sorption sites especially for hydrophobic organic contaminants, heavy metals, and radionuclides. Colloids have different origins. Their size ranges from a few nm up to several µm. They can be differentiated into organic colloids (most of the so called DOC "Dissolved Organic Carbon" is colloidal), inorganic colloids (Al-, Fe- and Mn-Oxides and –Hydroxides) and micro-organisms ("bio-colloids") (BUFFLE & LEEUWEN 1993). Partly they originate from human sources like industrial dusts and ashes, wash-out, as well as from natural formation. Soot colloids are of major importance concerning the displacement of hydrophobic organic contaminants in urban areas. Atmospherics colloids can reach the soil zone by wet and dry deposition. Depending on hydrochemical and hydraulic conditions significant colloid mobilization and transport can be expected. In contrast to the saturated zone the migration of colloid bound contaminants in the unsaturated zone is less understood.

2. Unsaturated column experiments

In unsaturated laboratory column studies the influence of hydraulic and hydrochemical parameters on colloid transport behavior are investigated in order to develop a predictive colloid release/soil-chart.

To determine how the soil grain size does influence colloid transport steady state experiments with different column filling materials were carried out. The soil grain size varied from the fine sand range to the gravel range. Fluorescent polystyrene colloids (diameter 1 µm, 1,05 g/cm³, Polyscience Inc.) were added as a quasi-dirac injection to the columns. Colloid concentration at the outflow was measured by fluorescent spectroscopy.

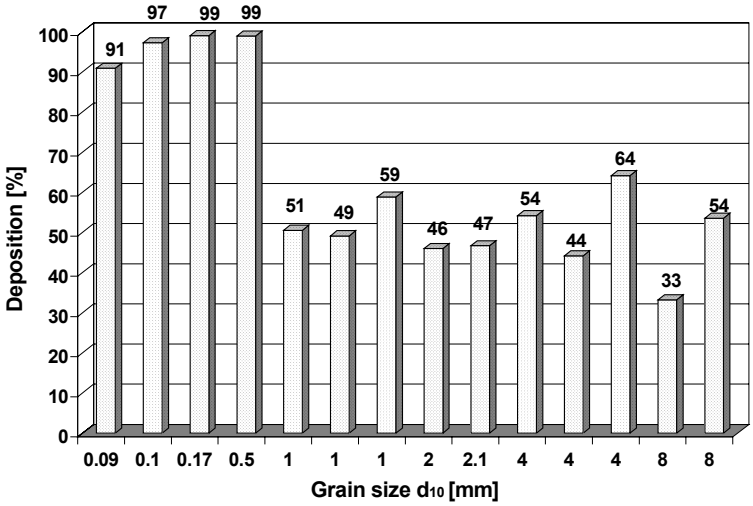

Figure 1: Deposition rates of 1µm polystyrene colloids depending on varying grain size of the column filling, irrigation intensity 36 mm/h

For gravel (d_{10} = 8 mm to 1 mm) colloid breakthrough curves seem to be very similar in velocity and shape. Colloid breakthrough in columns with fine grained material is much slower. Comparing the deposition rates a dichotomy in two groups of colloid deposition could be recognized (Fig. 1).

In the group of gravel materials (d_{10} = 8mm to 1mm) approximated 50 % colloid deposition can be observed. Compared to this the smaller grain size favors higher deposition rates of about 95 %. Despite the materials cover a wide range of grain sizes, only two deposition regimes are developed. Small grain size differences do not seem to be the main influencing factor for colloid deposition. Instead, the water content of the columns and thereby the flow regime plays a major role. In the fine grained columns flow regime is presumably dominated by matrix flow and a high water saturation. This also implies that more surfaces are in contact with the seepage flow and can sorb colloids. In coarse grained material macropore flow along distinct flow paths can be expected. Flow is faster, as proofed by the experiments, and the surface area for colloid attachment is lower, shear forces are higher. Thus, flow pattern (matrix vs. fingering/macropore flow) is dominating colloid transport. Further dye tracer experiments carried out at present may visualize these assumed effects. In addition, the gas-water interfacial area as well as the wetting history may play an important role.

Experiments where the colloid size was varied showed that colloid transport in the unsaturated zone behaves differently to the predictions by filtration theory (Fig. 2). According to filtration theory (RAJAGOPALAN & TIEN 1976, YAO 1968) a minimum in colloid deposition rate would have been expected for the experiments with 1 µm colloids. Contrary to the expectations, experimental data showed a minimum in colloid deposition displaced to smaller colloid sizes at 0.2 µm.

In the experiments the colloids reach the maximum concentration earlier than the tracer, whereby the smallest colloids are observed to be the fastest (Fig. 3). In filtration theory this can be explained for the large and very small colloids by a higher retention in respect to the tracer. Whereas the mean tracer arrival time is dominated by small and large pores, colloids only travel in the large “fast” pores (because they are retained in the small pore system). Model predictions show a typical minimum for colloid filtration around 1 µm for polystyrene spheres. Thus, the travel velocity of 1 µm colloids is expected to be closer to the tracer,

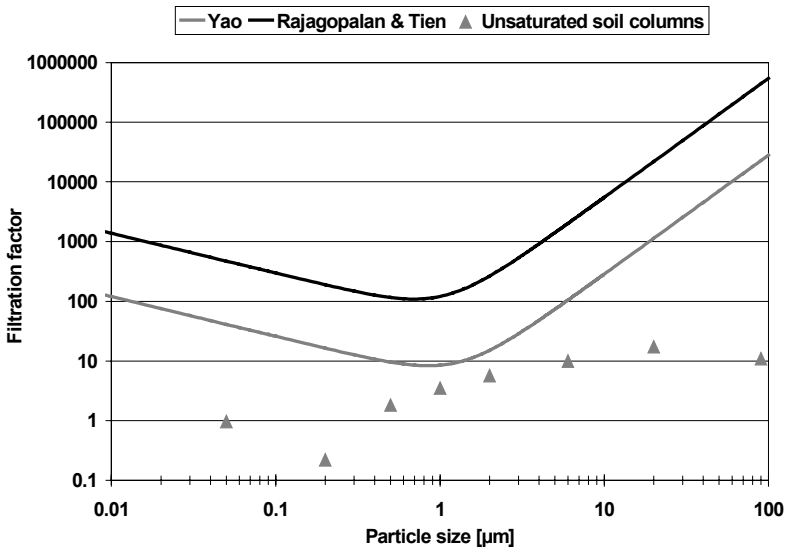

Figure 2: Comparison of filtration models and results from unsaturated column experiments: colloid size 0.05 µm - 90 µm, 36 mm/h

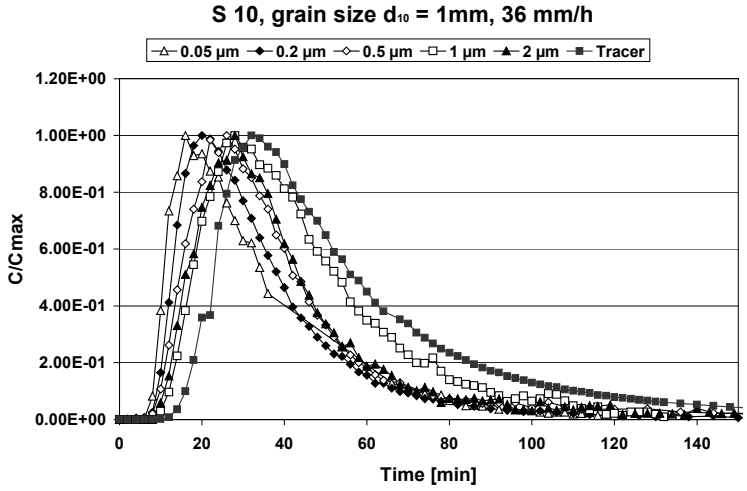

Figure 3: Colloid breakthrough curves of 0.05 µm to 2 µm polystyrene colloids, grain size = 1 mm, irrigation intensity 36 mm/h

contrary to larger and smaller colloids, which seem to arrive earlier (in fact, they do not arrive earlier, only the peak breakthrough is earlier).

The fact that in these laboratory experiments smaller colloids are transported faster through the unsaturated soil zone and that they show a smaller deposition rate can not be explained by filtration theory. Additional processes seem to play an important role in colloid transport in the unsaturated zone.This leads to the conclusion that the equations for sedimentation, interception, diffusion and filtration have to be modified to satisfy transport processes in the unsaturated zone. The processes are not finally identified and quantified. Sorption and transport at the gas-water interface are regarded to be important and described in several laboratory experiments (ABDEL-FATTAH 1998; WAN & TOKUNAGA 1997, WAN & WILSON 1994). In the case of a steady state gas-water interface colloids are deposited to a higher extend than in the saturated zone due to this additional deposition possibility.

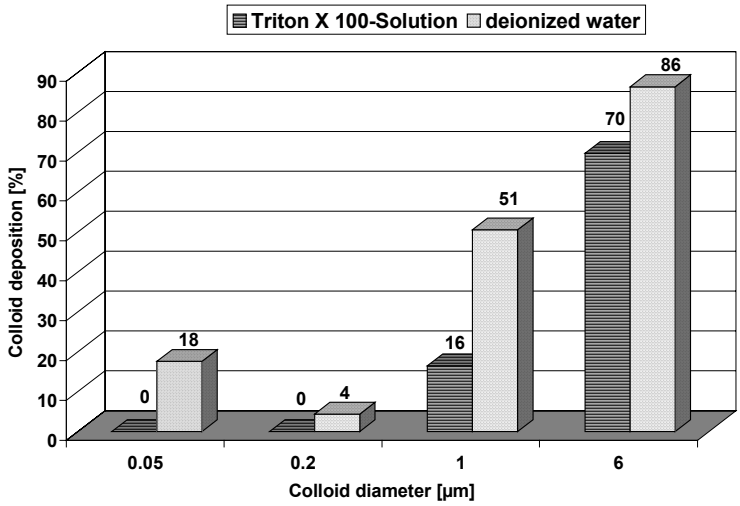

Figure 4: Comparison of deposition rates of polystyrol colloids (0,05 µm – 6 µm) in unsaturated column experiments using irrigation solution with varying surface tensions.

The relevance of the deposition at the gas-water interface was studied in further column experiments. The influence of surface tension to colloid filtration was investigated using a surfactant. The nonionic surfactant Triton X 100 was added to the irrigation water (1 Vol.% Triton X 100). The surface tension of the solution was significantly reduced to 27,5 mN/m. Beside a change of the surface attributes by formation of a surfactant adsorption layer further effects can be observed. After adding the surfactant, the water content in the column decreased significant (by 50 %), consequently altering the flow properties within the column. Sorption sites for colloids should be less available as a result of the lower amount of surface area and blocking of the sorption sites by surfactant molecules.

This assumption was confirmed in the column experiments. It can be shown that the deposition of 1 µm polystyrene colloids at an irrigation intensity of 36 mm/h is considerable reduced by irrigating the column with the surfactant solution (compared to a parallel experiment without surfactant, Fig. 4). The deposition of the 1 µm colloids is reduced by up to 35 %. 6 µm colloids show less reduction in the deposition rate (16 %). This could be due to a different influence of the gas-water interface on varying colloid sizes. The experiments give evidence that the smaller colloids are predominantly filtered at the gas-water interface, whereas the larger colloids are trapped in thinner water films, pore throats, or an immobile water meniscus between grains (and thus not affected to the same amount by the surfactant).

References:

ABDEL-FATTAH, A. & EL-GENK, M. (1998): On colloidal colloid sorption onto a stagnant air-water interface. Advances in Colloid and Interface Science 78:237-266.

BUFFLE, J. & van LEEUWEN, H.P. (eds.) 1993. Environmental colloids Vol. 2, London: Lewis Publishers.

RAJAGOPALAN, R. & TIEN, C.(1976): Trajectory analysis of deep-bed filtration with the sphere-in-cell porous media model. Am. Inst. Chem. Ing., 22, 523-533.

WAN, J. und WILSON, J.L. (1994): Colloid transport in unsaturated porous media. Wat. Resour. Res. 30:857-864.

WAN, J. & TOKUNAGA, T. (1997): Film straining of colloids in unsaturated porous media: conceptual model and experimental testing. Env. Sci. Tech. 31: 2413-2420.

YAO, K.M.(1968): Influence of suspended colloid size on the transport aspect of water filtration. Diss. Univ. of North Carolina, Chapel Hill.

Heterogeneity and scale issues in soil and groundwater

S.E.A.T.M. van der Zee

Wageningen University, Department of Environmental Sciences, Soil Quality, P.O.Box 8005, 6700 EC Wageningen, Netherlands, e-mail: Sjoerd.vanderZee@BodHyg.BenP.WAU.NL

Abstract: Soil and aquifers are intrinsically heterogeneous. Such a heterogeneity is apparent at different scales and can be observed for both physical, chemical and biological properties and processes. A number of illustrations is given to draw attention to heterogeneity.

The essence of heterogeneity is that because the medium of interest is heterogeneous, so are the processes that are important with respect to our appreciation of the environment and that are the basis of our management and the policy options for dealing with environmental issues. Hence, in some way we need to take heterogeneity into account if we wish to provide a good basis for environmental management. For illustration, several management and policy issues are related to heterogeneity of soil and ground water properties and processes.

Because heterogeneity occurs at every scale, we have to come up with a methodological approach that allows us to relate the different scales, and where possible, to develop a methodology that enables us to treat heterogeneity issues at each scale, indifferent to the actual scales we are interested in for a particular problem. A first step is to distinguish different scale levels, that are less arbitrary than other classifications as in Figure 1. An operational classification of scale levels is provided.

For upscaling, we are confronted with different problems, such as the problem that governing equations for processes at different scales differ and the increasing complexity of relevant processes as the scale we are interested in grows. These problems are essentially different and only for the earlier one, methodologies are available such as stochastic approaches, and mathematical analysis, such as aggregation, homogenisation, and regularization.

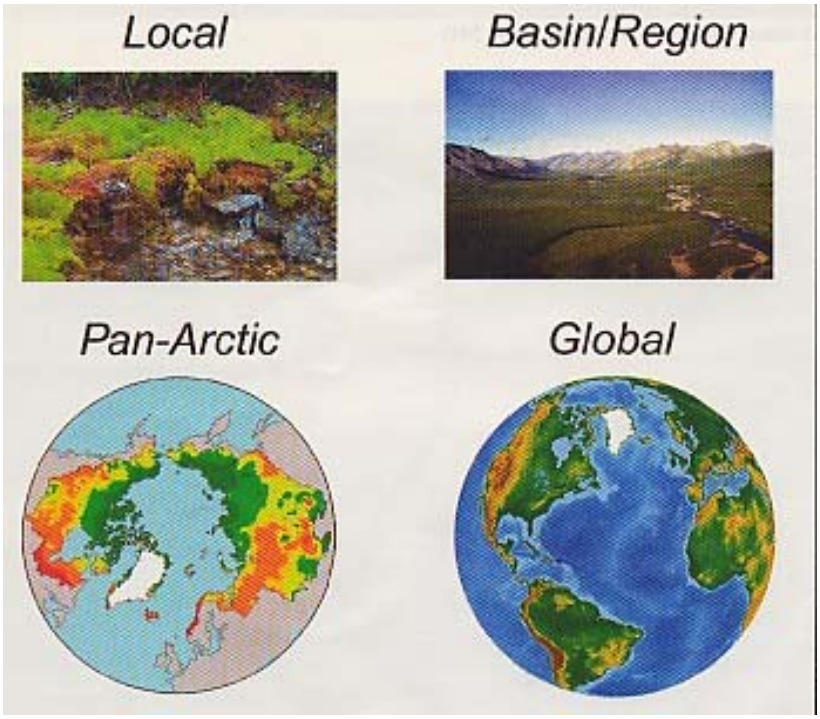

Figure 1: Example of a classification of scales that is rather arbitrary

For the increasing complexity issue, tools may be available in natural sciences, such as GIS, and fuzzy logic, but general theories and concepts may have to be borrowed from the socio-economic sciences. To enable further advances in upscaling, browsing socio-economical and mathematical approaches need to be related to outstanding practical issues related with environmental and particularly soil and ground water research.

Macronutrients, airborne acids, management tools applicable for protection zones – an overview

W. Walther[1], M. Pätsch[2], F. Reinstorf[3], C.,Konrad[1]

[1]*Corresponding author: Dresden University of Technology, Institute for Groundwater Management, Mommsenstr. 13, 01069 Dresden, Germany, Phone:+49 351257970, e-mail: grundwasser@mailbox.tudresden.de*
[2]*Karl-Marx-Strasse 1, 38104 Braunschweig, Phone: +49 531 700 9000, e-mail: Matthias.Paetsch@t-online.de*
[3]*Environmental Research Center Leipzig – Halle, Permoser Strasse 15, ´04318 Leipzig, e-mail: reinst@halle.ufz.de*

Abstract: Agricultural land use and airborne acids are sources of diffuse loads of waters. In water protection zones changes of land utilization can be one way to minimize emissions of nutrients. Tools are presented which enable the user to make scenario analysis and predict the reactions of the system before the agricultural soil use in larger areas or water protection zones starts to change. Furthermore an overview about reliable methods to identify the depth of the acidification front will be given here.

1. Introduction

The diffuse load on surface water and subterranean water has been considered an important problem for several decades in central Europe. This form of pollution reflects the economical development of Europe over more than 100 years. First publications that reported on the load on groundwater with nitrogen compounds that were used for the water supply appeared at the beginning of the 20th century. The centre of Europe is densely settled with an intense agricultural production, with an industry production on a relatively high level and with a relatively high amount of private and industrial traffic. The results are emissions which influence the aquatic systems through erosion and leaching.

Agricultural land utilization:

In countries with a high level of agricultural production like in Central Europe, the diffuse load on waters by nutrients, in particular nitrogen, or by persistent organic substances such as crop-protective-agents or antibiotics, often causes problems as mentioned before. In some regions an abstraction of drinking water is often only possible because decomposition processes such as denitrification decreases concentration below water standards.

The reaction of decomposition depends on the spatial distribution of reactive material in the aquifer. The life - span of reactive material is limited and therefore the life –span of water works too. However, the knowledge about these heterogeneous distributed processes and their impact on groundwater quality is of great importance for the protection of drinking water supply and it is still examined inadequately.

In countries of new members of EU changes in the intensity of agricultural soil use due to the conditions of the market is expected. In drinking water protection zones the change of land utilization can be one measure for minimizing the emissions of nutrients into groundwater.

Suitable instruments can be models describing water flux, substance transport and turnover in the compartments unsaturated and saturated zone. Special types of models for each compartment exist. The new issues urgently need a deeper insight in correlation of these compart-

ments. Our aim was to make a contribution for solving this problem. Tools have to be developed which enable the user to make scenario analysis and predict the reactions of the system before the agricultural soil use in larger catchment areas or water protection zones starts to change.

These general objectives were the tasks of a joint project carried out by our group (TU Dresden, co-ordinator) together with colleagues from Bulgaria, Poland and The Netherlands, Walther et al. (2002). Some results will be presented here.

Airborne Acids:

In central Europe aquifers are often contaminated from non point sources by airborne substances since many years. One group of important airborne substances are acids on the base of nitrogen from sources as large livestock farms (NH_3/NH_4) and traffic, sulfur from energy production. In consequence of the acidification of soils, metals are mobilised as a result of buffering reactions. The mobilisation of metals is caused by the exchange of M_b cations (this are K^+, Na^+, Ca^{2+} and Mg^{2+}) with hydrogen ions and the disintegration of clay minerals. The metal cations will be transported slowly to groundwater about the time distance of many years, when they will not be held by plant consumption for instance. In many regions of Germany, it can be observed that the level of contamination slowly migrates downwards. In some regions the acidification front has reached deeper zones of aquifers. In groundwater catchment areas, which are used for water supply, it is necessary to manage the problems on the side of the soils by suitable measures avoiding the leaching of substances or decreasing the velocity of migration to groundwater. A suitable measure in forest and agricultural used areas are the treatment of the soil with lime for example. Nevertheless, the main goal of preservation strategies should be the reduction of the deposition of strong acids. The task of the science should be, however, the development of reliable methods for identification of the position of the acidification front and for predictions of the migration. Particularly there is a lack of practicable methods, which are suitable for authorities and water workers for decision making. In the research project „Acidification of the Wingst Area (Northern Germany)“ some methods are applied to identify the status of the acidification and to make a prediction of the further trend, Walther et al. (2000), Reinstorf et al. (2001). This allows to give recommendations for counter measures. An overview about reliable methods to identify the depth of the acidification front will be given here.

2. Emssions in the field of agricultural land utilization, results of an research project

2.1 Test of suitable models

For the description of the nitrogen dynamics in the root zone, a great number of models with different stages of details exist. In general the practical application of the models goes back with increasing degree of specification since the expenditure to get the necessary parameters increases strongly. On the regional level of modelling often simplified approaches, so-called conceptual models are employed in order to solve the problems with the estimation of parameters. One example of that are the capacity approaches that employ the field capacity of a soil layer as a basis for the calculation of water flow. The corresponding models mostly have a higher degree of robustness but a lower sensitivity, e.g. the model HERMES (Kersebaum, 1995). One of the few model approaches that describe the dynamics of the balance of different substances such as phosphorus, oxygen and nitrogen, is implemented in the model SWAP/ANIMO (Van Dam et al., 1997, Groenedijk et al. 1993).

In the meantime a sufficiently large number of models to simulate flow and transportation of substances are available for the saturated zone. In recent years some efficient transportation - reaction models (multi-species) were presented, e.g. MT3D (Zheng, 1990).

For the **unsaturated zone** three models were assessed by the three research groups:

HERMES was developed for the advice of farmers in fertilisation. It is a conceptual model for water flux, nitrogen turnover and nitrogen flux. It requires a relatively low amount of data for parameterisation. But HERMES model is not able to react on fast changes of water content and nitrate transport in upper soil compartments. Leaching of nitrogen is computed because this information is needed for the farmer as a loss in the nitrogen balance. Therefore the applied version of HERMES considers leaching of nitrate only to a depth of 2 m below surface.

SWAP/ANIMO models are quite detailed models and they require a large amount of detailed input data and parameters. Both models are linked. Sometimes it is difficult to find detailed input information for the investigated areas. These models cannot be used by farmers but are very good tools for sophisticated research on the influence of agricultural land use on water quality. Both models are physically based for water flux and conceptual models on the side of nutrient turnover and flux.

WAVE model (Vanclooster et al., 1994) describes the nitrogen circle and it is similar to SWAP/ANIMO models.

All three models enable the user to account in detail for agricultural land use, organic and mineral fertiliser application, climate and soil conditions.

Groundwater flow and transport was modelled on the basis of MODFLOW (McDonald et al. 1988); combined with MT3D simulate two or three dimensional flow and predicts advective – disperse contaminant transport.

Nitrate decomposition in groundwater

In the German investigation area "Thuelsfeld", situated in the northern low plain, a very heterogeneous distribution of the denitrification capacity was found in connection to the distribution of concentration in groundwater (e.g. O_2, NO_3^-, SO_4^{2-}, Fe^{2+}) depending on the depth and on the distribution of reactive aquifer material. With the help of water age and nitrate concentration over the depth coefficient k of decomposition equations (1st order kinetics) were derived. The k-values lie between 0.2 and 0.5 1/year, Pätsch et al. (2001).

2.2 Results of model comparison:

Unsaturated zone:

The results can be summarised as follows: all three models SWAP/ANIMO, WAVE, HERMES are applicable for different soil types, agricultural practices and under various hydrological conditions. HERMES model is designed for farmer's advice. It requires a relatively low amount of additional measurements and parameters. But it has the limitation that it can only consider soil profiles until 2 m below the surface. The combination of SWAP and ANIMO models and also WAVE needs more specific data than HERMES. These models are very good tools for sophisticated study of influence of agricultural land use on water quality.

Saturated zones:

MODFLOW with MT3D is a commercial program, available world wide, and is updated constantly. The MT3D - model requires a data base which is more difficult in determination. Parameters such as the dispersion coefficients or the nitrate decay coefficient have to be estimated and adapted by calibration. The results would be more realistic if for example the coefficients k could be deduced from additional investigations in the catchment area. For the saturated zones in each investigation area, the previously mentioned combination is recommended.

Although results of model application were not completely satisfying –probably due to a lack of data– the models produced hints by scenario calculations, which impacts certain ways of land use will have on groundwater quality during the next decades.

Further investigation will be necessary to confirm our results.

3. Acidification of soils and groundwater, results of a test site situated in the northern low plain of Germany

3.1 Definition of acidification and buffering reaction

Acidification of the fluid and the solid phase in the saturated and unsaturated zone is the long-term decrease of the acid neutralisation capacity (ANC). The ANC can be measured as increasing the acidity respectively decreasing of the alcalinity in the whole system, Eq. 1:

$$Aci = 2\left[SO_4^{2-}\right] + \left[Cl^-\right] + \left[NO_3^-\right] + ... - \left[Na^+\right] - \left[K^+\right] - 2\left[Ca^{2+}\right] - 2\left[Mg^{2+}\right] \qquad (1)$$

Between acidity and alcalinity exists the following connection:

$$Aci = -Alk \qquad (2)$$

The concept leads methodically to the balance of strong acids and bases:

$$Aci = \sum strongacids - \sum strongbases \qquad (3)$$

Besides the buffering as phase internal process in the fluid phase soil water and groundwater the acid buffering takes place largely by interactions between the phases soil water / groundwater ⇔ solid phase. To this process belongs the weathering and the cation exchange. An important parameter for the size of the buffer (live time of the buffering process) is the base saturation (BS). The bigger BS the bigger acid amounts which can be retarded by exchange at the solid phase in the subsurface, without significant changes of pH.

The base saturation is defined as:

$$BS = \frac{\sum\left(Ca^{2+} + Mg^{2+} + Na^+ + K^+\right)}{CEC_{eff}} \cdot 100 \qquad (4)$$

with $CEC_{eff} = EffectivCationExchangeCapacity = \sum Ion - Equivalents = \sum \frac{n_i \cdot i^{z_i^+}}{z_i} \div m$ in [$\mu mol_{eq}/g$]; n_i = number of Mols of the cations to be sorbed i [-], z_i = valence of the cation i [-], m = weight basis [g].

The silicate and exchange buffer is particularly important for quantification of buffering capacity. Below the limit of 80 % BS the buffering capacity decreases drastically. Therefore, after ULRICH et al. (1989), a soil is acidified if the equivalent rate of M_b – cations ≤ 80% of CEC_{eff} anf the pH ($CaCl_2$) ≤ 5.

3.2 Method for estimation of status quo of acidification - Characterization of the acid–base–status of the solid phase

Subsequent, methods are presented which are suitable to estimate the status of the solid phase. Besides hydraulic parameters, e.g. hydraulic conductivity and effective porosity, and characteristic values of the soil substrate, e.g. bulk density, the essentially information are the hydrogeochmical parameters for (1) soil reaction, e.g. pH(H_2O), pH($CaCl_2$) in the Equilibrium soil solution (ESS), (2) ANC, e.g. estimation of the titration curves pH = f(Aci) and pH = f(Alk), and (3) soil chemical analysis, e.g. estimation of CEC_{eff} and BS. The mentioned parameters allows a assessment of the acid-base-status of the solid phase. The estimation of the parameters should be carried out at undisturbed drilling cores.

3.3 Methods of prognosis for movement of acidification front

Recent models for acidification could be allocated to following model groups: (1) balance models and (2) process oriented models.

(1) Balance models neglect the processes with are taking place in the inside of the system. Input, output and storage of a system are quantified and connected. Balance models are suitable for estimations of middle and long term trends and makes small demands on input data. An example is the model

- AcidProgress (MALESSA ET AL. 1997) for estimation of acidification velocity in the unsaturated zone up to the groundwater level. The model undertakes a balance between the acid load and the ANC.

(2) Process oriented models are based on physico-chemical laws for the description of anorganic soil chemical processes, e.g. acid-base-reactions, redox-reactions, solution / precipitation reactions, sorption / desorption, gas-water-reactions, complex formation, and ion interactions. Short, middle and long term trends are interesting with regard to the reactions in soil and groundwater zone. An example is the model:

- SAFE (SVERDRUP ET AL., 1994): This model is a relativ new version of the model PROFIL (WARFVINGE & SVERDRUP, 1992) with consideration of the time. SAFE calculates the chemical composition of the soil water for various soil layers and time steps on the basis of atmospheric deposition and local parameters of the soil chemistry.

We applicated AcidProgress and SAFE at the investigation area Wingst. The model SAFE simulates the concentration of several substances in the soil water and sum parameters. One nother result of the simulation was the velocity of the acidification front of approximately 3 m within 100 years in the case of the present input situation.

3.4 Acidification, conclusions

The acidification fronts in some regions of northern Germany have already been reached deeper aquifers. Partly, zones of the aquifers have already been acidified. Actually, we create suitable recommendations for acting to predict the status of acidification and the movement of the acidification front. This knowledge is required for deduction of the demand of acting.

There are a number of tools and methods for estimation of the acidification risk. Short term and local suitable counter measures are kown, too. Long term and sustainable management strategies are not known.

Therefore, the goal of our research was to test and verify model tools and methods at a catchment area with drinking water supply. The presented models and methods are selected from a

number of available tools and can recommend for application in the field of management tasks.

A further testing of the models and methods should also carry out at other location in northern Germany.

References

Groenedijk P., Kroes J.G. 1997: Modelling the nitrogen and phosphorus leaching to groundwater and surface water. ANIMO 3.5, Report 144, DLO – Winand Staring Centre, Wageningen.

Kersebaum K. C. 1995: Application of a simple management model to simulate water and nitrogen dynamics. Ecological Modelling 81 (1995) 145-156

Vanclooster, M., P. Viaene, J. Diels, and K. Christiaens, 1994: WAVE v.2.0: Mathematical model for simulating water and agrochemicals in the soil and vadose environment, Institute of land and water management, KUL, Leuven, Belgium, 139p.

Van Dam, J.C., J. Huygen, J.G. Wesseling, R.A. Feddes, P. Kabat, P.E.V. van Walsum, P. Groenendijk, P., and C.A. van Diepen 1997: Theory of SWAP version 2.0: Simulation of water flow, solute transport and plant growth in the Soil-Water-Atmosphere-Plant environment, Wageningen, The Netherlands, SC-DLO en WAU Report 71, 167p.

Walther, W., Mioduszewski, W., Diankov,Z., Querner, E., Pätsch, M., Fic, M., Velkovsky,, G., F. Reinstorf, Marinov, D., Weller, D., Slesicka, A., Radoslavov, S. J., Nitcheva, O., Roelsma, J., 2002: Development of tools needed for an impact analysis for groundwater quality due to changing of agricultural soil use. Final Report, 4th Framework Programme INCO-COPERNICUS of EU, Contract number IC 15-CT98-0131

Pätsch M., Weller D., Walther W., Reinstorf F., Harms E. 2001: Heterogenity of nitrogen removal processes in pleistocene aquifers, northern low plain of Germany. Groundwater quality 2001, Proceedings third International Conference on Groundwater Quality, University of Sheffield, UK. 18-21 June 2001.

Reinstorf, F.; Walther, W.; Heblack, K.; Cramer, T.: Tools for prognosis of the acidification of aquifers in sedimentary rocks. 6th Scientific Assembly of the IAHS, In: "Impact of Human Activity on Groundwater Dynamics", IAHS Publication no. 269, ISSN 0144-7815, Maastricht 18-27th July 2001.

Walther, W.; Pätsch, M.; Weller, D.; Reinstorf, F.; Harms, E.; Kersebaum, C.: Nutrient loads on a Northern German Sandy Aquifer, reduction Processes, their Distribution and Management tools. XXXI. IAH Congress. New approaches to characterising Groundwater Flow, 10th - 14th September 2001, Munich, ISBN 902651.

Malessa, V. (Koord.)(1997): Umsetzung von Forschungsergebnissen in Planungs- und Entscheidungsverfahren. Niedersächsisches Landesamt f. Bodenforschung: Arbeitshefte Boden, 3, 115 S.

Sverdrup, H.; Warfvinge, P.; Blake, L.; Goulding, K. (1995): Modelling recent and historic soil data from the Rothamsted Experimental Station, UK using SAFE. Agriculture, Ecosystems and Environment, 53, 161-177.

Ulrich, B.; Malessa, V. (1989): Tiefengradienten der Bodenversauerung. Z. Pflanzenernähr. Bodenk., 152, S. 81-84.

Walther, W; Cramer, T.; Reinstorf, F.; Heblack, K. (2000): Säureeinträge und Einträge von Stickstoff über den Luftpfad und deren Auswirkungen auf Boden und Grundwasser im Bereich der Wingst / Niedersachsen, Abschlußbericht, Institut für Grundwasserwirtschaft der TU Dresden.

Zheng, C. 1990: A Modular three-dimensional transport model for simulation advection, dispersion and chemical reactions of contaminants in groundwater system, Robert S. Kerr Environmental Research Laboratory, US EPA, Ada, Oklahoma

Acknowledgement

We would like to thank the European Commission and the Oldenburgisch-Ostfriesischer Wasserverband, Germany (Techn. Dir. E. Harms), that they have financially supported the research project in the frame of inco-copernicus. The authors thank also the Agency for Ecology of Lower Saxony / Germany for funding the research project “Wingst”.

POSTERS

GROUNDWATER RISK ASSESSMENT AT CONTAMINATED SITES

Detection of VOC in a large scale experiment: Evaluation of a field screening tool for site characterisation

Batereau, K., Mackenberg, S.

VEGAS, Institute of Hydraulic Engineering, University of Stuttgart

1. Background

Field screening instruments should be employed to carry out a more reliable site characterisation with a higher certainty of results with many low cost measuring points supplying real-time data directly in the field. This procedure makes the use of a flexible measuring grid possible which leads to more detailed information of the contaminant distribution and a better distinction between contaminant sources (Hot-Spot), lower contaminated and non contaminated areas (Fig. 1). The conventional site assessment procedure, based on a fixed measuring grid, consists of taking few soil, water and/or gas samples. Because of the heterogeneity of the subsurface and the heterogeneity of the contaminant distribution these few samples cannot represent the contaminated situation of the site [1].

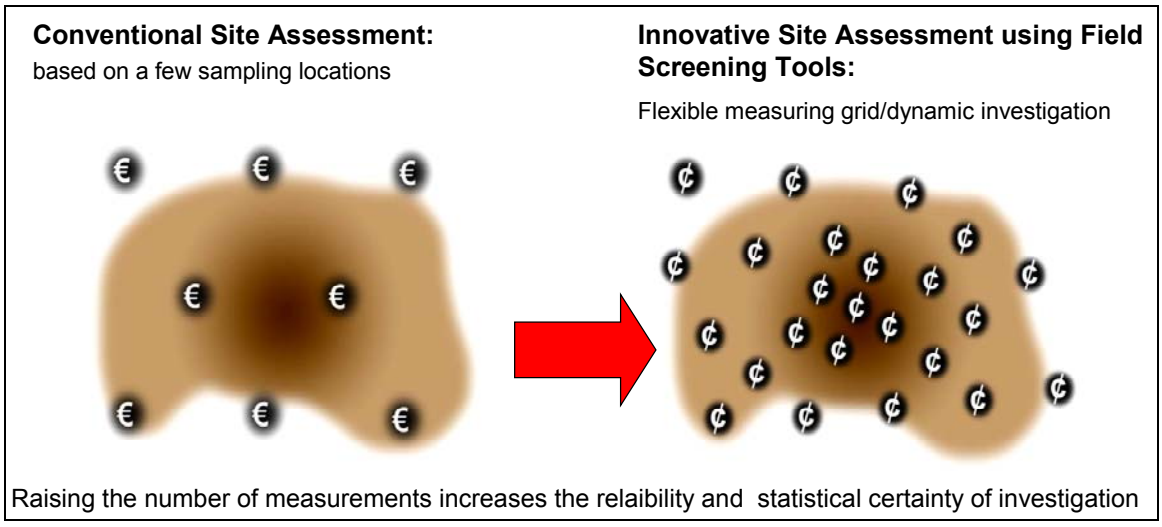

Figure1: Conventional site investigation and innovative site investigation

Since only limited field screening tools and detection systems which can be used for site characterisation are on the market, the development of field screening tools is an ongoing research topic. At *VEGAS* a prototype for the detection of VOC in the subsurface has been developed and already tested in the laboratory. The results show that it is suitable for the detection of contaminants typically found on brown fields. In the field the applicability of the prototype has been tested on various sites and it could be shown that:

- it is sensitive enough for the relevant contamination,
- it is selective enough for the target contaminant groups,
- it is robust and easy to handle in the field.

2. Objective and method

The aim of the large scale experiment is to evaluate the developed prototype at technical scale. In the experiment the application and limits are tested in a pilot study on a well known contamination. The experimental container in use at *VEGAS* (length: 9 m, width: 6 m, depth: 4.5 m has been contaminated under controlled conditions and an on-site investigation has been conducted with the sensor based field screening tool.

In figure 3 the experimental set-up is shown in side and top view. The container represents the unsaturated zone of a bedded subsurface. Different sand layers of varying thickness alternate from bottom to top. The slope of all layers is 5 %. The water content in the soil averages from 6 to 8 vol.-percent following a relative humidity in the soil gas close to natural conditions. For the infiltration of the chosen pollutant TCE a ½ inch tube of stainless steel with a 1 m perforated section was used. The perforated section is mainly located in the coarse-grained sand and reaches into the fine-grained sand below and the middle-grained sand above. The TCE-infiltration is carried out by vaporizing TCE and pumping the vapour into the container.

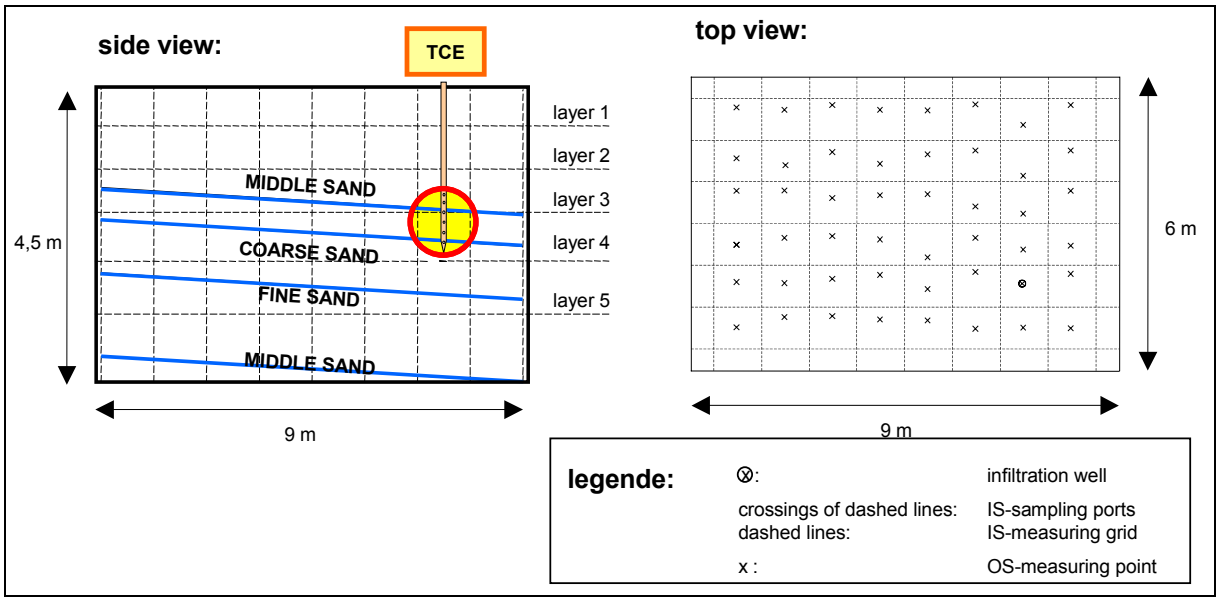

Figure 3: experimental container and set-up

The container is fitted by a tight grid of in-situ (IS) sampling ports (fig. 3). These sampling ports are arranged in five layers meter wise in each direction. Gas samples were taken out of these sampling ports with a syringe and injected directly into a head space vial. The gas samples were analysed by a GCMS-method (according to DIN 38 407 part 5 (F5)).

The grid for on-site (OS) measuring points (fig. 3) was defined according to the IS-sampling ports. Measurements have been carried out in the typical and proved field set-up [2]. The sensor based measuring device for VOC detection is linked to a conventional driving rod to establish the contact between soil gas and the analysing sensors. The assembly is shown in fig. 4 [3].

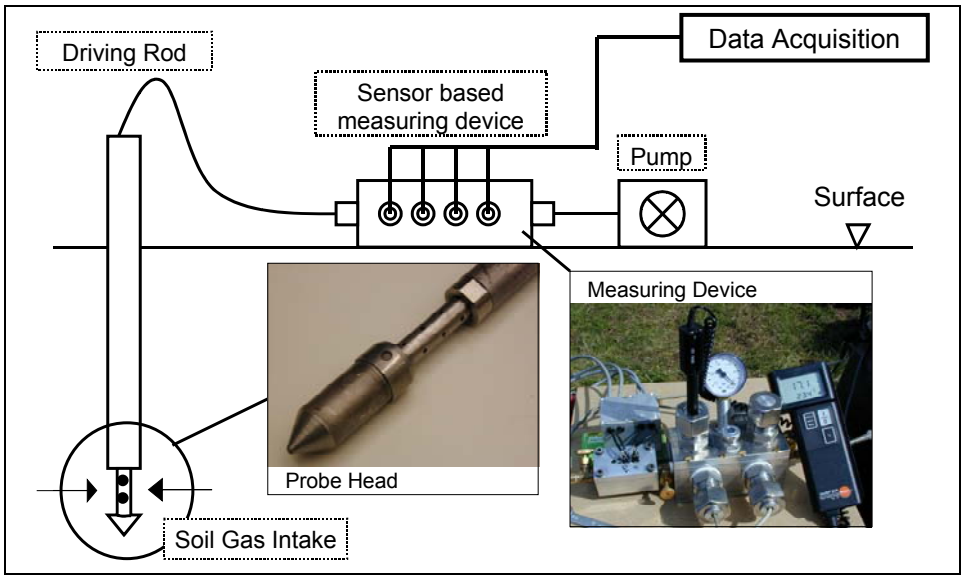

Fig. 4: Prototype of the field screening tool and measurement set-up in the field

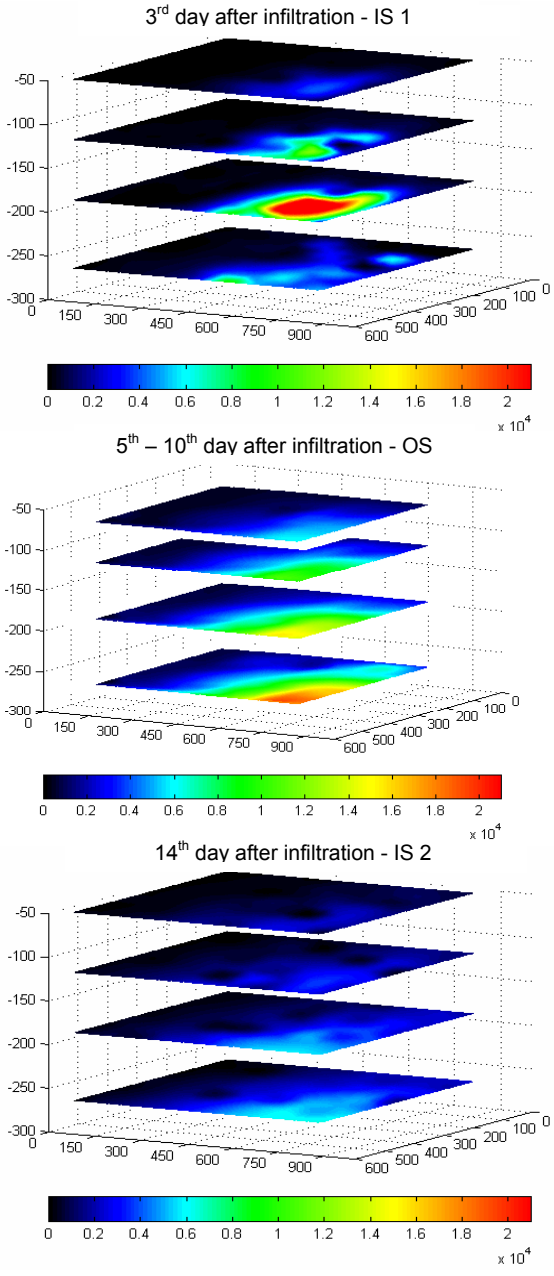

Fig. 5: TCE distribution for IS-measurements and OS-measurement [in µg/l]

The procedure of the experiment was the following:

Two days after the infiltration of TCE the first IS-sampling (IS 1) was carried out to get detailed information about the actual distribution of contamination. From the 5th day to the 10th day the contaminated situation was investigated by on-site measurements (OS). A total of 47 drillings were carried out. Because of an expected TCE distribution during the experiment devolution a second in-situ sampling (IS 2) has been carried out after the OS-measurement, 14 days after the infiltration.

3. Results of the experiment

The TCE-distributions resulting from the three different measurements of TCE concentration (IS 1, OS, IS 2) are shown in figure 5. All plots show a similar distribution of the TCE-concentration. The measured values clearly display the contaminant source and distribution of TCE into the container, horizontally according to the sand layers due to diffusion processes and vertically due to the density of TCE vapor.

Considering the temporal displacement of the three procedures of measurement there is an obvious interrelationship between the sampling time and the TCE-distribution:

At IS 1, just after infiltration, the highest concentrations of TCE were measured in the third level around the infiltration point. To examine the data resulting from OS-measurement the sensor which is most sensitive to TCE is taken into consideration. The results show the highest concentrations of the TCE-distribution in the forth level. Peak concentrations are lower than at IS 1 but therefore a further horizontal spreading of the contaminant plume has taken place. The figure of IS 2 shows a pattern for the TCE distribution similar to that of OS-measurements. Peak concentrations are lower again and the TCE is mostly spread horizontally and vertically compared to the infiltration situation. The driving forces for the distribution during the experiments progress are diffusion and gravity.

According to the different images of contaminant distribution a mass balance should give information about the total sum of TCE, measured with the different set-ups at different time steps. The sum of measured TCE at IS 1 is assumed as 100%. The recovered mass of TCE at the OS-measurement is 180% and at IS 2 70%. When comparing the data of IS 1 and IS 2, acquired with the same procedure, the strong effect of gravitation becomes apparent. The TCE is gravitated to the ground of the container, where it is not detectable because the deepest sampling-level is 1m above the container bottom. The sum of TCE at the OS-measurement is higher by a factor 2 than at IS 1 because of matrix effects.

4. Conclusion and Outlook

A new field screening tool for the assessment of contaminated sites has been applied in a large scale container. The contaminant distribution has been investigated with on-site measurements using the prototype. Since the container is fitted with a tight grid of in-situ sampling ports, before and after the on-site-measurement the distribution of the contaminants has been investigated with in-situ-samples analysed with GC/MS in the analytical laboratory of *VEGAS*. To evaluate the representativeness of the on-site measurements their results should be compared to the in-situ measurements. The results of all measurements show the same pattern of distribution of contaminants. The hot-spot and less contaminated areas are clearly defined in all set-ups. The application of the field screening tool is possible in a wide range of concentrations.

Due to the time factor of the different measurements (IS 1, OS, IS 2) a comparison of the absolute concentration is not possible. The total mass detected with the on-site measurements is two times higher than the total mass of the in-situ samples. For an estimation of the field applicability of the prototype this result is very good compared to the conventional site assessment because the sampling errors are often much higher. Also the field screening tool is useful to complete the current procedure of site characterisation because it is possible to carry out many low-priced point measurements. This leads to a more reliable picture of the heterogeneous distribution of contaminations at the field site and increases the certainty of investigation. Furthermore, on on-site measurements are useful to define suitable sampling locations for the analytical laboratory.

5. References

[1] Batereau, K. (2002): Application of sensors for site characterization, NICOLE Meeting: Cost-effective site characterization – Dealing with uncertainties, innovation, legislation constrains, Pisa, 2002

[2] Batereau, K., Klaas, N., Barczewski, B. (2001): On-Site Assessment of Contaminated Sites: Application of Sensors for On-Site Instrumentation, Field Screening Europe 2001, ISBN 1-4020-0739-6, Kluwer Academic Publishers, 2002

[3] Batereau, K., Barczewski, B., Müller, M. (2002): Application of sensors for site characterization, Response to New Pollution Challenges, 2nd SENSPOL Workshop, June 2002

Development of an easy-to-use tool for groundwater risk assessment: an application of geochemical modelling

Joris Dijkstra and Rob Comans

Energy Research Centre of The Netherlands (ECN), P.O. Box 1, 1755 ZG Petten, The Netherlands
Tel.: +31-224-564218; Fax: +31-224-568163; E-mail: comans@ecn.nl

Abstract: A possible alternative to remediation options of heavy metal-contaminated sites is natural (or stimulated) attenuation. Using geochemical models, an *attenuation indicator* has been developed, which provides the user a preliminary assessment of the possibility of sufficient (long term) attenuation based on the measurement of a few site-specific parameters and chosen target values for groundwater quality. The attenuation indicator consists of a pH/E_H diagram in which the colour of the different zones indicates the possibility of attenuation by either mineral precipitation or sorption. By plotting measured values of pH and E_H into the attenuation indicator, the user can interpret site-specific data in a rapid and simple manner. Among processes that are taken into account in the modelling are complexation in solution, mineral dissolution and precipitation, sorption to dissolved organic matter and to the solid phase.

1. Introduction

A possible alternative to remediation options of heavy metal-contaminated sites is natural (or stimulated) attenuation, particularly for large-scale contaminated areas. Costs of remediation can be possibly reduced if a preliminary assessment can be obtained of the possibility of sufficient (long term) attenuation, based on the measurement of a few site-specific parameters and specific groundwater targets. Using geochemical models, an attenuation indicator has been developed that provides the user such a preliminary assessment, as well as a qualitative to semi-quantitative indication of the binding capacity of the soil/aquifer. The approach followed may be valuable in the future for a wide variety of uses such as modellers, engineers as well as responsible legislators. The development of this tool is outlined in detail by Dijkstra and Comans (2003).

The graphical component of the attenuation indicator is a pH/E_H diagram in which the colours of the different zones provide an indication of whether attenuation is likely (green), uncertain (orange) or unlikely (red) (Figure 1). The boundaries of the green zones represent a specific groundwater limit value (see below); in theory this means that within these zones, solution concentrations are reduced to an acceptable level. Among processes that are taken into account in the modelling are complexation in solution, mineral dissolution and precipitation, sorption to dissolved organic matter and to the solid phase (cation exchange, specific sorption to Fe/Al-oxides and solid organic matter). Within each diagram, shaded zones (green or orange) indicate whether sorption to the solid phase is the predominant attenuation process.

2. Background: development of the instrument using geochemical models

The oxidation/reduction state of groundwater systems has appeared to be an important factor determining the distribution and transport of contaminants such as heavy metals (e.g., Christensen et al; 2000). Retention of heavy metal concentrations in the source or in the receiving medium may occur through formation of poorly soluble precipitates such as sulfides or through adsorption to reactive surfaces of minerals or solid/dissolved organic matter. Many

of these reactive surfaces, such as Fe-(hydr)oxides are sensitive to redox conditions due to their thermodynamic instability at low redox potentials.

The possible formation of mineral phases at natural groundwater conditions can be assessed with Geochemist's Workbench (Bethke, 1998). The main advantage of calculating "tailor-made" diagrams over using published diagrams (e.g., Brookins, 1988; Garrels and Christ, 1965) is that the user is able to choose relevant conditions (e.g., average groundwater composition, groundwater limit values). In the case of Figure 1, within the stability fields of minerals (such as ZnS) activities of Zn will be lower than the chosen Zn-activity (groundwater limit value) for which the diagram is calculated. These mineral stability fields may therefore be coloured green. The regions outside of the mineral stability fields are marked red as no precipitation is expected to the extent that Zn activity in solution would remain below the groundwater limit. The size of the green zones depends on the chosen activity of background components (e.g., the ZnS zone depends not only on the chosen Zn activity, but also on the chosen S^{2-} activity). Therefore, we performed our calculations with maximum as well as minimum groundwater concentrations of the relevant elements. The area captured between the stability fields calculated for high and low background concentrations are marked orange, because the actual concentrations will determine whether the mineral will precipitate in this field or not.

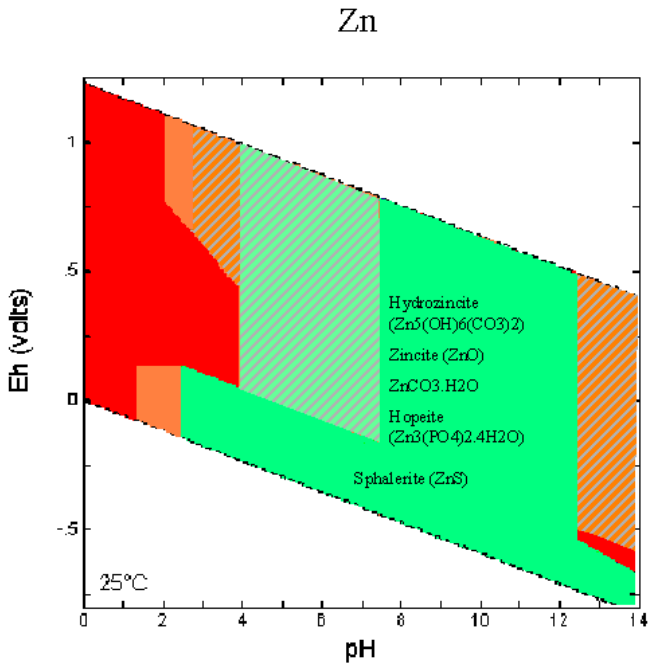

Figure 1. Example of an attenuation indicator for Zn. The coloured zones indicate whether sufficient (relative to a selected groundwater limit) attenuation is likely (green), uncertain (orange) or unlikely (red). The shaded areas indicate where adsorption is the most important attenuation process. In the areas without shading, precipitation of minerals is the dominant attenuation process. In these areas, potentially important solubility-controlling minerals are indicated (Dijkstra and Comans, 2003).

Stability diagrams for reactive (sorption) surfaces are calculated in the same way as outlined above. In the ranges where reactive surfaces are thermodynamically stable, sorption can take place. These regions can not be instantly marked green as the degree of sorption is dependent on the amount and type of reactive surfaces, the initially sorbed concentrations, competing ions etcetera. To distinghuish these zones from mineral stability fields, these zones are

shaded. The colours assigned to the different shaded areas are based on a worst-case scenario, with a given "poor" composition of the aquifer and a given loading of Zn (Dijkstra and Comans, 2003). However, to calculate the maximum binding capacity at which groundwater limit values are still met, site-specific binding capacities can be easily derived by the user with the help of spreadsheet calculations using contaminant-specific coefficients derived by geochemical modelling using ECOSAT (Keizer and van Riemsdijk, 1998). Among processes that are taken into account explicitely are sorption to Fe/Al-(hydr)oxides, cation exchange at clay surfaces and sorption to solid and dissolved organic matter under average groundwater conditions. More detail on the approach will be given in Dijkstra and Comans (2003).

3. Conclusions

The *attenuation indicator* has been developed as a potential easy-to-use tool for groundwater risk assessment. Because the development so far is based solely on theory and on a number of assumptions, field and laboratory testing is needed for validation of the tool and its usefulness. Currently, several contaminated sites are being evaluated; preliminary results show that natural or stimulated attenuation at some of the locations investigated is an effective alternative to more intensive and expensive remediation concepts.

4. References

Bethke CM, The Geochemist's Workbench™, version 3.2.1. A users guide to Rxn, Act2, Tact, React, and Gtplot. Hydrogeology Program, University of Illinois, 1998.

Brookins DG. E_H-pH Diagrams for Geochemistry. Springer-Verlag Berlin Heidelberg, 1988

Christensen TH, Bjerg PL., Banwart SA., Jakobsen R., Heron G., Albrechtsen HJ. Characterization of redox conditions in groundwater contaminant plumes. Journal of Contaminant Hydrology 45 (2000), pp 165-241.

Dijkstra, JJ, Comans, RNJ (2003). Submitted.

Garrels RM, Christ CL. Solutions, Minerals and Equilibria. Freeman, Copper & company, San Fransisco, USA, 1965.

Keizer MG, Van Riemsdijk WH, ECOSAT: Equilibrium Calculation Of Speciation And Transport, user manual, version 4, subdepartment of soil science and plant nutrition, Wageningen University and Research Centre, Wageningen, 1998.

Leaching of PAH's from soil: Comparison of two conceptually different column tests and a batch tests

Jesper Gamst[1]; Peter Kjeldsen[1]; Jette B. Hansen[2]; Kim Broholm[2]; Thomas H. Christensen[1],

[1]*Environment & Resources DTU, Technical University of Denmark, Building 115, DK-2800 Kgs. Lyngby, Denmark.*
[2]*Water & Environment, Danish Hydraulic Institute, Agern Allé 11, DK-2970 Hørsholm, Denmark.*

Introduction

Soils at former gaswork, tar producing sites as well as oil- and gasoline facilities are often contaminated with polycyclic aromatic hydrocarbons (PAH's). Due to the high toxic and carcinogenic potential of the PAH's this endangers the groundwater quality. In order to prevent an unacceptable contamination of groundwater and surface waters it is necessary to obtain knowledge of the mobility and potential leaching of these chemicals. This information are essential in risk assessment, when estimating the concentration of the PAH's in the water infiltrating and percolating through contaminated sites. Both central and local authorities and problem owners ask for better tools for risk assessments of contaminated soils and waste products containing organic compounds. Leaching tests may be an important tool in groundwater risk assessment if properly conducted and interpreted. Column and batch experiments are generally accepted methods to conduct leaching tests to determine release rates and effluent concentrations in contaminated soil materials. Thus it is important, that the results of the leaching tests are correctly interpreted, due to differences in test conditions. In this study two conceptually different column-leaching tests, (I) a maximal flux test and (II) an equilibrium tests, were evaluated and compared. Experimental conditions such as column size and type, bulk density of soils, flow velocity, and temperature were kept similar in both column tests, securing the possibility for comparison. Results from the column tests were also compared to results obtained in a batch test.

Materials and Methods

Two column tests were evaluated; (I) a maximal flux test developed by Weiß (1998) allowing for longer-term prediction of PAH release through determination of desorption rates ("maximal flux") (Fig. 1a), and (II) an equilibrium test allowing for determination of the "equilibrium" pore-water concentration of PAH's ("equilibrium") (Fig. 1b). The two leaching tests are conceptually different but experimental conditions such as column size (~15 cm length and ~6 cm diameter, ~425 cm^3) and type (glass), bulk density of soils, flow velocity (darcy velocity of 0.7 cm h^{-1}), and temperature (22 °C, ±2 °C) are similar in all column experiments conducted. The batch tests were conducted in large glass centrifuge vials (~680 mL) allowing for shaking and centrifugation in the same vial. Default experimental conditions of the column leaching tests are listed in Table 1. Also given in Table 1 is the default conditions for the batch leaching test that were compared with the column tests.

Soil from a former gaswork facility was used to compare and evaluate the results from the three different leaching tests, the soil used is a silty topsoil.

Table 1. Default conditions of the column and batch tests used in this study.

Test conditions	Column tests	Batch test
Test material	400-500 g	280 g
Porosity	0.25-0.5	~0.15
L/S-ratio	0.15-0.35 l kg^{-1} (in column) 20-30 l kg^{-1} (maximal flux, test) 0.8-1.2 l kg^{-1} (equilibrium, test)	2 l kg^{-1}
Contact time	1-30 d (maximal flux) 1-21 d (equilibrium)	1-14 d
Leachate	1 mM $CaCl_2$ 0.5 g l^{-1} NaN_3	1 mM $CaCl_2$ 0.5 g l^{-1} NaN_3
Solute/solid separation	-	Centrifugation (655 g for 20 min.)
PAH analysis	Cyclohexane extraction, GC MS	Solid Phase Extraction (SPE), GC MS

In the maximal flux test (Fig. 1a) the solution used in the test is initially pumped through a de-oxygenator (Arcangeli and Arvin, 1995) to a storage tank. From the storage tank the oxygen-free solution is pumped at a constant rate to the soil column. At the bottom and the top of the column a filter layer of quartz sand is placed to secure a steady inflow into the contaminated material and to prevent mobilisation of particles out of the column. The eluate is collected in a glass bottle containing cyclohexane allowing for extraction of the PAHs from the column eluate and finally determination of the outflow concentrations by GC MS analysis. The solution in the equilibrium test (Fig. 1b) is deoxygenated by N_2 before starting the experiment. Flow rate and packing of the column is similar to the maximal flux test, and all materials are kept in stainless steel and glass. The PAH concentration in the column eluate is determined by cyclohexane extraction and GC MS analysis at the end of the experiment. In the batch test, the concentration of the PAHs were determined by a solid phase extraction technique followed by GC MS analysis.

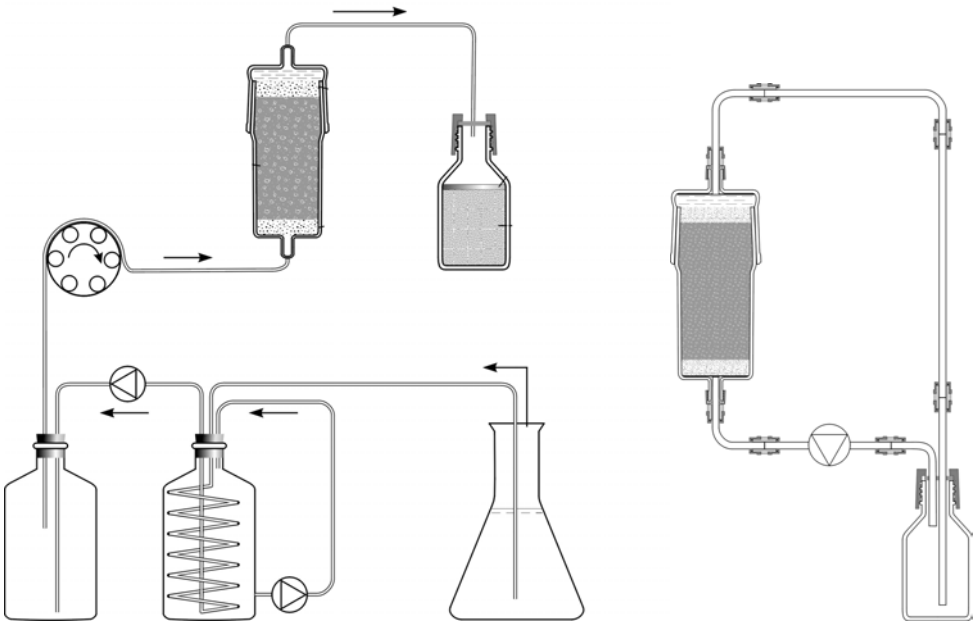

(a) (b)

Figure 1. Column leaching tests used in this study; (a) maximal flux test and (b) equilibrium test.

Results and discussion

The principle of the maximal flux test is, that by maintaining a relative high pore water velocity in the column, the system are supposedly operated far from equilibrium conditions, allowing for determination of the maximal release (desorption) rates of PAHs from the soil. In the equilibrium test similar pore water velocities are maintained in the columns, but the leachate from the column is recycled, allowing for determination of an "equilibrium" pore water concentration in the contaminated soil. Another assumption in the equilibrium test is, that self-filtration of particles and colloids in the column creates an almost realistic scenario, compared to e.g. a batch test.

The maximal flux test where evaluated using four columns in order to determine the release rates of the PAHs and to determine the repeatability of the leaching test. Figure 2 shows examples from this maximal flux test where the concentration of flouranthene and benzo(a)pyrene are shown as a function of L/S. Also shown are error bars representing the standard deviations. Except from a few single point observations, the observed standard deviations are very satisfactory. Effluent concentrations of the two PAHs decrease with increasing L/S, indicating that the system is not in an equilibrium stadium. In the first water sample taken from the effluent there were a significantly higher turbidity and total organic carbon (TOC) content (results not shown), indicating that the colloid/particle content of the effluent would be higher in these samples. However, the measured PAH-concentration was comparable to the other samples, indicating that the initial released colloids and particles did not contribute significantly to the apparent desorption rates of PAHs from this soil.

The equilibrium test was evaluated at different contact times. Figure 2 shows concentration of flouranthene and benzo(a)pyrene as a function of contact time. The concentration of these PAHs increases up to a contact time of approximately 7 days, indicating that equilibrium conditions are reached in the system. The system (glass column and stainless stell tubes) were rinsed with cyclohexane, analysis of the cyclohexane showed that some flouranthene (<10% by mass) adsorbed to the test materials and no benzo(a)pyrene could be determined. Turbidity and total organic carbon (TOC) content (results not shown) were almost similar and constant at all contact times and comparable to the first water sample in the maximal flux test, indicating that the colloid/particle concentration is comparable in these two tests.

The batch test was evaluated at different contact times and on Fig. 2 is shown concentration of flouranthene and benzo(a)pyrene as a function of contact time. The concentration of the two PAHs increases with increasing contact time and apparent equilibrium has not been reached in the system after 14 days of contact time. Turbidity increases with increasing contact time and where an order of magnitude higher than in the equilibrium tests, while total organic carbon (TOC) content (results not shown) where almost constant at all contact times and comparable to the equilibrium tests.

Comparison of the results from the two column tests shows, that the determined concentration levels of the two PAHs shown in Figure 2 are comparable. The concentration measured in the equilibrium test is higher, which is expected due to the longer contact time between solute and soil particles. However, the small concentration difference between the two column tests does indicate that the maximal flux system is not operated as far from equilibrium as intrinsically assumed in the test. The results also show that the equilibrium test appears to be a reliable test to determine an apparent equilibrium relationship between solute and soil particles.

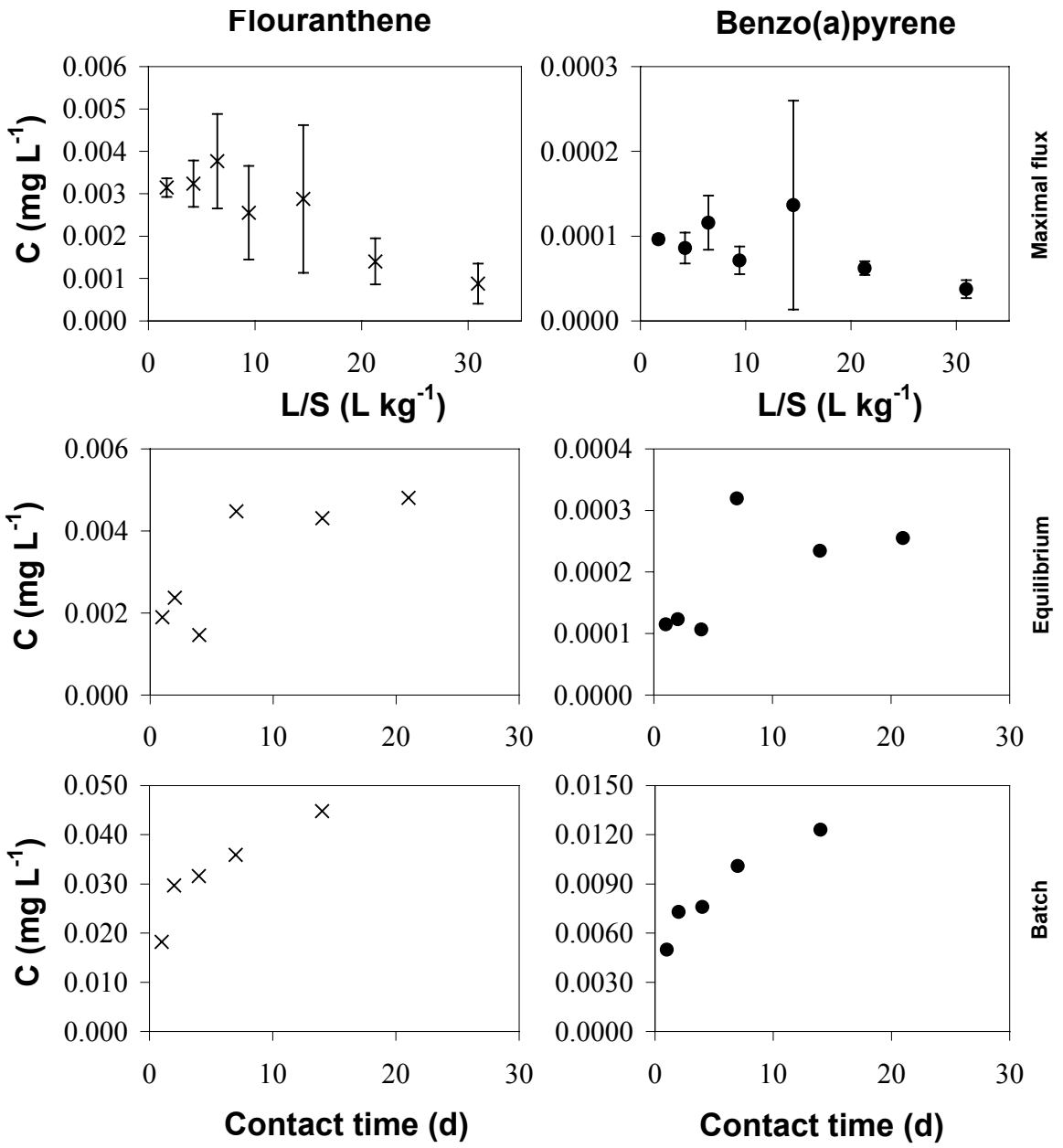

Figure 2. Concentration of flouranthene and benzo(a)pyrene determined in a soil from a former manufacturing gas plant in; the maximal flux test as a function of L/S, the equilibrium test as a function of contact time and the batch test as a function of contact time. Results from the maximal flux test are based on four column tests (indicating by the bars), while results from the batch and equilibrium tests are single-points.

The PAH concentrations measured in the batch test are more than an order of magnitude higher than determined in both column tests. This indicates that the physical affection of the soil particles caused by the shaking and rotating procedures in the batch test may result in colloid facilitated release of PAHs and consequently an overestimation of the solute PAH concentration for this soil. It is interesting that the significantly higher PAH concentrations determined in the batch tests only can be explained by a significantly higher turbidity of the solute, because the TOC level is comparable to the equilibrium and maximal flux tests. These results does though indicate that a larger fraction of the colloids must be separated from the

solute phase in the batch test in order to obtain results for the PAHs that are comparable to the column test.

The three different leaching tests were conducted on additionally four Danish soils. These leaching tests showed, the same pattern; that the maximal flux system is not operated as far from equilibrium in Danish soils as intrinsically assumed in the test and that the PAH concentration levels determined in the batch test were significantly higher than in the column tests.

Preliminary conclusions

The maximal flux test is a repeatable and reliable test for determination of release of PAHs from a contaminated soil. However, it is difficult to determine whether the system is operated far from equilibrium. The equilibrium test may be a good and reliable tool to determine this.

The equilibrium test is a reliable and repeatable test for determination of an apparent equilibrium between solute and soil particles.

The batch test must be used very carefully when determining leaching of PAH's because the physical affection of the soil supposedly results in colloid/particle facilitated release of the PAHs. It must though be noted, that for less hydrophobic compounds, leaching tests conducted on different soils have shown that results from the batch test are comparable to results obtained from the equilibrium test (results not shown).

References

Arcangeli, J.P. og E. Arvin. A membrane de-oxygenator for the study of anoxic processes, Water Resources 29:2220-2222, 1995.

Weiß, Hansjørg. Säülenversuche zur gefahrenbeurteilung für das grundwasser an PAK-kontaminierten standorten. Ph.D. dissertation and der Geowissenschaftlichen Fakultät der Universität Tübingen. 1998.

Hydraulically regulated alcohol circulation using a groundwater-circulation-well (GCW) for a precise in-situ remediation

K. Heinrich[1], U. Mohrlok[2]

[1]*Corresponding author: Institute for Hydromechanics (IfH), University of Karlsruhe, Kaiserstr. 12, D-76128 Karlsruhe, +49 (0)721 / 6087793, +49 (0)721 / 606180; heinrich@ifh.uka.de*
[2]*Institute for Hydromechanics (IfH), University of Karlsruhe, Kaiserstr. 12, D-76128 Karlsruhe*

Abstract: At the Institute for Hydromechanics (IfH), University of Karlsruhe, two dimensional experiments are conducted using a Groundwater-Circulation-Well (GCW) to analyse water and alcohol circulations. The aim of this research is the development of hydraulically regulated simultaneous circulation of water and alcohol in the saturated zone for a precise in-situ remediation. Therefore the circulation has to be defined by a specific form of potential lines with corresponding streamlines which have to be preserved even if alcohol is circulating. The specific construction of the infiltration and exfiltration area, each with moveable plates inside, enables the replacement of a distinct part of the water circulation by an alcohol circulation. In the area of alcohol circulation the hydraulic conductivity k_f is lower because of the higher kinematic viscosity ν_{alc} of the alcohol compared to the water. The alcohol flux then has to be reduced by the ratio of the kinematic viscosities of alcohol to water in order to conserve the specific form of potential lines with the corresponding streamlines. This hydraulically regulated simultaneous circulation of water and alcohol was proved in experiments.

1. Experimental setup

The experimental setup consists of a flume with two dimensional character (h = 1256 mm, w = 3168 mm >> d = 250 mm) filled homogeneously with a grainy sand mixture (n ≈ 0.33; $k_{f,water} \approx 1.5*10^{-2}$ m/s). There are 68 sampling ports for the determination of the groundwater flow and transport, where piezometric levels could be measured, and tracers as Uranin and alcohol could be sampled. The infiltration and exfiltration unit of the groundwater circulation well (GCW) consists of two stainless steel boxes, each with a total filter area of h = 303 mm, d = 250 mm and two moveable plates inside. The circulation then consists of an inner, a middle and an outer circulation area, each with corresponding compartments inside the infiltration and exfiltration unit (Fig. 1). This construction allows a precise injection of alcohol.

The piezometric level could be measured in each compartment of the filter units. The flow rate is regulated by valves in each compartment of the infiltration unit. At the exfiltration unit the potential in each compartment is regulated by height adjustable constant head reservoirs.

This setup provides a high flexibility to developing the technology of hydraulically regulated simultaneous circulation of water and alcohol in the saturated zone for a precise in-situ remediation.

2. Basic principles

For the precise alcohol injection for in-situ remediation, it is necessary to define the positions of the separating streamlines of the streamtube passing the contamination. These streamlines are defined by the positions of the movable plates inside the filter units (Fig. 1). The numerical models MODFLOW/MODPATH were used to determine these positions in the case of a predefined contamination. To be more precise, a water circulation of the GCW was

simulated and the pathlines of the particles set at the infiltration filter were calculated. Moreover the simulated water circulation was defined with constant heads at each filter. Such a water circulation could be described as a shear flow without "cross gradients" with a flow perpendicular to the filters. In this case there is no exchange across the separating streamlines (Fig. 1). This is important because the alcohol used here is a mixture which would segregate when too much water is added and its compounds could not be controlled hydraulically.

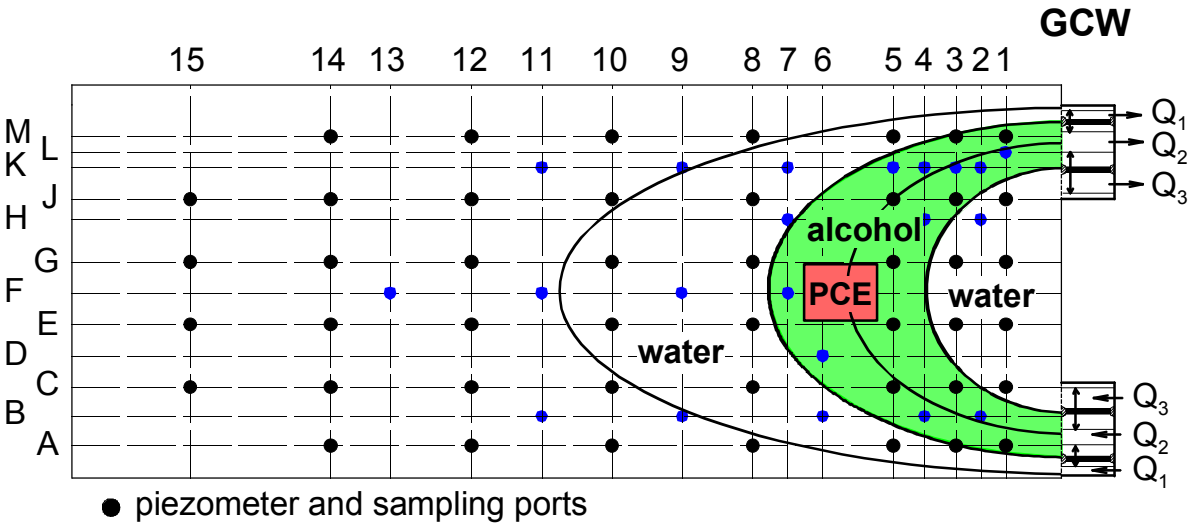

Figure 1:Experimental set-up of two dimensional experiments (schematic).

The defined water circulation shows a specific form of potential lines with corresponding streamlines which have to be preserved when water is subtituted by alcohol in the whole middle circulation area (Fig. 1). In the part of the alcohol circulation the hydraulic conductivity $k_f = k_{f,alc}$ is about 4.5 times lower than in the parts of the water circulation (Fig. 1) due to the kinematic viscosity ν_{alc} of alcohol which is about 4.5 times greater than the kinematic viscosity ν_{water} of water. Without a hydraulic regulation the change of hydraulic conductivity k_f would strongly affect the potential conditions and the streamlines. In order to preserve the streamlines, in the middle compartment of the infiltration unit, the flux of alcohol has to be reduced by the ratio of the kinematic viscosities $\nu_{alc}/\nu_{water} \approx 4.5$ (=> $Q_{2,alc} = Q_{2,water}/4.5$). In this case the water/alcohol circulation is in a steady state.

3. Results

The experimental concept includes several experiments like the visualization of pure water and water/alcohol circulation and Uranin tracer tests.

Figure 2 shows snap shots of a water/alcohol circulation experiment (Fig. 2a) and a pure water circulation (Fig. 2b) where the middle part of the circulation was colored with food coloring (darker area). While the alcohol was injected ($t_{alc,in}$ = 22.5 min, $Q_{2,alc}$ = 34.8 l/h = $Q_{2,water}/4.5$) the flow rate in the middle compartment of the infiltration unit was reduced by the ratio of the kinematic viscosities ν_{alc}/ν_{water} (Fig. 2a). The shapes of the circulations are similar which proves that the streamlines of both circulations are similar as well.

Figure 3 shows measurements of the piezometric level of the same water/alcohol circulation experiment. The three maps illustrate that the shapes of the potential lines before, during and after the alcohol injection were the same. This identical shape of the potential lines at any point proves the hydraulically regulated simultaneous water/alcohol circulation. It means that the streamlines are fixed and the flow of alcohol is controlled hydraulically.

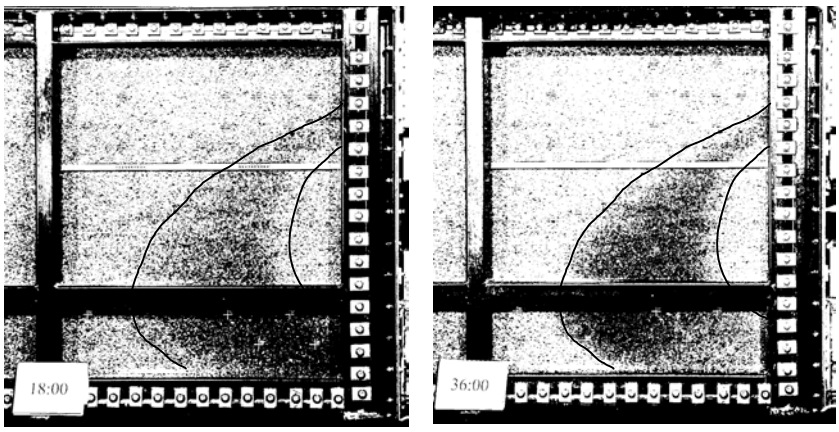

a) water/alcohol *b) water*

Figure 2: The middle circulation area was colored. a) simultaneous water/alcohol circulation, b) pure water circulation. The colored part of the circulation is emphasized by black lines.

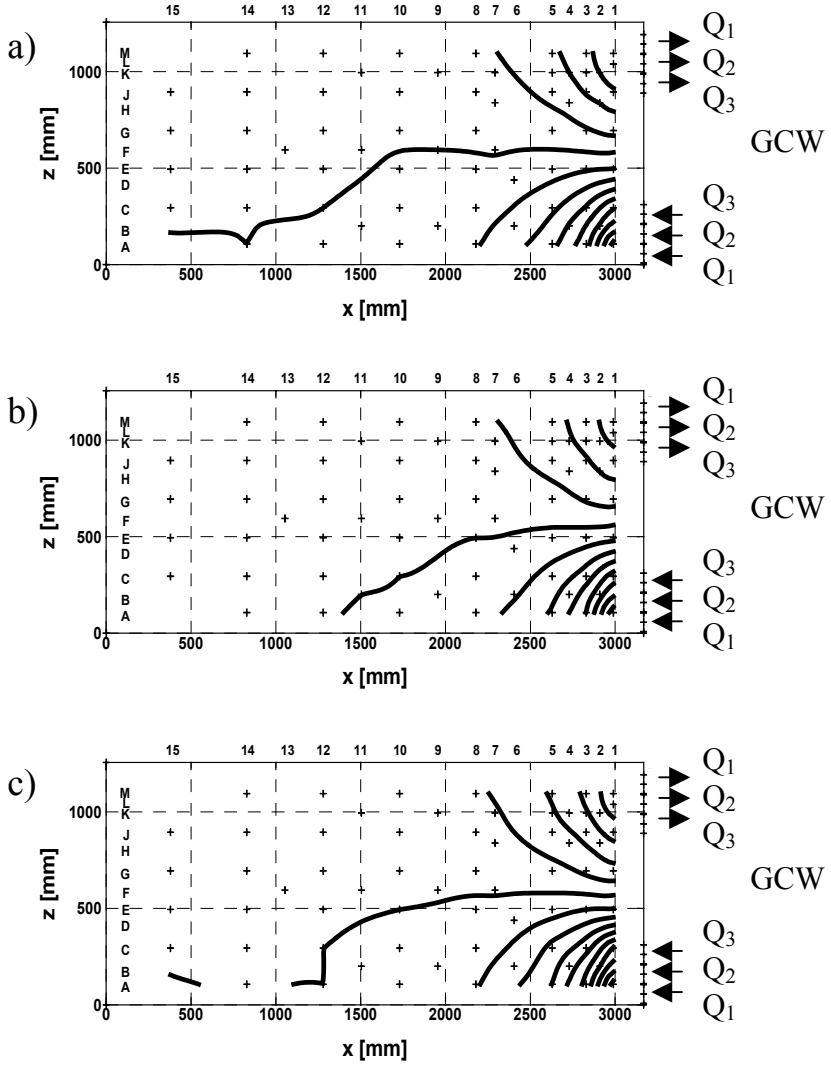

Figure 3: Measurements of the piezometric levels showing the same shape: a) before, b) during and c) after alcohol injection.

Relating soil physical and chemical properties to sorption and mobility of polar and nonpolar contaminants in soils

H. de Jonge[1], R. Celis[2], L.W. de Jonge[1], J. Cornejo[2]

[1]*Corresponding author: Danish Institute of Agricultural Sciences, Dept. of Crop Physiology and Soil Science, Research Centre Foulum, Blichers Allé 20, 8830 Tjele, Denmark, Phone: +45 89991758, Fax: +45 89991719, E-Mail: Hubert.deJonge@agrsci.dk*
[2]*Institute for Natural Resources and Agrobiology of Seville, CSIC. Avda Reina Mercedes 10, Apdo 1052; 41080 Sevilla, Spain.*

Abstract: Sorption, desorption and leaching are key processes determining the bioavailability of organic pollutants in soil and dispersion of pollution to ground water. Identification of parameters controlling sorption and mobility of organic pollutants in soil is crucial to improve assessment of ecological risk and to select the most suitable remediation technologies. As part of a recently started EU project, in this work we present preliminary results of sorption and leaching experiments designed to elucidate key physical and chemical properties affecting the bioavailability of organic pollutants in soil. Soils from different edafoclimatic regions of Europe and chemicals with different structural characteristics were selected. Relevant soil characteristics were determined and relationships between sorption/leaching behaviour and the characteristics of the soils and organic compounds were investigated.

1. Introduction

Tools for ranking contaminated sites according to risks and prioritisation of clean up measures for brown field redevelopment need to be established. The newly started EU project *Liberation* aims to provide a decision support system for management of contaminated land, based on biological and chemical tools, to decide whether pollutants from a contaminated site or landfill are available for ground water contamination or pose a risk for soil and freshwater organisms. The present work reports preliminary results on sorption, desorption and leaching of contaminants of different polarity for a range of soils and reference materials. The aim of this work is to elucidate key-physical and chemical properties affecting the behaviour of the compounds under investigation.

Selected contaminants include PAHs (phenanthrene, pyrene), PAH metabolites (salicylic acid, phthalic acid), and heterocyclic-aromatic compounds (dibenzofuran). Reference soils were selected across Europe, and clay fractions (< 2 μm) were purified. In addition, single, binary and ternary model particles containing montmorillonite, ferrihydrite and humic acid were synthesised. The soils and model materials are thoroughly characterised, including standard soil physical/chemical properties, surface area, elemental analysis, infrared spectroscopy, X-ray diffraction and Hg-porosimetry measurements. Sorption, desorption and leaching experiments are carried out using traditional batch analysis, and isotope-exchange, spiking/desorption and column leaching experiments. Preliminary results will be presented here including soil characterisation, and batch, leaching and isotope-exchange experiments.

2. Soil materials

A range of six non-contaminated soils from across Europe were selected (Table 1). The soils were collected, air-dried, sieved over 2 mm, homogenised and stored at room temperature until use.

Table 1. Available data from soil characterisation and isotope-exchange experiments.

	Askov	Borris2	Flakke-bjerg	IFA	Ket-tering	P2
Land of origin	DK	DK	DK	AU	GB	SP
pH ($CaCl_2$)	6.3	6.4	7.1	7.7	6.7	7.9[1]
pH (H_2O)	7.0	6.7	7.5	8.4	6.9	
CEC (Ca^{2+}, meq/100g)	9.70		16.46	0		
CEC (K^+, meq/100g)	0.30		0.39	0		
CEC (Mg^{2+}, meq/100g)	0.48		0.69	0		
CEC (Na^+, meq/100g)	0.12		0.27	17.4		
CEC (total, meq/100g)	10.6		17.81	17.4		9.0[1]
Organic C (g/100 g)	1.39	1.63	1.25	1.84	2.09	0.40[1]
Inorganic C (as $CaCO_3$, g/100g)	n.d.	n.d.	n.d.	0.61	n.d.	
Total C (g/100 g)	1.39	1.67	1.25	2.45	2.13	
Coarse sand 200-2000 μm (g/100g)	39.7	30.3	12.2	7.2	34.0	
Fine sand 50-200 μm (g/100g)	28.7	39.5	29.4	23.8	13.2	
Coarse silt 20-50 μm (g/100g)	9.2	11.4	11.3	19.8	10.2	
Fine silt 2-20 μm (g/100g)	9.6	9.1	24.8	16.3	14.5	
Clay <2 μm (g/100g)	10.4	6.9	20.2	24.7	24.5	20.0[1]
Organic matter (g/100 g)	2.4	2.8	2.1	3.1	3.6	
Surface Area (EGME, m^2/g)	17.4	10.4	37.0	39.1	52.3	
Phenanthrene distrib. coeff. (L/kg)	210	238	154	115		29
Koc	15100	14600	12400	6250		7150
Phenanthrene irreversibly sorbed (-)	0.28	0.31	0.22	0.18		0.05

[1]provisionary results from another batch of soil then used in the present study

The clay (< 2 μm) fraction of 4 reference soils (Borris2, Askov, Kettering and P2) was purified by sedimentation, after carbonate elimination. Clay fractions were saturated with Ca^{2+} by 3 successive treatments with 1 N $CaCl_2$, washed with deionised, and then freeze-dried.

Model soil particles were prepared following the procedure described by Celis et al. (1998). Sodium-Wyoming montmorillonite, freshly-precipitated ferrihydrite and soil-extracted humic acid were used as starting materials. Montmorillonite-ferrihydrite binary particles were prepared by Fe(III) precipitation in the presence of montmorillonite particles, whereas montmorillonite-humic acid and ferrihydrite-humic acid binary particles were prepared by shaking of dissolved humic acid in the presence of montmorillonite or ferrihydrite. Ternary particles were obtained by shaking dissolved humic acid in the presence of a binary montmorillonite-ferrihydrite complex. All solids were dialysed to remove excess of salts and freeze-dried prior to use.

3. Results and Discussion

3.1 Characterisation

Table 1 summarises the main physical and chemical features of the selected soils. It shows a broad range in soil texture, surface area and counter-ion composition. However, all soils have rather similar organic carbon (OC) contents, excluding the Spanish P2 soil that is poor in OC. The soil database will be extended in the second year of the project to include more high-organic matter content soils.

Table 2. Characteristics of the model particles and sorption coefficients for dibenzofuran†.

	Sorbent	Sorbent composition			Kd	Koc	pH	SSA
		SW	Ferrih	HA				
		——— % ———						m^2/g^{-1}
Single model sorbents	SW	100	0	0	14 ± 6	-	7.0	25
	Ferrih	0	100	0	4 ± 4	-	5.8	346
	HA	0	0	100	2731 ± 224	5160	2.3	< 1
Binary associations	SW-Ferrih$_0$	100	0	0	116 ± 3	-	6.3	25
	SW-Ferrih$_8$	92.7	7.3	0	36 ± 8	-	4.7	58
	SW-Ferrih$_{16}$	86.3	13.7	0	35 ± 8	-	4.8	83
	SW-HA$_0$	100	0	0	19 ± 2	-	6.5	43
	SW-HA$_4$	95.7	0	4.3	98 ± 9	4340	5.2	4
	SW-HA$_8$	93.3	0	6.7	140 ± 15	3960	5.2	3
	Ferrih-HA$_0$	0	100	0	4 ± 4	-	6.6	348
	Ferrih-HA$_4$	0	96.3	3.7	47 ± 8	2370	6.0	334
	Ferrih-HA$_8$	0	93.1	6.9	88 ± 4	2400	6.4	290
Ternary associations	SW-Ferrih-HA$_0$	85.2	14.8	0	64 ± 14	-	5.2	82
	SW-Ferrih-HA$_4$	82.5	14.6	2.9	91 ± 7	5910	5.8	57
	SW-Ferrih-HA$_8$	81.0	13.5	5.5	172 ± 35	5850	5.3	32

† SW: Wyoming montmorillonite; Ferrih: ferrihydrite; HA: humic acid; Kd: distribution coefficient; Koc: organic carbon-normalised Kd value; SSA: N_2-specific surface area..

The amount of clay recovered from the soils increased in the following order: Borris2 < Askov < Kettering = P2. Results of elemental analysis of the soil clays revealed that the OC content was inversely related to the clay content: Borris2 (24%) > Askov (6%) > Kettering (3%) > P2 (1%). The high OC content of the clay fraction of Borris2 soil should be noted; about 50% of this clay corresponds to organic matter. X-ray diffractograms of the soil clays revealed that the clay mineral content of Borris2 soil was very low; just traces of kaolinite and illite/mica were identified. Montmorillonite and kaolinite predominated in P2 and Kettering soil, respectively. Askov soil had the most heterogeneous clay fraction, containing significant amounts of kaolinite, illite/mica and montmorillonite/vermiculite displaying some resistance to swelling.

Some characteristics of the model particles prepared are given in Table 2. Characterisation of the model particles revealed that the properties of the binary and ternary model colloids were not the simple sum of their individual constituents, suggesting that the inter-association processes could greatly influence the sorptive behaviour of complex soil colloids. In particular, the humic acid displayed a great affinity for ferrihydrite and low affinity for montmorillonite. It is reasonable to hypothesise that ferrihydrite-bound humic acid may display sorptive properties different from those of free humic acid. Thus, the model particles will help investigate the role of the main active soil components in contaminant sorption, not only as individual constituents, but also when associated in complex particles.

Table 3 shows the pore volumes for different pore size ranges for reference soils measured by mercury intrusion porosimetry. Interestingly, Borris2, Askov and Kettering soils had very different pores size distributions; the volume of smaller pores increased in the following order: Borris2 < Askov < Kettering. The Spanish P2 soil had an intermediate pore size distribution. Because of their different pore structures, the soils selected appear good candidates to investigate the effect of soil porosity on contaminant bioavailability.

Table 3. Porosity characterisation of four reference soils by Hg intrusion porosimetry. Volume of pores (mm^3/g) for different pore size ranges.

SOIL	$r_p > 10$ µm	$10 > r_p > 0.1$ µm	$r_p < 0.1$ µm
BORRIS2	**67 ± 3**	56 ± 3	5 ± 1
ASKOV	26 ± 4	**106 ± 3**	16 ± 2
KETTERING	22 ± 1	71 ± 4	**54 ± 1**
P2	**75 ± 1**	44 ± 4	21 ± 2

3.2 Batch sorption experiments

Figure 1 shows that the isotherms of Askov, Borris and Kettering adsorbing phenanthrene are almost identical, despite the differences in their textural composition, organic matter, surface area (Table 1), and pore size distribution (Table 3). IFA and Flakkebjerg soils adsorb considerably less, which only for Flakkebjerg may be explained by a lower OC content. The unique difference of the IFA soil in relation to the other soils is the presence of carbonates and CEC saturation with sodium (Table 1). This may have an effect on physico-chemical state of the soil colloids, and may explain the lower sorption affinity for phenanthrene.

Isotopic exchange experiments with phenanthrene (Table 1, method after Celis and Koskinen, 1999) confirm the trend of the sorption isotherms. In this study, the P2 soil was also concluded. Clearly, this soil has the lowest sorption affinity for phenanthrene of all the investigated soils. K_{oc} values vary considerably, but are within one order of magnitude. Interestingly, the lowest K_{oc} values are found for the soil with the highest pH.

Sorption of dibenzofuran to single model sorbents (Table 2) clearly showed preferential sorption of this chemical to the humic acid, as was expected. Interestingly, the K_{oc} values in binary associations are reduced by the interaction with the clay mineral and especially with ferrihydrite. In contrast, the K_{oc} values for the ternary associations are higher than that measured for pure humic acid. So, there is a complex feedback of interaction between mineral and organic model particles on the sorption of dibenzofuran, and it is not possible to predict the sorption of binary and ternary associations as the simple sum of their individual constituents.

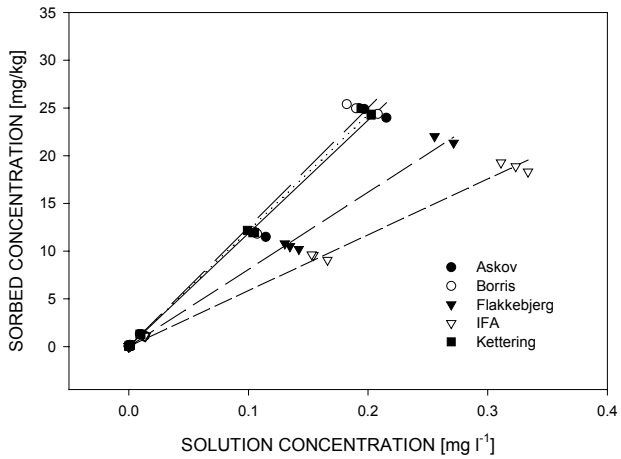

Figure 1: Sorption isotherms of phenanthrene to five reference soils.

3.3 Column leaching experiment

Leaching profiles for phthalic acid, salicylic acid, and dibenzofuran in hand-packed soil columns (20 cm-long x 3 cm i.d. glass columns filled with Spanish P2 soil) are shown in Figure 2. Phthalic acid, and to a lesser extent salicylic acid, rapidly moved through the soil column. In contrast, no dibenzofuran was detected in the leachates even after application of 300 mL of water, which corresponds to a cumulative rainfall of 400 mm. It is interesting to note that very little phthalic and salicylic acid were extracted from the soil columns at the end of the leaching experiment, whereas dibenzofuran accumulated in the top 0-5 cm of soil. These results suggest little risk of vertical movement through matrix flow mechanisms for highly sorbed, hydrophobic compounds, such as dibenzofuran, even in soils with relatively low retention capacities such as the Mediterranean P2 soil used in our study. In contrast, the great leaching of anionic compounds observed in this preliminary experiment deserves further investigation.

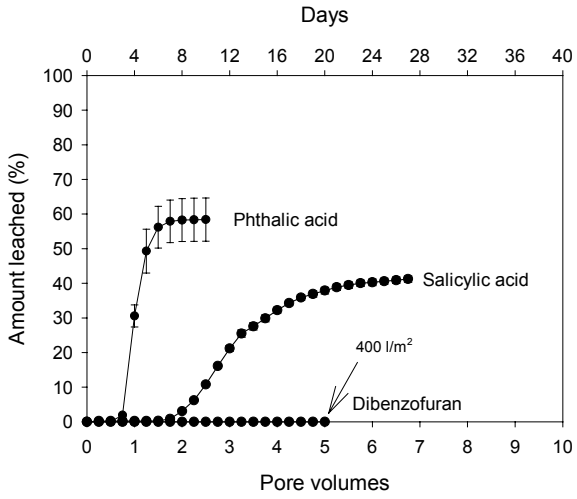

Figure 2: Breakthrough curves (BTCs) of phthalic acid, salicylic acid, and dibenzofuran in hand-packed soil columns (Mediterranean P2 soil).

4. Conclusion

A broad range of soils, soil clays, and model particles were collected and characterised according to their chemical and physical properties. The preliminary results presented here do suggest that sorption affinity of such diverse soil materials for phenanthrene cannot be simply predicted with single soil parameters such as organic carbon or clay content. Sorption effects with model particles show the complex feedback of mineral-humic associations towards sorption of dibenzofuran. Solute transport in a low-organic carbon Spanish soil was clearly controlled by the solute polarity.

5. Acknowledgement: This work has been supported by the FP5 EU project EVK1-CT-2001-00105 (LIBERATION) [http://www.liberation.dk].

6. References

1. Celis R., Cornejo J., Hermosín M.C., Koskinen W.C. 1998. Soil Sci. Soc. Am. J. 62, 165-171.
2. Celis R., Koskinen W.C. 1999. J. Agric. Food Chem. 47, 782-790.

Pollutant leaching from demolition waste

Kalbe, Ute; Eckardt, Jürgen; Berger, Wolfgang; Christoph, Gabriele; Grabner, Angela

[1] *Federal Institute for Materials Research and Testing (BAM),*
Unter den Eichen 87, 12205 Berlin, Phone: ++49 30 81043862, Fax: ++49 30 81041437,
e-mail: ute.kalbe@bam.de

Abstract: The assessment procedure for the soil-groundwater pathway has changed following the introduction of the German Ordinance on Soil Protection and Contaminated Sites (Bundes-Bodenschutz- und Altlastenverordnung, BBodSchV). Transfer of pollutants to the groundwater can be estimated by a leachate forecast procedure using in-situ investigations or laboratory tests. This study contributes to the investigation of the leaching behaviour of PAH and sulfate from demolition waste by using laboratory leaching experiments (multiple-stage batch tests, column tests). While the sulfate contents decreased continuously (column test) or relatively rapid (multiple-stage batch tests), the PAH contents remained relatively constant throughout the experiment.

1. Introduction

In Germany, demolition waste is being increasingly reused, however pollutants contained in them may affect the potential of reuse. In order to clear their applicability the leaching behaviour with respect to groundwater compatibility must be evaluated, especially when demolition waste is disposed of on the ground.

Since the passing of the German Ordinance on Soil Protection and Contaminated Sites (Bundes-Bodenschutz- und Altlastenverordnung) [1] risk assessment of the soil - groundwater pathway can be performed by a leachate forecast. The estimation of pollutants transfer to the groundwater can be performed using in-situ investigations or laboratory tests (column experiments, batch tests).

The study presented here is a contribution to the investigation of the leaching behaviour by using different leaching experiments.

2. Materials and Methods

The demolition waste material investigated in this study contains different parts of crushed concrete, bricks, asphalt and gypsum. Only the grain size fraction < 4 mm (demolition debris fines) was examined.

Further parameters of demolition waste solid material are:

- pH-value (H_2O) approx. 12,
- carbonate content approx. 5 % by weight,
- water permeability approx. 4×10^{-6} m/s.

Characteristic pollutants are PAH, MHC, phenole, sulfate and traces of heavy metals. Apart from sulfates no other anions are present in significant quantities in any of the eluates.

In order to characterise the leaching behaviour of this demolition waste material, different leaching tests were performed:

- Column tests with an experimental set-up in accordance with DIN V 19736 [2]

- Multiple-stage batch leaching tests with a liquid / solid ratio of 2 : 1 (2 l/ kg) per E DIN EN 12457-1 [3]

Column tests were performed with glass columns of approx. 615 cm³ total filling volume (6 cm in diameter and 20 cm in length). Ascending percolation with de-ionised water was applied. The flow rate was nearly 0.8 ml/min. The pore volume was determined by weighing before and after placing the sample into the column. The sample masses used averaged 540 g.

In this study the pollutants PAH and sulfate were only considered. In addition, parameters pH, DOC, turbidity and conductivity were determined in the eluates.

PAH-compounds in the eluates were measured by HPLC according to DIN 38 407 - 18 [4].

Sulfate concentration in the eluates was analysed by anion chromatography according to EN ISO 10304-2 [5].

3. Results

The presence of PAH in the demolition waste material results from the contained asphalt component of road construction material. Figure 1 presents the results of the column tests for PAH (sum PAH, acenaphthene, phenanthrene, fluoranthene). The sum of PAH in the eluates was found to be approx. 50 µg/l. The pattern of PAH substances found in the eluates of the column tests is similar to that obtained from the batch leaching (2 l/ kg). The order of magnitude of the quantity of water per mass of sample and the contact time water/sample for the column tests on the first day and the batch leaching test were similar.

However, the results of the both tests are not directly comparable due to the different preparation steps of the eluates. As currently running tests show, a decrease in flow rate and a simultaneous increase in contact time do not result in substantially different PAH elution at the same number of replaced pore volumes. The eluted quantity of PAH can be taken from Figure 1 after up to 70 exchanged pore volumes. That corresponds to a mere small fraction of PAH in the solid samples of demolition waste, which means that the PAH leaching process is not completed yet.

The simultaneous batch and column tests accomplished on the same demolition waste material show satisfactory reproducibility of the results. An averaged relative standard deviation of 7 % regarding the PAH sum resulted for example from three repetitions accomplished at the same time.

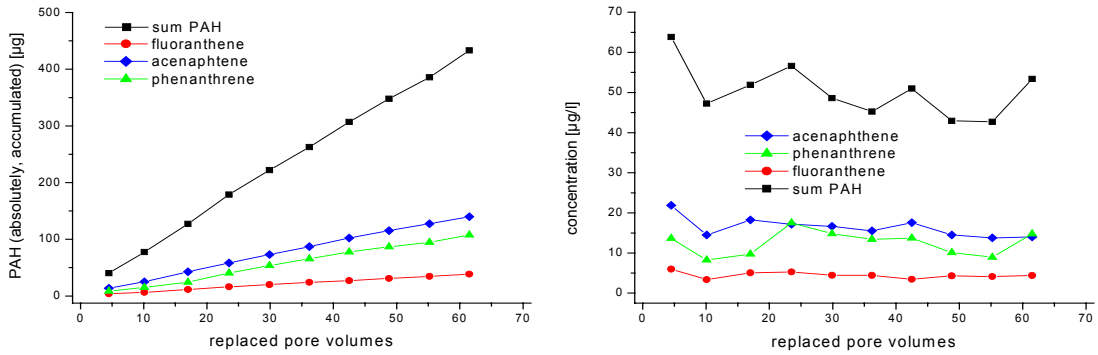

Figure 1: Example of column tests on the demolition waste investigated

The source of sulfate in the demolition waste eluates was gypsum dissolution.

High sulfate concentration was found in the batch test eluates (2 l/ kg) and it exceeds water solubility of gypsum.

The sulfate content leaching from debris fines decreased during the column experiments continuously. After approx. 70 replaced pore volumes within the column tests the sulfate concentration was reduced by approx. 90 % (Fig. 2). In this period a quantity of approx.12 g dissolved $CaSO_4$ per kg building debris was calculated.

In comparison to the column tests decreases the sulfate content in the eluates within the multiple-stage batch tests more rapidly.

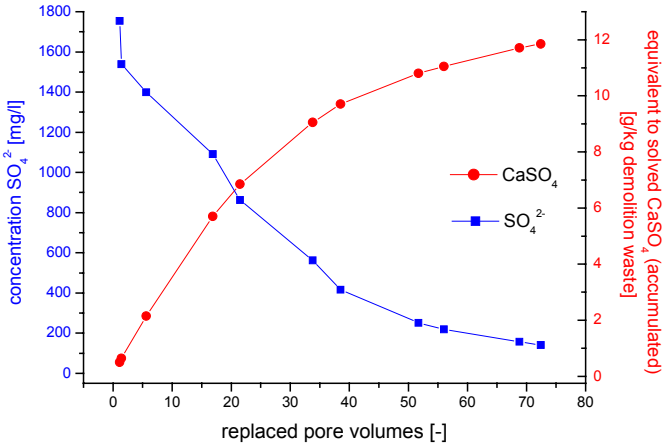

Figure 2: Results from a column test with demolition waste regarding sulfate

In addition, the measured parameters pH-value, conductivity, turbidity and DOC are presented in Figure 3 for the column tests eluates.

The pH-values of all eluates collected in the batch and column tests were alkaline between 12 and 13 (see Fig. 3). During column elutions the pH-value was somewhat reduced, which corresponds to the decrease in conductivity and may be attributed to the reduction of sulfate concentration. DOC content in the column eluate samples decreased considerably even during the replacement of 15 pore volumes to a relatively constant low level. (Fig 3).

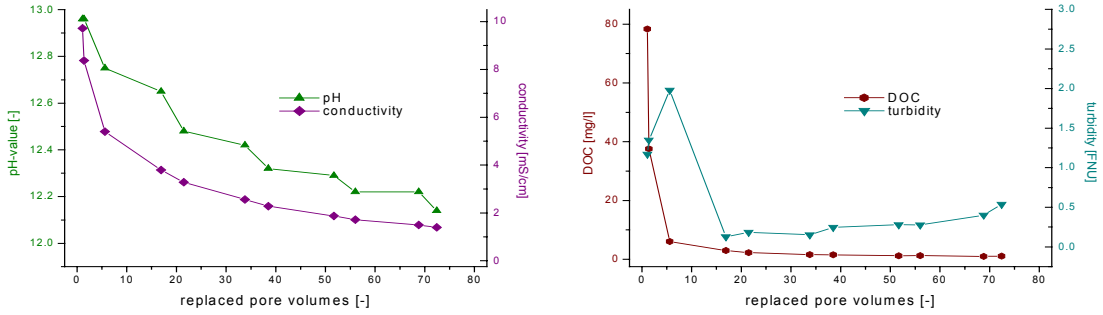

Figure 3: pH-values, conductivity, DOC-content and turbidity in a column test on demolition waste

4. Conclusions

PAH elution is still not completed after approximately 70 replaced pore volumes in column tests on the demolition waste investigated.

At the same stage of the column experiments the sulfate concentration was strongly reduced but could be eluted further in small rates. With the help of the multiple-stage batch tests the sulfate content decreases still faster. This results are comparable with other investigations on the leaching behaviour of demolition waste found in literature [6].

Sulfate concentrations greater than solubility limit due to gypsum dissolution were measured in the eluates in both batch and column tests. This indicates that different other factors had influenced the leaching behaviour.

Multiple-stage batch tests are suitable to obtain the total elutable amount of difficultly soluble pollutants in relatively short time.

Column elution offers the benefit that elutable amounts and changes in physical-chemical parameters can simultaneously be determined. This provides important information on the leachate forecast of contaminants under the specific boundary conditions.

5. References

[1] Bundes-Bodenschutz- und Altlastenverordnung (BBodSchV) BGBl. I, 1554ff (16.07.1999).

[2] DIN V 19736: 10.98: Ableitung von Konzentrationen organischer Stoffe im Bodenwasser.

[3] E DIN EN 12457-1:02.00: Charakterisierung von Abfällen, Eluierung - Deklarationstest für die Auslaugung von körnigen Abfällen und Schlämmen. Teil 1: Einstufiges Schüttelverfahren mit einem Flüssigkeits-/Feststoffverhältnis von 2 l/kg und einer Korngröße unter 4 mm (ohne oder mit Korngrößenreduzierung).

[4] DIN 38407 - 18:05.99: Deutsche Einheitsverfahren zur Wasser-, Abwasser- und Schlammuntersuchung - Gemeinsam erfaßbare Stoffgruppen (Gruppe F) - Teil 18: Bestimmung von 15 polycyclischen aromatischen Kohlenwasserstoffen (PAK) durch Hochleistungs-Flüssigkeitschromatographie (HPLC) mit Fluoreszenzdetektion (F 18)

[5] EN ISO 10304-2:11.96: Wasserbeschaffenheit; Bestimmung der gelösten Anionen mittels Ionenchromatographie, Teil 2: Bestimmung von Bromid, Chlorid, Nitrat, Nitrit, Orthophosphat und Sulfat in Abwasser.

[6] JANG, Y.-C. & TOWNSEND, T.(2001): Sulfate leaching from recovered construction and demolition debris fines. – Advances in Environmental Research 5, pp. 203-217.

Material Investigations to determine the leaching behaviour of PAHs at elevated temperatures

Iris Madlener, Rainer Henzler and Peter Grathwohl

Center for Applied Geoscience, Sigwartstr. 10, 72076 Tübingen, Germany;
Phone: +49-7071-2977452, Fax: +49-7071-5059
E-mail: iris.madlener@uni-tuebingen.de

Abstract: The extraction of polycyclic aromatic hydrocarbons (PAHs) from solid environmental matrices has traditionally been done using non-automatic approaches, e.g. Soxhlet extraction. Recent developments focus on using automated techniques like the Accelerated Solvent Extration (ASE) (Dean, 2000). With the ASE it is possible to follow the desorption behaviour of PAHs at different temperatures. Aqueous eluates were produced by extracting materials several times at a pressure of 100 bar and step-wise temperature increases from 25 °C to 100°C. With increasing temperatures the PAHs concentration in the water extract increase exponentially. This relationship can be described by the van´t Hoff equation, if the mass of the sorbed PAHs on the solid material does not decrease significantly, during the leaching test. The van't Hoff equation allows to determine the desorption enthalpy ΔH *and it is possible* to extrapolate to equilibrium concentrations at lower temperatures (e.g. groundwater temperatures).

Introduction

Objective of this study was to investigate how increased temperatures affect the desorption behaviour of polycyclic aromatic hydrocarbons (PAHs) in fine and coarse grained materials. Aqueous leachates were produced with a temperature-programmed automatic Accelerated Solvent Extractor (Dionex, ASE 300). Each sample was leached several times at eight different temperatures from 25 °C up to 100 °C and a constant pressure of 100 bar.
If equilibrium condition occurs, then the aqueous concentration C_w [µg L^{-1}] depends on the contaminant concentration in the solids C_s [µg kg^{-1}] and the sorption distribution coefficient K_d [L kg^{-1}]:

$$C_W = \frac{C_S}{K_d} \qquad [1]$$

If the sorbed concentration of polycyclic aromatic hydrocarbons (PAH) does not decrease significantly during the leaching procedure, then the equilibrium concentration in water is approximately inverse proportional to the equilibrium distribution coefficient K_d [L kg^{-1}]:

$$C_W \sim \frac{1}{K_d} \qquad [2]$$

By increasing the temperature, the polarity of the water decreases (the dielectric constant decreases), and thus the solubility of PAHs increases. In addition increasing temperatures lower the viscosity and the surface tension of water (API 1998, Miller 1998, Johnson 2001). Accordingly the increasing temperatures shift the sorption equilibrium towards the aqueous phase and thus the K_d value decreases. The influence of different temperatures at equilibrium conditions can be described with the van´t Hoff equation:

$$\Delta H = -R \frac{d \ln\left(\frac{1}{K_d}\right)}{d\left(\frac{1}{T}\right)} \quad [3]$$

where ΔH is the desorption enthalpy [kJ mol^{-1}], R the universal gas constant [kJ mol^{-1} k^{-1}], K_d the sorption distribution coefficient [L kg^{-1}] and T the temperature [K].

As shown in equation [2] the term $1/K_d$ can be replaced by C_W and a modified van't Hoff equation can be formulated:

$$\Delta H \approx \frac{d(\ln C_W)}{d\left(\frac{1}{T\ R}\right)} \quad [4]$$

Plotting ln C_W versus $1/(T\ R)$ gives in an ideal case a straight line and the enthalpy ΔH can be determined directly from its slope. If the desorption enthalpy ΔH (slope of the regression line) is known, than it is possible to extrapolate to lower, e.g. in-situ concentrations in the field.

Materials and Methods

Fine and coarse grained materials

Materials which occur in large quantities, like building demolition waste and dredged river sediments were investigated in this study. Representative for these materials following four samples were chosen: *Demolition Waste* (reference material from Bundesanstalt für Materialforschung und –prüfung), *Recycling Demolition Waste* from Mainz (Germany), *Bilbao Harbour Sludge* from Spain and *Iffezheimer Rhine sediment* from Germany.

The demolition waste samples were crushed down to a grain size less than 4 mm. The materials exist of 90 % concrete and rock fragments and the rest consists of slag, wood and asphalt.

The fine grained materials, Bilbao Harbour Sludge from Spain and Iffezheim Rhine sediment from Germany, were dried for several days at 50° C. After drying, they were pulverised to get a homogeneous mixture. For getting a higher permeability, 2/3 of fine grained sediment was mixed with 1/3 of coarse quartz sand.

Accelerated Solvent Extractor (ASE)

Accelerated solvent extraction (ASE) is a relatively new extraction technique (Fig. 1) that uses high temperatures similar to Soxhlet extraction, but applied in addition high pressures up to 100 bar. The ASE allows the extraction to be completed within a short time period and with a relatively small quantity of solvent (Gan 1999). In this study the concentrations of PAHs in water at different temperatures and the concentration in soil were determined.

The schematic function of the ASE is described in detail in Henzler et al. 2002. The solvent is pumped into the sample cell until a pressure of 100 bar is reached. The cell moves in to the oven and is heated until the extraction temperature is reached. After the extraction time the cell is flushed. The leachate is collected in a bottle and prepared for analysis.

Aqueous leaching

The extraction temperature program of the ASE is listed in Table 1. The extraction at 53 °C was performed two times, with a duration of 30 and 99 minutes, respectively if both extracts have nearly the same concentration than equilibrium conditions can be assumed.

Tab. 1: Temperature program of ASE

Extraktion No.	Temperature [°C]	Duration of extraction [min]
1	25	99
2	25	99
3	25	99
4	40	99
5	47	99
6	53	30
7	53	99
8	64	99
9	75	99
10	87	99
11	100	99
12	100	99

Solvent extraction

After aqueous leaching the material was first extracted with acetone at 100 °C and then two times with toluene at 150°C to determine the PAHs concentrations in the solid phase (Tab. 3). Hubert et al (2001) and Hawthorne (2000) showed that toluene at 150°C is a very good solvent for PAHs. Before the toluene extraction the material has to be extracted with acetone in order to remove water from the sample.

Table 3: Extraction parameter of solvent extraction

Extraction No.	Temperature [°C]	Duration of extraction [min]	Solvent
13	100	10	acetone
14	150	10	toluene
15	150	10	toluene

Results and Discussion

In Table 4 the results of the concentrations on the solid phase (C_s) and in water (C_w) at 25 °C are listed for the different materials. For the PAHs the sum of the 16 EPA PAH without Naphthalene (15 EPA PAH) is shown and also the distribution coefficient *Kd*.

Table 4: Results of the water- and solvent extraction with the ASE for the investigated materials.

Material	15 EPA PAH C_s [mg kg^{-1}]	15 EPA PAH C_w at 25 °C [µg L^{-1}]	K_d at 25 °C [L kg^{-1}]
Demolition Waste	***49,9***	***27***	***1850***
Recycling Demolition Waste	***10,2***	***2,2***	***4640***
Bilbao Hafenschlick	**9,6**	0,7	13710
Iffezheimer Rhine sediment	**3,1**	0,1	31000

Fig. 2 shows the concentrations of Phenanthrene (Phe) in water for increasing temperatures for the Bilbao Harbour Sludge. At 25 °C the Phe concentration is only 0.1 µg L^{-1} (close to the detection limit) and at 100 °C thirty times higher (3.0 µg L^{-1}). The comparison of the extraction steps at 53 °C show similar concentrations of 0.4 µg L^{-1} and 0.42 µg L^{-1} after 30 minutes and 99 minutes. This is an indication that equilibrium concentrations exist. Thus water becomes a better solvent for the nonpolar PAHs. Accordingly increasing temperatures cause a decrease in sorption coefficient K_d of the PAHs.

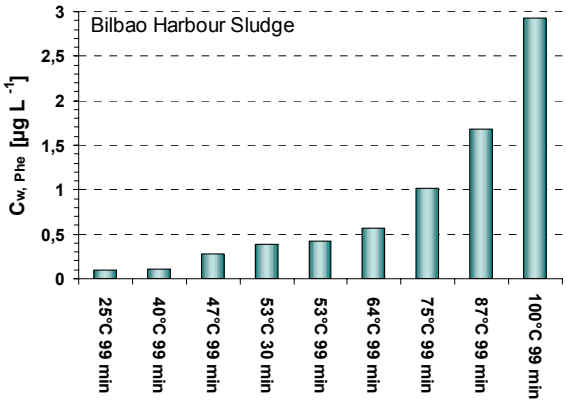

Fig. 2: Phenanthrene (Phe) concentration of the Bilbao Harbour Sludge at increasing temperatures

The increasing PAHs concentrations with increasing temperatures can be described by the van´t Hoff equation (Eq. 4), if the mass of the sorbed PAHs on the solid material (C_S) remains constant during the leaching steps and if equilibrium conditions are established. The slope of the regression is equivalent to the desorption enthalpy ΔH.

The van't Hoff equation fits very well to the results of the investigated materials (Fig. 3 A-D), especially for the 3- and 4-ring PAHs like Phenanthrene and Fluoranthene. For Phenanthrene a desorption enthalpy of the four materials range from –32 kJ mol^{-1} to -58 kJ mol^{-1} and for Fluoranthene from –44 kJ mol^{-1} to –76 kJ mol^{-1}. The investigated materials show, that with increasing molecular weight and hydrophobicity of PAHs the desorption enthalpy increases.

The sorption of the heavier 5 -ring PAHs like Benzo(a)pyrene (Fig. 3-B) is very strong (higher K_d values) and so the concentrations in the aqueous leachate are often near or below the detection limit. At higher temperatures the concentrations for Benzo(a)pyrene are detectable and fit to the van't Hoff equation.

The differences in the desorption enthalpy are probably caused by different sorption properties of the materials, which depend mainly on the type of organic material. Thus the desorption enthalpy is an indicator for the strength of sorption of the organic matter in the sample.

For the Iffezheimer Rhine sediment (Fig. 3-C) the concentrations in water at field conditions (10°C) would be near or below the detection limit (0,01 µg l^{-1}). With the techniques discussed here it is possible to extrapolate to these concentrations.

Conclusions

The results of the eight different temperature steps show that they are fitted very well by the van´t Hoff equation. With the determined desorption enthalpies of the PAHs it is possible to estimate the equilibrium concentrations for lower temperatures (e.g. groundwater temperatures).

In the future, more materials will be investigated to establish a database, in which the enthalpies for PAHs in a variety of materials are collected. If specific classes of material have characteristic enthalpy values, then the characteristic enthalpy value allows to estimate the equilibrium concentrations at field temperature based at a extraction step at elevated temperature.

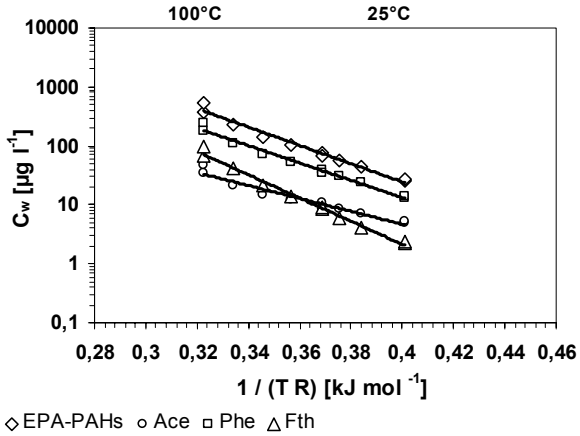

A

Demolition Waste

Desorption Enthalpy ΔH [kJ mol^{-1}]

EPA PAH: -41.3 ± 2.8
Ace: -22.8 ± 1.6
Phe: -32.4 ± 0.9
Fth: -43.7 ± 0.9

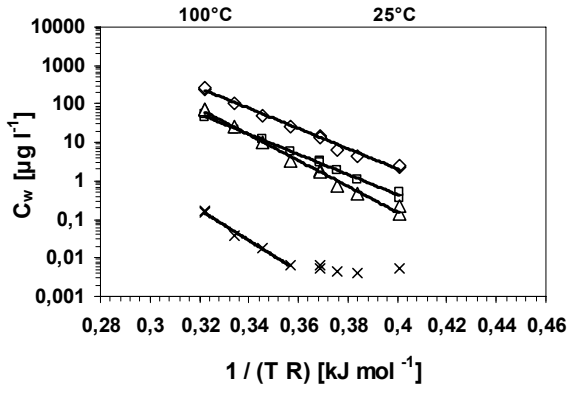

B

Recycling Demolition Waste

Desorption Enthalpy ΔH [kJ mol^{-1}]

EPA PAH: -60.0 ± 2.6
Phe: -57.7 ± 1.2
Fth: -75.5 ± 3.4
BaP: -91.5 ± 5.1

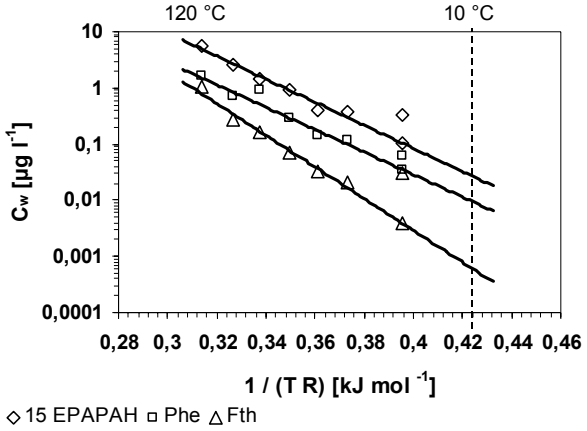

C

Iffezheimer Rhine sediment

Desorption Enthalpie ΔH [kJ mol^{-1}]

EPA PAH: -47.3 ± 2.7
Phe: -46.0 ± 2.2
Fth: -65,0 ± 2.9

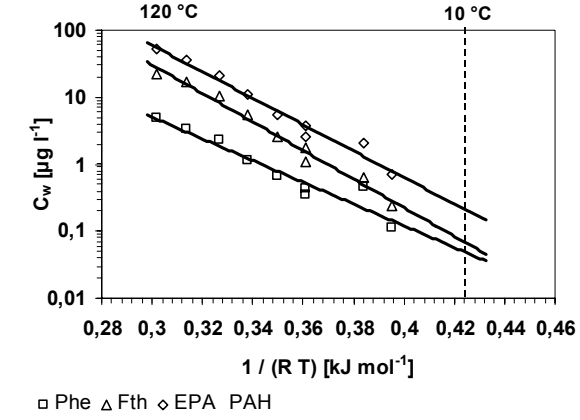

D

Bilbao Harbour Sludge

Desorption Enthalpy ΔH [kJ mol^{-1}]

EPA PAH: -45.5 ± 2.8
Phe: -37.4 ± 4.0
Fth: -49.2 ± 2.5

Fig. 3 A-D: Van´t Hoff plots for Demolition Waste, Recycling Demolition Waste, Iffezheimer Rhine Sediment and Bilbao Harbour Sludge. The desorption enthalpy ΔH [kJ mol^{-1}] was directly determined from the slopes of the regression lines.

(16 EPA PAHs without Naphthalene (EPA PAH), Phenanthrene (Phe), Fluoranthene (Fth), Chrysene (Chr), Benzo(a)pyrene (BaP).

References

American Petroleum Institute (1998): Selective Subcritical Water Extraction of Aromatic and Aliphatic Organic Pollutants from Petroleum Industry Soils and Sludges. – AIP Soil & Groundwater Research Bulletin, No. 4, July 1998.

Dean, J.; Xiong, G. (2000): Extraction of organic pollutants from environmental matrices: selection of extraction technique. - Trac-Trends in Analytical Chemistry 19(9): 553-564.

Dionex (2000): Extraktion von PAK aus umweltrelevanten Proben mit ASE (Accelerated Solvent Extraction). - Dionex GmbH Idstein. Applikationsnote 313.

Gan, J.; Papiernik, S. (1999): Evaluation of accelerated solvent extraction (ASE) for analysis of pesticide residues in soil. – Environ. Sci. & Technol. 33(18): 3249-3253.

Henzler, R.; Madlener, I. & Grathwohl, P. 2002:

Hawthorne, S.; Grabanski, B. (2000): Comparisons of Soxhlet extraction, pressurized liquid extraction, supercritical fluid extraction and subcritical water extraction for environmental solids: recovery, selectivity and effects on sample matrix. - Journal of Chromatography A 892(1-2): 421-433.

Hubert, A.; Wenzel, K. (2001): Accelerated solvent extraction - More efficient extraction of POPs and PAHs from real contaminated plant and soil samples. - Reviews in Analytical Chemistry 20(2): 101-144.

Johnson, M.; Weber, W. (2001): Rapid prediction of long-term rates of contaminant desorption from soils and sediments. - Environ. Sci. & Technol. 35(2): 427-433.

Miller, D.J.; Hawthorne, S. (1998): Method for determining the solubilities of hydrophobic organics in subcritical water.- Analytical Chemistry 70(8): 1618-1621.

Occurrence and transport of MTBE in a contaminated groundwater plume from Düsseldorf

M. Rosell[1], S. Lacorte[1], H. P. Rohns[2], C. Forner[2] and D. Barceló[1]

[1]*Department of Environmental Chemistry, IIQAB-CSIC. Jordi Girona 18-26, 08034 Barcelona, Catalonia, Spain. Phone: +34 93 400 61 69, Fax: +34 93 204 59 04,E-mail: slbqam@cid.csic.es*
[2]*Stadtwerke Düsseldorf AG, OE 236 Qualitätsüberwachung Wasser, Wiedfeld 50, 40589 Düsseldorf, Germany*

Abstract: In a contaminated site of Düsseldorf (middle-west of Germany), a one-year monitoring program has been carried to determine the presence and evolution of some gasoline additives in groundwater. The origin of contamination was a spill or underground storage tank leakage from a gas station. The target compounds were: methyl *tert*-butyl ether (MTBE), its main degradation products, *tert*-butyl alcohol (TBA) and *tert*-butyl formate (TBF); other gasoline additives, oxygenate dialkyl ethers: ethyl *tert*-butyl ether (ETBE), *tert*-amyl methyl ether (TAME) and diisopropyl ether (DIPE); aromatics: benzene, toluene, ethylbenzene and xylenes (BTEX) and other compounds causing odor events in groundwater such as dicyclopentadiene (DCPD) and trichloroethylene (TCE). Purge and trap coupled to gas chromatography – mass spectrometry (P&T-GC/MS) method was used for the simultaneous determination of the above mentioned compounds and permitted to detect concentrations at ng/L (ppt) or sub-ppb concentrations. All samples analysed contained MTBE at levels varied between 0.05 –645 μg/L (ppb). Three contaminated *hot spots* were identified with levels up to *US. Environmental Protection Agency drinking water advisory* (20 – 40 μg/L) and one of them doubling Danish suggested toxicity level of 350 μg/L. Samples with high levels of MTBE contained 0.1 – 440 μg/L of TBA, indicating (but not proving) *in situ* degradation of parent compound. In all cases, BTEX were at low concentrations or not detected showing less solubility and persistence than MTBE.

1. Introduction

Fuel oxygenates are added to gasoline to increase combustion efficiency and to reduce air pollution. Since the ban of tetraalkyl lead compounds, methyl *tert*-butyl ether (MTBE) is the most commonly used octane enhancer and one of organic chemical with the highest production volume worldwide. In European gasoline the average MTBE content is around 2 vol. %, though its use varies considerably between countries (for instance Germany has 1.35% whereas Spain has 3.4%). Some of this MTBE is inevitably released to the environment during the manipulation or storage of petrol fuel and become a groundwater pollutant due to its high solubility, easy mobility and slow degradation.

In addition to health effects concerns (toxicity and discussed carcinogenity), there is much interest in the aesthetic implications of MTBE in drinking water. Taste and odor thresholds for this compound in water have been reported at very low concentrations, approximately 25-60 μg/L for flavour and 40-70 μg/L for odor at 25ºC. For this reason, the U.S. Environmental Protection Agency (USEPA) has established a drinking water advisory for aesthetic concerns of 20 to 40 μg/L.

Furthermore, whether the resulting contamination will become an important environmental issue depends, in part, on the rates and products of MTBE degradation. Although the rates are generally slow, the major products of its degradation are tert-butyl formate (TBF) by atmospheric photooxidation and tert-butyl alcohol (TBA) in the aqueous phase. These resulting products are not easily detected using conventional methods. For such purpose, a

fully automated Purge and Trap coupled to Gas Chromatography – Mass Spectrometry (P&T-GC/MS) method and Headspace Gas Chromatography with Flame Ionization Detection (HS-GC-FID)[i] have been optimised and intercompared for the analysis of Catalonian groundwater samples[ii]. In a recent monitoring study the above mentioned compounds and other fuel additives such as oxygenate dialkyl ethers were detected at ppb concentrations in groundwater where there had been a fuel spill or a underground storage tank leakage. Afterwards, new target compounds were added to the method because its presence can cause odor episodes in groundwater such as dicyclopentadiene (DCPD, a minority compound in gasoline formulation but very low odor threshold at 0.01 – 0.025 µg/L)[iii] and trichloroethylene (TCE, an industrial organochlorinated solvent used as a metal degreaser in automobile production). The objectives of the present study were to follow a contaminated groundwater plume which originated after gasoline spill episode.

2. Study site

A monitoring program has been carried to determine 14 gasoline additives in a total of 11 groundwater wells and one surface sample of Rhine river that were located in Düsseldorf city near a petrol service station where leaking from underground storage tanks or accidental spill occurred. As a result of odor incidents, five campaigns have been done since November of 2001, but only 2 wells were studied permanently (*10688* and *10979*). Significant concentrations of MTBE have reached the local groundwater, and the contamination plume, currently over 400 meters long, is moving under a neighbourhood thus putting the end-users at risk. In addition, this shallow aquifer – between 4-7 meters depth from surface and groundwater level of 38-39 meters M.S.L. (mean sea level)- which consist of gravel, coarse and fine sand lying on Tertiary bedrock, has very low oxygen content (around 0.2 mg/L) and subsequently in anaerobic conditions the biodegradation of pollutants is expected to be more unlikely. Other groundwater characteristics are: conductivity of 930-1030 µS/cm, pH between 6.4 – 6.6 and temperature around 12-13 ºC (measured in April 2002).

In November of 2002, three new monitoring wells were built in the line between older ones *10688* and *10979* with the object of finding the centre of the contamination plume that it was suspect very narrow due to low concentrations in the south wells (*12452* and *12451*). Besides, two of these new ones (called *MTBE1* and *MTBE2*) are multilevel wells; it means that there are filters in different depths. As a result, the groundwater samples were taken out of different depths and should therefore be representative for water in that special region of the aquifer whereas conventional monitoring wells, which have a continuous filter between 4-5 meters and 11-12 meters depth, show more or less an average or representation of the whole aquifer.

3. Methods

Sampling

Standard water sampling techniques for volatile organic compounds (VOCs) were used according to USEPA[iv] except that some replicates were not preserved by acidification (to avoid hydrolysis of TBF)[v]. Besides, some different sampling methods (direct separation into separated vials (A), previously mixed in a big bottle (B) and with or without acidifying (300 µl 25 % sulphuric acid)) for analysis of MTBE and its degradation products were investigated.

The samples from the different wells were collected in triplicate after water had run for several minutes in order to eliminate the stagnant water. A portable pump of 1.1 m^3/h was

used, except in emergency well *17/02* with its own pump at 10 m^3/h. Amber glass vials (40 mL, EPA quality, Tekmar) with Teflon-faced silicone septa were directly filled, avoiding air bubbles passing through the sample, until overflow to prevent volatilisation during sampling and storage. However, some different methods of sample handling were proved combining this usual way (directly into separated vials) against previously mixed in a big bottle with or without acidification to notice differences.

Immediately after collection, samples were placed inside a portable freezer and were transported to the laboratory where they were refrigerated at 4ºC and analysed in less than 2 weeks. If samples were suspected of being highly polluted, a diluted sample was analysed first to avoid contamination of the system.

P&T-GC/MS conditions

A commercial Purge and Trap Concentrator Tekmar 3100 was used coupled to an Aquatek 70 Liquid Autosampler (Tekmar-Dohrmann, USA), which automatically dispensed 10 mL sample aliquots into a purging devise. VOCs were purged from water samples for 13 minutes by bubbling helium (35 mL/min) and absorbed onto a Tenax®-Silica Gel-Charcoal trap (Supelco) at room temperature. After sample loading, the trapped sample components were desorbed at 225ºC during 4 minutes and transferred directly to the GC/MS system.

A Trace GC coupled to a Voyager MS (ThermoQuest Finnigan, USA) was used. Extracts were transferred onto a 75 m x 0.53 mm i.d. DB-624 (J&W Scientific, USA) fused silica capillary column with a 3-μm film thickness where they were separated due to a temperature oven program.

The mass spectrometer was operated in electron impact (EI) mode at 70eV. Peak detection and integration were carried out by use of XCalibur software. Commercial standards were used in order to determine the characteristic ions and the retention times used for identification of selected analytes and calibration. For increased sensitivity and specificity, final quantification was performed in Selected Ion Monitoring (SIM) mode using three ions for each compound (except TBA due to its too low molecular weight confirming ions). Finally, the quantitation was performed by the internal standard procedures.

4. Results and Discussion

Whereas the rapid degradation of BTEX compounds, which, in all cases, showed very low concentrations (<0.2 μg/L) or below their limits of detection, MTBE is more persistent along the contaminant flowpath and, due to its higher relative solubility moves faster. This fact confirms the suitability of MTBE as a tracer or indicator of long-term gasoline contamination than the historically used BTEX. The results are clear, MTBE was detected in all samples analysed at concentrations that mainly varied between 0,05 – 188 μg/L (measured in the conventional monitoring wells as Figure 1 shows) and a maximum detected level of 645 μg/L at the depth of 11 meters (in a new multilevel well, *MTBE1* as Figure 2 shows). Samples with high levels of MTBE contained TBA and TBF at maximum concentration of 440 and 3 μg/L respectively, and the first one shows a similar profile in depth, which could indicate a potential degradation of parent compound.

In relation to different sampling methods investigated, as expected, MTBE did not show significant differences between pre-treatment methods, since it shows very slow biodegradation[vi]. Although the mixed-acidified samples were always highest, there was not a common behaviour for the rest. Besides, the RSDs (relative standard deviation) were below

7% between replicates. On the other hand, acidified samples showed clearly higher TBA concentrations than not acidified ones. These differences were significant due to its RSD above 20%, whereas TBA concentrations were very similar between separated and mixed samples. But, in acid conditions the other degradation product, TBF, is not detected and in addition it can be hydrolysed to TBA.

In view of MTBE values, three monitoring wells were identified as *hot spots* that exceeded the USEPA maximum permissible levels of taste and odor in water. Although until last campaign it seemed that MTBE concentration was decreasing in the contaminated site, finally, high concentrations of this compound were found in depth. Maximum detected level practically doubled Danish suggested toxicity level of 350 µg/L in water. Moreover, taking into account stricter measures, as Swiss guideline value for groundwater of 2 µg/L based on precautionary principle (MTBE as a tracer for gasoline presence in water) or primary and secondary action levels of the state of California, which were fixed at 13 and 5 µg/L respectively, other wells might be considered as risk sites. Obviously, that aquifer water shouldn't be utilized for domestic use and the problem must be monitored so other wells might be contaminated in close areas due to the ability of MTBE to travel significant distances and persist for long periods in the subsurface.

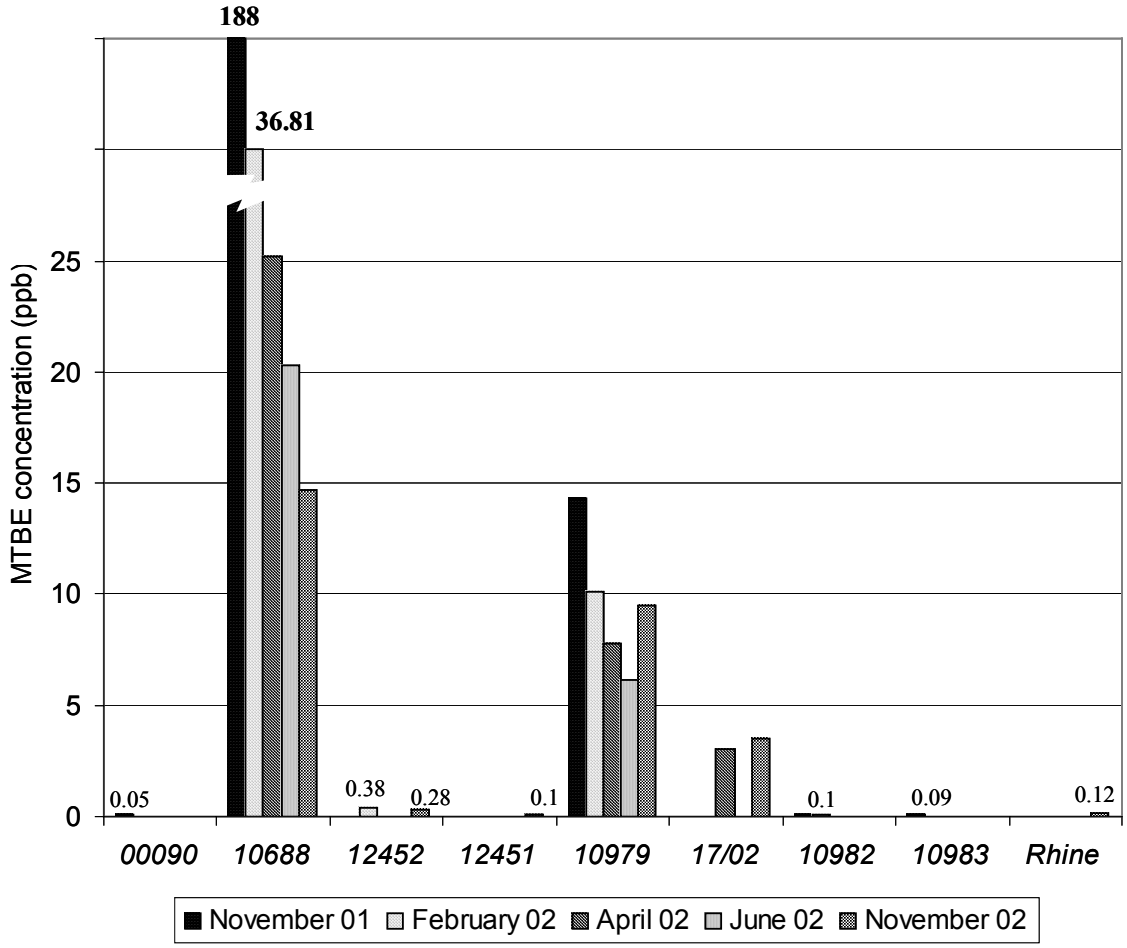

Figure 1: Evolution of MTBE concentration in monitored groundwater wells from Düsseldorf contaminated site.

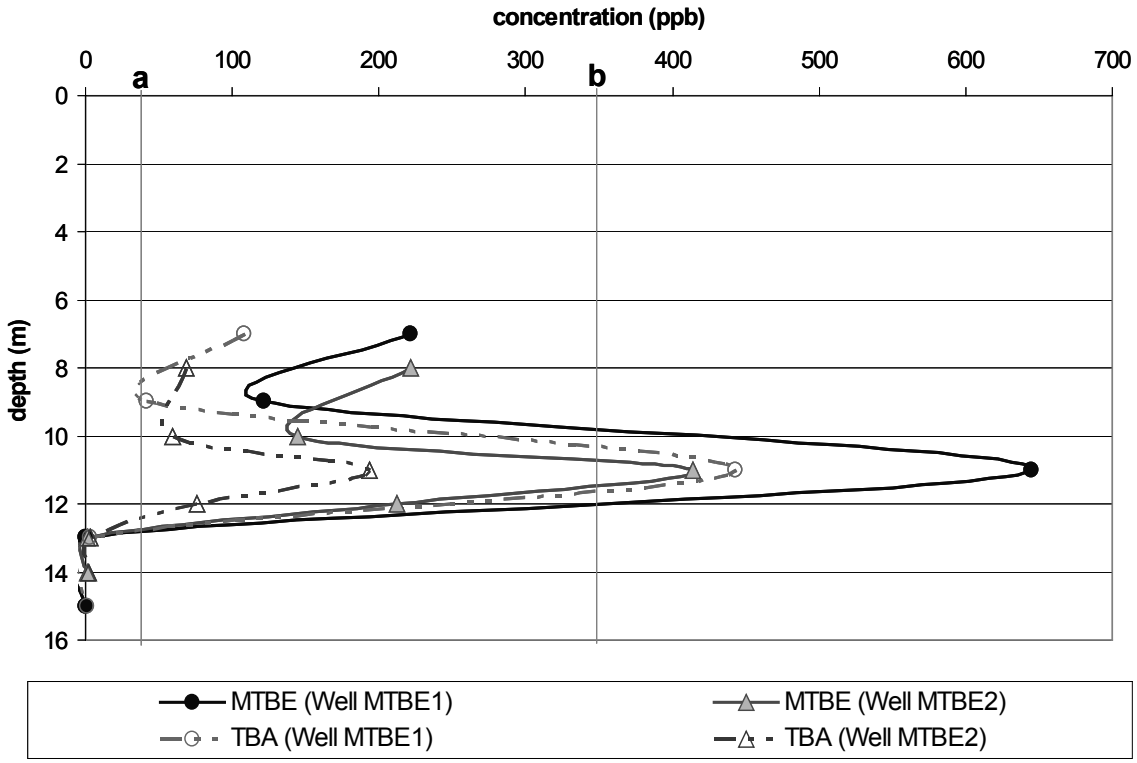

Figure 2: Concentrations of MTBE and TBA in the two new multilevel groundwater wells in November 2002. MTBE guide values of: (a) USEPA drinking water advisory and (b) Danish suggested toxicity level in water are shown.

Acknowledgements

This research is part of the WATCH (EVK1–CT–2000–00059) EU project that is being funded by the EU Environment and Sustainable Development sub-program and from the Ministerio de Ciencia y Tecnología (REN2001-5039-E). We thank Dr. Hans-Peter Rohns and Claudia Forner from Stadtwerke Düsseldorf AG for their kind collaboration. This work is supported by *Departament d'Universitats, Recerca i Societat de la Informació de la Generalitat de Catalunya*.

References

[i] Lacorte, S.; Olivella, L.; Rosell, M.; Figueras, M.; Ginebreda, A. and Barceló, D., *Cross-Validation of Methods Used for Analysis of MTBE and other Gasoline Components in Groundwater*, Chromatographia **2002**, 56, 739-744.

[ii] Rosell, M; Lacorte, S. and Barceló, D., *Simultaneous determination of MTBE and its degradation products, other gasoline oxygenates and BTEX in Catalonian groundwater by P&T-GC/MS* (submitted).

[iii] Ventura, F., Romero, J. and Pares, J., *Determination of Dicyclopentadiene and Its Derivatives as Compounds Causing Odors in GroundwaterSupplies*, Environ. Sci. Technol. **1997***,* 31, 2368-2374.

[iv] Eichelberger, J.W., Munch, J.W. and Bellar, T.A. *USEPA METHOD 524.2. Measurement of Purgeable Organic Compounds in Water by Capillary Column Gas*

Chromatography/Mass Spectrometry (Revision 4.0); Environmental Monitoring Systems Laboratory, Office of Research and Development USEPA, **1992** Cincinnati, Ohio 45268.

[v] Church, C.D., Isabelle, L.M., Pankow, J.F., Rose, D.L. and Tratnyek, P.G. *Method for Determination of Methyl tert-Butyl Ether and Its Degradation Products in Water*, Environ. Sci. Technol., **1997**, 31, no.12, p. 3723-3726.

[vi] Schmidt, T.C., Duong, H., Berg, M. and Haderlein, S.B. *Analysis of fuel oxygenates in the environmental*, Switzerland and Vietnam, Analyst, **2001**, 126, pp.405-413.

MTBE: An emerging problem in groundwaters from Catalonia

M. Rosell[1], L. Olivella[2], M. Figueras[2], A. Ginebreda[2], S. Lacorte[1] and D. Barceló[1]

[1] *Department of Environmental Chemistry, IIQAB-CSIC. Jordi Girona 18-26, 08034 Barcelona, Catalonia, Spain. Phone: +34 93 400 61 69, Fax: +34 93 204 59 04,E-mail: slbqam@cid.csic.es*
[2] *Catalan Water Agency, Generalitat de Catalunya, Provença 204-208, 08036 Barcelona, Catalonia, Spain.*

Abstract: Head space gas chromatography with flame ionization detection (HS-GC-FID) and purge and trap gas chromatography-mass spectrometry (P&T-GC-MS) were used and compared for the determination of methyl-*tert*-butyl ether (MTBE) and benzene, toluene and xylenes (BTEX) in groundwater.For that purpose, Catalonian groundwater samples corresponding to a contaminated area due to a fuel spill and tank leakage were analyzed using both systems. For high concentration levels, a good correlation between both methods was achieved. In relation to the levels obtained with P&T, 20 out of the 21 samples analyzed in vulnerable areas contained MTBE at concentrations up to 666 $\mu g.L^{-1}$. 7 samples exceeded US-EPA drinking water advisory (20-40 $\mu g.L^{-1}$) and 13 of the samples had levels between 0.28 and 17.9 $\mu g.L^{-1}$. However, HS-GC-FID provided two-three orders of magnitude lower sensitivity and concentrations of 6-10 $\mu g.L^{-1}$ could not always be detected, producing false negatives. The same behavior was observed for the analysis of BTEX, where GC-MS confirmation was always necessary. Therefore, we describe the applicability of two widely used analytical methods for routine monitoring of VOCs and the need to survey trace concentrations of persistent MTBE in vulnerable aquifers.

1. Introduction

In order to replace antiknock leaded derivatives in gasoline which caused toxic emissions of CO, O_3 and volatile organic compounds towards the atmosphere, oxygenates derivatives such as alcohols and aliphatic ethers are utilized as octane booster. Methyl tert-butyl ether (MTBE) is the most widely used ether oxygenate and is added to gasoline at concentrations up to 15% by volume, depending on the country. MTBE enters the environment during all phases of the petroleum fuel cycle (e.g. auto emissions, evaporative losses from gasoline stations and vehicles, storage tank releases, pipeline leaks and accidental spills, and refinery stock releases). Inhalation of fumes while fueling automobiles is the main source of human exposure to MTBE. However, humans are also exposed when drinking water is contaminated with MTBE. Due to its high solubility (25-50 g/L), low Kow (0.94 - 1.43) and Henry's Law constant (55.3 Pa m^3/mol), MTBE remains dissolved in surface water, where it can volatilize to the atmosphere. A small fraction can partition into soil and eventually reach ground water. Once in anaerobic conditions of ground water under, it is slow to biodegrade and can persist for more than 200 days. Thus, a major issue regarding the survey of MTBE concerns its detection at low levels in ground water. In this paper, we report two analytical techniques that permit the detection of MTBE and BTEX in groundwaters. The first one consists in headspace extraction followed by gas chromatography and flame ionization detection. The second one is based in automated purge and trap coupled to gas chromatography with mass spectrometric detection. Quality parameters such as recoveries, precision, limits of detection and robustness are reported for both techniques. For comparability purposes, groundwater samples corresponding to an area where there had been odor problems due to a fuel spill were analyzed using both systems.

2. Experimental

Chemicals and Reagents. Standard mixture of benzene, toluene, ethylbenzene, m+p-xylene, o-xylene and methyltertbutylether (MTBE) were obtained from SUPELCO (Barcelona) and were prepared in methanol and added on organic-free water. For the static headspace GC-FID analysis, α,α,α-trifluorotoluene was used as internal standard. For P&T GC-MS, deuterated MTBE was used and fluorobenzene for the BTEX.

Sampling Procedure. For the comparison exercise, 21 groundwater samples were taken from two "hot spot" areas in Catalonia (Northeast Spain) in which (i) an accidental gasoline spill in a petrol service station (La Batlloria) had occurred in 1997 and (ii) leakage of oil refinery storage tanks (Tarragona). These areas have been monitored since then and residue levels between 10 and 600 $\mu g.L^{-1}$ are still being encountered [1]. Groundwater samples were collected using a Niskins bottle. For P&T analysis, samples were directly transferred to homologated 40 mL Tekmar amber glass vials (EPA Method 524.2), which were thereafter used for analysis. No sample acidification was performed, samples were analyzed within 7 days after collection.

Headspace and GC-FID. 10 mL of water sample were sealed in a 22 mL headspace vial with an open-centre aluminium cap and PTFE-faced butyl rubber septum and analysed by static headspace with a flame ionization detector [2]. Previously, samples were spiked with 10 μL of 100 $\mu g.mL^{-1}$ internal standard solution of α,α,α-trifluorotoluene. The headspace analysis was performed in a Varian Genesis Headspace Autosampler connected to a Varian Star 3600 gas chromatograph. Samples were equilibrated at 70ºC for 4 min, mixed at 80% of full power for 7 min, and post mixing stabilized for 1 min. Sample loop was 1 mL; line and valve were maintained at 150ºC and vials pressurized at 7 psi. A fused-silica column DB-624 (75m x 0.53 mm x 3 μm) from J&W was used.

Purge and Trap and GC-MS. Tenax®-SilicaGel-Charcoal cartridges of the Purge and Trap Concentrator Tekmar 3100 were used. An Aquatek 70 Liquid Autosampler (Tekmar-Dohrmann) was used to automatically dispense 13 mL sample aliquots into a 25 mL purging devise. The sample was purged with a stream of He at 35 $mL.min^{-1}$ for 11 min at ambient temperature. After sample loading, the trapped sample components were desorbed by heating the Tenax® cartridges at 225ºC and passing He gas at 3 $mL.min^{-1}$ during 3 min and the injector was left in splitless mode. These conditions were chosen since gave maximum response for a large number of volatile organic compounds [3]. The analysis was performed using a Trace GC coupled to a Voyager MS (ThermoQuest, England) in electron impact mode at 70 eV (EI) with a 75 m x 0.53 mm i.d. DB-624 (J&W Scientific, Inc.) fused silica capillary column with a 3 μm film thickness. Acquisition was performed in time scheduled selected ion monitoring using three ions per compound.

3. Results

Quality parameters. Basically HS is rather suitable for highly polluted samples which can cause matrix and carry over problems. P&T enrichment, following EPA method 624 [4], is the most widely used method for the analysis of MTBE and volatile organic compounds in general due to large number of compounds that can be simultaneously analyzed and easy automation. Table I reports the quality parameters obtained with both methods.
As regards to the linear range, HS-GC-FID permits the detection of MTBE and BTEX from the limit of detection up to 15 $mg.L^{-1}$ and 1 $mg.L^{-1}$, respectively. For P&T-GC-MS, the system permits the detection of compounds up to 10 $\mu g.L^{-1}$. Exceeding this concentration, the

system suffers from memory effects and poor linearity, and therefore, highly polluted samples should be diluted prior to analysis. On the other hand, both methods provided excellent recoveries and intra-day variation, as indicated by a maximum standard deviation of 12.2%. However, the main difference between both methods rely in their sensitivity. Whereas P&T has a limit of detection of 0.002 $\mu g.L^{-1}$ for all studied analytes, HS has much lower sensitivity, with levels up to 5.7 $\mu g.L^{-1}$ for MTBE and 0.3-0.6 $\mu g.L^{-1}$ for the BTEX which might not be sensitive enough for the trace level determination of MTBE in groundwaters, where residue levels might be encountered at the low $\mu g.L^{-1}$ level. An additional problem of HS-GC-FID is the need for confirmatory analysis of all positive samples. Both techniques offer a high precision and easy use.

Table 1. Quality parameters obtained with static HS-GC-FID and P&T-GC-MS

Compound	Upper $\mu g.L^{-1}$		R^2		%R		Std (%)		LOD (µg/L)	
	HS	P&T	HS	P&T	HS	P&T	HS	P&T	HS	P&T
MTBE	15000	10.0	0.999	0.9954	102.4	101.0	7.9	11.0	5.7	0.001
Benzene	1000	10.0	0.999	0.9991	95.1	97.7	12.2	10.6	0.6	0.002
Toluene	1000	10.0	0.999	0.9901	100.6	111.8	11.7	4.6	0.6	0.001
Ethylbenzene	1000	10.0	0.999	0.9992	100.4	94.1	8.2	8.1	0.4	0.001
m+p-xylene	1000	10.0	0.999	0.9992	99.9	96.0	4.8	10.6	0.3	0.001
o-xylene	1000	10.0	0.999	0.9967	101.2	96.6	6.3	7.8	0.4	0.002

Table 2. Cross-validation of results using static HS-GC-FID and P&T-GC-MS for oxygenate additives. Concentrations are given in $\mu g.L^{-1}$.

Sample id.	MTBE		Benzene		Toluene		Ethylbenzene		m+p-xylene		o-xylene	
	HS	PT	HS	PT	HS	PT	HS	PT	HS	PT	HS	PT
Tarragona												
Sevil-Caseta	< ld	8.50	< ld	1.47	< ld	8.89	< ld	2.53	< ld	1.76	< ld	1.30
Sevil-road	n.a.	28.02	n.a.	1491	n.a.	1351	n.a.	312.0	n.a.	508.5	n.a.	454.9
Sevil-sinia	< ld	11.26	< ld	1.59	< ld	10.18	< ld	3.15	< ld	2.10	< ld	1.58
Gate-well	12.7	20.66	< ld	1.71	< ld	9.05	< ld	2.55	< ld	1.79	< ld	1.28
Sorts	610	666.3	< ld	5.88	< ld	3103	< ld	25.94	< ld	24.05	< ld	5.47
Ferrerota	65	74.48	< ld	4.60	< ld	30.31	< ld	7.76	< ld	4.43	< ld	2.77
Tarragonins	< ld	5.62	< ld	1.74	< ld	8.30	< ld	2.18	< ld	1.59	< ld	1.08
Pineda-2	115	42.66	35.0	8.75	8.0	269.4	< ld	36.07	50	31.23	65	43.12
Camping	6.0	10.53	< ld	1.96	< ld	9.88	< ld	2.74	< ld	2.02	< ld	1.34
Repsol-73	< ld	10.13	1.6	1.53	< ld	9.52	0.7	3.25	13	2.15	< ld	1.58
Repsol-83	< ld	8.23	< ld	1.84	< ld	11.08	< ld	3.60	< ld	2.24	< ld	1.57
La Batlloria												
Formigueta	< ld	0.28	< ld	< ld	< ld	0.03	< ld	< ld	< ld	< ld	< ld	< ld
Comptesa	20.0	48.09	< ld	< ld	< ld	0.13	< ld	0.04	< ld	< ld	< ld	< ld
Ferreria 1	11.0	13.81	< ld	0.02	< ld	0.37	< ld	< ld	< ld	< ld	< ld	< ld
Ferreria 2	57.0	32.85	< ld	< ld	< ld	1.43	< ld	< ld	< ld	< ld	< ld	< ld
Ferreira 3	< ld	2.37	< ld	< ld	< ld	0.05	< ld	< ld	< ld	< ld	< ld	< ld
Xemani	5.4	8.97	< ld	0.09	< ld	0.14	< ld	0.06	< ld	< ld	< ld	< ld
Xemani 2	< ld	< ld	< ld	< ld	< ld	0.07	< ld	< ld	< ld	< ld	< ld	< ld
Auladell	< ld	0.62	< ld	< ld	< ld	< ld	< ld	< ld	< ld	< ld	< ld	< ld
Viñas	15	17.97	< ld	0.02	< ld	< ld	< ld	< ld	< ld	< ld	< ld	< ld
Blancher	< ld	1.36	< ld	< ld	< ld	0.09	< ld	< ld	< ld	< ld	< ld	< ld

< ld = lower that the detection limit of each compound, see Table I.
n.a.=not analyzed

Cross Validation Studies in Real Environmental Waters. A total of 21 groundwater samples were analyzed in parallel using HS-GC-FID and P&T-GC-MS for comparison studies. Table II reports the MTBE and BTEX levels found. In Tarragona, where there was a

permanent tank leakage from big underground tanks in a petrol service-stations, levels up to 600 $\mu g.L^{-1}$ of MTBE were encountered and for samples with concentrations higher than 10 $\mu g.L^{-1}$ good agreement between both methods. Detritus coarse materials, sands and conglomerates constitute the aquifers involved and had 8-10 m depth. These levels are quite relevant since MTBE is highly water soluble and moves nearly as fast as the groundwater itself and it is considered recalcitrant in the subsurface environment.

In sample Pineda 2, two different phases were clearly observed when sampling and this affected the reproducibility of the analysis, especially for BTEX. The four samples with highest concentration of MTBE had also highest BTEX levels varying from 387 to 4116 $\mu g.L^{-1}$ total BTEX. For the rest, the levels varied from 5 to 74 $\mu g.L^{-1}$.
In La Batlloria, five years after the spill, it was still possible to detect traces of MTBE from 0.28 to 48 $\mu g.L^{-1}$ and from 0.02 to 1.43 $\mu g.L^{-1}$ for BTEX. A good agreement was observed for the "negative" values which were not detected with P&T nor with HS. In the other way round, in some cases and specially for toluene, HS could not detect the target analytes at 0.1 $\mu g.L^{-1}$ level.

4. Conclusions

Levels up to 600 µg/L were encountered with a good correlation between both methods. In relation to the levels obtained, 45% of the samples out of 49 analyzed in vulnerable areas exceeded the maximum permissible levels of odor and taste set by the US-EPA (20-40 µg/L). 14% of the samples had levels below 0.1 µg/L. Taking into consideration the organoleptic threshold of MTBE in groundwaters, which are often used for irrigation or domestic use, and the spread presence of this compound at high concentrations, its survey is necessary to determine its final fate and establish remediation strategies.

Acknowledgements

This research, which has been published recently [5], is part of the WATCH (EVK1-CT-2000-00059) project that is being funded by the EU Environment and Sustainable Development sub-program and from the Ministerio de Ciencia y Tecnología (REN2001-5039-E). This work is supported by *Departament d'Universitats, Recerca i Societat de la Informació de la Generalitat de Catalunya*.

References

[1] U.S. Environmental Protection Agency. **1984**. Method 624- Purgeables. 40 CFR Part 136, 43373; Federal Register 49, No. 209.
[2] Fraile, J., Niñerola, J.M., Olivella, L., Figueras, M., Ginebreda, A., Vilanova, M., Barceló, D. *TheScientificWorldJournal* **2002**, *2,* 1235-1242.
[3] Stuart, J.D., Roe, V.D., Lacy, M.J., Robbins, G.A. *Anal. Chem.* **1989**, *61*, 2584-2585.
[4] Martinez, E., Lacorte, S., Llobet, I; Viana P., Barceló, D. *J. Chromatogr. A* **2002**, *959*, 181-190.
[5] Lacorte, S., Olivella, L., Rosell, M., Figueras, M., Ginebreda, A., Barceló, D. *Chromatographia* **2002**, 56, 739-744.

Mass Transfer of Contaminants in Urban Groundwater and Evidence for Natural Attenuation

T. Schiedek, M. Beier, C. Lerch

Applied Geosciences, TU Darmstadt, Schnittspahnstr. 9, 64287 Darmstadt, Phone +49(0)6151 166018, Fax +49(0)6151 166539, E-Mail: schiedek@geo.tu-darmstadt.de

Abstract: Groundwater in high-density areas, e.g. big cities, industrialized areas, is often contaminated with organic and inorganic compounds. Due to the many potential emission sources in such areas the delineation of an existing contaminant plume and the quantification of groundwater contamination using groundwater wells is very difficult. Thus, remediation of contaminated sites in a city is challenging. Natural attenuation is one of the few possible clean-up strategies but not well investigated. The quality of urban groundwater and the mass transfer of typical urban contaminants along the flow path under the city of Darmstadt, Germany, was investigated, using a mass balance concept. Several ground water samples were taken from winter 1999 to summer 2002 in the area of the city (urban and rural). Organic and inorganic contaminants (such as PAHs, fuel related contaminants, chloride, sulfate, iron, etc.) could be found in various concentrations in the urban groundwater (especially inner-city groundwater), sometimes reaching the water regulations of the State Hessia. The mass balance clearly shows an increase of the contaminant load in the city. At some sites, highly contaminated with organic compounds, a decrease of potential electron acceptors (e.g. nitrate, sulfate) and/or an increase of iron (II) or manganese shows, that natural attenuation takes place.

1. Introduction

The usage of groundwater in high-density areas, e.g. big cities, industrialized areas, is often limited rather due to availability than to certain quality requirements. In such areas emission sources (housing areas, industrial areas, roads, sewers, gas stations, etc.) are usually located close to the water users, hence, the flow path of a groundwater contaminant to potential receptors (e.g. wells) is short (with respect to time and distance). The delineation of an existing contaminant plume using groundwater wells is very difficult as well, because of the many potential emission sources and the probability of overlapping plumes. Moreover, the usually dense setup of buildings, roads, pipelines etc., makes it almost impossible to install a (good practice) sampling well network. Thus, recognition and quantification of contaminated sites e.g. in a city need more integrative approaches. Natural attenuation is one of the few possible clean-up strategies but not well investigated as far as hardly accessible, spatial contamination is concerned. The following report presents preliminary results of an ongoing study.

2. Methods

To quantify the groundwater contamination in a high-density area we choose the city of Darmstadt (Germany, highly industrialized, 140.000 inhabitants) as a test site to develop an integrative method based on a mass balance concept (Beier & Ebhardt 2002). We established a hydrogeological model (Lerch 2001) of the area of Darmstadt using all relevant data (Justen 1999, Greifenhagen 2000), such as geological profiles from borings, groundwater recharge (considering precipitation, surface sealing, etc.) and discharge (surface, industrial, etc.). The hydrogeological data were processed as a 3-D-model with the commercially available code Visual Modflow. Based on this model, the study area was divided into 3 control planes (defined by the accessible sampling and monitoring wells: upstream-, city-, downstream-

plane) perpendicular to the main groundwater flow. 6 model budget zones (MBZ, fig. 1, left) with a maximum of 6 subzones were defined within the city-plane and the downstream-plane and the water budget for each zone was calculated (fig. 1, right). Several ground water sampling campaigns were carried out from winter 1999 to summer 2002 using the groundwater monitoring wells (GMW) of the area of Darmstadt city (fig. 1, left). Inorganic (cations, anions, several anthropogenic elements) and organic parameters (such as PAH, BTEX) were analyzed using standard methods. The concentrations of the contaminants and the water budget were used to calculate a mass balance (from upstream to downstream) for each contaminant. Due to the specific geological conditions in the model area, the water budgets and mass balances could be calculated for a maximum depth of ca. 100 m below surface, details are described in Beier & Ebhardt (2002).

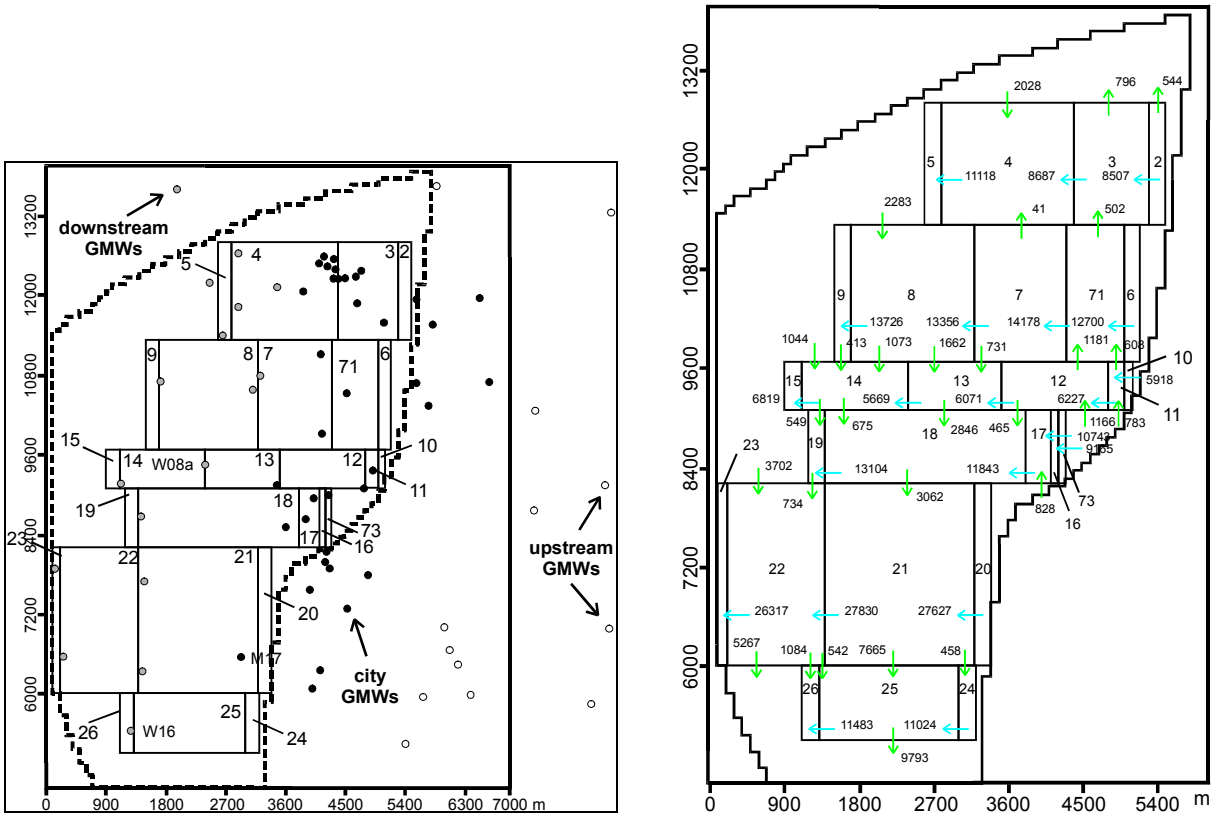

Figure 1: Model area (dashed line) with groundwater monitoring wells (GMW) and the defined 26 budget zones/subzones (left), and the calculated water budgets for each zone (right, m^3/d); general groundwater flow from E to W.

3. Results and Discussion

The analysis of the hydrogeological data showed that groundwater flow in the subsurface of the city is generally from East to West, relevant alteration of flow direction, except at zone 1, 22 and 25, could not be detected. Since there is no mentionable contaminant source upstream, it was clear that all contamination to be found resulted from urban input. This appraisal is confirmed by the chemical data. The GMWs in the upstream-plane showed normal geogenetic background values for all relevant naturally occuring inorganic species. Organic compounds, typical for urban environments, such as PAHs, BTEX and CHCs could only be found in traces in many samples, and may stem from atmospheric input.

The contaminant concentrations, inorganic and organic, increased in groundwater in the city-plane, directly influenced by emissions from road traffic, gas stations, etc., partly orders of magnitude (see e.g. tab. 1). In the downstream-plane usually a drop of concentrations could be observed.

Fig. 2 shows the calculated fluxes of chloride and PAHs in the various zones and sub-zones. For the non-reactive chloride a positive budget (pale-grey areas) could be calculated in 5 sub-zones, which shows that additional chloride from urban sources is reaching groundwater in relevant masses. These areas match well with main roads, which points at contaminant sources such as leaking sewers (road salting is also a chloride source, but not very likely for that summer sampling campaign). All other sub-zones show negative budgets (dark-grey areas fig. 2), which could be mostly explained with dilution phenomena. In general, all zones down-stream show a value close to the background level of the chloride flux.

The PAH fluxes (fig. 2, right) correspond well with industrial areas and main roads. In one sub-zone the source is probably known. In the city area, fluxes increase extremely to a maximum calculated value of 554 ng/d*m. All other sub-zones show values approximately two orders of magnitude lower. The group of the PAHs are well known to sorb onto soil and aquifer material (e.g. Kleineidam et al. 1999), showing a broad variation of the sorption coefficients from 2-ring to poly-ring compounds. This may explain the relatively strong decrease of PAH-fluxes from zones of urban input (pale-grey areas) to the following downstream zone, but can also be a hint for a natural degradation of some of these compounds. Nevertheless, PAH fluxes downstream are explicitly higher compared to the upstream fluxes, indicating a strong influence of the city area on groundwater quality.

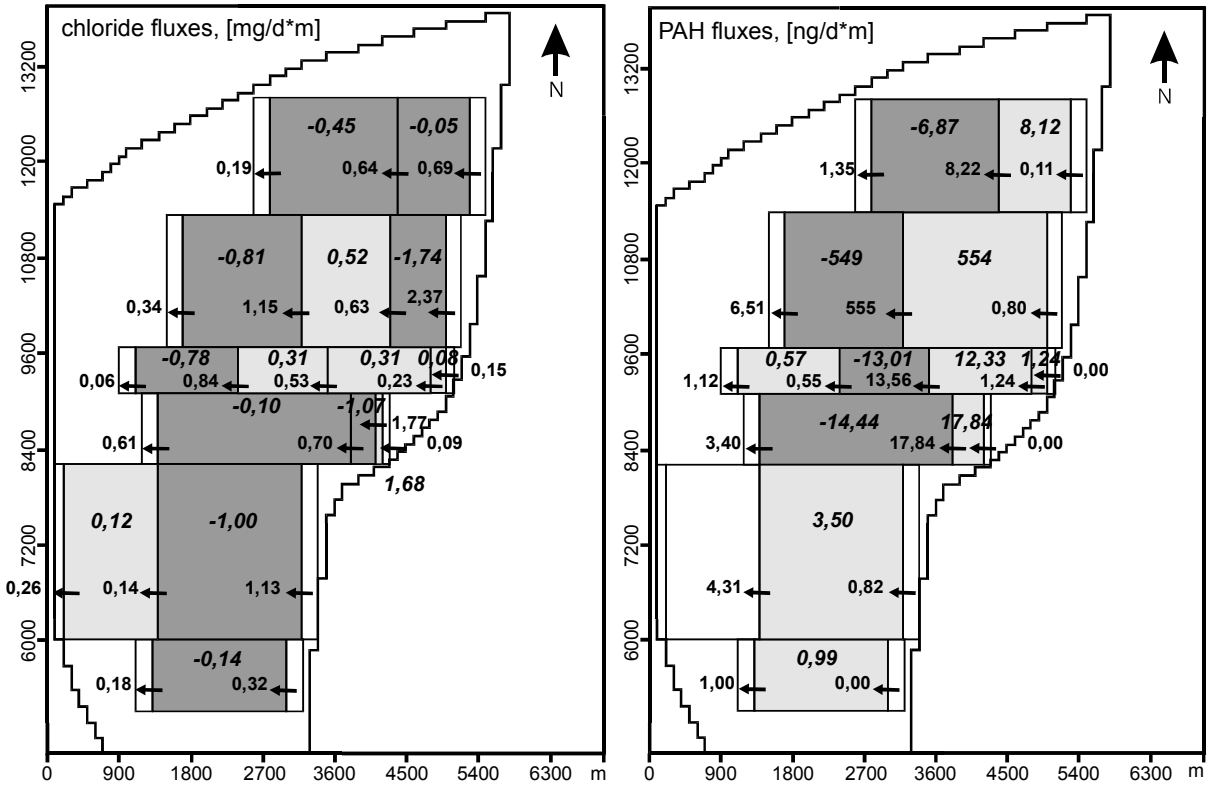

Figure 2: Calculated mass fluxes for chloride (left) and PAHs (right, sum of 17 PAH from analysis in autumn 2001); general groundwater flow from E to W; numbers in italic represent the balanced value for the budget zone.

After e.g. Wiedemeier et al. (1995) a biological degradation of organic compounds in groundwater can be recognized with decreasing concentrations of potential electron acceptors, such as sulfate, nitrate, and the occurrence or increase of Fe^{2+} and Mn^{2+} (reduction of X^{3+}-minerals). Table 1 shows a comparison of concentrations of organic compounds and potential electron acceptors for selected GMWs. It can be observed that with increasing contaminant concentrations, the concentration of nitrate is decreasing. In GMW 56, with the highest organic contamination, nitrate could not be detected. For all GMWs an increase of Mn^{2+} concentration could be observed, Fe^{2+} shows increased concentrations if a higher concentration of a organic compound is detected.

Particularly with regard to the results of the mass balances presented above, we conclude that this concentration pattern is due to natural attenuation processes, including biological degradation. Ongoing research will focus on this topic.

Table 1 – Concentrations of Fuel-related Compounds and Potential Inorganic Natural Attenuation Indicators (Electron Acceptors) at Selected Groundwater Monitoring Wells; Sampling Campaign 03/2001.

[a]GMW-NO.	sum PAH without Nap [ng/l]	SO_4 [mg/l]	NO_3 [mg/l]	Fe^{2+} [mg/l]	Mn^{2+} [mg/l]
		[b]46,7	[b]35,2	[b]0,11	[b]0,03
47	205,8	8,0	25,6	0,10	0,05
29	232,5	111,2	67,4	0,10	0,08
88	354,1	65,4	63,2	0,02	0,10
1	1159,5	97,4	550,0	0,90	0,12
12	2339,9	130,0	3,7	0,84	0,32
73	7540,2	201,8	4,0	0,14	0,61
56	23439,5	126,2	0,0	0,45	0,28
	sum BTEX [ng/l]				
73	67	201,8	4,0	0,14	0,61
18	77	125,7	84,9	0,10	0,09
43	96	128,8	147,6	0,04	0,03
75	199	23,0	16,2	0,09	0,07
74	379	64,9	58,4	0,57	0,05
56	113355	126,2	0,0	0,45	0,28

[a]Groundwater monitoring well; [b]mean value upstream

4. Acknowledgement

We gratefully acknowledge the financial support of the Hessian Landesamt für Umwelt und Geologie HLUG, Prof. B. Toussaint, and the support and discussion of Prof. P. Grathwohl and the lab-team (Dr. T. Wendel, R. Seelig) at ZAG, University of Tübingen.

5. References

Beier, M.; Ebhardt, G. (2002): Urbane Stoffeinträge in das Grundwasser unter dem Stadtgebiet Darmstadt.- In: W. Rosendahl & A. Hoppe (Hrsg.): Schrift. d. Deutsch. Geol. Gesell., Heft 15: 75-84; 8 Abb., 4 Tab., Hannover.

Greifenhagen, G. (200): Untersuchungen zur Hydrogeologie des Stadtgebietes Darmstadt mit Hilfe eines Grundwasserinformationssystems.- Dissertation, Technische Universität Darmstadt, S. 221.

Justen, N. (1999): Grundwassermodellierung und hydrogeologische Untersuchungen zur Infiltration von Dachflächenwasser im Raum Darmstadt-Ahrheiligen unter Berücksichtigung der gewerblichen Gewässerentnahmen.- unpubl. Diploma-Thesis, Technische Universität Darmstadt, S. 69.

Kleineidam, S., Rügner, H., Liguis, B., Grathwohl, P. (1999): Organic matter facies and equilibrium sorption of phenanthrene.- Environ. Sci. Tech., 33, 10, 1637 - 1644

Schiedek, T.; Heckwolf, M.; Ebhardt, G. (2000): Fuel Related Contaminants In The Groundwater Of The City Of Darmstadt, Germany.- Abstract, Geophysical Research Abstracts, 25th General Assembly EGS2000, Nice, Volume 2.

Wiedemeier, T.H.; Swanson, M.A.; Wilson, J.T.; Kampbell, D.H.; Miller, R.N.; Hansen, J.E. (1995): Patterns of intrinsic bioremediation at two U.S. Air Force Bases.- in: Hinchee, R.E.; Wilson, J.T.; Downey, D.C. Columbus (Hrsg.): 3. International In Situ and On-Site Bioreclamation Symposium, San Diego, Ca/USA, 1995, 24.-27.Apr, Battelle Press. Oh, USA 1995, Bd 3(1): 31-51.

Optimized experimental design for the determination of effective release rates of organic contaminants using column outflow experiments

Wehrer, M.[1], Totsche, K.U.[2], Jann, S.[2], Knorr, K.-H.[2] and Huwe, B.[1]

[1]*Abteilung Bodenphysik, Universität Bayreuth, 95440 Bayreuth, Phone: 0921/552330, Fax: 0921/552246;email: markus.wehrer@uni-bayreuth .de*
[2]*Lehrstuhl für Bodenkunde, Department für Ökologie, Wissenschaftszentrum Weihenstephan für Ernährung, Landnutzung und Umwelt, Technische Universität München, 85350 Freising*

1. Introduction

Column outflow experiments are a common means to determine the release and transport parameters of organic contaminants in soils. It has been shown that experimental designs based solely on the determination of breakthrough curves as a response to continuous-feed input-boundary conditions may result in a non-unique parameter estimation due to equifinality (Koch and Flühler 1993a; Totsche 1998, 2001; Wehrer and Totsche 2003). This deficiency can be overcome by modifying the course of the experiment, i.e., the experimental design.

One means to observe kinetic limitations is the application of different flow velocities and stop flow events (flow interruptions). A flow interruption shows a distinctive effect during the elution of a substance that is released by a rate–limited process (Brusseau et al., 1997). In case the flow interruption has been long enough, the effluent concentration after restart of flow is higher than before: The higher residence time allowed for prolonged equilibration and such resulted in increased effluent concentration. However, if the rate of release is small, the duration of the stop flow might be too short to obtain a difference in effluent concentrations. Under these circumstances, a substance being subject to very slow release might not be distinguished from an instantaneously desorbing contaminant. Neither one will show a concentration difference after a flow interruption. However, the pore water concentration of the latter substance is at equilibrium, while that of the first one is not. Nevertheless, it is possible to discriminate between the two cases.

The extent of the flow interruption effect is not only depending on the release rate itself but on the ratio of release-reaction time scale to transport time scale, the so called Damköhler-number *Da*.

Damköhlernumber: $$\mathrm{D}a = \frac{\mathrm{R} \cdot \mathrm{k}}{(v/L)}$$ Equation 1

R: Coefficient of Retardation

k: Rate parameter

L: Column Length

v: Mean pore water velocity

The Damköhler-number is a measure for the extent of the non-equilibrium. If this ratio is lowered during the experiment, for example, by increasing the flow velocity, non-equilibrium conditions are enforced. In case of prevailing equilibrium at the low flow velocity, a first

interruption would not cause a effluent concentration difference, while in a second it could be observed. On the other hand, if non-equilibrium already prevailed and no concentration-effect could be observed, a further enforcement of the nonequilibrium would not result in a concentration effect, because the absolute release is just to slow. Consequently, performing one experiment with two different flow velocities and a flow interruptions can help to identify the Damköhler-number. Furthermore, from the extent of the concentration difference before and after flow interruption, the release rate can be quantified. However, this method requires at least two flow interruptions of different length (Wehrer and Totsche, 2003).

The objective of this study was to investigate, whether the described experimental design can be used in real world experiments for the identification of Damköhler-number and release rate. Soil columns containing oil-contaminated soil material were percolated under saturated conditions and subjected to two flow interruptions. Different flow velocities were applied to two parallel columns at the same time in order to keep the duration of the experiment as short as possible. To support the interpretation of the BTCs, the observed behavior was simulated numerically, applying the same boundary conditions and parameters as in the experiments.

2. Methods

2.1 Soil column set up

The columns were repacked with air dried contaminated coarse textured carbonaceous soil samples. The materials were sampled from the unsaturated zone of a petrochemical plant at Munich, Germany. Two columns were used in parallel. The columns were saturated from bottom to top at a low flow rate to allow entrapped air to escape. The set up is given in figure 1. For the percolation experiment, the columns were run at two different flow velocities: 1pv/24h and 1pv/4h, termed *'q slow'* and '*q fast*' respectively. The percolation solution contained 10^{-2}M $NaClO_4$-solution for constant ionic strength and 10^{-5}M $AgNO_3$ to inhibit microbial activity. Both columns were percolated by the same number of pore volumes, using the named flow velocities, and then subjected to flow interruptions of equal duration. Within the efflux, DOC, pH, electrolytic conductivity, spectral absorptivity at 254nm and 436nm and turbidity at 869nm (DIN 38404). In order to determine the longitudinal hydraulic dispersivity a chloride pulse was applied. PAHs were analyzed employing SPE and GC/MS and quantified via internal standard/recovery-standard method.

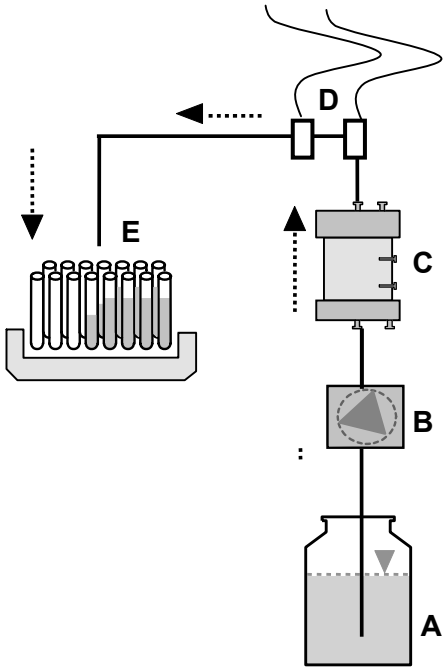

Figure 1: Set up of the column experiment. A) Percolation-solution, B) Peristaltic pump C) soil column, D) circulation cells with combination electrodes E) fraction collector

Simulation of the BTC´s was conducted using the model CARRY (Totsche, 2000), which is based on the Advection-Dispersion-Equation in combination with first order mass-transfer and nonlinear isotherms. In the model, the same flow boundary conditions were applied as in the experiment. Parameters are according to table 1, with some parameters determined in the experiment and others adjusted by trial and error.

Table 1: Parameter values used in the numerical simulations with CARRY.

Parameter	slow q	fast q
Length L [cm]	15 1)	15
Water content θ	0.33 1)	0.33
Flow velocity q [cm/d]	**4.6 1)**	**25 1)**
Bulk density [g/cm^3]	1.7 1)	1.7
Diffusion D [cm^2/d]	1.4 2)	1.4
Tortuosity τ	2.5 2)	2.5
Dispersion λ [cm]	0.5 3)	0.5 3)
Rate parameter k [1/d]	0.7 3)	0.7 3)
Distribution coefficient K [cm^3/g]	2.0 3)	2.0 3)
Freundlich Exponent p	0.5 3)	0.5 3)
Inflow conc. [g/cm^3]	0 1)	0
Initial solid phase Conc. [g/cm^3]	1 3)	1 3)

1) Experimentally determined
2) 'Worst-case scenario' for the identification of release rates. High diffusion might counterbalance the effect of flow interruption (Koch und Flühler, 1993b).
3) Tuned by trial and error

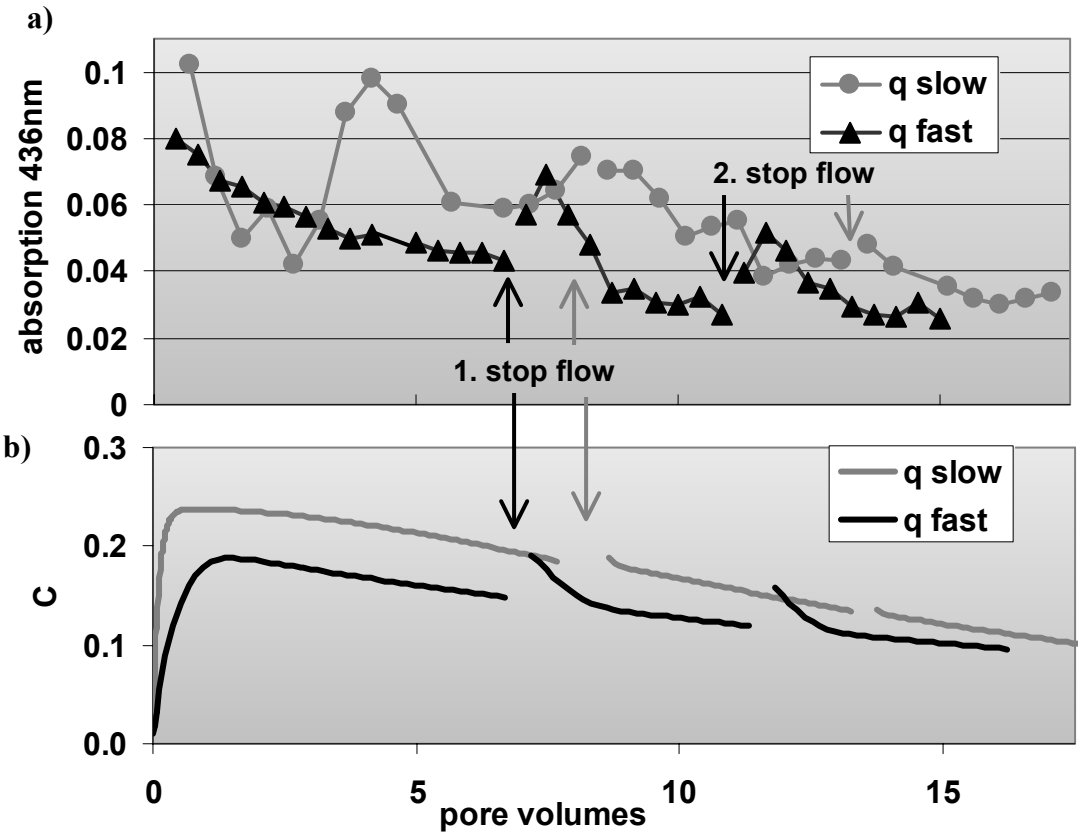

Figure 2: (a) Breakthrough-curves of spectral absorptivity at 436 nm in two soil columns applying different flow velocities, (b) numerical simulation (see text). The arrows indicate flow interruptions ('stop flow') of 120 h (first) and 48 h (second).

3. Results and Discussion

Some breakthrough-curves of the experiment described above comply with the behavior that was expected from the numerical scenarios described in Wehrer and Totsche (2003). Figure 1a shows two BTCs of the slow and the fast experiment in terms of the relative absorption at

436nm against number of exchanged pore volumes. This wavelength is absorbed by ferric oxides, clay minerals and humic substances, which might serve as carrier for organic or inorganic contaminants. Both BTCs gradually decline from the beginning to the end. While 'q slow' strays generally above 'q fast', it also shows quite high fluctuations, especially at the beginning. 'q fast' reveals a smoother course and a distinctive rise of concentration after the flow interruptions. The second efflux-fraction after the flow interruption exhibits even higher levels.

To facilitate the understanding of this behavior, figure 1b shows the results of simulations revealing qualitatively similar properties. These sets are characterized by the same release-reaction properties (k, K and p) and, like in the real world experiment, differ only in the applied flow velocity q (Table 1). Obviously, 'q slow' strays higher than 'q fast'. Both show a general decline except for the very beginning. 'q fast' also exhibits the rise of concentration after a flow interruption. These two findings clearly indicate that at 'q slow' the system is at equilibrium and at 'q fast' it is not. The transition between the two cases is attributable to a very narrow range of the Damköhler-number (Wehrer and Totsche, 2003). Thus, knowing one unknown of Equation 1, the release-reaction time scale can be derived. Furthermore, by the height of the concentration difference before and after the two flow interruptions, the release rate can be determined.

Some experimental findings deviate from the expected behavior. Firstly, no initial rise could be observed. This hints to the point that the initial condition of the experiment and the simulation differ dramatically. The initial high release is due to the export of readily available fraction of mobilizable organic and inorganic materials (Münch et al. 2002; Weigand and Totsche, 2003). Such materials are endogenous (microbial activity) or exogenous (preparation of the sample by drying and sieving) and result in a "first flush" behavior.

The behavior of Σ PAH is displayed in Figure 3. It shows an initial rise of the concentration during the first half of the experiment (until approximately the second flow interruption) and a final decline. Similar to the example discussed above, the concentration level of the slow column strays above that of the fast one. With respect to the fast experiment, again a rise of the concentration after the flow interruptions becomes obvious. This is not the case for the 'slow' column. Even a decline of concentration after the second flow interruption occurs. Both BTCs show some fluctuations of PAH concentrations.

Again, it can be concluded that the slow flow velocity system is near equilibrium with respect to PAH release, while the fast one is not. However, the initial rise of the concentration during the first part of the experiment needs further investigation, as it is not totally explainable by the conceptual model (Figure 2b). In the simulation, the initial rise of the concentration lasts for 1.5 pv only, it can be extended to a maximum of 2 pv by further parameter adjustment (data not shown). A possible reason for an enduring rise of the concentration can be found in the wetting behavior of the soil sample. It can be assumed that the transfer of contaminant from dry regions to the mobile phase is inhibited. Because the contamination is hydrophobic in nature, energy and consequently, time is needed to moisten the source regions of the PAHs, which were air dry prior to the experiment. Because incompletely wetted surfaces in the soil might lead to variations of flow paths, this might explain the erratic fluctuations of the PAH concentrations. After complete wetting of the system, the expected decline of concentration can be observed along with a smoother curve.

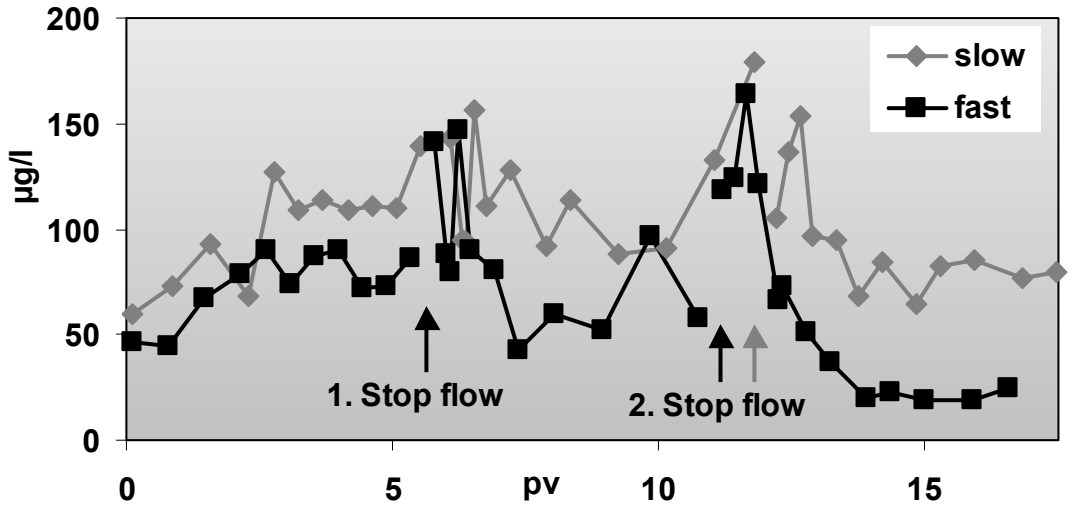

Figure 3: BTC of PAHs of two soil columns, employing two flow velocities and two flow interruptions (duration 24 h and 120 h, respectively)

4. Conclusions

- The described experimental design, using different flow velocities in two parallel soil columns and applying two flow interruptions, can be used for the quantification of release rates and Damköhler-numbers.
- The initial period of the column experiment has proved critical for the analysis, especially if the soil is homogenized (dried and sieved) prior to application. In particular, if the soil reacts hydrophobic, the release rate of PAHs can not uniquely be identified. It must be recommended, that either the efflux of the first few pore volumes has to be discarded or the experiment has to be run in closed flow design initially.

5. References

Brusseau, M.L., Qihong, H. and Sristava, R., 1997. *Using flow interruption to identify factors causing nonideal contaminant transport*. Journal of Contaminant Hydrology, 24, 205-219.

Koch, S., Flühler, H., 1993a. *Solute Transport in aggregated porous media. Comparing model independent and dependent parameter estimation*. Water, Air and Soil Pollution, 68, 275-289.

Koch, S., Flühler, H., 1993b. *Nonreactive solute transport with micropore diffusion in aggregated porous media determined by a flow-interruption method*. Journal of Contaminant Hydrology, 14, 39-54.

Totsche, K.U., 1998, 2001. *Reaktiver Stofftransport in Böden: Optimierte Experimentdesigns zur Prozeßidentifikation*. Bayreuther Bodenkundliche Berichte, Band 75. Universität Bayreuth, Bayreuth.

Totsche, K.U., 2000. CARRY Version 6.1. Reference Manual.

Wehrer,M., Totsche, K.U., 2003. Non-equilibrium transport of reactive solutes: identification of processes and sensitivity analysis by means of break-through curves in column outflow experiments. Z. Pflanzenernährung und Bodenkunde, accepted.

Weigand H. & Totsche K. U. 1998. Flow and reactivity effects on dissolved organic matter transport in soil columns. *Soil Sci. Soc. Am. J.* 62:1268-1274

Münch, J.M., Totsche K. U., Kaiser K. 2002. Physicochemical factors controlling dissolved organic carbon release in forest subsoils - a column study. *European J. Soil Sci*., 53:311-320

POSTERS

LARGE SCALE DIFFUSE POLLUTION: INTEGRATED SOIL AND WATER PROTECTION

Large scale input to soil and water environments - Evaluative scenarios with a spatially resolved multimedia model linking a soil-water box model to an air quality model

Till M. Bachmann, Rainer Friedrich

Institute of Energy Economics and the Rational Use of Energy, University of Stuttgart, Hessbruehlstr. 49a, 70565 Stuttgart, Germany
Phone: +49 (0)711 78061-66, Fax: +49(0)711 7803953 E-Mail: Till.Bachmann@ier.uni-stuttgart.de

Abstract: In recent years the impact of hazardous pollutants due to diffuse exposures has been realized to pose a threat to human and ecosystem's health. In order to assess such impacts also via ingestion a multi-media environmental fate framework has been developed at the European scale. This modeling framework is based on the spatially resolved impact pathway approach that has been developed and implemented in the software tool 'EcoSense' for to assess external costs from human activities. The integrated WATer and SOil environmental fate, exposure and impact assessment model of Noxious substances for Europe (WATSON - Europe) has been added to 'EcoSense' by linking an air quality backward trajectory model to a level III/IV multi-media type water and soil model. This coupling allows to assess impacts of persistent, bioaccumulative and toxic (PBT) substances especially on human health also via ingestion. Coming from emissions to air, the coupling of an air quality model to a soil and water box model without back-emissions to air is justified for most of the PBT substances due to negligible back-transfer to air. Evaluative results of the environmental fate of lead and Benzo[a]pyrene are shown for the Rhine catchment.

1. Introduction

In recent years the impact of hazardous pollutants due to diffuse exposures has been realized to pose a threat to human and ecosystem's health. In order to assess such impacts also via ingestion a multi-media environmental fate framework has been developed at the European scale. This modeling framework is based on the spatially resolved impact pathway approach that has been developed and implemented in the software tool 'EcoSense' (e.g. Krewitt et al., 1998) for to assess external costs from human activities developed within the EU-funded project series 'Externalities of Energy' (ExternE, European Commission, 1999). External costs are a measure in environmental economics to show whether all impacts on the environment e.g. by the production or use of a product are accounted for in its price. External costs occur if the market does not take such impacts into account. The impact pathway approach estimates external costs in that it links emissions by a human activity to an impact on receptors, i.e., either on human health or the environment (reading figure 1 from top to bottom). For this the concentrations in the different media (air, water, soil) need to be computed in order to assess a receptor's exposure to the harmful substance. As a last step these impacts are transformed into monetary units by means of monetization, preferably by contingent valuation studies.

The integrated WATer and SOil environmental fate, exposure and impact assessment model of Noxious substances for Europe (WATSON – Europe, Bachmann, in preparation) has been added to 'EcoSense' by linking an air quality backward trajectory model to a level III/IV multi-media type water and soil model. This coupling allows to assess impacts of persistent, bioaccumulative and toxic (PBT) substances especially on human health also via ingestion. Coming from emissions to air, the coupling of an air quality model to a soil and water box model without back-emissions to air is justified for most of the PBT substances due to negligible back-transfer to air (Margni et al., submitted).

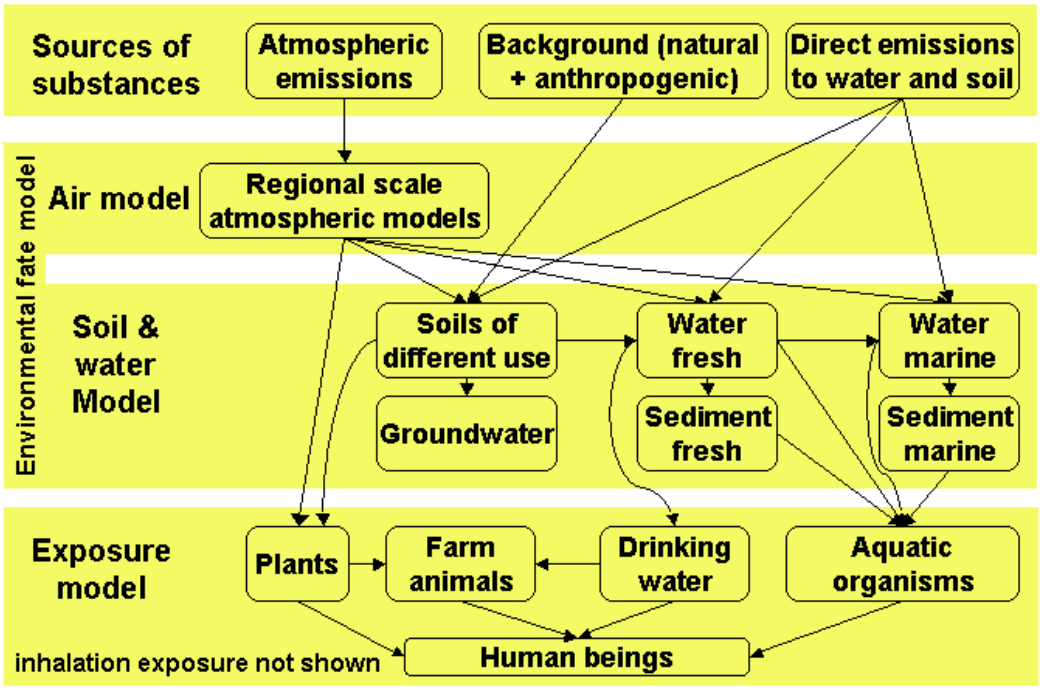

Figure 1: Conceptual structure of the multi-media model and the exposure assessment (arrows denote a substance's environmental pathway)

2. Method

The environmental fate of substances is influenced by various processes (e.g. advective transport by water: matrix leaching in soils, surface runoff, discharge, soil erosion; sediment resuspension; diffusion). In order to describe these processes, typical values for hydrological data and land use have been mostly adopted from the literature (watershed data: U.S. Geological Survey's EROS Data Center (1996); hydrology: Baumgartner& Liebscher (1990), Döll et al. (2002), Döll et al. (2003); land use: European Environment Agency (2000), Lehner et al.(2001); sediment and related processes: Brandes et al. (1996); erosion: EC, (1996)).

The model parameters and emission data specified for lead and Benzo[a]pyrene (BaP) are given in table 1 and 2, respectively. In order to cope with the different environmental behaviour of the PBT substances the partitioning between the aqueous and solid phases of heavy metals and lipophilic organic compounds is defined as a function of the key parameters pH and organic carbon content, respectively (note that considering chemical speciation at this spatial resolution is practically not feasible). In order to evaluate the influence of spatial variability at the regional scale, the Rhine catchment is subdivided into 90 base regions. Each base region generically consists of different compartments. These were distinguished according to a land use's different characteristics in terms of permeability, soil erosion and exposure to human beings. The following compartments are, thus, considered: freshwater bodies and corresponding sediments, glaciers/permanent snow, semi-natural ecosystems, arable land, pastures, non-vegetated land, and urban/built-up areas.

The main working hypothesis is that different processes are important for the environmental fate and hence the assessed impact of different (groups of) substances. For instance, the

process of transformation is not needed when doing a mass balance for a (non-radioactive) element. In WATSON, pollutants are assigned to substance types for which processes are defined allowing a flexible (database-based) way to adjust the model to the user's needs.

Table 1 - Properties and emissions of Pb

Parameter	**value**
K_d[a] [m^3/kg] for pH range of	
4.0-6.0	0.88
6.5-8.5	3.11
9.0-9.5	7.00
atmospheric deposition[b] [µg/m^2/d]	
wet	10.85
dry	5.29

[a] solid-water partitioning coefficient (K_d) values derived from Anonymous (1999)

[b] average Pb depositions to the Rhine catchment resulting from regional air quality modelling of emissions for 1990 given by Berdowski et al. (1997)

Table 2 - Properties and emissions of BaP

Parameter	**value**
log Kow[a] [-]	6.13
half-lives[b] [d]	0.88
water	60
sediment	900
built-up areas	258
non vegetated areas	400
semi natural ecosystems	197
pasture	200
arable land	200
atmospheric deposition[c] [µg/m^2/d]	
wet	4.08
dry	1.88

[a] value for the octanol-water partitioning coefficient taken from (Rippen und Voigt, 1998)

[b] values set to values similar to those given in (Rippen und Voigt, 1998)

[c] average Pb depositions to the Rhine catchment resulting from regional air quality modelling of emissions for 1990 given by Berdowski et al. (1997)

3. Results

The poster will present concentrations for lead and BaP in the steady-state and dynamic situation. Additionally, the 'time to steady-state' will be assessed. This is the time until which a defined fraction of the steady-state solution is achieved. The latter is a good indicator when the steady-state solution will actually come into effect.

4. Acknowledgements

The authors gratefully acknowledge the financial support of the European Commission through the "Energy, environment and sustainable development"-programme given to the ***NewExt*** (New elements for the assessment of external costs from energy technologies, EC Project number: ENG1-2000-00129) and ***GREENSENSE*** projects (An applied integrated environmental impact assessment framework for the European union, EC Project number: EVG1-2000-00022) as well as through the "Sustainable and Competitive Growth"-research programme given to the ***OMNIITO***X-project (Operational Models aNd Information tools for Industrial applications of eco/TOXicological impact assessments, EC Project number: G1RD-CT-2001-00501).

We also acknowledge the collaboration with David W. Pennington and Olivier Jolliet (Swiss Federal Institute of Technology in Lausanne, EPFL). For further details related to their spatial model for Europe please contact David W. Pennington (david.pennington@epfl.ch).

5. References

Anonymous, 1999. Understanding variation in partition coefficient, K_d, values - Volume II: Review of Geochemistry and Available K_d Values for Cadmium, Cesium, Chromium, Lead, Plutonium, Radon, Strontium, Thorium, Tritium (^3H), and Uranium. Herndon, VA, USA, Office of Radiation and Indoor Air Office of Solid Waste and Emergency Response, U.S. Environmental Protection Agency; Office of Environmental Restoration, U.S. Department of Energy.

T.M. Bachmann (in preparation): Application of the impact pathway approach to the media soil and water at the regional scale : coupling of the EcoSense Europe multi-source model with the integrated WATer and SOil environmental fate, exposure and impact assessment model of Noxious substances (WATSON) for Europe. Doctoral thesis, in preparation, University of Stuttgart. p.

A. Baumgartner and Liebscher, H.-J., 1990. Allgemeine Hydrologie, quantitative Hydrologie. Gebrüder Borntraeger, Stuttgart, p. 673.

J.J.M. Berdowski, Baas, J., Bloos, J.P.J., Visschedijk, A.J.H. and Zandvend, P.Y.J., 1997. The European Atmospheric Emission Inventory of Heavy Metals and Persistent Organic Pollutants for 1990. Berlin, Apeldoorn, Umweltbundesamt; TNO Institut für Umwelt, Energie und Verfahrensinnovation.

L.J. Brandes, den Hollander, H. and van de Meent, D., 1996. SimpleBox 2.0: a nested multimedia fate model for evaluating the environmental fate of chemicals. Bilthoven, the Netherlands, National Institute of Public Health and the Environment (RIVM).

P. Döll, Kaspar, F. and Lehner, B., 2003. A global hydrological model for deriving water availability indicators: model tuning and validation. Journal of Hydrology 270 (1-2): pp. 105-134.

P. Döll, Lehner, B. and Kaspar, F., 2002. Global modeling of groundwater recharge. In: G.H. Schmitz (Eds), Proceedings of Third International Conference on Water Resources and the Environment Research, Technical University of Dresden, Germany. pp. 27-31.

European Commission, 1996. EUSES, the European Union System for the Evaluation of Substances. Ispra, Italy, National Institute of Public Health and the Environment (RIVM), the Netherlands. Available from the European Chemicals Bureau (EC/JRC), Ispra, Italy.

European Commission, 1999. Externalities of Fuel Cycles - ExternE Project. Brussels - Luxembourg, European Commission DG XII, Science Research and Development, JOULE.

European Environment Agency, 2000. CORINE land cover database.

W. Krewitt, Mayerhofer, P., Trukenmüller, A. and Friedrich, R., 1998. Application of the Impact Pathway Analysis in the Context of LCA. The International Journal of Life Cycle Assessment 3 (2): pp. 86-94.

B. Lehner and Döll, P., 2001. A global wetlands, lakes and reservoirs data set. Kassel, Center for Environmental Systems Research, University of Kassel, Germany.

M. Margni, Pennington, D.W., Bennett, D.H. and Jolliet, O., submitted. Redefining Multimedia Modelling: Coupling Single-Medium Models and the importance of Feedback. Environmental Science & Technology: pp.

G. Rippen and Voigt, K., 1998. Handbuch Umweltchemikalien : Stoffdaten, Prüfverfahren, Vorschriften : mit Datenquellen. ecomed, Landsberg/Lech, p.

U.S. Geological Survey's EROS Data Center, 1996. HYDRO1k geographic database developed from the USGS' 30 arc-second digital elevation model (DEM) of the world (GTOPO30), U.S. Geological Survey (USGS) in cooperation with UNEP/GRID Sioux Falls. 2001.

Field persistence of atrazine and metribuzin in soils of Argentina

Francisco Bedmar[1], José L. Costa[2], and Peter E. Daniel[1]

[1]*Facultad de Ciencias Agrarias, Universidad Nacional de Mar del Plata, CC 276 (7620) Balcarce, Argentina;*
[2]*Instituto Nacional de Tecnología Agropecuaria (INTA), EEA Balcarce, CC 276, (7620) Balcarce, Argentina; E-mail: fbedmar@balcarce.inta.gov.ar*

Introduction

The herbicides atrazine (2-chloro-4-ethylamino-6-isopropylamino-1,3,5-triazine), and metribuzin (4-amino-6-tert-butyl-3-methylthio-1,2,4-triazin-5(4H)-one) have been and are extensively used in Argentina for control of a wide variety of broadleaf and grassy weeds. Atrazine is at present the most used herbicide in corn, while metribuzin was extensively applied in soybean up to the coming of RR soybean varieties applied with glyphosate. At present, metribuzin is extensively used in Argentina in potato and horticultural crops.

The processes of degradation and nonlabile residue (bound residue) formation determine, to a large extent, the persistence of pesticides in soils. Walker (1976) found that the first-order rate law, when fitted to simazine and prometryne degradation data produced correlation coefficients significant at P=0.001, and thus assumed first order kinetics. A simulation model, which Walker developed, satisfactorily estimated the persistence of these herbicides under field conditions. In subsequent years the modified version of this model adequately predicted field persistence of several pesticides from laboratory derived first order rate constants (Smith and Walker, 1989; Walker et al., 1992).

Persistence defines the "lasting-power" of a pesticide. Most pesticides break down or "degrade" over time as a result of several chemical and micro-biological reactions in soils. Sunlight breaks down some pesticides. Generally, chemical pathways result in only partial deactivation of pesticides, whereas soil microorganisms can completely break down many pesticides to carbon dioxide, water and other inorganic constituents. Some pesticides produce intermediate substances, called "metabolites" as they degrade. The biological activity of these substances may also have environmental significance. Because populations of microbes decrease rapidly below the root zone, pesticides leached beyond this depth are less likely to be degraded. However, some pesticides will continue to degrade by chemical reactions after they have left the root zone.

Degradation time is measured in "half-life." Each half-life unit measures the amount of time it takes for one-half the original amount of a pesticide in soil to be deactivated. Half-life is sometimes defined as the time required for half the amount of applied pesticide to be completely degraded and released as carbon dioxide. Usually, the half-life of a pesticide measured by the latter basis is longer than that based on deactivation only. This is especially true if toxic or nontoxic metabolites accumulate in the soil during the degradation.

The objective of this study was to characterize atrazine and metribuzin dissipation sprayed at field in two soils of Argentina.

Materials and Methods

Field studies were conducted in 1999-2000 and 2000-2001 in two different locations (Balcarce, and Tres Arroyos) within the humid pampa region in the southeast of Buenos Aires province (Argentina). The Balcarce and Tres Arroyos soils are both classified as a clay loam (fine, thermic, illitic, Typic Argiudoll). The Balcarce soil has a pH of 5.6, organic matter content of 6.7%, cation exchange capacity of 27.6 cmol/kg, and sand/silt/clay percentages of 32.8/38.3/28.9, respectively. The Tres Arroyos soil has a pH of 6.0, organic matter content of 4.2%, cation exchange capacity of 22.2 cmol/kg, and sand/silt/clay percentages of 40.5/31.5/28.0, respectively.

Both soils are commonly used in agricultural production, and all soil characteristics presented describe the 0 to 10 cm soil zone. The area was disked with a tandem disk two times starting in September to bury all residue each year in both locations. The final tillage pass was performed with a field cultivator equipped with a rototiller. Herbicides were applied superficially on November 5, 1999 in Balcarce and Tres Arroyos, and on November 3 and 30, 2000 in Tres Arroyos and Balcarce respectively. No crop was planted each year in any location. Treatments were arranged in a randomized complete block design with three replications. Atrazine at 2000 g/ha, and metribuzin at 480 g/ha were applied with a CO_2-pressurized sprayer in 170 L/ha at 276 kPa to 5.0- by 8.0-m plots.

Soil samples were collected with a hand-held core sampler from the 0 to 10 cm soil depth 0, 17, 39, 69, and 122 days after treatment (DAT), and 0, 26, 42, 71, 97 and 139 DAT in Balcarce in 1999-2000 and 2000-2001 respectively, while in Tres Arroyos samples were taken 0,19, 39, 66, and 122 DAT in 1999-2000 and 0, 14, 28, 68, 98, and 136 DAT in 2000-2001. Ten cores per plot were collected using a 3 cm diameter plugger to a depth of 10 cm. Once collected in the field, soil samples were immediately stored at –18° C until chemical analysis, later thawed and air dried, ground to pass through a 2-mm sieve, thoroughly mixed and a sub sample retained for chemical analysis. Cumulative rainfall data following herbicide application in each year is provided in Table 1.

Before analysis, the soil samples were thawed and homogenized. Immediately afterwards two aliquots were taken, one for extraction of the herbicides, the other for determination of water content.

Extraction Procedure

25 g of homogenized, wet soil were extracted with 50 ml of 90% pesticide grade methanol in deionized water by sonication during 15 minutes. After sonication, de slurry was filtered through a 0.45µ pore size membrane and the residue was washed with a 10 ml portion of deionized water. The combined filtrate was quantitatively transferred to a beaker of 1 liter capacity, the volume was brought to 500 ml with deionized water and 3 g of NaCl were added. This solution was passed through a preconditioned Varian Bond-Elute® Atrazine SPE cartridge at a flow of approximately 6 ml / min. Herbicides were eluted from the cartridge with 4 ml of HPLC grade methanol and the eluate transferred to vials for analysis by HPLC.

Chemical analysis

Finally, the eluate was analyzed by means of a Hewlett-Packard 1100 system HPLC (Agilent Technologies, Hewlett Packard Strasse 8, 76337 Waldbronn, Germany), consisting of a quaternary pump system, a diode array detector programmed at 224 nm (atrazine) and 214 nm (metribuzin) and an autosampler, using a Varian ChromSpher 5 Pesticide column with dimensions of 150 mm by 4.6 mm and a guard column in front of the analytical column. A flow of 1.2 ml min^{-1} of 100 % buffer was used during 1 min followed by a gradient to reach

24 % of acetonitrile, in a period of 13 min. The buffer composition was: 95% 0.025M Na H_2PO_4, pH=5.0 + 5% acetonitrile.

Statistical analysis

Herbicide concentration data were empirically fitted to first-order kinetics (Walker 1987). The atrazine or metribuzin soil concentrations were converted to the natural logarithm and then linearly regressed against time in days to the following equation:

$$\ln (C/C_0) = -kt$$

where C is the concentration in ppb at time t, C_0 is the initial concentration in ppb, k is the first-order constant, and t is the time in days after treatment. The first-order rate constant was estimated for each herbicide through regression analysis by plotting $\ln (C/C_0)$ as a function of time. The slope of the resultant line was considered the first-order rate constant (Walker 1987). A dissipation half-life (DT_{50}) was calculated for each soil, each herbicide and each year from the equation:

$$DT_{50} = 0.693/k$$

where DT_{50} is the herbicide half-life in days, and k is the first-order dissipation rate constant. DT_{50} confidence intervals were calculated based on the 95% confidence intervals around the k value for each soil, each herbicide, and each year. Each year + soil + herbicide treatment combination was considered as an individual regression line, and herbicide dissipation was examined by comparing confidence intervals. If the confidence intervals overlapped, then the dissipation rate was not different. This is a conservative approach because two standard deviations are given for each rate constant, resulting in a 99% probability level (Brown et al. 1996).

Table 1. Cumulative precipitation following herbicide application in 1999-2000 and 2000-2001.

Location	Year	Application date	Weeks after application									
			2 mm	4	6	8	10	12	14	16	18	20
Balcarce	1999	November 5	23	38	58	103	137	151	304	398	461	567
	2000	November 30	56	83	175	191	211	223	326	398	436	464
T.Arroyos	1999	November 5	38	82	100	188	254	279	383	421	526	544
	2000	November 3	20	20	52	74	134	194	233	252	351	388

Results and discussion

The first-order dissipation rate constant (k) for each herbicide differed highly significant (p = 0.01) between years for the same location. In general, values of k were quite similar for both herbicides, locations and years except for metribuzin in Tres Arroyos where the higher values for both years were achieved (Table 2 and 3). Half life (DT_{50}) of atrazine was quite similar between locations and years, ranging between 13 and 15 days for Balcarce and averaging 13 days in Tres Arroyos (Table 2). In the case of metribuzin, DT_{50} values ranged from 14 to 16 days for Balcarce and from 8 to 9 for Tres Arroyos (Table 3). The low DT_{50} values obtained in Tres Arroyos would be related to high dissipation rates achieved for that location. Half life values obtained in this work are in general lower that those reported in average for laboratory experiments. In that case, 60 days for atrazine and 30-60 days for metribuzin are usually reported (Ahrens 1994). However, our results agree with DT_{50} reported by Gallaher and Mueller (1996) who obtained in no-crop situations at field values of 17-27 days for atrazine and 16-17 days for metribuzin.

Correlations between atrazine or metribuzin k and DT_{50} and selected soil properties were calculated (Table 4). Atrazine k and DT_{50} values were not significantly correlated ($p = 0.05$) with any soil properties, while metribuzin with exception of clay, correlated highly ($p = 0.01$) with all soil properties. Correlation analysis for metribuzin indicated a positive relationship of DT_{50} with OC, CEC and clay, while a negative correlation was observed for pH, silt and sand (Table 4).

Stepwise multiple linear regression was used to further evaluate the relationship between atrazine or metribuzin persistence and soil properties. This procedure indicated in the case of atrazine that although only organic carbon content was related to half life, this correlation was poor ($r^2 = 0.25$, $DT_{50} = 10.98 + 0.70$ OC). For metribuzin, half life was positively related to organic carbon content and negatively related to silt content (r2 = 17.32 + 9.02 OC – 0.98 silt).

Results obtained for atrazine do not agree with soil properties although a weak relationship with organic carbon content could partially explain persistence. In the case of metribuzin, persistence was explained mainly by organic carbon content and to a less extent by silt content. It is probable that a complex interaction between climatics and edaphics conditions could explain the results. Besides this, as was exposed by Dinelli et al (2000), variability in persistence of atrazine and metribuzin could also be due to the variability at field in microbian biomass distribution and activity. For various pesticides, it has been shown that dissipation rate may vary greatly, not only with soil type but with temperature and soil water content (Walker, 1976; Walker et al., 1992; Obrador et al., 1993). In many instances, however, the effects of temperature and moisture on the kinetics of disappearance of pesticides are not well enough understood to be described quantitatively by temperature and moisture functions in simulation models.

Table 2. First-order degradation rate constants (k) and DT_{50} values for atrazine in Balcarce and Tres Arroyos soils for the 1999-2000 and 2000-2001 seasons[a].

Location	Year	k	C.I.	r^2	DT_{50}	C.I.
		----------d^{-1}----------			----------d----------	
Balcarce	1999	0.0549	0.0508-0.0591	0.98	13	12-14
	2000	0.0468	0.0397-0.0540	0.92	15	13-18
T.Arroyos	1999	0.0553	0.0468-0.0637	0.94	13	11-15
	2000	0.0543	0.0518-0.0567	0.99	13	12-14

[a]k= first order constant; DT_{50} = half-life in days.
[b]C.I. = 95% confidence interval for k and DT_{50} values.

Table 3. First-order degradation rate constants (k) and DT_{50} values for metribuzin in Balcarce and Tres Arroyos soils for the 1999-2000 and 2000-2001 seasons[a].

Location	Year	k	C.I	r^2	DT_{50}	C.I.
		----------d^{-1}----------			--------d---------	
Balcarce	1999	0.0447	0.0416-0.0479	0.99	16	15-17
	2000	0.0511	0.0355-0.0666	0.79	14	10-20
T.Arroyos	1999	0.0853	0.0718-0.0989	0.95	8	7-10
	2000	0.0797	0.0604-0.0989	0.90	9	7-12

[a]k= first order constant; DT_{50} = half-life in days.
[b]C.I. = 95% confidence interval for k and DT_{50} values.

Table 4. Correlation of atrazine and metribuzin persistence calculated parameters with selected soil properties.

	Pearson correlation coefficients[a]			
	Atrazine[b]		Metribuzin[b]	
Independent variables	k	DT_{50}	k	DT_{50}
OC[c]	-0.49	0.49	-0.94**	0.94**
CEC[d]	-0.49	0.48	-0.91**	0.91**
pH	0.46	-0.47	0.90**	-0.91**
Clay	-0.18	0.17	0.57	0.60*
Silt	-0.43	0.44	-0.89**	-0.90**
Sand	0.42	-0.43	0.91**	-0.92**

[a] **, * denote significance at the $P \leq 0.01$, and 0.05 levels respectively. [b]k= first order constant; DT_{50} = half-life in days.
[c]OC = organic carbon, [d]CEC = cation exchange capacity.

References

Ahrens WH. (Ed). 1994. Herbicide Handbook, 7th edition. Weed Science Society America, Champaign, Illinois, USA, 352 pp.

Brown BA, Hayes RM, Tyler DD, and Mueller TC. 1996. Effect of long-term vetch (Vicia vilosa) cover crop and tillage system on fluometuron dissipation from surface soil. Weed Science, 44:171-175.

Dinelli G, Accinelli C, Vicari A, Catizone P. 2000. Comparison of the persistence of Atrazine and metolachlor under field and laboratory conditions. Journal of Agriculture and Food Chemistry. 2000:3037-3043.

Gallaher K, and Mueller T. 1996. Effect of crop presence on persistence of atrazine, metribuzin and clomazone in surface soil. Weed Science, 44:698-703.

Obrador A, Lechon Y, and Tadeo JL. 1993. Simulation of atrazine persistence in Spanish soils. Pesticide Science, 37:301-308.

Smith AE, and Walker A. 1989. Prediction of the persistence of the triazine herbicides
atrazine, cyanizine, and metribuzin in Regina heavy clay. Canadian Journal of Soil Science, 69:587-595.

Walker A. 1976. Simulation of herbicide persistence in soil. I. Simazine and prometryne. Pesticide Science, 7:41-49.

Walker A. 1987. Herbicide persistence in soil. Rev. Weed Science, 3:1-17.

Walker, A, Moon Y, and Welch SJ. 1992. Influence of temperature, soil moisture and soil characteristics on the persistence of Alachlor. Pesticide Science, 35:109-116.

Biodegradation of phenanthrene in unsaturated soil columns

Andreas Tiehm, Iris Brost, Michael Stieber

Water Technology Center, Department Environmental Biotechnology, Karlsruher Str. 84, 76139 Karlsruhe, Germany, +49(0)721-9678 220 (phone), +49(0)721-9678-101 (Fax); tiehm@tzw.de

Abstract: Understanding and quantifying biodegradation in the subsurface is a prerequisite for the application of transport models and assessing the environmental risk of contaminated materials deposition. In our study, biodegradation of phenanthrene was examined in two unsaturated soils (quartz sand and a natural sorptive sand) with a moderate flow rate and under conditions representing heavy rain. In columns inoculated with an adapted mixed culture, the influent phenanthrene was degraded immediately resulting in effluent concentrations below the detection limit. After 250 h of constant operation, an increased flow rate resulted in rapid phenanthrene breakthrough. Without inoculation, phenanthrene was eliminated by retardation in the natural sorptive sand during initial moderate flow conditions. Afterwards, the accumulated phenanthrene was degraded by the microflora initially present in the soil. During subsequent heavy rain conditions, the highly active microflora was capable to eliminate the influent phenanthrene completely. In conclusion, constant average flow rates seem not to be suitable to represent field conditions. Different scenarios with varying microbial activity and flow rates, but also with varying frequencies of moderate and heavy rain, have to be considered to model pollutant elimination during transport in unsaturated soil.

1. Introduction

Elimination of environmental pollutants during transport through unsaturated soil layers is essential to protect groundwater resources. The main elimination processes in the subsurface are sorption and biodegradation. For many environmental pollutants, the subsurface soil represents a buffer system retaining the contaminants, with pollutant retardation being a function of organic carbon content and lithology (Kleineidam et al., 1999; Rügner et al., 1999). However, if pollutants continuously accumulate, thresholds for storage and buffering finally will be exceeded and sudden contaminant release can occur. Microbial degradation in sorptive materials results in pollutant elimination and restoration of the buffer capacity (Tiehm et al., 2002). Understanding and quantifying biodegradation in the subsurface is a prerequisite for the application of transport models and assessing the environmental risk of contaminated materials deposition.

To assess the fluxes of pollutants, a sufficient understanding of sorption and biodegradation processes is needed. Most studies into pollutant biodegradation have involved continuously mixed systems or column studies under saturated conditions. A previous study has shown that degradation kinetics can vary considerably in saturated batch, saturated column, and unsaturated column experiments (Estrella et al., 1993). Therefore, the use of unsaturated soil columns is expected to produce biodegradation rates that would more closely represent those of vadose zone conditions. Under unsaturated conditions, moisture content (Sleep and Mulcahy, 1998) and residence times (Thomsen et al., 1999) have been considered to effect biodegradation. Furthermore, transformation of organic chemicals depend strongly on their retention by the solid phase. Sorption tends to decrease the degradation rate due to reduction of its availability to microbial attack (Tiehm et al., 1997).

It is the objective of our study to examine the effect of biodegradation on pollutant transport in unsaturated soil. Phenanthrene was chosen as a hydrophobic model compound. In first

experiments, phenanthrene elimination was studied for varying flow regimes (i) in two soil types, and (ii) with the original soil microflora and after additional inoculation of adapted microorganisms.

2. Materials and Methods

The experiments were done in a column system equipped with a vacuum unit. Four columns were operated simultaneously. Each column (volume: 6 L) was filled with 8-9 kg soil and operated below atmospheric pressure (fig. 1). Sorption and biodegradation were examined in inert quartz sand and for a natural sorptive soil. The quartz sand had a grain size of 0.1 – 0.5 mm and an organic carbon content < 0.01%. The sorptive soil had a grain size of 0.1 – 10 mm and 0.4% organic carbon.

The soil columns were percolated with autoclaved mineral medium (Lockhead & Chase, 1973) with flow rates representing moderate (3.4 L/m^2*h) or heavy rain (47.5 L/m^2*h) conditions, corresponding to a water content of 10% and 28% in the quartz sand, and 7% and 23% in the natural sorptive sand, respectively. Influent phenanthrene concentrations between 200 – 400 µg/L were adjusted. Biodegradation was studied without inoculation, i.e. with the microflora initially present in the soil, or after additional inoculation with a phenanthrene adapted mixed culture. In order to study elimination by adsorption only, 1 g/L azide was added to inhibit microbial activity. Aqueous phase phenanthrene concentrations were determined by GC/FID and GC/MS after extraction with cyclohexane.

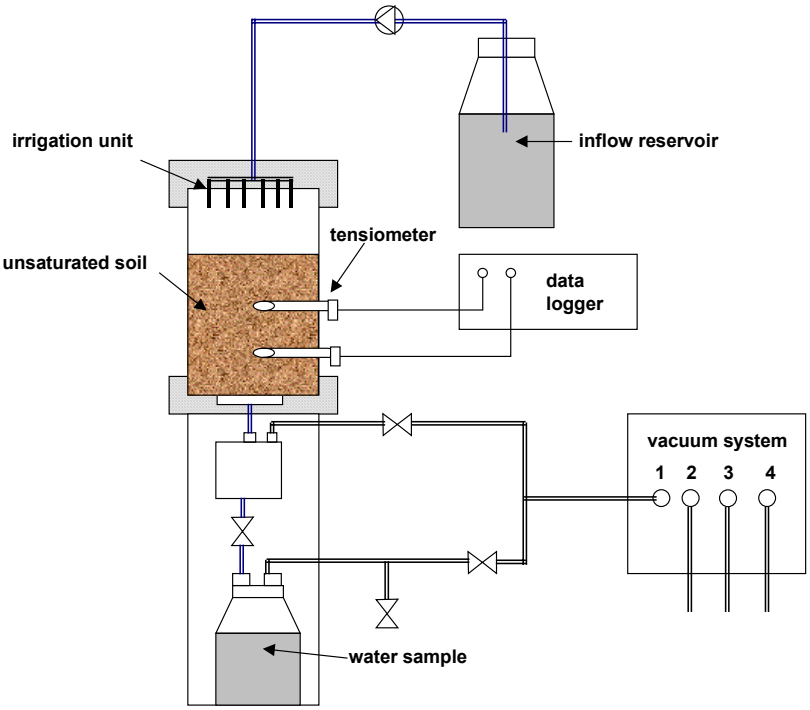

Figure 1: Set-up of the laboratory column experiments.

3. Results and Discussion

Adsorption only

Sorption was studied after addition of 1 g/L Na-azide in order to inhibit microbial activity. Operation of the unsaturated quartz sand column with a hydraulic loading of 3.4 L/m^2 * h

resulted in a phenanthrene breakthrough after 35 h. The effluent concentration plateaued at a C/C_0 value of about 1 after about 250 h (fig. 2 A). In contrast to the quartz sand, a significant retardation was observed in the natural sorptive sand. Phenanthrene breakthrough was observed for the first time after 150 h. 80% of the influent phenanthrene was still retained after 250 h (fig. 2 B).

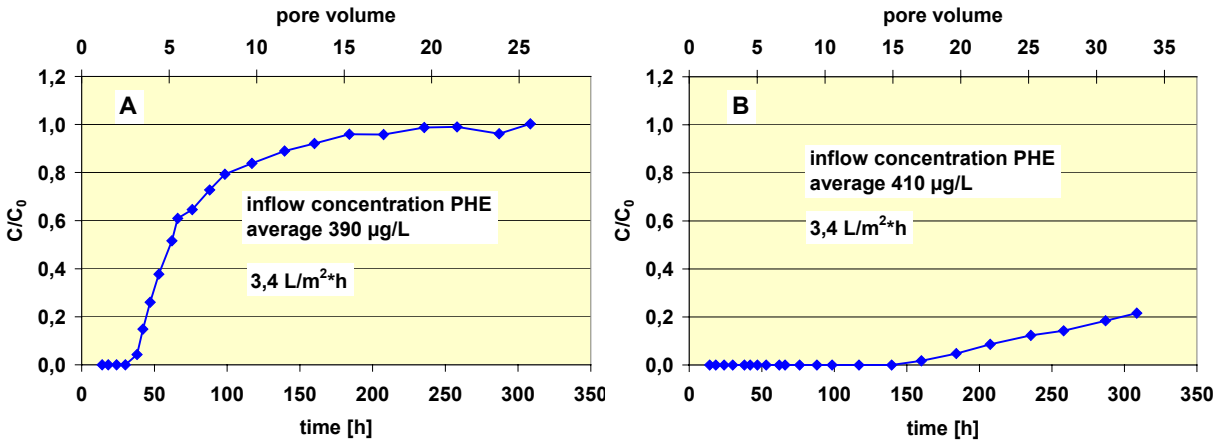

Figure 2: Breakthrough of phenanthrene in the biologically inactivated (A) quartz sand and (B) sorptive sand.

Adsorption and Biodegradation

Quartz sand:

Biodegradation in the quartz sand column inoculated with an adapted mixed culture resulted in a complete elimination of phenanthrene under slow flow conditions (3.4 L/m^2 * h). An increased flow rate for 7.5 h – simulating heavy rain (47.5 L/m^2 * h) – resulted in a maximum effluent concentration of about 200 µg/L (fig. 3). Obviously, the microbial community could not adapt quick enough to the increased substrate mass flow.

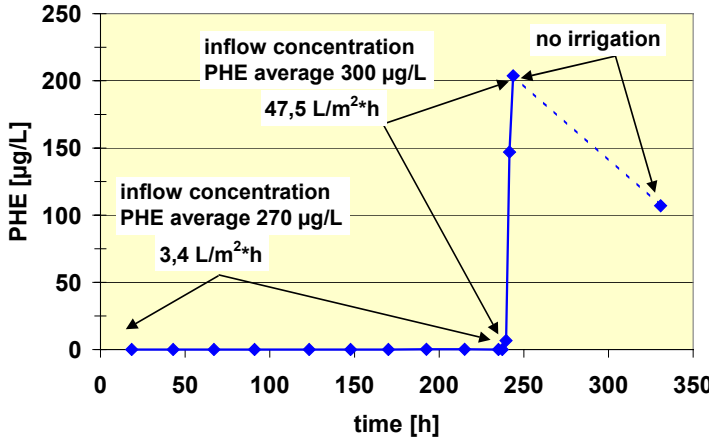

Figure 3: Quartz sand column inoculated with an adapted mixed culture: Effect of flow rate on effluent phenanthrene concentration.

In the quartz sand column initially operated with addition of azide (fig. 2 A), azide addition was stopped after 300 h. During subsequent percolation for 350 h, no biodegradation was observed (data not shown). Obviously, initial microbial numbers in the quartz sand were too low to result in significant phenanthrene biodegradation.

Natural sorptive sand:

In the first experiment, percolation was started after inoculation with an adapted phenanthrene degrading mixed culture. In this column, phenanthrene was not detectable in the effluent under moderate flow conditions (3.4 L/m^2 * h) indicating an efficient biodegradation. An increased flow rate for 7.5 h – simulating heavy rain (47.5 L/m^2 * h) – resulted in increasing effluent concentrations with a maximum of about 60 µg/L (fig. 4). The lower effluent concentration as compared to the quartz column (fig. 3) demonstrated the higher buffer capacity of this type of soil.

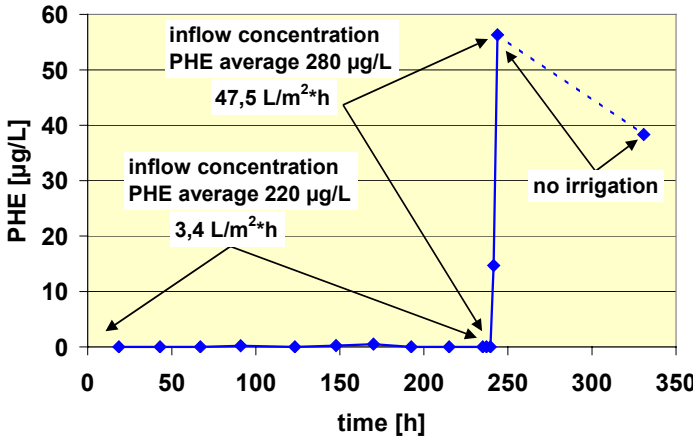

Figure 4: Natural sorptive sand column inoculated with an adapted mixed culture: Effect of flow rate on effluent phenanthrene concentration.

In the second experiment, phenanthrene elimination was studied after an initial period of inhibited bioactivity (shown in fig. 2 B) and without adding an pre-adapted phenanthrene degrading mixed culture. Under moderate flow conditions (3.4 L/m^2 * h), the phenanthrene effluent concentration increased for 150 h up to 45% of the influent loading of 220 µg/L. After 190 h of operation, effluent phenanthrene was below the detection limit of 0.2 µg/L (fig. 5). Obviously, the microbial community initially present in the sorptive sand was capable to degrade phenanthrene. Increasing phenanthrene elimination with longer operation time indicated biomass growth and adaptation. The phenanthrene eliminated by sorption in the initial period, subsequently was subject to biodegradation resulting in a regeneration of the sorption capacity of the soil. Due to the high amount of active biomass present at the onset of heavy rain conditions (47.5 L/m^2 * h), phenanthrene was completely eliminated also during the high loading period (fig. 5). As a result of the differences in mass and physiological status of the microbial community in the two experiments, significantly different phenanthrene effluent concentrations were obtained (fig. 4, fig. 5).

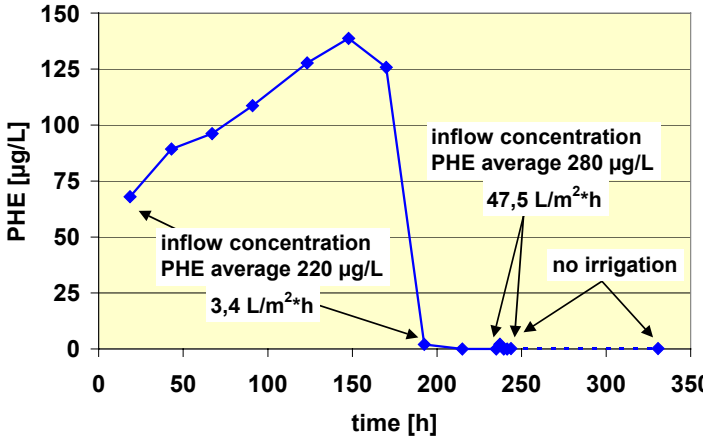

Figure 5: Natural sorptive sand column without inoculation of an adapted mixed culture: Effect of flow rate on effluent phenanthrene concentration.

4. Conclusions

The results demonstrate the important role of microbial adaptation, biomass, and physiological status on biodegradation kinetics. In the inoculated quartz sand and natural sorptive sand columns, the microbial community immediately degraded the influent phenanthrene resulting in effluent concentrations below the detection limit. After 250 h of continuous operation at low flow rate, an increased flow rate – representing heavy rain – resulted in a breakthrough of phenanthrene. Without inoculation, biodegradation of phenanthrene was not significant initially, but phenanthrene was eliminated by retardation in the natural sorptive sand. Subsequently, the accumulated phenanthrene was degraded resulting in a highly active microbial community after 200 h. This microbial community was capable to eliminate the influent phenanthrene completely during heavy rain conditions.

In conclusion, the pollutant biodegradation in unsaturated test systems is not only a function of influent concentrations and hydraulic retention time, but also of the mass and physiological state of the microflora. Constant average flow rates seem not to be suitable to represent field conditions. Different scenarios with varying flow rates, but also with varying frequencies of low and heavy rain, have to be considered to model pollutant elimination during transport in unsaturated soil.

5. Acknowledgement

The authors gratefully acknowledge financial support by the German Ministry of Education and Research (BMBF No. 02WP0201).

6. References

Estrella, M R, Brusseau M L, Maier R S, Pepper I L, Wierenga P J and Miller R M (1993) Biodegradation, sorption, and transport of 2,4-dichorophenoxyacetic acid in saturated and unsatirated soils. *Appl. Environ. Microbiol.* **59**(12): 4266-4273

Kleineidam S, Rügner H, Ligouis B, Grathwohl P (1999) Organic matter facies and equilibrium sorption of phenanthrene. *Environ. Sci. Technol*. **33**(10): 1637-1644

Lockhead A G, Chase F E (1973) Quantitative studies of soil microorganisms. V. Nutritional requirements of the predominant bacterial flora. *Soil Sci.* **55**: 185-195

Rügner H, Kleineidam S, Grathwohl P (1999) Long term sorption kinetics of phenanthrene in aquifer materials. *Environ. Sci. Technol*. **33**(10): 1645-1651

Sleep B E, Mulcahy L J (1998) Estimation of biokinetic parameters for unsaturated soils. *J. Envir. Engrg.* **124**(10): 959-969

Thomsen A B, Henriksen K, Gron C, Moldrup P (1999) Sorption, transport and degradation of quinoline in unsaturated soil. *Environ. Sci. Technol.* **33**(10): 2891-2898

Tiehm A, Gozan M, Müller A, Schell H, Lorbeer H, Werner P (2002) Sequential anaerobic/aerobic biodegradation of chlorinated hydrocarbons in activated carbon barriers. *Water Sci. Technol.* **2**(2): 51-58

Tiehm A, Stieber M, Werner P, Frimmel F H (1997) Surfactant-enhanced mobilization and biodegradation of polycyclic aromatic hydrocarbons in manufactured gas plant soil. *Environ. Sci Technol.* **31**(9): 2570-2576

Nitrate and atrazine leaching from corn in the "Argentinian Humid Pampas"

J. L. Costa[1], F. Bedmar[2], P. E. Daniel[2], V. C. Aparicio[2]

[1]Corresponding author: INTA, CC 276 (7620) Balcarce Argentina, Phone:54 2266 439100;Fax: 54 2266 4391001; E-Mail:jcosta@balcarce.inta.gov.ar
[2]FCA UNMDP, CC 276 (7620) Balcarce Argentina, Phone:54 2266 439100;Fax: 54 2266 4391001

Introduction

Water flow in the unsaturated zone of agricultural soils is of great importance in determining the fate of surface-applied soluble nutrients and pesticides. Concern for water quality in the rural Argentina has increased in the past decade. Costa et al., (2002), working in a rural setting of the Upper Pantanoso Stream Basin (UPSB) in the southeast of Buenos Aires Province, Argentina, reported that the fertilizers and soil organic carbon mineralization were the main sources of nitrogen in groundwater. The excess of NO_3^- in drinking water constitutes a risk for the human health. (Sasson, 1993; Weisemburger, 1991). Related to this problem the Environmental Protection Agency (USEPA 1995) in USA established for drinking water a critical value of 10 mg L^{-1} for NO^-_3 – N and the European Union was enacted a directive to prevent groundwater contamination caused by nitrates from agricultural sources (CEC, 1991). The drinking water regulations in the Province of Buenos Aires, Argentina established a critical value of 50 mg l-1 of NO^-_3 (11.3 mg L^{-1} for NO^-_3 – N).

The NO_3^- may have different ways of losses. It undergoes volatilization and denitrification, but those are of low magnitude and they would not explain the total losses of N which occur in different farm systems (Garcia et al., 1999; Sainz Rosas et al., 2001). Nitrate leaching appears as the main form of N loss, however the information about leaching of N from specific crops in the "humid pampas" is scarce.

The herbicides represent the main class of pesticides responsible for the contamination of groundwater (Funari et al., 1995). Atrazine is one of the herbicides more utilized in Argentina for weed control in corn. The doses of application are variables, however 2 kg ha^{-1} are usual in most parts of the country when applied alone, while in mixtures, mainly with Acetoclor, the dose oscillates between 1 and 1.5 kg ha^{-1}. Although the presence of Atrazine in groundwater is frequently reported (Flury, 1996; Kolpin et to the. 1997; Pasquarell and Boyer, 1996; USEPA, 1990), in Argentina the detection of pesticides in drinking water supplies is extremely rare. However, reliable water quality management requires more research to minimize future possible contamination. The objective of this work was to estimate the leaching losses of nitrate and atrazine in an agricultural cycle under field conditions.

Materials and methods

The experiment was conducted in a field plot on Mar del Plata soil at Balcarce County, Buenos Aires, Argentina. Some of the soil physical and chemical properties are shown in Table 1.

Neutron probe access tubes were installed into each subplot at a depth of 2 m. Ceramic soil-water suction samplers were installed to depths of 1, 1.5 and 2 m. The suction samplers were made with a 5-cm diameter, 20-cm long section of polyvinyl chloride (PVC) pipe. A ceramic

cup was cemented to one end and the opposite end was sealed with a two hole stopper. Two tubes were placed into the suction sampler through the stopper. One of them was used to apply vacuum and the other to collect the water sample.

To install the suction probe, a vertical hole was drilled by means of a soil auger with a diameter similar to that of the probe. To get good contact between the suction cup and the soil a slurry of the material from the soil auger was made and put back into the hole before inserting the suction probe. Once the suction sampler was located at the right depth, half of the hole was filled with the slurry. After that, a layer of bentonite was added to the hole. The rest of the hole was then filled with the slurry.

The tubes from the soil-water suction samplers were maintained buried at 30 cm depth below the plots to allow tillage operation. At the end of the plots the tubes were connected to a manifold where a vacuum pump supplied a suction averaging 4.2 and 5.6 kPa (Figure 1). Similar designs was previously used by Costa et al., (1994). During the period from August 11, 2001 to May 16, 2002 the concentration of nitrate and atrazine in the suction water samples were measured at different depths. Water sample were collected any time that the rainfall was grater than 30 mm.

In the water samples the N concentration was analyzed using colorimetric methods, KBr by ion-specific electrode, and atrazine by HPLC.

The plots were planted with corn and watered during the growing season using a drip irrigation system. The irrigation dripperlines were installed with a separation of 30 cm and the dripper on the dripperlines at intervals of 30 cm.

For determining deep percolation of water or drainage, the mass balance approach was used as follow:

$$DPR=I+P-\Delta S-Et-R \quad [1]$$

where DPR is the daily soil water percolation in mm, I the irrigation water applied during day in mm, P the rainfall during day in mm. ΔS the change in soil water storage in mm, Et the crop water use or evapotranspiration in mm during day calculated from the FAO Penman Montieth equation (Clarke et al., 1998) and R is the run-off in mm.

Nitrate and atrazine flux (Ln) below the root zone, at a depth of 1,1.5, and 2 m, was calculated from the equation:

$$Ln=DPR\ C_d \quad [2]$$

where DPR is the water drainage calculated at a depth of *d* m from Eq. 1 and Cd the NO3-N concentration in the soil solution sampled by soil water samplers at the *d* depth.

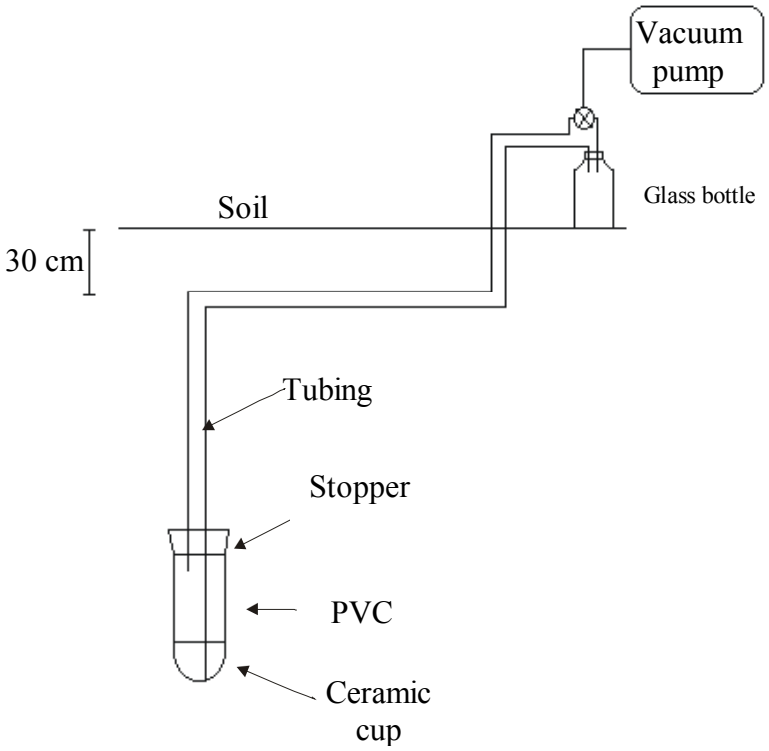

Figure 1: Set-up of ceramic cup field experiment.

Table 1. Organic carbon (OM), Clay, silt, sand, pH and cationic exchange capacity (CEC) from the Mar del Plata series soil.

Depth	OC	Textural analysis			pH	CEC	Gravimetric soil moisture at different soil tension in MPa		
		Clay	Silt	Sand			0.033	0.1	1.5
cm	----------%----------					cmol kg^{-1}	----------%----------		
0-10	3.9	28.9	38.3	32.8	5.6	27.6	30.6	29.1	14.7
10-20	3.8	29.5	37.6	32.9	5.6	25.7	29.1	24.7	15.6
20-30	2.5	30.2	33.8	36.0	5.8	25.9	29.1	23.5	15.6
30-40	1.8	34.8	29.8	35.4	6.1	23.6	31.3	25.8	17.1
40-50	1.2	40.7	26.2	33.1	6.4	25.9	34.9	29.6	19.6

Results and discussion

Nitrate

The amount of leached nitrate increased with the increasing dose of applied N (Table 2), these data confirm the hypothesis previously presented by Sainz Rozas et al. (2001) that the main losses of N would be through leaching more than the other kind of N losses. The initial peak concentration of N was detected in November 22 after 123 mm of accumulated drainage (from October 20 through November 22) (Figure 1). The high rainfall conditions after the fertilizer applications (November 13) could lead to this considerable nitrate losses by leaching.

Atrazine

We also detected a loss of atrazine of 0.013 kg ha^{-1} below the 1.5 m depth, which represents the 0.9% of the total applied atrazine (Table 2). Like in the case of nitrate, the atrazine concentration peak was detected after the application of the herbicide to the soil (Figure 1). Also the peak of Br^- concentration was produced at the same moment as the nitrate and atrazine peaks, which would indicate that part of atrazine moved at the same velocity as the non interactive tracer.

Bedmar et al., (1999), working with a similar soil but in packed soil columns found a retardation in the atrazine concentration peak of more than 4 pore volumes. Since there was no retardation in the manifestation of the atrazine peak in this study, we think that the water flow that produced the atrazine movement took place through the macropores of the soil. We assume also that the presence of macropores in these well structured soil could increased the loss of atrazine toward the groundwater.

Table 2. Nitrate and Atrazine losses from root zone from 11/10/01 through 16/5/02.

Applied		Leached		
Atrazine	NO_3-N	Atrazine	Nitrate[1]	
kg ha^{-1}				
-	0	-	26.4	c
-	100	-	50.3	b
-	200	-	92.9	a
2	-	0.018	-	

[1]Different letters means significant differences (LSD; $p<0.05$)

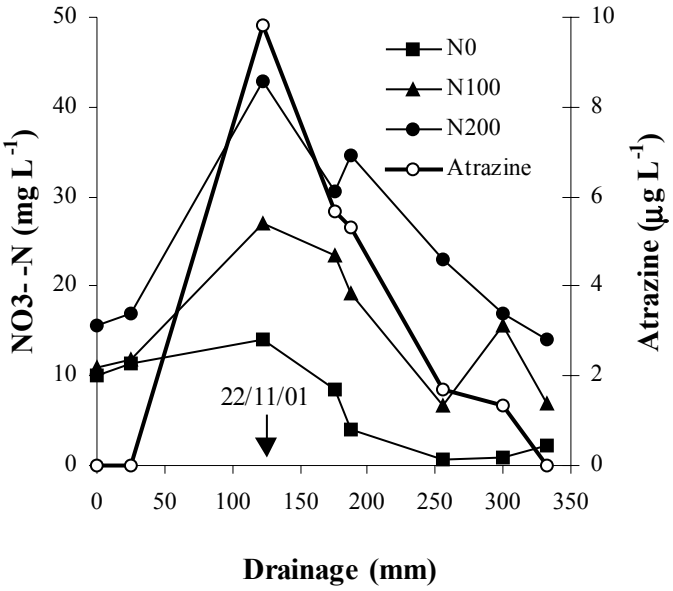

Figure 1. Nitrate and atrazine concentration at 1.5 m depth from the soil profile as a function of the amount of drainage water.

References

Bedmar, Francisco y José Luis Costa. 1999. Transporte de atrazina, metribuzin y bromuro en suelos. 14 Congreso Latinoamericano de la Ciencia del Suelo. Pucon Chile.

CEC, 1991. Council Directive of 12th December 1991 Concerning the Protection of Waters Against Pollution Caused by Nitrates from Agricultural Sources (91/676/EEC). Official Journal of the European Communities (30/12/91 L135/1 to 8).

Clarke, D., Smith, M., El-Askari, K., 1998. New software for crop water requirement and irrigation scheduling ICID J. 47,45-58.

Costa J L, H Massone, E Suero, M Vidal Y F Bedmar. 2002. Nitrate contamination of a rural aquifer and accumulation in the unsaturated zone. Agricultural Water Management.

Costa, J. L., R. E. Knighton, and L. Prunty. 1994. Model comparison of unsaturated steady-state solute transport in a field plot. Soil Sci. Soc. Am J 58:1277-1287.

Flury, M. 1996. Experimental evidence of transport of pesticides through field soils-A review. Journal of Environmental Quality, 25 : 25-45.

Funari, E., Donati, L., Sandroni, D., And Vighi, M. 1995. Pesticide levels in groundwater : Value and limitations of monitoring. Chapter 1 : 3-44. In : Pesticide risk in groundwater. Editors : Vighi, M., and Funari, E. CRC Press, Inc. Boca Raton, Florida, USA, 275p.

García, F. O., K. P. Fabrizzi, L. Picone y L. Justel. 1999. Volatilización de amonio a partir de fertilizantes nitrogenados aplicados superficialmente bajo siembra directa y labranza convencional en Argentina. En: Actas 14º Congreso Latinoamericano de la Ciencia del Suelo. Temuco. Chile. 8 al 12 de noviembre. Pp. 304.

Kolpin, D.W., Sneck-Fahrer, D., Hallberg, G.R., And Libra, R.D. 1997. Temporal trends of selected agricultural chemicals in Iowa's groundwater, 1982-1995 : Are things getting better ?. Journal of Environmental Quality, 26 :1007-1017.

Pasquarell, G.C., And Boyer, D.G. 1996. Herbicides in Karst groundwater in Southeast West Virginia. Journal of Environmental Quality, 25 :755-765.

Sainz Rozas, H., Echeverría, H.E., Picone, L.I., 2001. Denitrification in maize under no-tillage: effect of 296 nitrogen rate and application time. Soil Sci. Soc. Am. J. 65, 1314–1323.

Sasson A. 1993. La alimentación del hombre del mañana. UNESCO. Reverté S.A.

U. S. Environmental Protection Agency. 1995. Drinking water regulations and health advisories. Washington D.C., Office of Water, U. S. Environmental Protection Agency, 11

Usepa (U.S. Environment Protection Agency). 1990. National survey of pesticides in drinking water wells, phase I report. USEPA Rep. 570/9-90-015.

Weisenburger, D. D. 1991. Potential Health Consecuences of Ground-water Contamination by Nitrates in Nebraska. Nato Asi Series. Vol. G30. Ed. by Bogardi and Kuselka. Springer-Verlag Berlín Heildelberg.

Release and Transport of Polycyclic Aromatic Hydrocarbons from a Coarse Textured, Calcareous Contaminated Soil

Steffen Jann[1], Kai U. Totsche[1], Klaus-Holger Knorr[1], Markus Wehrer[2] and Ingrid Kögel-Knabner[1]

[1]Lehrstuhl für Bodenkunde, Department für Ökologie, Wissenschaftszentrum Weihenstephan für Ernährung, Landnutzung und Umwelt, Technische Universität München, 85350 Freising, Phone: 08161/ 71 31 47, Fax: 08161/ 71 44 66 email: sjann@wzw.tum .de
[2]Institut für Bodenkunde, Abteilung Bodenphysik, Universität Bayreuth, 95440 Bayreuth

Abstract: Release and transport of polycyclic aromatic hydrocarbons (PAH) and dissolved and colloidal phase organic carbon (DCOC) was studied with saturated column outflow experiments. The effect of the residence time on the release was investigated by different flow rates and two stop-flow events of different duration. The release of DCOC was characterized by a high initial export followed by a steep decrease. Each flow interruption resulted in an increased release. Qualitatively, the same results are found for the release of PAH: Each stop flow results in an increased export. Thus, the export and the release of both PAH and DCOC are clearly rate dependent. Due to this non-equilibrium behavior the release of PAH at contaminated sites is strongly controlled by the soil water residence time and thus influenced by the climatological boundary conditions and the soil physical properties.

1. Introduction

The widespread occurrence of hydrophobic organic contaminants in soil and groundwater has become an important environmental concern. Within the group of the hydrophobic contaminants, the polycyclic aromatic hydrocarbons (PAH) play a prominent role because of their human- and ecotoxicity and their persistence. The PAH comprise more than hundred single compounds, all of which are composed of at least two annealed benzene rings. The knowledge on the release and transport of PAH is mandatory for the risk assessment of soil and groundwater pollution. PAH feature high recalcitrance against microbial and chemical transformation, very low aqueous solubility and hydrophobicity. Due to these properties, PAH are considered immobile within the unsaturated zone at contaminated sites. Transport with the seepage water is supposed to be of minor importance, as PAH have a high affinity to the immobile solid phase, in particular to the organic fraction of the soil matrix. This results in strong sorption and such in an effective retardation in the unsaturated soil zone. However, the presence of mobile colloidal particles may substantially affect PAH mobility in soils (Totsche et al. 1997). Colloids act hereby as mobile sorbents for PAH and other strongly sorbing solutes and could thus facilitate their transport.
Besides the colloids of inorganic origin like clay minerals, iron and other metal hydr/oxides, the organic colloids (humic substances, viruses, bacteria, fungi, soot particles) act as a possible sorbent for hydrophobic contaminants and are thus possible pollutant carriers. Therefore, the release and transport of soil-borne colloidal particles is substantial for the understanding of the mobility of hydrophobic or surface-complexing contaminants. The fate of dissolved and colloidal phase organic carbon (DCOC) within soils is controlled by the release from and the interactions with the immobile solid phase as well as by the flow regime. DCOC is referred to as the amount of organic carbon in the liquid phase after filtration < 0.45 µm. Below this limit, components are by definition designated as “dissolved” but as the size of colloids range from 1 nm to 1 µm this filtration removes only a part of the colloids possibly present.

To investigate the effect of residence time on the release and transport of PAH and DCOC two saturated column outflow experiments with different flow rates were carried out. Additionally, two flow interruptions of 24 and 120 hours duration were imposed (Wehrer & Totsche 2003).

2. Materials and Methods

Saturated column experiments were performed using stainless-steel columns (9.4 cm diameter, 14.6 cm height) equipped with porous plates as bottom and top capping. The columns were repacked with air-dried and homogenized soil material. The soil material is a fluvial deposit of mainly calcareous gravel, with fine material less than 20% by weight, from beneath a tar oil blob at a contaminated site. A peristaltic pump was used to feed the percolation solution. To prevent microbial activity the solutions were poisoned by 0.5 mM sodium azide. The properties of the solutions are given in Table 1. During the experiments the temperature was kept constant at 20°C. All tubes except the pumping tube were made of stainless steel. Column effluent was collected with a fraction collector (Figure 1). Prior to the experiments the columns were water saturated from bottom to top. Analysis of the flow regime was done with chloride as a non-reactive tracer and fitting the breakthrough curves with the nonlinear least squares inversion model CXT-FIT (Parker & van Genuchten, 1984).

Solution	PH	elec. conductivity [µS cm^{-1}]	chloride [mol l^{-1}]
0.01 M $NaClO_4$ * H_2O	6.8	1160	< d.l.
0.01 M NaCl	7.0	1234	0.01

Table 1 - Physicochemical properties of the percolation solutions

The effect of the residence time on the release of PAH and DCOC was investigated by different flow rates and two stop-flow events of different duration (24 and 120 hours). Except for the stop flow events, the mean volumetric flow rate was kept constant throughout the experiments at 11 ml h^{-1} (*slow*) and 50 ml h^{-1} (*fast*), respectively. Analysis of the effluent samples comprised the determination of DCOC as non-purgeable organic carbon using a TOC-Analyzer after filtration with fiber-glass-filters (pore size 0.45 µm), pH by an ion-sensitive electrode, electrolytic conductivity by a conductivity cell and turbidity by absorption at 860 nm. The analysis of the 16 EPA-PAH in the liquid and the colloidal phase (extraction of the 0.45 µm filters) was done by GC-MSD using deuterated internal and injection standards. The extraction and determination of PAH is described in detail by Hartmann (1996).

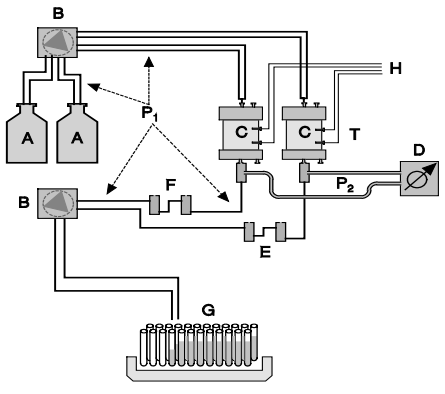

Figure 1: Set-up of laboratory column experiment.

3. Results and Discussion

An evaluation of the breakthrough curves for the non-reactive tracer chloride with CXT-FIT was used to detect non-uniform macroscopic flow due to poor packing of the column or poorly satisfied boundary conditions. These conditions would result in an early breakthrough of the tracer and/or in an extended tailing of the breakthrough curve.

Table 2 – Results of the inverse modeling of the chloride breakthrough data

Experiment	Pore water velocity [cm h^{-1}]	R	λ [cm]	r^2
slow: LEA	0.63	1.57	1.27	0.998
fast: LEA	2.86	1.22	2.65	0.997

(LEA: linear equilibrium adsorption; R: retardation; λ: dispersivity; r^2: coefficient of determination)

The breakthrough curves were of sigmoidal shape and were completed after 4 pv had been exchanged. Neither early breakthrough nor tailing was observed. The linear equilibrium model showed good agreement with the observed values (Table 2). The results of the parameter fitting identified no significant amount of immobile soil water. Slight retardation of chloride was observed due to anion exchange on the solid phase. The retention was even more pronounced in the *slow* column because of the higher residence time. The large longitudinal dispersivities reflect the fact that coarse textured materials (80% > 2mm !) were used with the columns. The column dispersivities are around 1.27 cm for the *slow* and 2.65 cm for the *fast* flow rate. The larger dispersivities for the *fast* column are due to the higher flow velocities.
The pH of the effluent solutions of the *slow* and *fast* column remained more or less constant around 7.4 and 7.0, respectively. The higher value at lower velocity is due to dissolution of carbonate. The flow interruptions showed little effect on the pH in the fast and no effect in the slow column. The electrolytic conductivity increased rapidly at the beginning of the experiment in response to the infiltration of the percolation solution. Both stop flow events resulted in temporarily increased electric conductivities with further decreasing values (data not shown).

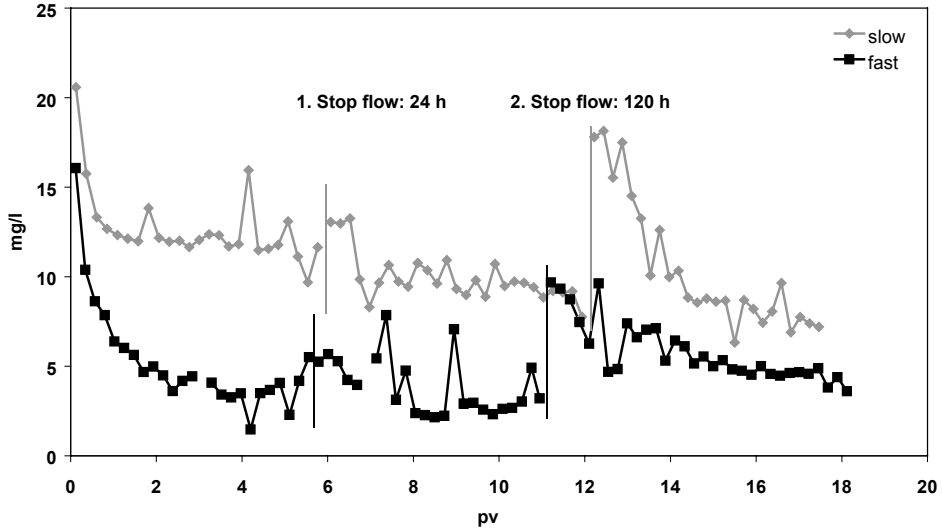

Figure 2: Concentrations of dissolved and colloidal phase organic carbon (DCOC) in the effluent of the slow and fast column with the effect of stop flow events

Figure 2 shows the concentrations of DCOC in the outflow of the *slow* and *fast* column. Starting irrigation caused a high initial release of DCOC followed by a steep decrease. This is explained by the export of readily available DCOC and the prolonged saturation previously. Under continued irrigation, the concentrations reached a constant level of about 10 mg l^{-1} for the *slow* and 5 mg l^{-1} for the *fast* column. Each flow interruption resulted in an increased release indicating that the release of DCOC is controlled by non-equilibrium conditions. However, the first stop flow was provoked to early before the release of readily available DCOC was completed. Thus, the effect of the stop flow on the DCOC release is more expressed for for the second an longer stop flow.
Qualitatively, the same results are found for the release of PAH (Figure 3). In general, higher concentrations were observed in the *slow* column. Maximum concentrations reached about 130µg l^{-1}.

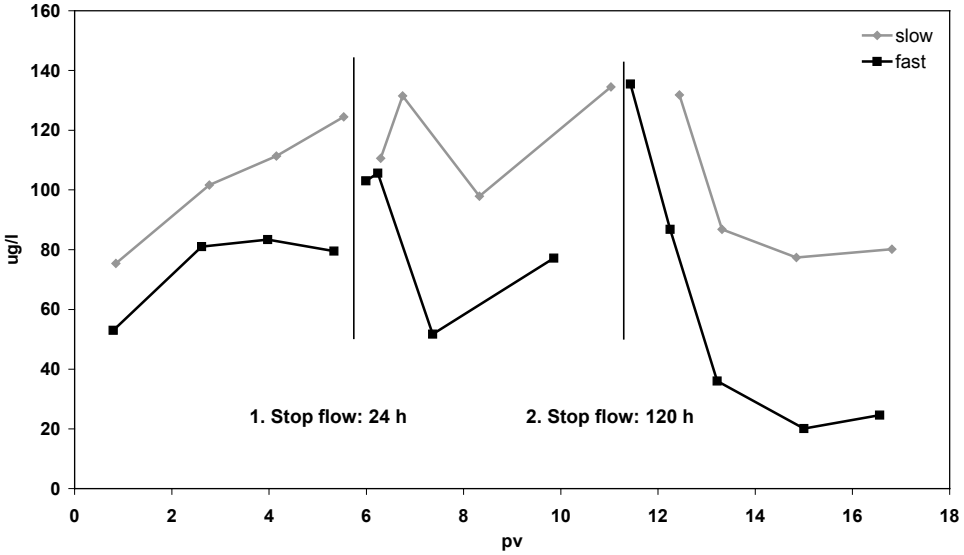

Figure 3: Concentrations of polycylic aromatic hydrocarbons (PAH) in the effluent of the slow and fast column with the effect of stop flow events

The initial release of PAH revealed rather low but increasing concentrations for both columns. The increase was steeper and reached higher levels at the low flow rate. This initial release pattern seems to be due to incomplete wetting of the tar-oil contaminated soil material right at the start of the experiment. However, with propagating time, all surfaces get water wet. From then on, the complete solid-liquid interface adds to the release of PAHs.
The stop flow events at the high flow velocity results in an increased export followed by a steep decrease. This points to a rate limited release of PAHs. Within the slow column, this effect is not that expressed. At the end of the experiment the effluents showed constant concentrations of 80 µg l^{-1} and 20 µg l^{-1}, respectively.
The release of PAH sorbed to colloids and suspended particles larger 0.45 µm is shown in Figure 4. First a high initial release with a steep decrease is observed: This release behavior is followed by continued decrease in the effluent concentrations. In contrast to the DCOC situation, the stop-flow events result in decreased concentration of PAH sorbed to colloids and suspended particles. The decrease is even more expressed for the fast than for the slow column. This was to be expected as the shear forces and thus the ability to mobilize larger particles are higher within the fast fraction.
The export of PAH in the colloidal and particle fraction is two orders of magnitude higher than in the liquid phase. Colloid and suspended-particle facilitated transport seems to be the

dominating process for the migration of PAH and other hydrophobic organic contaminants in the unsaturated zone of soils at contaminated sites.

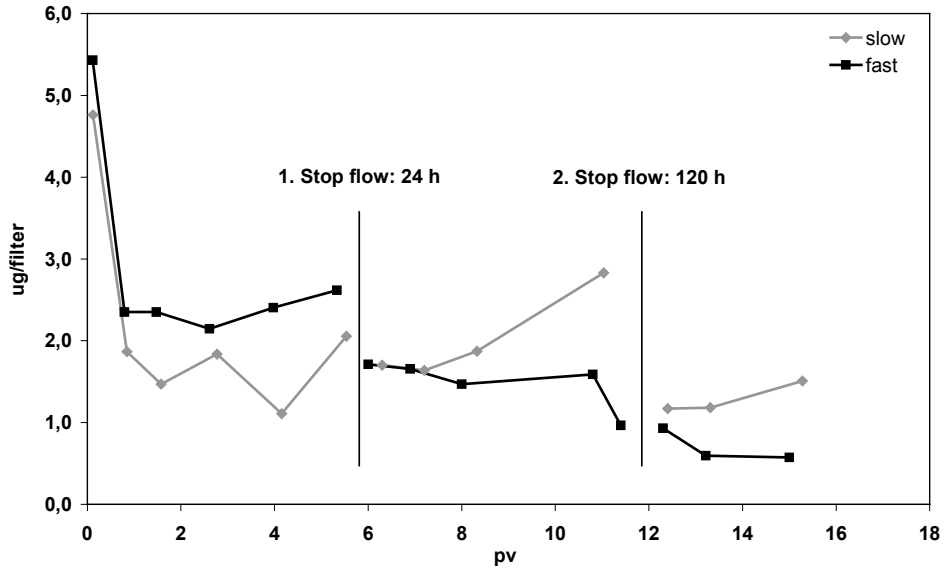

Figure 4: Concentrations of polycylic aromatic hydrocarbons (PAH) in the retentate (extracted filters) of the slow and fast column with the effect of stop flow events

Both the release of PAH and DCOC are rate dependent. Moreover, the export of DCOC, colloids and suspended particles is characterized by high initial concentrations. The residence time of the soil water is a function of the capillary-pressure conductivity curve, the actual soil moisture content, the vulnerability of the soil for preferential flow and the amount and temporal distribution pattern of the precipitation. Proper risk assessment and reliable monitoring strategies have to consider both the heterogeneous soil profile and the local micrometeorological conditions at the site.

4. References

Hartmann, R. (1996): Polycyclic aromatic hydrocarbons (PAHs) in forest soils - Critical evaluation of a new analytical procedure. *Intern. J. Environ. Anal. Chem*., 62: 161-173.

Parker, J.C. & van Genuchten, M.T. (1984): Determining transport parameters from laboratory and field tracer experiments. Virginia Agricultural Experimental Station, *Bulletin* 84-3.

Totsche, K.U., Danzer J. & Kögel-Knabner I. (1997): DOM-Enhanced Retention of polycyclic aromatic hydrocarbons in Soil Miscible Displacement Experiments. *J. Environ. Qual.* 26(4): 1090-1100.

Wehrer, M. & Totsche, K.U. (2003): Detection of non-equilibrium in soil solumns: Delineation of experimental conditions by numerical solution. *J. Plant Nutr. Soil Sci.* Accepted for publication:

Sorption of atrazine and three of its degradation products in different soils and tillage systems

J C Montoya[1], F Bedmar[2], P Daniel[2] & J L Costa[3]

[1]*Instituto Nacional de Tecnología Agropecuaria (INTA), EEA Anguil, CC 11 (6326) Anguil, La Pampa, Argentina. jmontoya@anguil.inta.gov.ar*
[2]*Facultad de Ciencias Agrarias, Universidad Nacional de Mar del Plata, CC 276 (7620) Balcarce, Buenos Aires, Argentina.*
[3]*Instituto Nacional de Tecnología Agropecuaria (INTA), EEA Balcarce, CC 276 (7620) Balcarce, Buenos Aires, Argentina.*

Introduction

Sorption studies are useful to assess the movement and fate of pesticides in soils. Soils have different capacity to sorb organic chemicals, depending on soil texture and organic matter (OM) content (Koskinen & Harper, 1990).

Atrazine (2-chloro-4-ethylamino-6-amino-1,3,5-triazine) is one of the more extensively used herbicides in agriculture. In Argentina, it is the second most extensively used pesticide after glyphosate. In soil it is transformed by chemical hydrolysis to hydroxyatrazine (2-chloro-4-amino-6-isopropilamino-*s*-triazine) (HA) and the first step of microbiological pathway results in desisopropilatrazine (2-hydroxy-4-ethylamino-6-isopropilamino-1,3,5-triazine) (DIA) and desethylatrazine (2-chloro-4-amino-6-isopropilamino-1,3,5-triazine) (DEA) (Rusell *et al*., 1968). Atrazine and its metabolites have pollution potential.

During the last decade, in Argentina, the use of atrazine had a significant increment and at present it is the second most used pesticide after glyphosate. The intensification of agriculture and the replacement of conventional tillage (CT) by no tillage (NT) caused more frequent herbicide applications.

No tillage produces changes in chemical soil properties like an increase in organic carbon (OC) content at 0-5 cm depth (Needelman *et al*., 1999). Sorption data for atrazine and its main metabolites in different soils and tillage systems are needed. In Argentina, there have been few studies of sorption of pesticides and their behavior in soils (Daniel *et al*., 2002; Hang *et al.,* 1996).

Because of this intensification of agriculture, the need arises from the public and scientists' concerns about the behavior and fate of these compounds with different physical and chemical soil characteristics. The objective of this study was to characterize the soil sorption of atrazine, HA, DEA and DIA as affected by soil type and tillage system.

Materials and methods

Three soils of the "humid pampas" region in the southeast of Buenos Aires Province (Argentina), each under both NT and CT systems, were selected for a relatively wide range of OM content (Balcarce, Bal; Tres Arroyos, TA and Coronel Dorrego, Dor). These soils were classified as follows: Bal, silty clay loam (fine, thermic, illitic, Typic Argiudoll); TA, clay loam (fine, thermic,

illitic, Typic Argiudoll), and Dor, loam (fine, thermic, mixed illitic-mortmorillonitic, Typic Argiudoll). The NT systems date from 10 years ago, while the CT systems always had this management. Soil samples were collected from the 0-15 cm upper layer which is the plow depth in CT system. Atrazine had never been applied in those soils.

A batch equilibrium method was employed to characterize sorption of atrazine, DEA, DIA and HA (OECD, 1995). Concentrations for the all compounds were 0.04, 0.1, 0.2, 0.5, 1.0, 2.0 and 5.0 mg L^{-1}, each one of this was replicated three times. The selected concentrations represented the dilution of a range from 0.072 to 9.0 Kg ha^{-1} of technical grade compound in the upper 0-15 cm layer of soils.

Two SAS procedures were used for fitting Freundlich equation, PROC NLIN and PROC REG (Myers, 1986; Sit & Poulin-Costello, 1994).

The mean square error (MSE) criterion was used to compare the regression models, where the lowest values imply the better model. As a subjective consideration for a ‘‘better’’ model, the two models and the observed data were plotted.

In the Freundlich equation, when n = 1, K_f becomes equal to the K_d (L Kg^{-1}), the distribution coefficient for adsorption. When K_d is normalized by the soil OC fraction, the organic carbon normalized adsorption coefficient is obtained (K_{oc} = [K_d / OC%] 100).

The K_f and K_d values were tested with ANOVA and Duncan test and Sliced test was used for interactions. A correlation analyses and a stepwise multiple linear regression procedure ($P < 0.15$ to enter or remove a component) for soils and adsorption parameters was performed (SAS Institute Inc. 1985).

Results and discussion

Soil properties

Soil properties relevant to sorption processes are shown in Table 1. There were significant differences between soil types for all variables ($P<0.01$) except for pH. Organic carbon content for the three soils was Bal > TA > Dor ($P<0.05$), CEC was higher in Bal and TA than Dor ($P<0.05$). TA and Bal had higher clay content than Dor ($P<0.05$); TA presented the highest silt content ($P<0.05$); Dor and Bal had more sand than TA ($P<0.05$). There were no significant differences between tillage systems in any soil properties.

Table 1 *Particle size distribution, organic carbon (OC), pH and cation exchange capacity (CEC) from Balcarce (Bal), Tres Arroyos (TA) and Cnel. Dorrego (Dor) under conventional (CT) and no tillage (NT) systems.*

Soil	Tillage	Particle size			OC	pH	CEC
		Sand	Silt	Clay			
		%			g Kg^{-1}		$mmol_c$ Kg^{-1}
Bal	CT	34.5(2.2)*	36.8(1.0)	28.6(3.1)	3.6(0.1)	6.1(0.3)	32.4(2.0)
Bal	NT	35.4(1.7)	36.1(1.6)	28.6(1.4)	3.5(0.3)	5.5(0.2)	30.7(1.3)
TA	CT	25.6(3.1)	42.5(1.2)	32.0(4.2)	2.7(0.2)	6.0(0.2)	31.5(1.8)
TA	NT	24.0(2.5)	44.6(1.3)	31.3(2.3)	3.1(0.2)	6.0(0.2)	30.1(2.1)
Dor	CT	41.0(4.0)	36.3(2.4)	22.7(1.6)	1.6(0.0)	6.0(0.3)	23.4(5.3)
Dor	NT	34.6(2.5)	38.3(0.6)	27.2(1.9)	1.8(0.2)	6.5(0.7)	25.4(3.0)

*Numbers in parentheses are standard deviations for three replicates.

Adsorption isotherms

The use of the non-linear form of the Freundlich equation (PROC NLIN) was more appropriate than the linearized form (PROC REG) to describe the sorption process (Table 2). In the soils studied adsorption isotherms of atrazine, DEA and HA were well described by Freundlich for K_f; while for DIA the use of K_f or K_d varied depending on soils and tillage.

The K_f and K_d values for each compound showed the same pattern in the order of adsorption for HA > atrazine > DIA > DEA (Table 2 and 3). There were no clear sorption tendencies because of tillage systems however the higher 1/n value under NT system in TA and Dor could reflect a large presence of young amorphous OM, when compared to CT. Lesan and Bhandari (2000) found similar results when 1/n values from forest soils were compared with agricultural soils.

Table 2 *Freundlich adsorption coefficients and 1/n estimated by the linearized and non-linear Freundlich equation for atrazine, desethylatrazine, desisopropilatrazine and hydroxyatrazine.*

Soil	Till	Linearized Freundlich equation			Normal Freundlich equation		
		K_f^{ac}	$1/n^{ac}$	MSE[d]	K_f^{bc}	$1/n^{bc}$	MSE[d]
		$mg^{1-1/n} L^{1/n} Kg^{-1}$	L Kg^{-1}		L Kg^{-1}		
				Atrazine			
Bal	CT	8.85(1.05)	0.94(0.02)	1.50	9.07(0.40)	0.93(0.08)	1.47
Bal	NT	9.12(1.05)	0.98(0.02)	0.95	9.20(0.29)	0.90(0.06)	0.81
TA	CT	6.11(1.05)	0.95(0.02)	0.25	6.25(0.15)	0.79(0.03)	0.21
TA	NT	5.75(1.03)	0.93(0.01)	1.48	7.34(0.14)	0.82(0.03)	0.15
Dor	CT	5.99(1.04)	0.91(0.02)	1.26	6.37(0.22)	0.75(0.04)	0.45
Dor	NT	7.39(1.07)	0.97(0.03)	0.48	5.83(0.11)	0.82(0.02)	0.12
				Desethylatrazine			
Bal	CT	3.74(1.03)	0.93(0.02)	0.24	3.58(0.17)	0.95(0.05)	0.22
Bal	NT	4.14(1.06)	0.92(0.03)	0.77	4.46(0.20)	0.75(0.05)	0.32
TA	CT	2.08(1.07)	0.88(0.04)	1.18	3.57(0.22)	0.67(0.06)	0.50
TA	NT	2.39(1.08)	0.99(0.04)	0.57	2.79(0.24)	0.92(0.08)	0.48
Dor	CT	3.19(1.07)	0.89(0.04)	0.93	2.43(0.20)	0.61(0.07)	0.42
Dor	NT	2.69(1.08)	0.89(0.04)	1.75	2.90(0.27)	0.66(0.08)	0.80
				Desisopropilatrazine			
Bal	CT	6.05(1.06)	0.92(0.04)	0.71	6.44(0.25)	0.83(0.05)	0.58
Bal	NT	7.03(1.04)	0.87(0.03)	1.05	7.36(0.27)	0.76(0.05)	0.74
TA	CT	3.46(1.10)	0.70(0.04)	2.05	5.23(0.16)	0.92(0.04)	0.21
TA	NT	3.25(1.01)	0.62(0.04)	2.74	6.11(0.20)	0.98(0.05)	0.33
Dor	CT	5.10(1.08)	0.68(0.04)	2.49	3.41(0.20)	1.05(0.06)	0.30
Dor	NT	5.70(1.08)	0.65(0.03)	3.18	3.06(0.25)	1.07(0.08)	0.48
				Hydroxyatrazine			
Bal	CT	14.59(1.07)	0.72(0.03)	1.31	13.65(0.38)	0.62(0.04)	0.84
Bal	NT	13.33(1.04)	0.63(0.02)	0.72	13.01(0.22)	0.57(0.02)	0.40
TA	CT	10.59(1.03)	0.82(0.01)	3.41	10.88(0.46)	0.58(0.05)	2.20
TA	NT	9.12(1.07)	0.91(0.05)	1.52	15.56(0.43)	0.80(0.06)	1.48
Dor	CT	11.02(1.05)	0.71(0.02)	0.84	10.62(0.29)	0.87(0.05)	0.83
Dor	NT	15.33(1.06)	0.81(0.03)	0.96	9.02(0.32)	0.98(0.06)	0.96

[a] Parameters estimated by linearized form of Freundlich equation.

[b] Parameters estimated by non-linear form of Freundlich equation.

[c] Numbers in parentheses are standard errors.

[d] MSE Mean Square Error.

Sorption was mainly attributed to soil organic carbon (OC), however the significant correlation with CEC implies that the mineral fraction also contributes to the sorption process (Table 4, 5 and 6). The K_{oc} described adequately the ability of the studied soils to adsorb HA, DIA and DEA. However atrazine had an inverse tendency between K_{oc} and OC (Table 3). This would reveal that not only OC is responsible of atrazine sorption, but also there would be other interactions with the inorganic matrix of soil.

Table 3 *Distribution coefficient for adsorption (K_d) and organic carbon normalized adsorption coefficient (K_{oc}) for atrazine, desethylatrazine, desisopropilatrazine and hydroxyatrazine.*

Soil	Tillage	K_d[a] L Kg^{-1}	R^2	K_{oc} L Kg^{-1}	K_d[a] L Kg^{-1}	R^2	K_{oc} L Kg^{-1}
		Atrazine			**Desethylatrazine**		
Bal	CT	8.83(0.28)	0.96	244.14	4.19(0.10)	0.98	115.29
Bal	NT	8.84(0.22)	0.97	256.95	4.19(0.22)	0.94	131.08
TA	CT	7.33(0.29)	0.96	342.60	4.30(0.33)	0.87	124.42
TA	NT	6.56(0.14)	0.98	244.83	2.52(0.16)	0.88	136.32
Dor	CT	7.09(0.27)	0.93	389.35	2.57(0.05)	0.99	124.46
Dor	NT	6.59(0.11)	0.99	310.65	2.00(0.13)	0.82	147.27
		Desisopropilatrazine			**Hydroxyatrazine**		
Bal	CT	5.75(0.17)	0.96	157.97	31.63(3.42)	0.54	973.17
Bal	NT	8.33(0.23)	0.98	242.38	22.71(1.29)	0.89	662.27
TA	CT	4.94(0.08)	0.99	181.92	14.82(0.73)	0.92	545.25
TA	NT	5.89(0.12)	0.98	192.48	20.87(0.53)	0.98	579.48
Dor	CT	3.55(0.08)	0.98	215.85	14.51(0.64)	0.95	581.25
Dor	NT	3.24(0.09)	0.97	177.05	8.83(0.23)	0.97	553.60

Table 4 *Correlation analyses for the non-linear Freundlich coefficient (K_f) and distribution coefficient of adsorption (K_d) and soil properties.*

	K_f				K_d			
	atrazine	DEA	DIA	HA	atrazine	DEA	DIA	HA
OC	0.87**	0.71**	0.95**	0.74**	0.63**	0.70**	0.84**	0.80**
pH	-0.69**	-0.67**	-0.75**	-0.45	-0.57*	-0.64**	-0.86**	-0.38
CEC	0.63**	0.68**	0.84**	0.60**	0.51*	0.73**	0.70**	0.65**
Clay	0.17	0.42	0.56**	0.45	0.04	0.39	0.44	0.20
Silt	-0.34	-0.24	0.08	0.34	-0.50*	-0.17	-0.04	-0.18
Sand	0.10	-0.08	0.33	-0.42	0.26	-0.11	-0.21	-0.00

*P<0.05 **P<0.01

Table 5 *Estimated models for Freundlich adsorption coefficients (K_f) obtained by the non-linear Freundlich equation for atrazine, desethylatrazine (DEA), desisopropilatrazine (DIA) and hydroxyatrazine (HA).*

Compound	R^2	Estimated model
Atrazine	0.98	$\mathbf{K_f}$ = 8.8 + 2.20 [OC] – 0.26 [Clay]
DEA	0.54	$\mathbf{K_f}$ = 1.54 + 0.64 [OC]
DIA	0.99	$\mathbf{K_f}$ = 10.42 + 1.56 [OC] – 1.88 [pH] + 0.04 [Silt]
HA	0.59	$\mathbf{K_f}$ = 6.13 + 2.20 [OC]

Table 6 *Estimated models for K_d for atrazine, desethylatrazine (DEA), desisopropilatrazine (DIA) and hydroxyatrazine (HA).*

Compound	R^2	Estimated model
Atrazine	0.92	$\mathbf{K_d}$ = 12.26 – 0.19 [Silt] + 0.98 [OC]
DEA	0.60	$\mathbf{K_d}$ = - 3.45 + 0.23 [CEC]
DIA	0.94	$\mathbf{K_d}$ = 22.11 + 1.19 [OC] – 3.33 [pH]
HA	0.71	$\mathbf{K_d}$ = - 5.61 + 9.28 [OC]

References

Daniel PE, Bedmar F, Costa JL, Aparicio VC. 2002. Atrazine and metribuzin sorption in soils of Argentinean humid pampas. *Environmental Toxicology & Chemistry* 21, 2567-2572.

Hang S, M Bocco & R Sereno. 2000. Adsorción de atrazina en dos perfiles de suelos argentinos, bajo siembra directa. Agrochimica XLIV, 115-122.

Koskinen WC, Harper SS. 1990. The retention process: Mechanisms. In*: Pesticides in the Soil Environment* (ed. HH Cheng). SSSA Book Series nº 2, 51-77. Soil Science Society of America, 677 S. Segoe Rd., Madison, WI 53711, USA.

Myers RH. 1986. Classical and Modern Regression with Applications. PWS Publishers, 20 Park Plaza, Boston, Massachusetts 02116. 359 pp.

Lesan HM & A Bhandari. Evaluation of atrazine binding to surface soils. Proceedings of the 2000 Conference on Hazardous Waste Research, 76-89 pp.

Needelman BA, Wander MM, Bollero GA, Boast CW, Sims GK & Bullock DG. 1999. Interaction of tillage and soil texture: Biologically active soil organic matter in Illinois. *Soil Science Society of American Journal* 63, 1326-1334.

OECD. 1995. Test guideline programme, final report of the OECD. Guideline 106. Workshop on selection of soils/sediments, Belgirate, Italy, 18-20 January 1995.

Rusell JD, Cruz M & White JL. 1968. Mode of chemical degradation of s-triazine by montmorillonite. *Science* 160, 1340-1342.

SAS Institute Inc. 1985. User's guide. Statistics. Version 5. SAS Institute Inc., Cary, North Carolina, USA.

Sit, V and M. Poulin-Costello. 1994. Catalog of Curves for Curve Fitting. Bergerud W. &V. Sit (eds.). Biometrics Information Handbook Series Nº 4. Province of British Columbia, Ministry of Forests. Forest Science Research Branch, Ministry of Forests, 31 Bastion Square, Victoria, B.C. V8W 3E7.116 pp.

Soil protection: in-situ sampling versus leaching tests

Nele Schuwirth, Dietmar Schenk, Thilo Hofmann

Johannes Gutenberg Universität Mainz, Becherweg 21, 55099 Mainz, Phone: 06131-3923771, Fax: 06131-3924769; E-Mail: thilo.hofmann@uni-mainz.de

Abstract: Today in Germany, one of the problems for risk assessment of the soil-groundwater transfer is that there is no effective guideline for choosing proper leaching/extraction tests or in-situ sampling techniques. In the past a wide range of leaching tests has been developed for different problems. The difficulty is to decide, which method should be used to answer which question. This decision depends on the contaminants as well as on the soil type and local conditions. The most suitable method has to be chosen in each individual case. In a project founded by regional authorities of Rhineland-Palatinate strategies will be developed for the realization of a groundwater risk assessment for typical inorganic contaminations in this state.

1. Background

Leaching tests are an important tool for the source term investigation because most of them are cheap and fast. Usually batch tests are, used which are not very close to reality, and hence may lead to unrealistic results. An other possibility are column tests under saturated or unsaturated conditions which may be much closer to reality but have a large time-need. An intelligent strategy is needed to establish how different tests relate to another, when keeping in mind that for regulatory control and quality control short procedures are needed. For understanding mechanisms and leaching processes, which are used to define and optimize theses shorter procedures for specific purposes, more fundamental and elaborate tests are required. Distinction should be made based on the amount of a priori knowledge, material quantity, and proper balancing between testing and management costs to achieve economic efficiency. Finally, the results also must unambiguously guide the evaluator to a well founded decision. Leaching tests are the only possibility for risk assessment of materials that will be used for landfill or disposal in future.

In-situ sampling procedures like suction lysimeters or centrifugation have the advantage that they are leading straight to realistic concentrations in the seepage water. If samples are taken at different depths it is although possible to make some time-dependent assumptions. Disadvantages are problems regarding interpolation, because of the small soil volume which is characterized by each sampling point. Statistical certainty of sampling is investigated by Liedl & Teutsch (1998). Spatial distribution of sampling points and statistical certainty of investigation grids are discussed by Reichert & Roemer (1997).

2. Investigations

The main intention of this project is to develop strategies for the realization of a groundwater risk assessment for typical inorganic contaminations in Rhineland-Palatinate. There are two typical contamination scenarios: Flotation dumps from ore mining in the low mountain ranges of Germany and abandoned industrial sites which are common in the neighborhood of rivers.

An exemplary realization of a source term investigation for two test sites is to be worked out with several different methods. Different in-situ sampling techniques like suction cups and centrifugation are tested and also several leaching/extraction tests (e.g. saturation soil extraction, the German S4 test, pH static tests at pH 4, ammonium nitrate extraction and

modifications of common procedures) in order to enable a well founded statement on practicability and suitability of these techniques. The leachates and seepage water samples are analyzed to measure heavy metals and metalloids such as zinc, lead, copper, cadmium, and arsenic using ICP-MS. Field parameters like electrical conductivity and pH and although the major anions and cations are investigated as well. Aside this soil samples are analyzed to investigate the total amounts of elements using XRF and aqua regia extracts as well as to identify mineral phases using XRD.

One of the test sites is a flotation dump from the zinc and lead ore mining. Since the age of the Romans until 1961 non-ferrous metals have been mined there. The dump consists of clay and silt and its thickness varies from four to seven meters. Field surveys show significant contaminations with lead, zinc, copper, cadmium, and arsenic. The other test site is an arsenic contaminated former production site of sulphuric acid and aluminium. It is an anthropogenic affected accumulation of ground excavation and building rubble. Arsenic, lead and fluoride can be found here in elevated concentrations.

Currently, selection criteria for leaching tests are developed and an evaluation of significance and correlation of in-situ sampling procedures and leaching tests is to be worked out. Geochemical behavior of different inorganic contaminants and geochemical conditions in different leaching tests are to be taken into account as well.

References:

Bundes-Bodenschutz- und Altlastenverordnung (BBodSchV) vom 12. Juli 1999, BGBl. I, S. 1554.

FRENZ, W. (2000): Bundesbodenschutzgesetz (BBODSCHG), Kommentar. C.H. Beck Verlag, München.

LIEDL, R. & TEUTSCH, G. (1998): Statistische Absicherung der Probenahme bei der Gefahrenherderkundung. Abschlußbericht LAG 98-01-0460. Eberhard-Karls-Universität Tübingen, Tübingen.

REICHERT, J.K. & ROEMER, M. (1997): Probenahme- und Untersuchungsmethoden. In GDCH (Eds.), Chemie und Biologie der Altlasten, VCH, Weinheim.

DE ROOIJ, G. & STAGNITTI, F. (2002): Spatial and temporal distribution of solute leaching in heterogeneous soils: analysis and application to multisampler lysimeter data. Journal of Contaminant Hydrology 54:329-346.

VAN DER SLOOT, H. A., HEASMAN, L. & QUEVAUVILLER, PH. (1997): Harmonization of Leaching/Extraction tests. Elsevier, Amsterdam.

GROSSMANN, J., BREDEMEIER, M. & UDLUFT, P. (1990): Sorption of trace metals by suction cups of aluminium oxide, ceramic and plastics. Z. Pflanzenernähr. Bodenk. 153:359-364.

In der Reihe C der Tübinger Geowissenschaftlichen Arbeiten (TGA) sind bisher erschienen:

Nr. 1: Grathwohl, Peter (1989): Verteilung unpolarer organischer Verbindungen in der wasserungesättigten Bodenzone am Beispiel der leichtflüchtigen aliphatischen Chlorkohlenwasserstoffe. 102 S.

Nr. 2: Eisele, Gerhard (1989): Labor- und Felduntersuchungen zur Ausbreitung und Verteilung leichtflüchtiger chlorierter Kohlenwasserstoffe (LCKW) im Übergangsbereich wasserungesättigte/wassergesättigte Zone. 84 S.

Nr. 3: Ehmann, Michael (1989): Auswirkungen atmogener Stoffeinträge auf Boden- und Grundwässer sowie Stoffbilanzierungen in drei bewaldeten Einzugsgebieten im Oberen Buntsandstein (Nordschwarzwald). 134 S.

Nr. 4: Irouschek, Thomas (1990): Hydrogeologie und Stoffumsatz im Buntsandstein des Nordschwarzwaldes. 144 S.

Nr. 5: Sanns, Matthias (1990): Experimentelle Untersuchungen zum Ausbreitungsverhalten von leichtflüchtigen Chlorkohlenwasserstoffen (LCKW) in der wassergesättigten Zone. 122 S. **(Vergriffen!)**

Nr. 6: Seeger, Thomas (1990): Abfluß- und Stofffrachtseparation im Buntsandstein des Nordschwarzwaldes. 154 S.

Nr. 7: Einsele, Gerhard & Pfeffer, Karl-Heinz (Hrsg.) (1990): Untersuchungen über die Auswirkungen des Reaktorunfalls von Tschernobyl auf Böden, Klärschlamm und Sickerwasser im Raum von Oberschwaben und Tübingen. 151 S.

Nr. 8: Douveas, Nikon G. (1990): Verwitterungstiefe und Untergrundabdichtung beim Talsperrenbau in dem verkarsteten Nord-Pindos-Flysch (Projekt Pigai-Aoos, NW-Griechenland). 165 S.

Nr. 9: Schlöser, Heike (1991): Quantifizierung der Silikatverwitterung in karbonatfreien Deckschichten des Mittleren Buntsandsteins im Nordschwarzwald. 93 S.

Nr. 10: Köhler, Wulf-Rainer (1992): Beschaffenheit ausgewählter, nicht direkt anthropogen beeinflußter oberflächennaher und tiefer Grundwasservorkommen in Baden-Württemberg. 144 S.

Nr. 11: Bundschuh, Jochen (1991): Der Aquifer als thermodynamisch offenes System. – Untersuchungen zum Wärmetransport in oberflächennahen Grundwasserleitern unter besonderer Berücksichtigung von Quellwassertemperaturen (Modellversuche und Geländebeispiele). 100 S. **(Vergriffen!)**

Nr. 12: Herbert, Mike (1992): Sorptions- und Desorptionsverhalten von ausgewählten polyzyklischen aromatischen Kohlenwasserstoffen (PAK) im Grundwasserbereich. 111 S.

Nr. 13: Sauter, Martin (1993): Quantification and forecasting of regional groundwater flow and transport in a karst aquifer (Gallusquelle, Malm, SW-Germany. 150 S.

Nr. 14: Bauer, Michael (1993): Wasserhaushalt, aktueller und holozäner Lösungsabtrag im Wutachgebiet (Südschwarzwald). 130 S.

Nr. 15: Einsele, Gerhard & Ricken, Werner (Hrsg.) (1993): Eintiefungsgeschichte und Stoffaustrag im Wutachgebiet (SW-Deutschland). 215 S.

Nr. 16: Jordan, Ulrich (1993): Die holozänen Massenverlagerungen des Wutachgebietes (Südschwarzwald). 132 S.

Nr. 17: Krejci, Dieter (1994): Grundwasserchemismus im Umfeld der Sonderabfalldeponie Billigheim und Strategie zur Erkennung eines Deponiesickerwassereinflusses. 121 S.

Nr. 18: Hekel, Uwe (1994): Hydrogeologische Erkundung toniger Festgesteine am Beispiel des Opalinustons (Unteres Aalenium). 170 S. **(Vergriffen!)**

Nr. 19: Schüth, Christoph (1994): Sorptionskinetik und Transportverhalten von polyzyklischen aromatischen Kohlenwasserstoffen (PAK) im Grundwasser - Laborversuche. 80 S.

Nr. 20: Schlöser, Helmut (1994): Lösungsgleichgewichte im Mineralwasser des überdeckten Muschelkalks in Mittel-Württemberg. 76 S.

Nr. 21: Pyka, Wilhelm (1994): Freisetzung von Teerinhaltsstoffen aus residualer Teerphase in das Grundwasser: Laboruntersuchungen zur Lösungsrate und Lösungsvermittlung. 76 S.

Nr. 22: Biehler, Daniel (1995): Kluftgrundwässer im kristallinen Grundgebirge des Schwarzwaldes – Ergebnisse von Untersuchungen in Stollen. 103 S.

Nr. 23: Schmid, Thomas (1995): Wasserhaushalt und Stoffumsatz in Grünlandgebieten im württembergischen Allgäu. 145+ 92 S.

Nr. 24: Kretzschmar, Thomas (1995): Hydrochemische, petrographische und thermodynamische Untersuchungen zur Genese tiefer Buntsandsteinwässer in Baden-Württemberg. 142 S. **(Vergriffen!)**

Nr. 25: Hebestreit, Christoph (1995): Zur jungpleistozänen und holozänen Entwicklung der Wutach (SW-Deutschland). 88 S.

Nr. 26: Hinderer, Matthias (1995): Simulation langfristiger Trends der Boden- und Grundwasserversauerung im Buntsandstein-Schwarzwald auf der Grundlage langjähriger Stoffbilanzen. 175 S.

Nr. 27: Körner, Johannes (1996): Abflußbildung, Interflow und Stoffbilanz im Schönbuch Waldgebiet. 206 S.

Nr. 28: Gewald, Thomas (1996): Der Einfluß der Desorptionskinetik bei der Freisetzung von Trichlorethen (TCE) aus verschiedenen Aquifersanden. 67 S.

Nr. 29: Schanz, Ulrich (1996): Geophysikalische Untersuchungen im Nahbereich eines Karstsystems (westliche Schwäbische Alb). 114 S.

Nr. 30: Renner, Sven (1996): Wärmetransport in Einzelklüften und Kluftaquiferen – Untersuchungen und Modellrechnungen am Beispiel eines Karstaquifers. 89 S.

Nr. 31: Mohrlok, Ulf (1996): Parameter-Identifikation in Doppel-Kontinuum-Modellen am Beispiel von Karstaquiferen. 125 S.

Nr. 32: Merkel, Peter (1996): Desorption and Release of Polycyclic Aromatic Hydrocarbons (PAHs) from Contaminated Aquifer Materials. 76 S.

Nr. 33: Schiedek, Thomas (1996): Auftreten und Verhalten von ausgewählten Phthalaten in Wasser und Boden. 112 S.

Nr. 34: Herbert, Mike & Teutsch, Georg (Hrsg.) (1997): Aquifersysteme Südwestdeutschlands - Eine Vorlesungsreihe an der Eberhard-Karls-Universität Tübingen. 162 S.

Nr. 35: Schad, Hermann (1997): Variability of Hydraulic Parameters in Non-Uniform Porous Media: Experiments and Stochastic Modelling at Different Scales. 233 S.

Nr. 36: Herbert, Mike & Kovar, Karel (Eds.) (1998): GROUNDWATER QUALITY 1998: Remediation and Protection - Posters -.- Proceedings of the GQ'98 conference, Tübingen, Sept. 21-25, 1998, Poster Papers. 146 S.

Nr. 37: Klein, Rainer (1998): Mechanische Bodenbearbeitungsverfahren zur Verbesserung der Sanierungseffizienz bei In-situ-Maßnahmen. 106 S.

Nr. 38: Schollenberger, Uli (1998): Beschaffenheit und Dynamik des Kiesgrundwassers im Neckartal bei Tübingen. 74 S.

Nr. 39: Rügner, Hermann (1998): Einfluß der Aquiferlithologie des Neckartals auf die Sorption und Sorptionskinetik organischer Schadstoffe. 78 S.

Nr. 40: Fechner, Thomas (1998): Seismische Tomographie zur Beschreibung heterogener Grundwasserleiter. 113 S.

Nr. 41: Kleineidam, Sybille (1998): Der Einfluß von Sedimentologie und Sedimentpetrographie auf den Transport gelöster organischer Schadstoffe im Grundwasser. 82 S.

Nr. 42: Hückinghaus, Dirk (1998): Simulation der Aquifergenese und des Wärmetransports in Karstaquiferen. 124 S.

Nr. 43: Klingbeil, Ralf (1998): Outcrop Analogue Studies – Implications for Groundwater Flow and Contaminant Transport in Heterogeneous Glaciofluvial Quaternary Deposits. 111 S.

Nr. 44: Loyek, Diana (1998): Die Löslichkeit und Lösungskinetik von polyzyklischen aromatischen Kohlenwasserstoffen (PAK) aus der Teerphase. 81 S.

Nr. 45: Weiß, Hansjörg (1998): Säulenversuche zur Gefahrenbeurteilung für das Grundwasser an PAK-kontaminierten Standorten. 111 S.

Nr. 46: Jianping Yan (1998): Numerical Modeling of Topographically-closed Lakes: Impact of Climate on Lake Level, Hydrochemistry and Chemical Sedimentation. 144 S.

Nr. 47: Finkel, Michael (1999): Quantitative Beschreibung des Transports von polyzyklischen aromatischen Kohlenwasserstoffen (PAK) und Tensiden in porösen Medien. 98 S.

Nr. 48: Jaritz, Renate (1999): Quantifizierung der Heterogenität einer Sandsteinmatrix (Mittlerer Keuper, Württemberg). 106 S.

Nr. 49: Danzer, Jörg (1999): Surfactant Transport and Coupled Transport of Polycyclic Aromatic Hydrocarbons (PAHs) and Surfactants in Natural Aquifer Material - Laboratory Experiments. 75 S.

Nr. 50: Dietrich, Peter (1999): Konzeption und Auswertung gleichstromgeoelektrischer Tracerversuche unter Verwendung von Sensitivitätskoeffizienten. 130 S.

Nr. 51: Baraka-Lokmane, Salima (1999): Determination of Hydraulic Conductivities from Discrete Geometrical Characterisation of Fractured Sandstone Cores. 119 S.

Nr. 52: M^{c}Dermott, Christopher I. (1999): New Experimental and Modelling Techniques to Investigate the Fractured System. 170 S.

Nr. 53: Zamfirescu, Daniela (2000): Release and Fate of Specific Organic Contaminants at a Former Gasworks Site. 96 S.

Nr. 54: Herfort, Martin (2000): Reactive Transport of Organic Compounds Within a Heterogeneous Porous Aquifer. 76 S.

Nr. 55: Klenk, Ingo (2000): Transport of Volatile Organic Compounds (VOC's) From Soilgas to Groundwater. 70 S.

Nr. 56: Martin, Holger (2000): Entwicklung von Passivsammlern zum zeitlich integrierenden Depositions- und Grundwassermonitoring: Adsorberkartuschen und Keramikdosimeter. 84 S.

Nr. 57: Diallo, Mamadou Sanou (2000): Acoustic Waves Attenuation and Velocity Dispersion in Fluid-Filled Porous Media: Theoretical and Experimental Investigations. 101 S.

Nr. 58: Lörcher, Gerhard (2000): Verarbeitung und Auswertung hyperspektraler Fernerkundungsdaten für die Charakterisierung hydrothermaler Systeme (Goldfield/Cuprite, Yellowstone National Park). 158 S.

Nr. 59: Heinz, Jürgen (2001): Sedimentary Geology of Glacial and Periglacial Gravel Bodies (SW-Germany): Dynamic Stratigraphy and Aquifer Sedimentology. 102 S.

Nr. 60: Birk, Steffen (2002): Characterisation of Karst Systems by Simulating Aquifer Genesis and Spring Responses: Model Development and Application to Gypsum Karst. 122 S.

Nr. 61: Halm, Dietrich & Grathwohl, Peter (Eds.) (2002): Proceedings of the 1st International Workshop on Groundwater Risk Assessment at Contaminated Sites (GRACOS). 280 S.

Nr. 62: Bauer, Sebastian (2002): Simulation of the genesis of karst aquifers in carbonate rocks. 143 S.

Nr. 63: Rahman, Mokhlesur (2002): Sorption and Transport Behaviour of Hydrophobic Organic Compounds in Soils and Sediments of Bangladesh and their Impact on Groundwater Pollution – Laboratory Investigations and Model Simulations. 73 S.

Nr. 64: Peter, Anita (2002): Assessing natural attenuation at field scale by stochastic reactive transport modelling. 101 S.

Nr. 65: Leven-Pfister, Carsten (2002): Effects of Heterogeneous Parameter Distributions on Hydraulic Tests - Analysis and Assessment. 94 S.

Nr. 66: Schwarz, Rainer (2002): Grundwasser-Gefährdungsabschätzungen durch Emissions- und Immissionsmessungen an Deponien und Altlasten. 100 S.

Nr. 67: Abel, Thekla (2003): Untersuchungen zur Genese des Malmkarsts der Mittleren Schwäbischen Alb im Quartär und jüngeren Tertiär. 187 S. (**Im Druck**).

Nr. 68: Prokop, Gundula & Bittens, Martin & Cofalka, Piotr & Roehl, Karl Ernst & Schamann, Martin & Younger, Paul (Eds.) (2003): Summary Report on the 1st IMAGE-TRAIN Advanced Study Course “Innovative Groundwater Management Technologies”. 119 S.

Nr. 69: Halm, Dietrich & Grathwohl, Peter (Eds.) (2003): Proceedings of the 2nd International Workshop on Groundwater Risk Assessment at Contaminated Sites (GRACOS) and Integrated Soil and Water Protection (SOWA). 260 S.